The petrology and geochemistry of the Ortakoy area, Central Turkey

by

Kerim Koçak, B.Sc., M.Sc.

Thesis submitted for the degree of Doctor of Philosophy

Department of Geology&Applied Geology,

University of Glasgow, Glasgow. February, 1993

ProQuest LLC.
789 East Eisenhower Parkway
P.O. Box 1346
Ann Arbor, MI 48106 – 1346

Dedicated to my parents with all my love

Declaration

The material presented herein is the result of independent research carried out between June 1989 and February 1993 in the Department of Geology and Applied Geology, University of Glasgow, under the supervision of Professor B.E.Leake.

This thesis is based on my own research and any previously published results of other research used by me has been given full acknowledgement in the text.

Kerim Kocak

Acknowledgements

I wish to express my gratitude to the following people for their support and contributions to my work during my PhD.

First, thanks to the Rector of Selcuk University (Konya,Turkey), Dean of the Engineering & Architecture Faculty and staff members of the Geology Department to give an opportunity to pursue this degree. Thanks especially to my supervisor, Professor B.E.Leake for his continuous help, patience, encouragement, constant advice throughout my project, valuable help in the field (both in Ireland and Turkey) and for his hospitality at Christmas. Thanks are due to Professor H. Bas for his supervision and guidance in the field; to Professor A. Ayhan for his various help in Turkey and to I.Ergin for his considerable help during my field studies.

I am indebted to Dr.T.Dempster for his help with metamorphic petrology, to Dr.G.Tanner who assisted me in my structural interpretation, to Dr.C.Burton for his identification of the fossil, to Dr. C.Farrow for help with computing and to Dr.C.Braithwaite for his identification of the limestone. Also in the department, thanks to R.Morrison for his logistic support, to R.McDonald who helped with the microprobe analyses, to J.Gallagher for running major and trace element analyses, and to M. MacLeod and D.Turner for their assistance in the geochemistry laboratory, thanks to J.Gilleece and A.Jones for supplying thin section and polished sections.

Thank-you, also, to those in Turkey, particularly T.Sert for organising accommodation during my field studies and A.Taskiran and B.Akarsu for

their support during my field work. Thanks to H. Kurt, V.Zedef , B.Hekimbasi, M.Arslan and G. Keaney for social and psychological support during my stay in Britain.

Most importantly, thanks to my parents, brothers and sister for their constant support, understanding and encouragement during my life and this PhD.

Contents

List of figures

List of tables

List of photographs

page

ABSTRACT

The Middle Anatolia Massif is one of the largest igneous and metamorphic complexes in Turkey. The western part of the massif is the subject of the present study.

The main purposes of the work are to map the different igneous and metamorphic rocks; to identify their mineralogical, petrographical and geochemical characteristics and by considering their relationships to each other, determine the metamorphic, magmatic and geological evolution of the Ortakoy area.

The geological map of the Ortakoy area(Appendix-Ia) shows that the oldest identified rocks are the Seksenusagi Formation of Silurian-Devonian age and the conformably overlying Gobektepe Formation of Upper Palaeozoic age. The Ekecekdagi gabbro comprises hornblende-gabbro and minor banded gabbro and may have been emplaced onto the metamorphic rocks as an allochthonous unit or intruded into the metasediments before the intrusion of the Ortakoy pluton. The metasediments were intruded and hornfelsed by the voluminous Upper Cretaceous - Paleocene Ortakoy pluton containing hornblendite, hornblende diorite, biotite-hornblende granitoid, microgranite and quartz-alkali syenite. The massif is overlain by the Pecenek Formation of Pliocene age composed of rhyolitic tuff; clay and sand with some gravels; and lacustrine limestone. Colluvium and alluvium are the youngest formations in the area.

The Ortakoy part of the Middle Anatolia Massif underwent four phases of deformation: D1 during the formation of the metamorphic rock fabric, D2 which produced folds varying from isoclinal to tight while D3

folds have open limbs and developed in approximately an E-W direction. D4 folds are usually open with steep axial planes and plunge roughly towards the S-E. The massif was then uplifted inducing the development of the WSW-ENE dominated joint sets in the Ekecekdagi gabbro, diorite and granitoid and the formation of WNW-ESE faults.

During or after D1 deformation, the Ortakoy metasediments underwent a single episode of regional metamorphism corresponding to the upper amphibolite facies conditions (second sillimanite grade), which is confirmed by geothermometer studies from the different metamorphic assemblages which yield between 608-761 °C at 4 kb. pressure. The high grade metamorphic rocks have undergone limited retrogression to greenschist facies assemblages which is shown by the replacement of sillimanite and K-feldspar by muscovite, and breakdown of garnet to biotite.

The Ortakoy metasediments occur as roof pendants, and as a result of this, they suffered intensive contact metamorphism, which resulted in the formation of pelitic hornfels consisting of biotite, cordierite, orthoclase and plagioclase; paragneissic granites and their pelitic inclusions, both of which are made of cordierite, biotite, plagioclase (An 26-40%), orthoclase and garnet; skarn zones in carbonate xenoliths, and andalusite in the semipelitic gneiss. The temperature ranged from 681(±50) to 533 (± 50) °C at 4.17(±0.29) kb in contact metamorphism.

Evaluation of the geochemical analyses of the hornblende diorite, biotite-hornblende granitoid and microgranite indicates that these igneous units represent different batches of a magma which was possibly formed by mixing of mantle and lower crustal derived magmas, coupled with fractional crystallisation with a possible small degree of high level contamination. The melt dominated character of the I-type acidic rocks is

evidenced by decreasing K/Rb with increasing SiO2. Y/Nb variation in the granitoids also implies heterogenity at the source of the granitoids. Hybridisation processes such as mixing and mechanical transfer affected the chemical composition of the granitoids.

The Ortakoy metasediments may have been derived from pre-Silurian weathering of Gondwanaland which was made of mainly acidic igneous and volcanic rocks with possible minor basic-ultrabasic contributions and deposited in an active continental margin and possibly in part in a continental island arc. The general transgressive character of the Ortakoy metasediments is indicated by the decreasing semipelite and psammite layers and increasing carbonate. The within plate character of the continental amphibolites that were emplaced into the metasediments imply a change in the geotectonic environment from an active continental margin to a passive continental one between the Silurian and Permian time. The sediments were later intruded by voluminous post-tectonic granitoids of active continental margin type in Upper Cretaceous-Paleocene time. As a tensional tectonic regime was dominant in the Anatolia block between Permian and Upper Cretaceous times (Sengor &Yilmaz,1981), the metamorphism in Ortakoy would be Permian-Carboniferous. The non-existence of the pre-Upper Cretaceous formations in the Middle Anatolia Massif indicates that the massif acted as a rigid block after the metamorphism, between the Permian and Upper Cretaceous.

I INTRODUCTION

The area studied is located in the Ortakoy region, Central Turkey (Fig.1). The main mountains in the area are Ekecekdagi (2137m), Harundagi (1505m.) and Yerlitepe (1538m) made up hornblende gabbros and biotite-hornblende granitoids, otherwise the topography is muted.

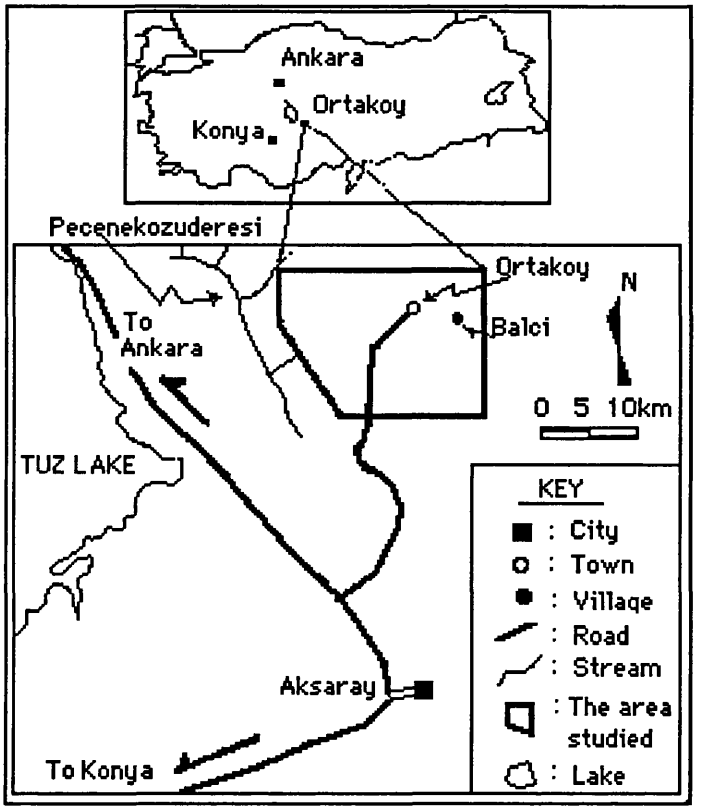

Figure 1: Location map of the area studied

The area is composed of marbles, semipelites, psammites, quartzites and amphibolites of Silurian-Devonian (possibly Carboniferous) age metamorphosed in pre-Cretaceous time. These rocks were intruded and hornfelsed by hornblendite, hornblende diorite and granitoids during Late Cretaceous to Paleocene time. The metasediments also contain post regional metamorphic gabbros but the contacts with the metasediments are

not exposed and it is unclear whether the gabbros intrude, or are thrust into, the metasediments. All these rocks are variably covered unconformably by Pliocene limestone, tuff and unmetamorphosed sediments.

I.1 AIM AND METHODS

The area studied is situated in the western part of the Middle Anatolia Massif (MAM) which can be defined as an association of igneous and metamorphic rocks around Kirsehir,Nigde (Okay, 1954) and Akdagmadeni, Yozgat (Erkan, 1980-b) (Fig. 2). No detailed study has been performed before in this part of the massif. Therefore, the main aims of this study were to map the different metamorphic and igneous units, identify their mineralogical, petrographical and geochemical characteristics and evaluate the magmatism and metamorphism of the area and its geological evolution.

Field studies started in 1987 and finished in 1991, resulting in 1/25 000 geological maps of the Ortakoy area (~380 km square) including mapping of Sirayalardagi at 1/5 000 scale (2 km square). About 650 samples from different lithologies were collected, ~200 thin sections examined and, major and trace element analyses of ~100 samples determined and REE analyses of 17 samples performed on selected representative fresh samples. To determine the modal mineralogical compositions point counting of 14 thin sections were carried out. A major problem has been the difficulty of obtaining fresh samples of many of the rocks, especially the semipelitic rocks.

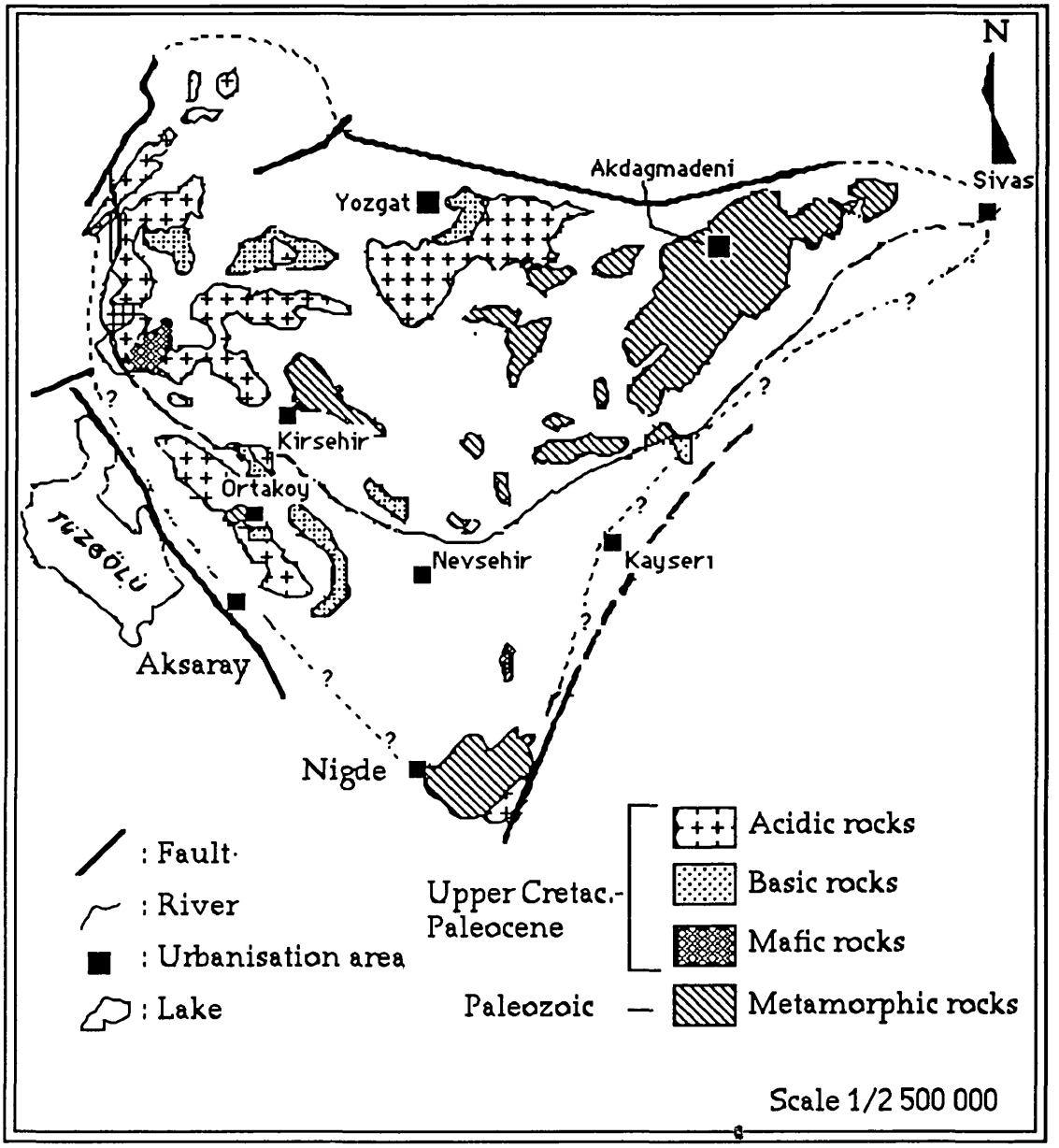

Figure 2 : Geological map of the Middle Anatolia Massif (border of the massif adopted from Bingol, 1974)

I.2 HISTORY OF RESEARCH

Many studies have been carried out by different authors in the Middle Anatolia Massif, the second biggest complex in Turkey. These are, however, mostly undetailed researches and often unpublished. In last two decades, considerable work has been carried out especially by Erkan (1976 a-b, 1977, 1978, 1980 a-b), Goncuoglu (1977), Tulumen (1980) and Seymen (1981, 1982). No detailed study had been carried out in the present area of study before the present work began. The principal publications dealing with the massif as a whole are summarised chronologically :

Around Kirikkale and Kirsehir, Baykal (1941) reported granitic xenoliths in dolerite and that the dolerites cut the granite.

The area between Nigde-Incesu, Kizilirmak, and Tuz Golu was studied in term of the general geology by Tromp (1942) who discovered the existence of Upper Cretaceous units called the Asmabogazi Formation at the east side of Tuz Lake.

Lahn (1949) tried to explain the basement in the Middle of Anatolia. He indicated that it was composed of metamorphic and igneous rocks of several old massifs, e.g., the Kirsehir, the Yukari Sakarya and the Akdagmadeni massifs. He proposed that there existed similar unexposed massifs covered by the younger deposits of the Konya and Tuz Golu basins.

The first extensive geological mapping was by Buchardt (1954). He published a geological map of the area at 1/100,000 between Kirsehir and the Kizilirmak river and concluded that the gabbros and dolerites represent the initial magmatism of Cretaceous age while the granite is of Laramide age

i.e. the Cretaceous-Tertiary boundary. A geological map of the massif at the eastern side of Kirsehir was produced at the same scale by Erguvanli (1954).

The Middle Anatolia Massif was defined for the first time as the igneous and metamorphic rocks of the Nigde and Kirsehir terrains by Okay (1954).

Roenner (1958) dealt with skarn mineralisation at the granite-marble contact, in the Kirsehir area, and he proposed that the sedimentary age of the marbles was Palaeozoic or Mesozoic.

Pisoni's (1961) work was the first in Ortakoy. He showed that a Palaeozoic metamorphic complex was made of gneiss with quartzite and amphibolite intercalations, and highly recrystallized marble.

In the Kirsehir terrain, the granite was observed to cut through gabbro which itself was intruded into ophiolite (Ayan, 1963).

The first geological map of the major part of the massif at 1/500.000 which includes the area of study, was published by Ketin (1963) who confirmed Ayan (1963)'s opinion, that is, gabbro cut the ophiolitic sequence.

Vache's (1963) first suggested the existence of a discordance in the metamorphic units at the Akdag mountain belt. He explained that the basement is composed of marbles discordantly over the basal series of gneiss. Above the marbles are mica schists and quartzite.

The volcanic area, between Aksaray and Hasandagi was mapped by Beekman (1966) who identified many tuff, tuffite, ignimbrite and lava

units. He suggested that some eruption may have originated along the Sereflikochisar-Aksaray fault which is on the east side of Tuz Golu.

Around Kirsehir, the isotopic ages of plutonism in the massif were studied by Ataman (1972). He recorded a 71 my. age to the Cefalikdag granodiorite using the Rb-Sr method.

Bingol (1974) produced the metamorphism map of Turkey. He showed that the meta-sedimentary rocks in the massif have been metamorphosed under medium pressure-greenschist facies conditions.

In 1975, Arikan described the geology of the Tuz Golu basin including the gravels containing granite and granitic gneiss clasts in the Haymana Formation which is of Upper Cenonian age.

The first detailed study in the massif was carried out by Erkan (1976 a) who identified high grade greenschist-amphibolite facies rocks reaching to the sillimanite+K-feldspar isograd around Kirsehir. Plagioclase became more calcic and hornblende richer in Ti, K, Al and garnet poorer in Mn with increasing metamorphic grade (Erkan, 1976-b,1977, 1978).

At the south end of the massif; near Nigde, an important study was Goncuoglu (1977) who identified gneiss and amphibolite of the Gumusdere Formation, marble-gneiss-quartzite alternations of the Kaleboynu Formation and marble of the Asigedigi Formation. These units are cut by metabasic rocks and the Uckapili Granodiorite, respectively.

Erkan (1980 a) suggested that the amphibolites in the massif have a sedimentary origin. He also concluded that the meta-sedimentary rocks

metamorphosed under high-amphibolite facies conditions around Akdagmadeni-Yozgat belong to the Middle Anatolia Massif (Erkan, 1980-b). Tulumen (1980), however, identified ten different petrographic and metamorphic facies ranging from muscovite-bearing schist to almandine-bearing gneiss in the same area. The degree of metamorphism increases from southwest to northeast with increasing anorthite content of the plagioclase from An8 to An26.

Another important study was carried out by Seymen(1981,82) on the Kirsehir terrain which is 50 km from the area of study. He identified gneiss, granulite and amphibolite schist of the Kalkanlidag Formation, marble-schist-gneiss alternations with interbanded quartzite of the Tamadag Formation, marble of the Bozcaldag Formation, gabbro in the Karakaya Ultramafite and granitoid in the Baranadag Pluton. He considered that the gabbro is tectonically overlying the meta-sedimentary units. He also determined greenschist and a transition zone amphibolite to granulite facies and four phases of deformation.

The sedimentology of the Tuz Golu Basin was studied by Yasar et al. (1982). They discovered granite pebbles in the Kartal Formation of Upper Cretaceous age. They also showed that the 150 km. length Sereflikochisar-Aksaray fault is an oblique-slip fault.

In 1984, Gorur et al. tried to interpret the events developed in the Tuz Golu Basin in terms of global tectonics. They pointed out that the Baranadag Pluton which initiated its intrusion during the Maastrichtian and continued into the Paleocene, shows the features of an Andean type continental arc. It was situated along the plutonic axis of the Sereflikochisar-Aksaray fault.

Seymen (1984) explained the geological evolution of the Kaman Group of meta-sedimentary rocks in the massif. He suggested that the Kaman Group was developed transgressively at an Atlantic type of continental margin. Then the Group was deformed and intruded by igneous rocks at a Pacific type of continental margin. .

Yaman stated that the basic and acidic igneous rocks show transition to each other (Yaman, 1985).

In 1987, Atabey et al. described schist and gneiss of the Kalkanlidag Formation, schist, marble, calc-schist, marble and amphibolite alternations of the Tamadag Formation, marble of the Bozcaldag Formation, and acidic-basic intrusive rocks of the Ortakoy granitoids.

Bayhan and Tolluoglu(1987) identified microcline bearing syenites, felsic vein rocks, and nepheline bearing syenites around Kirsehir.

II STRATIGRAPHY

The metasediments in the Middle Anatolia Massif, "MAM", are generally well-exposed both in the north, northeast, or south of the massif (Kirsehir, Akdagmadeni, Nigde) (Fig. 2). In the western part of the massif, they are almost non-existent due to being altered and covered by extensive Tertiary formations. In the studied area, gneisses can only be seen around the village of Seksenusagi

II.1 PALEOZOIC

II.1.1 Seksenusagi Formation

This formation is typically exposed near the village of Seksenusagi, and is mainly made of migmatitic gneiss, semipelitic and psammitic schist and gneisses with lesser quartzite, calcite marble, calc-silicate gneiss and amphibolite.

Fresh semipelitic and psammitic gneisses are mainly beige, brownish and varying tones of gray in colour with the altered surfaces being yellow and pale brownish. The gneisses occupy lower topography in the field due to being weathered easily. They occupy the cores of major anticlines (Appendix-1a, b).

The marble members, 20-30 m in thickness are made of metamorphosed limestones interbedded with quartzites, semipelites and psammite. The bedding in the quartzite and marble is almost parallel to the main foliation and the bed thicknesses range between 0.1 cm -7 cm and 3 cm - 1 m., respectively although it is recognised that these thicknesses will not be the original sedimentary values.

The bottom of the formation is nowhere seen while towards the top of the formation, the marble beds within the formation increase in proportion and the semipelitic and psammitic gneiss decrease. Fig. 3 shows the sequence and relationship between quartzite, marble and psammitic and semipelitic gneiss in Navruztepe. The formation which has a thickness of > 300 m is conformably overlain by the Gobektepe Formation with a transitional contact, the boundary being drawn by calcite marbles occupying >50% in the sequence.

II.1.2 Gobektepe Formation

This formation which typically occurs at Gobektepe mainly consists of calcite marble with lesser quartzite, semipelitic and psammitic gneiss, rare amphibolite and tremolite bearing gneiss. The migmatite and migmatitic gneisses have not been observed in the formation.

The marbles are medium-coarse grained (calcite crystals can reach up to 5 cm in length), fractured and often deformed. Semipelitic and psammitic gneiss levels occur at the bottom of the formation and become rarer upwards as marble becomes almost the sole lithology with rare quartzites or metacherts. The amphibolite with dark green(fresh) and brownish(altered) colours forms small lenses or thin layers(~5cm) between marble layers.

The marbles and quartzites vary in bedding between 5 cm- >1 m and 2 mm-24 cm, respectively. The thickness in the Ca-silicate bands ranges from 3 to 9 cm. Calcite is ubiquitious in the marble but in a few places dolomite is also found. Siliceous dolomite in which tremolite and actinolite formed has been seen only at the summit of Armutlutepe. The formation is > 500

m in thickness.

Neither the Seksenusagi nor the Gobektepe formation preserve way-up sedimentary structures to indicate the sequence order.

II.1.3 The age of metasediments

The sedimentation and metamorphic ages of the MAM metasediments are subject to differing views:

Kober(1931), Arni(1938), Leuchs(1943) and Blumenthal(1946) stated that the metasediments were Paleozoic or Precambrian in age. In contrast, Ketin (1955, 1959, 1963, 1966) postulated a Paleozoic-Mesozoic geosyncline metamorphosed by the Laramide orogeny. Brinkman (1971) suggested, on the basis of his observation on the Tauros mountains that the age of metamorphism was pre-Ordovician -Devonian. A pre-Mesozoic age for the metasediments is suggested by Seymen(1982) with respect to the relation of the Ankara melange of Jura-Campanian age to that of the metasediments. At the southernmost massif of Nigde, Goncuoglu(1977) accepted a Paleozoic age for the metamorphism.

From mica schist or gneiss and amphibolites, Erkan and Ataman(1981) obtained 69, 70 and 74 my. ages which probably correspond to the emplacement or cooling of the acidic igneous intrusions using K/Ar dating method.

Around Kirsehir, the isotopic ages of plutonism in the massif were studied by Ataman (1972). He recorded a 71 my. (i.e. Cretaceous) age to the Cefalikdag granodiorite using the Rb-Sr method. In agreement with this, acidic

rock pebbles were found in the Kartal formation of Upper Cretaceous age (Yasar et al.,1982).

There is no reliable age of sedimentation of the metasediments except they must pre-date 70-80 my. To determine the sedimentation age of the metasediments microfossils were separated from marble samples of the Seksenusagi Formation by treatment with acetic acid. The residue obtained contained a very low diversity polynomorph assemblage dominated by three species of the sphaeromorph acritarch Leiosphaeridia and also Lophosphaeriduim sp. Together with these were found possible graptolite fragments-questionably of Retiolites sp. The assemblages indicates a Cambrian to Devonian age.

The very low diversity assemblage is best attributed to a restricted circulation in a shelf environment in view of the existence of a coral. The lack of any spores in the sample would suggest deposition away from areas of sediment derived from a vegetated terrestrial environment.

The first certain macro fossil was discovered near Sirayalardagi in marble near the top of the Seksenusagi Formation. Although the sample was rather re-crystallised, Heliolitinae (Heliolitidae fam.) Paeckelmannophora sp can be recognised, which is Lower Silurian to Upper Devonian.

In conclusion, the acritarchs give a broad Cambrian to Devonian range, while the coral gives a range of Lower Sil urian to Upper Devonian. The more questionable attributions of a Silurian age for Reliolites sp and a Lower Dev onian age for Paeckelmannophora sp (Weissermel, 1939), are also consistent with a range of Silurian to Lower Devonian. The regional

metamorphism of metasediments must have taken place between the Devonian and the Upper Cretaceous. If the rifting in Anatolia, which started in Permo-Trias time and continued to the Lower Cretaceous (Sengor&Yilmaz, 1981), is taken into the consideration, the metamorphism would be Carboniferous-Permian (Hercynian?). The lack of pre-Upper Cretaceous formations in the massif show that the massif acted as a rigid block after the metamorphism

II.2 POST METAMORPHIC INTRUSIONS

The oldest igneous unit is the Ekecekdagi gabbro, cut by the granitoids as seen in the Ekecekdagi, followed by the hornblendite, hornblendediorite and granitoids. The hornblendites exposed in a limited area shows transition to the hornblende-diorites, and have not been seen with the granitoids. The biotite-hornblende granitoids cut the hornblende-diorites as is shown by fragmented diorite xenoliths (Photo 1) at the granitoid-diorite contact but as there are also small separate diorite intrusions into the granitoids e.g. in north of Sirayalardagi (Appendix-2), it seems as if the granitoids and diorites were intruded at the same time. The granitoids were later intruded by the microgranitoid and quartz-alkali syenite. The restricted occurence of the microgranites and quartz-alkali syenites do not allow determination of their relative order of intrusion.

The Ekecekdagi gabbro may be an allochthonous unit. The contact with the metamorphic rocks has not been seen. Similar rocks were named as Karakaya ultramafite of pre-Upper Maastrichtian age (Seymen, 1981) and of Upper Paleozoic age (Yasar et al.,1982) in the massif. However, Goncuoglu (1977) identified metagabbros which cut through the metasediments in Nigde, southern massif. In the area studied, only some

hornblende gabbro, rare banded gabbro and sheet dykes (Fig. 4) of the Ekecekdagi gabbro can be seen and the rest of the ophiolitic sequence such as peridotite and pillow lava have not been observed. On the basis of field evidence, it is not possible to determine whether the Ekecekdagi gabbro is allochthonous or autochthonous. In the geological map of the Ortakoy area (Appendix-1a), the gabbro is shown with the granitoids as Upper Cretaceous - Paleocene.

II.3 NEOGENE FORMATIONS

II.3.1 Pecenek Formation

This was named after the Pecenek valley by Yasar et al. (1982) and mainly consists of rhyolitic tuff; clay and sand with some gravels; and lacustrine limestone

The tuffs, vitric and rhyolitic, are white and yellowish cream and contain granitoid, diorite, marble gravels and hornblende-basalt. They are exposed near Kepir.

The limestones include clasts of the tuff and gastropoda fossils. They occur east of Ortakoy village.

Clay and sand are more widespread than both the tuff and the limestone. The red colour of the clay and sands, and the white colour of the tuffs are typical in distinguishing the formation in the field. These colours shows transition into each other depending on the relative proportion of the tuff or clay and sand.

Nonmarine sediments were deposited in a basin formed by block faulting in the Pliocene(Yasar et al.,1982).

II.3.2 Collovium

This only forms at the north side of the Ekecekdagi in relation with the development of the faults. Angular particles of the gabbros in the formation range from sand to block in size.

II.3.3 Alluvium

This occurs along the streams which flow off the granitoids. The alluvium contains rounded and poor-sorted, gravel, sand and clay which were derived from many lithologies, but the granitoids seem to be comparatively dominant.

Photo 1: Fragmented diorite (dark coloured) xenoliths within the granitoids (light coloured) , ENE Seksenusagi. Black colour on the picture refers some moss.

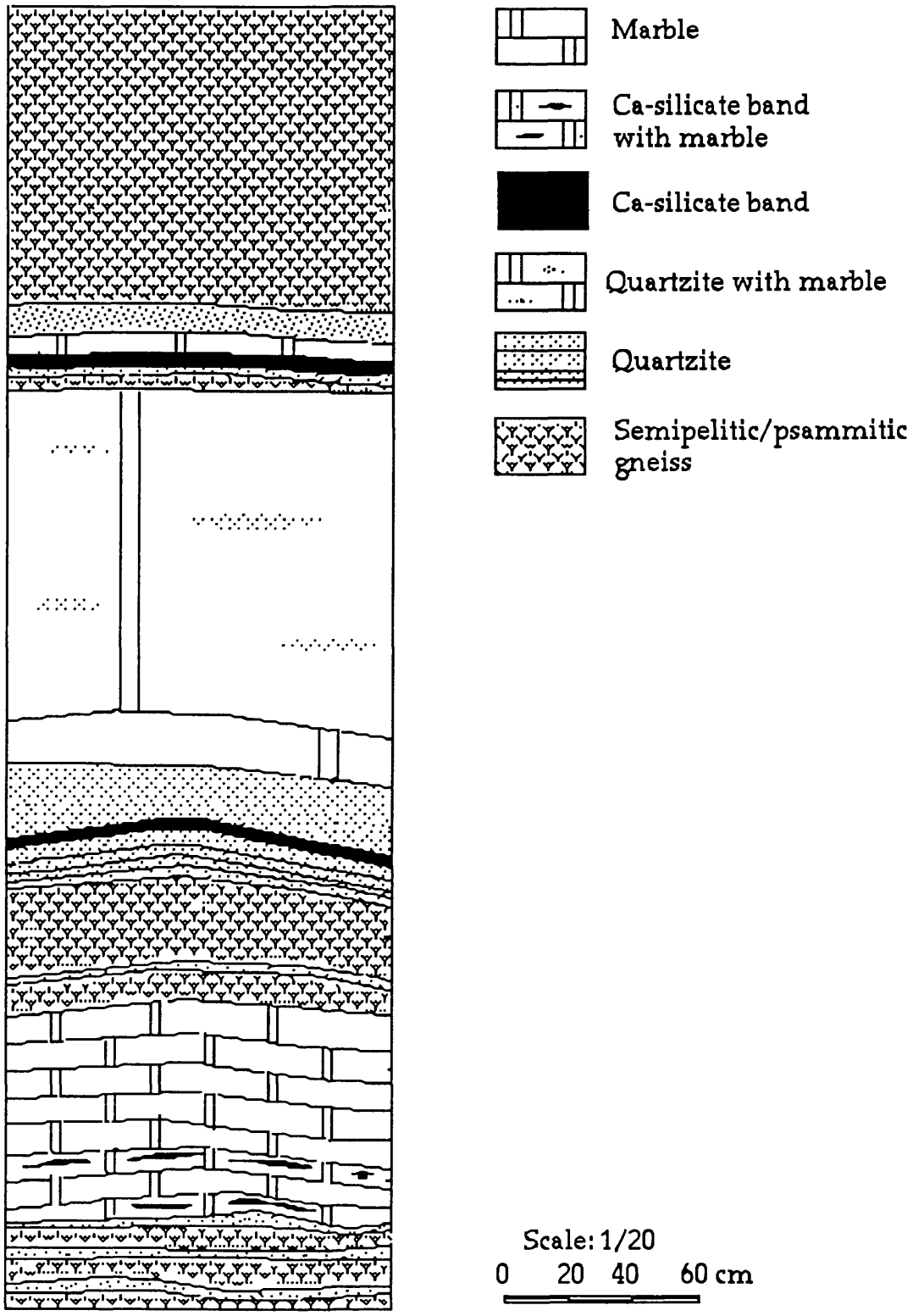

Figure 3: Stratigraphic column showing the intercalations of the marble, quartzite and Ca-silicate in the semipelitic and psammitic gneisses at the top of the Seksenusagi Formation, north side of the Navruz tepe.

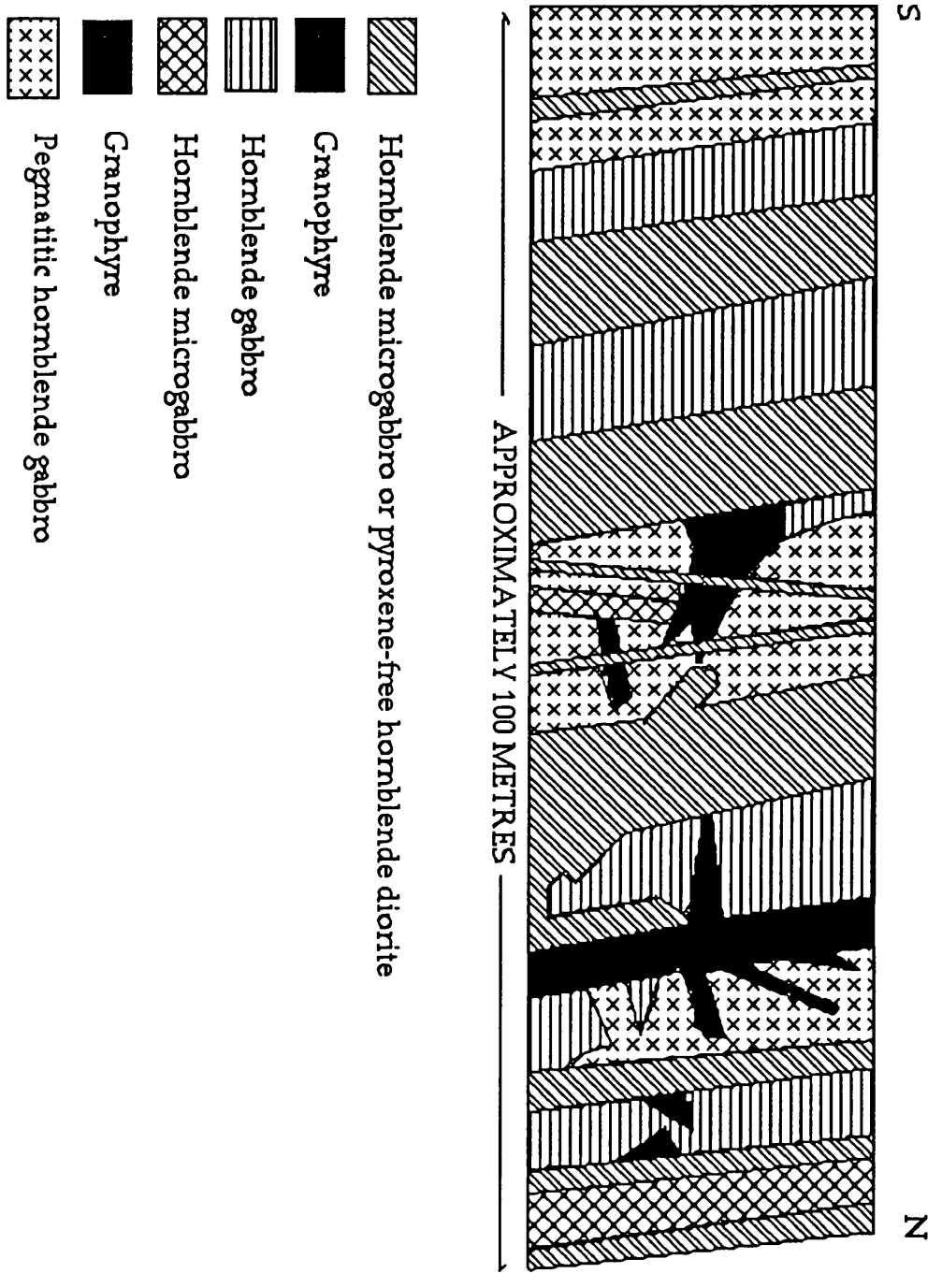

Figure 4: Schematic cross section of dyke sheets at the Ortakoy dam.

III PETROGRAPHY

III.1 PALEOZOIC

III.1.1. Seksenusagi Formation

This formation is mainly migmatitic gneiss, migmatitic granite, semi-pelitic and psammitic schist/gneiss with lesser calc-silicate gneiss, tremolite-bearing gneiss, amphibolite, quartzite and marble sometimes with chert. There is gradational contact between the Seksenusagi and the overlying Gobektepe formation. The typical outcrop of the unit occurs around the village of Seksenusagi. The bottom of the formation has not been seen anywhere..

III.1.1.1 Migmatitic gneiss and migmatitic granite

The migmatitic gneiss contains biotite, sillimanite fibrolite and ilmenite restite and granitic textured quartz, K-feldspar and plagioclase leucosome varying from a few mm. to a metre. This gneiss generally shows schollen (raft) structure, often exhibits deformation structure due to shearing; phlebitic (vein) structure possessing the paleosome traversed irregularly by vein-like neosomes; or stromatic (layered) structures (Menhert, 1968).

The muscovite-garnet-bearing granite and pegmatitic granite appear to be generated by migmatisation of metasediments. The migmatitic granite, the earlier formed migmatites in depth, pierce through the metasediments and occurs as veins.

The mineralogy of the migmatitic gneiss consists of perthitic K-feldspar (~45%), 0.15 to 3.1mm, much altered to sericite and muscovite;

quartz (~30%), 0.01 to 3.0 mm and oligoclase (~20%) which varies in An content from 23 % to 29 % (Fig. 5) being 0.3 to 0.07 mm. Myrmekite is sometimes present and light brown to reddish biotite (5%), often replaced by fibrolite sillimanite; ilmenite; and accessory rutile and zircon. The chemical compositions of feldspar, biotite and ilmenite are given in Table 1 and Table 2.

Using the two feldspars geothermometer of Haselton et al. (1983), 603°C temperature is determined at 4 kb (data in Table 1, Ort2 and Plg1).

In the late fractionate from migmatitic granite, K-feldspar(~40%), 0.55 to 0.1 mm., generally shows perthitic texture and is commonly altered to clay mineral or replaced by muscovite. Quartz (35%) and albite (20%) , 0.8 to 0.5 mm, are also present and quartz inclusions within garnet of composition Alm (81.58)*, Sps (15.67), Prp (2.09), Adr(0.66). The garnet is slightly zoned with a core relatively rich in Mn and the rim richer in Fe, due to fractionation (Hollister,1966 ; Atherton,1968 ; Miyashiro and Shido,1973 ; Tracy,1982). Gahnite; andalusite enclosed in its alteration products, sericite; schorl with strong pleochroism ranging from dark blue (no) to light blue (ne) and very rare ilmenite are also present.

Chemical analyses of muscovite, garnet and feldspars are given in Tables 3a and 3b.

* : The abbreviations for rock forming minerals are made according to Kretz (1983)

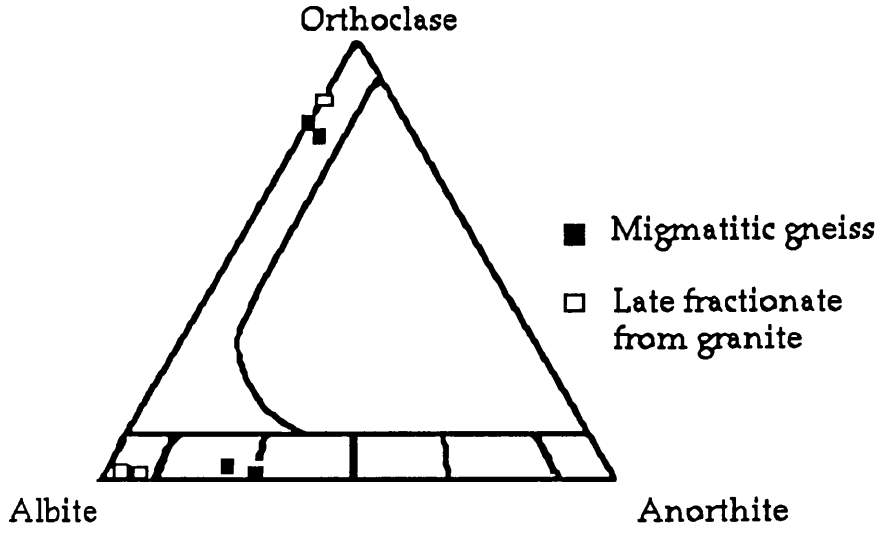

Figure 5: The composition of feldspars in the migmatitic gneiss and late fractionate from migmatitic granite

Table 1: Representative analyses of feldspars in the migmatitic gneiss

Sample (694-A)	Or(1)	Or(2)	Pl(1)	Pl(2)
SiO2	64.21	64.311	60.04	61.24
TiO2	0.06	0.16	0.00	0.02
Al2O3	18.71	18.92	24.54	23.72
FeO*	0.00	0.00	0.00	0.04
MgO	0.14	0.05	0.10	0.14
MnO	0.06	0.07	0.03	0.00
CaO	0.06	0.14	6.26	4.89
Na2O	2.01	1.9	8.20	8.61
K2O	13.46	3.85	0.22	0.37
Total	98.72	99.39	99.40	99.03
Formula based on 32 oxygens				
Si	11.92	11.87	10.77	10.98
Ti	0.01	0.02	0.00	0.00
Al	4.09	4.12	5.19	5.01
Fe^{2+}	0.00	0.00	0.00	0.01
Mg	0.04	0.01	0.03	0.04
Mn	0.01	0.01	0.01	0.00
Ca	0.12	0.03	1.20	0.94
Na	0.72	0.68	2.85	2.99
K	3.19	3.27	0.05	0.09
Mol % An	0.30	0.68	29.32	23.35

*: Fet is assumed as Fe^{2+}

Table 2: Representative analyses of biotite and ilmenite in the migmatitic gneiss

Sample	694-A (Bt)	737 (Ilm)
SiO2	35.02	0.15
TiO2	2.38	54.47
Al2O3	19.63	0.01
Fe2O3*	2.78	0.00
FeO	17.05	43.97
MgO	8.50	0.01
MnO	0.09	2.76
CaO	0.26	0.00
Na2O	0.48	-
K2O	8.48	-
Total	94.65	100.79
Formula based on 22 oxygens for biotite and 6 oxygens for ilmenite		
Si	5.36	0.01
Ti	0.27	2.04
Al	3.54	0.00
Fe^{3+}	0.36	0.00
Fe^{2+}	2.18	1.83
Mg	1.94	0.00
Mn	0.01	0.12
Ca	0.04	0.00
Na	0.14	-
K	1.65	-

* : $Fe^{2+}/(Fe^{2+} + Fe^{3+})$ is assumed 0.86 (Kretz , 1990)

Table 3a: Representative analyses of muscovite and garnet in the late fractionate from migmatitic granite

Sample (696)	Muscovite	Garnet	
SiO2	45.20	SiO2	36.16
TiO2	0.06	TiO2	0.00
Al2O3	36.83	Al2O3	20.79
Fe2O3^	0.19	Fe2O3*	2.13
MgO	0.10	FeO	35.57
MnO	0.00	MgO	0.51
CaO	0.07	MnO	6.68
Na2O	0.46	CaO	0.22
K2O	9.92	Cr2O3	0.02
Total	92.83	NiO	0.01
		Total	102.09
Formula based on 22 oxygens for muscovite and 24 oxygens for garnet			
Si	6.11	Si	5.87
Ti	0.01	Ti	0.00
Al	5.87	Al	3.98
Fe^{3+}	0.02	Fe^{3+}	0.26
Mg	0.02	Fe^{2+}	4.83
Mn	0.00	Mg	0.12
Ca	0.01	Mn	0.92
Na	0.12	Ca	0.04
K	1.71	Cr	0.00
		Ni	0.00

* : Fe+3 is calculated according to Drop, 1987

^ : Fet is assumed as Fe^{3+}

Table 3b: Representative analyses of feldspars in the late fractionate from migmatitic granite

Sample (696)	Pl (1)	Pl (2)	Or
SiO2	65.72	67.42	65.03
TiO2	0.06	0.02	0.00
Al2O3	21.08	20.05	18.83
FeO*	0.09	0.01	0.05
MgO	0.13	0.00	0.00
MnO	0.05	0.00	0.00
CaO	1.43	0.73	0.05
Na2O	10.95	11.14	1.41
K2O	0.11	0.17	14.70
Total	99.61	99.54	100.08
Formula based on 32 oxygens			
Si	11.60	11.85	11.93
Ti	0.01	0.00	0.00
Al	4.39	4.15	4.07
Fe^{2+}	0.01	0.00	0.01
Mg	0.03	0.00	0.00
Mn	0.01	0.00	0.00
Ca	0.27	0.14	0.01
Na	3.75	3.79	0.50
K	0.02	0.04	3.44
Mol % An	6.66	3.45	0.00

*: Fet is assumed as Fe^{2+}

III.1.1.2 Semipelites and psammites

These are generally fine grained with a medium to good foliation depending on the relative proportions of mica and sillimanite to quartz and feldspars. Quartz segregations vary from 0.1 to 1cm in length. In the hand specimen, fibrolite appears as white, curved patches, up to 0.2 mm in length. These gneisses are interbedded with quartzite, marble and amphibolite and cut by aplite and migmatitic granite.

The main constituents in these rocks are quartz (10-65%), plagioclase, (0-25%), K-feldspar (5-35), biotite (0-65%), muscovite (0-25%), sericite (0-80%), sillimanite (0-30%), chlorite and sometimes garnet (up to 5 %) in a lepidoblastic texture. These metasediments are occasionally cut by chlorite veins. The rocks have suffered sericitisation, chloritisation and tourmalinisation.

They contain quartz, 0.1 to 10 mm; sericite; light brown to reddish biotite, 0.05 to 0.44 mm, altered to chlorite, calcite, epidote and leucoxene; plagioclase varying in anorthite content from 2% to 23%, and 0.07 to 0.3 mm which is normally zoned and albite twinned, with myrmekite; orthoclase, 0.5 to 2.8 mm with perthitic texture; microcline which inverted from orthoclase (only in 287),1.1 to 1.4 mm; and muscovite formed as a secondary mineral from sericite is 0.4-0.5 mm. Fibrolite sillimanite is replaced by sericite and sometimes by small andalusite prisms. Garnet with a composition of Alm(68.35)*, Sps(22.74), Prp(6.79), Adr(2.12) is 0.1 to 0.5 mm, almost homogeneous, and is broken down to produce biotite.

* : The abbrevations for rock forming minerals are made according to Kretz (1983)

The chemical compositions of garnet and biotite are not eligible for using as a geothermometer with Ferry and Spear (1978) 's equation owing to having high Mn in the garnet and high Al^{VI} in the biotite. Tourmaline shows strong pleochroism varying from greenish yellow to yellow. Accessory apatite, zircon, sphene, rutile, picotite associated with magnetite, ilmenite and cassiterite in one sample (565) only are also present.

Retrograde metamorphism results in albite, sericite and chlorite forming from feldspars, sillimanite, biotite and garnet. Tourmalinisation is a common phenomenon in the rock showing these alterations and andalusite growth and is probably derived either from boron in the metasediments or from boron metasomatism caused by igneous activity.

Chemical analyses of garnet, feldspar and biotite are given in Tables 4 and 5.

Table 4: Representative analyses of garnet.

Sample (587)	Core	Rim
SiO2	36.26	36.59
TiO2	0.14	0.04
Al2O3	20.55	21.14
Fe2O3	1.82	0.58
FeO*	30.64	31.31
MgO	1.66	1.53
MnO	9.74	9.55
CaO	0.72	1.20
Total	101.53	101.94
Formula based on 24 oxygens		
Si	5.86	5.87
Ti	0.02	0.00
Al	3.92	4.00
Fe^{3+}	0.22	0.07
Fe^{2+}	4.12	4.20
Mg	0.40	0.37
Mn	1.33	1.30
Ca	0.12	0.21

* : Fe^{3+} is calculated according to Drop (1987).

Table 5: Representative analyses of feldspar and biotite.

Sample	287Pl (core)	287Pl (rim)	Bt(587)
SiO2	62.32	67.44	32.93
TiO2	0.00	0.09	3.67
Al2O3	24.23	19.67	20.34
Fe2O3*	-	-	3.31
FeO	0.00	0.00	20.33
MnO	0.05	0.00	0.41
MgO	0.19	0.05	4.12
CaO	4.85	0.33	0.03
Na2O	8.75	10.76	0.25
K2O	0.18	0.15	8.55
Total	100.57	98.49	93.94
Formula based on 32 oxygens for feldspar and 22 oxygens for biotite			
Si	10.98	11.93	5.19
Ti	0.00	0.01	0.44
Al	5.03	4.10	3.77
Fe^{3+}	-	-	0.44
Fe^{2+}	0.00	0.00	2.68
Mn	0.01	0.00	0.05
Mg	0.05	0.01	0.97
Ca	0.91	0.06	0.00
Na	2.99	3.69	0.07
K	0.04	0.03	1.72
An%	23.20	1.66	

* : $Fe^{2+}/(Fe^{2+} + Fe^{3+})$ is assumed 0.86(Kretz,1990).

III.1.1.3 Pelitic inclusions in the paragneissic granite

In the paragneissic granite, these are irregular elliptical clots, typically 12-15 cm in diameter (range 7 to 24 cm.) slightly schistose and mark of biotite, sillimanite, plagioclase, orthoclase, cordierite and garnet in order of abundance and with accessory magnetite, zircon, apatite and cassiterite. The texture ranges from nematoblastic to lepidoblastic with pressure shadows.

Biotite, 1.05 and 0.04 mm, has strong pleochroism from light to reddish brown with pleochroic haloes enclosing zircon, commonly associated with ilmenite and some chlorite replacement along its cleavage. Sillimanite, varying from prismatic to fibrolitic, generally replaced biotite. Albite-periclinic twinning is characteristic for plagioclase, 0.9 to 0.25 mm, ranging in anorthite content from 28% to 40%, sometime with myrmekitic texture. Cordierite formed by the breakdown of garnet and is itself considerably pinitised being 0.7 to 1.2 mm. K-feldspar, 1.25 to 0.5 mm, sometimes perthitic is also present and both feldspars have undergone sericitisation. The earliest recognisable mineral in the rock is garnet, Alm (72), Prp (21.55), Adr (4.64), Sps (1.69), Grs (0.06), Uv (0.06), varying from euhedral to anhedral depending on its replacement by cordierite, biotite, plagioclase, orthoclase and sillimanite which totally destroy inner inclusion trails of the garnet though some of quartz inclusions are preserved in it. Chemical zoning in the garnet is shown by enrichment of core in Mg and of rim in Fe and Mn (Fig. 6) owing to the homogenization and retrograde zoning which is characteristic of high grade metamorphism (Tracy et al.,1976; Woodsworth,1977; Yardley,1977a; Tracy,1982). Accessory magnetite, rounded zircon, apatite and very rare rounded cassiterite, in one sample (709) only are also present.

Table 6 shows modal mineralogical composition of the pelitic inclusion. The chemical analyses of garnet, cordierite, mica and feldspars are given in Tables 7, 8 and 9.

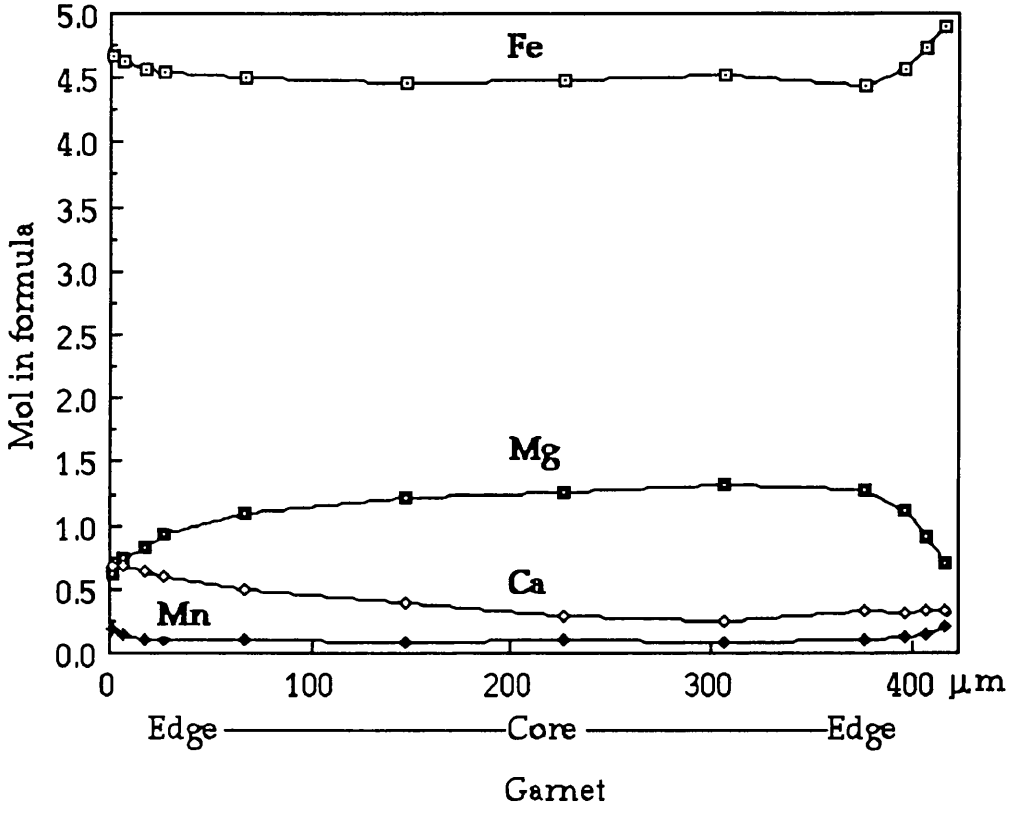

Figure 6 : Chemical zoning in garnet belong to the pelitic inclusion(340)

Table 6 : Modal mineralogical composition of the pelitic inclusion

Sample	712 (500points)*	340 (600 points)
Biotite	32.2±4	24.5±3.5
Sillimanite	11.0±2.8	34.0±3.9
Plagioclase	24.0±3.8	22±3.2
Cordierite	4.4±1.5	5.0±2.2
Orthoclase	5.2±2	5.0±2.2
Quartz	8.4±2.5	2.5±1.2
Garnet	3.0±2	2.5±1.2
Chlorite	3.4±2.2	3.0±1.2
Iron ore	8.4±2.5	1.5±1.0
Total	100.0	100.0

* : The ranges of mineral volumes in the samples are given with a 95 % confidence(Van der plas and Tobi,1965)

Table 7: Representative analyses of garnet and cordierite in the pelitic inclusion

Sample (340)	Grt (core)	Grt (rim)	Crd
SiO2	37.36	36.64	47.53
TiO2	0.01	0.01	0.00
Al2O3	21.48	20.68	32.69
Fe2O3*	0.59	0.99	0.00
FeO	33.43	33.42	11.84
MgO	5.39	2.64	6.19
MnO	0.78	1.34	0.27
CaO	1.66	3.94	0.05
Cr2O3	0.05	0.03	-
Na2O	-	-	0.21
K2O	-	-	0.03
Total	100.75	99.69	98.81
Formula based on 24 oxygens for garnet and 18 oxygens for cordierite			
Si	5.88	5.92	4.96
Ti	0.00	0.00	0.00
Al	3.99	3.94	4.02
Fe+3	0.07	0.12	0.00
Fe+2	4.39	4.51	1.03
Mg	1.27	0.64	0.96
Mn	0.10	0.18	0.02
Ca	0.28	0.68	0.01
Cr	0.01	0.00	-
Na	-	-	0.04
K	-	-	0.00

* : Fe+3 in garnet is calculated according to Drop (1987) and it is assumed as zero in cordierite.

Table 8: Representative analyses of micas in the pelitic inclusion

Sample	Bt (340)	Bt (708)	Ms (710)
SiO2	33.84	33.87	46.74
TiO2	1.57	3.20	1.05
Al2O3	20.97	19.42	33.37
Fe2O3*	3.19	3.48	1.59
FeO	19.60	21.36	0.00
MgO	6.36	5.45	1.39
MnO	0.05	0.07	0.00
CaO	0.00	0.03	0.05
Na2O	0.13	0.46	0.71
K2O	9.46	9.02	9.72
Total	95.17	96.36	94.62
Formula based on 22 oxygens			
Si	5.24	5.21	6.25
Ti	0.18	0.37	0.11
Al	3.83	3.52	5.26
Fe+3	0.41	0.4	0.00
Fe+2	2.54	2.75	0.18
Mg	1.47	1.25	0.28
Mn	0.01	0.01	0.00
Ca	0.00	0.00	0.01
Na	0.04	0.14	0.18
K	1.87	1.77	1.66

* : Fe+3 is calculated according to Drop, 1987 for biotite, and Fet is assumed as Fe^{3+} in muscovite.

Table 9 : Representative analyses of feldspars in the pelitic inclusion

Sample	Pl-2(710)	Pl-3(710)	Or (340)
SiO2	60.25	56.84	63.81
TiO2	0.02	0.00	0.19
Al2O3	24.37	26.70	18.69
FeO*	0.16	0.26	0.12
MgO	0.00	0.04	0.04
MnO	0.01	0.00	0.00
CaO	6.10	8.55	0.00
Na2O	8.45	6.96	1.65
K2O	0.20	0.03	14.17
Total	99.56	99.38	98.67
Formula based on 32 oxygens			
Si	10.79	10.25	11.87
Ti	0.00	0.00	0.03
Al	5.15	5.68	4.10
Fe	0.02	0.04	0.02
Mg	0.00	0.01	0.01
Mn	0.00	0.00	0.00
Ca	1.17	1.65	0.00
Na	2.93	2.44	0.60
K	0.05	0.08	3.36
Mol % An	28.19	40.34	0.00

* : Fe is assumed as FeO

To determine the PT conditions of last equilibrium for the pelitic inclusions, the garnet-biotite geothermometer and the compositions of phases in the garnet-biotite-sillimanite-plagioclase-cordierite-quartz assemblage for geobarometry are used. In geothermometry calculations, the composition of garnet in contact with biotite is taken as these minerals are in equilibrium each other although they might show retrogressive effect. The biotite-garnet pairs taken are for biotite low in Ti and for garnet low in Ca, and Mg as recommended by Ferry and Spear (1978). The temperature for biotite (Table 8, bt 340) and garnet (Table 7) in equilibrium in the pelitic inclusion at 4 kb. is 681.8±50 ^{o}C as determined by using Ferry and Spear's(1978) experimental calibration. For the geobarometry calculation, a computer program(Powell and Holland,1988), using Holland and Powell(1990)'s updated thermodynamic dataset with uncertainties and correlations is used. The pressure calculated for possible reactions at 600^{o}C and 575^{o}C with 95% confidence are given in Table 10.

Table 10 : The geobarometer calculations on the pelitic inclusion using the method of Powell and Holland (1988) and the dataset of Holland and Powell(1990)

---

a.Suggested T=575°C for H2O =1

reactions	P(T)	sd	dP/dT	ln K
1. ann+crd=alm+east+3qtz	2.8	0.8	0.0073	-0.302
2.alm+6phl+12sil=ann+5east+4crd	3.5	1.32	0.0087	2.156
3.3alm+3east+9qtz=2phl+ann+3fcrd	3.7	0.81	0.0078	-2.738

av	sd	sig
3.96	0.30	1.10

b.Suggested T=600°C for H2O=1

reactions	P(T)	sd	dP/dT	lnK
1. 2phl+4sil=2east+crd+qtz	4.0	1.98	0.0092	0.618
2. ann+crd=alm+east+3qtz	3.3	0.82	0.0076	-0.148
3. 3alm+3east+9qtz=2phl+ann+3fcrd	4.1	0.83	0.0082	-3.201

av	sd	sig
4.17	0.29	1.06

III.1.1.4 Marble

This is poor to well bedded depending on the recrystallisation and varies in thickness from 3 cm to 1 metre. Calcite marble is a dominant rock type in the unit although dolomite bearing calcite marble is sometimes exposed. Semipelitic and/or siliceous layers containing biotite, muscovite, plagioclase, quartz, and sometimes opaque iron ore are also developed. The transition from marble to quartzite is often seen in varying stages. The mineralogy mainly consists of carbonate minerals (95%), predominantly calcite and very rare dolomite, showing twinning, 0.25 to 0.025 mm., minor muscovite; dark and light brown biotite, generally altered to chlorite; plagioclase; quartz and iron ore in a granoblastic texture.

III.1.1.5 Ca-silicate gneiss/schist

This is made of tremolite-actinolite (10-20%) showing weak pleochroism in tones of pale green,2.9 to 0.02 mm.; quartz (0-75%) and diopside (0-25%) being 1.3 to 0.12 mm with granoblastic or nematoblastic texture depending on the relative proportions of quartz to tremolite and diopside. Accessory clinozoisite(0.2 to 0.05 mm.) associated with tremolite-actinolite, garnet, rutile, zircon , apatite and opaque iron ore are also present

III.1.1.6 Metabasic vein in marble

In one place only, within the marble situated within the Seksenusagi Formation is a ~10 cm thick basic vein. It is folded altogether with the host rock. Feldspar and ferromagnesian minerals, pyroxene and/ or amphibole in the rock are considerably altered to sericite and chlorite. Porphyritic

texture with a weak flow foliation is still preserved. It is often cut cross by chlorite, calcite and opaque iron veins and is a metabasic dyke.

III.1. 2 Gobektepe Formation

This mainly consists of marble intercalated with quartzite, semipelitic and psammitic gneiss, rare amphibolite and tremolite bearing schist or gneiss. At the bottom of the formation pelitic and semipelitic gneisses are often exposed. Marble becomes the major lithological rock unit towards the top of the formation and occasionally contains metachert.

III.1.2.1 Semipelitic and psammitic gneiss

These are often at the bottom of the formation with the alternation of amphibolite, tremolite bearing gneiss, quartzite, and marble becoming dominant towards the top of the unit. The main rock forming minerals are quartz (35%), biotite (30%) and feldspars (35%) with granoblastic texture.

The mineralogy consists of quartz, 0.67 to 0.01 mm; biotite, 0.28 to 0.02 mm, showing strong pleochroism from reddish brown to light brown, generally replaced by chlorite along the cleavage; feldspars, 0.03 to 0.35 mm. is generally altered sericite, muscovite. Plagioclase occasionally shows polysynthetic twinning which indicates An_{40} . Accessory zircon, apatite, rutile and opaque iron ore are also present.

III.1.2.2 Amphibolite

This is poor to well foliated with or without crenulation cleavage and medium to coarse grained. It is often cross cut by quartz, calcite and epidote veins. It is mainly magnesio-hornblende, plagioclase, biotite, diopside and quartz in a nematoblastic texture. The modal composition of amphibolite is given in Table 11.

Bluish green to light green hornblende, 0.02 to 3.4 mm., is the dominant rock forming mineral. It is occasionally converted to biotite, showing strong pleochroism from dark to light brown and altered to chlorite. The plagioclase is 0.05 to 0.7 mm and replaced by sericite. Albite twinning is characteristic and the anorthite content ranges from 94 to 48. Quartz, diopside, accessory sphene and apatite are also present. Chemical analyses of plagioclases, pyroxene and amphiboles are given in Table 12.

To determine the origin of the An-rich (92 %) and An-poor (48 %) plagioclase, the feldspar was investigated by means of Scanning Electron Microscope (SEM). A back scattered image shows (Photo 2) that the andesine does not show transition to the anorthite. The image also shows that the andesine is situated both at the centre and the edge of the anorthite either as relict or later replacing feldspar. The andesine at the centre of the plagioclase is not related to cracks nor is the marginal andesine clearly related to the edges of the anorthite. It is therefore not certain which of the two compositions is earliest which is latest. If the andesine is earliest then Ca-enrichment has occured possibly related to the breakdown of diopside (23 % CaO) to hornblende (12 % CaO). If the andesine is the latest then Na movement into the anorthite has occured.

Table 11: Modal composition of the amphibolite

Minerals*	684 (1000 points)
Hornblende	54.1±3.2
Plagioclase	43.0±3.2
Sphene	1.7±0.5
Quartz	0.6±0.5
Biotite	0.6±0.5

* The range of mineral volumes in the sample are given with a 95% confidence(Van der plas and Tobi, 1965)

III.1.2.3 Tremolite bearing schist or gneiss

This is situated near marble and quartzite. Crenulation cleavage formed by crystallisation of actinolitic hornblende is generally well developed in addition to the main foliation. Tremolite is a main constituent accompanied by minor amount of magnesio-hornblende and ilmenite in the rock.

Representative analyses of the amphiboles are given in Table 13.

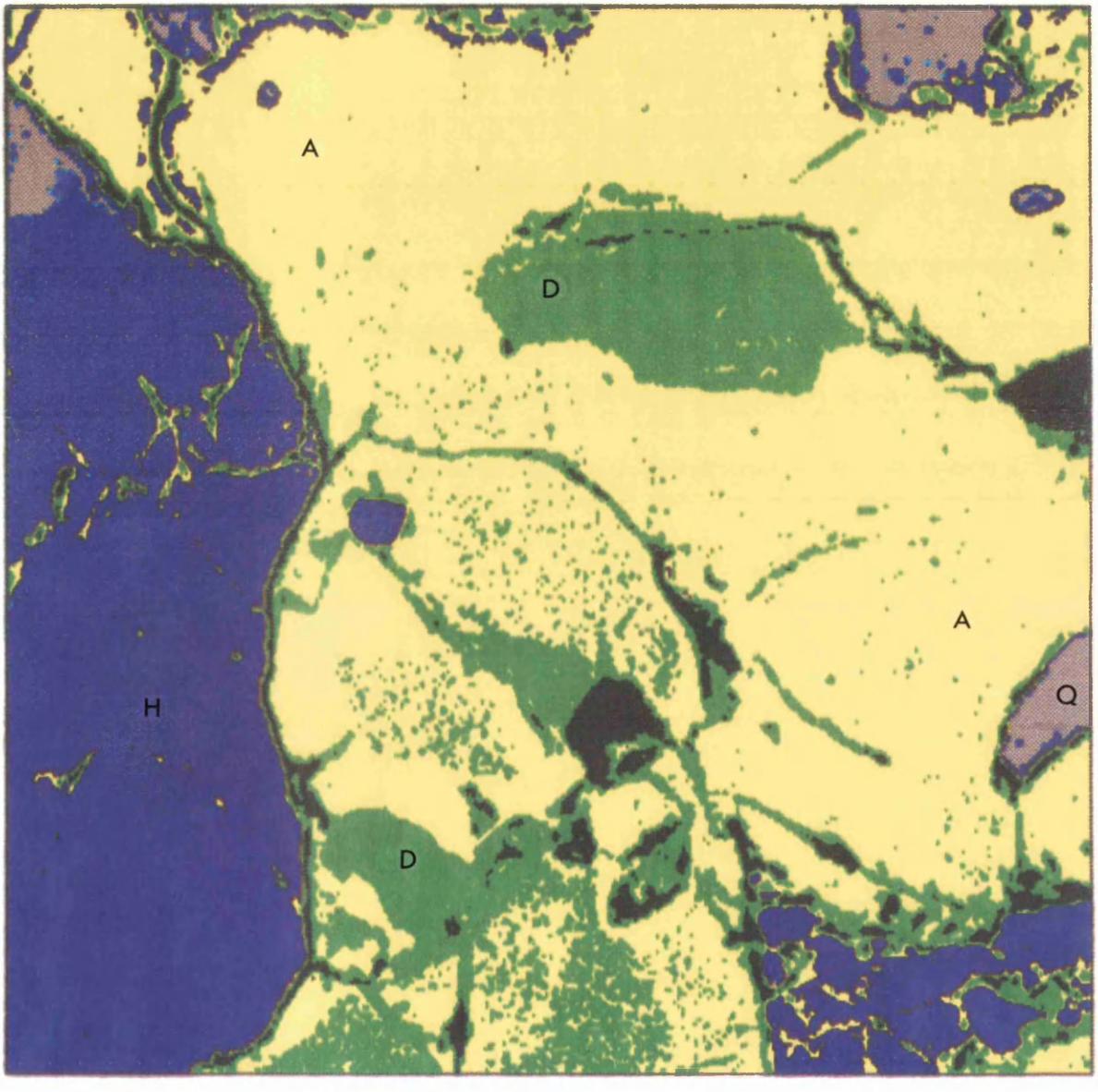

Photo 2: Back scattered image of the amphibolite(689) (H: hornblende, A: anorthite, D: andesine, Q: opaque.

Table 12 : Chemical compositions of the amphibolite plagioclases, pyroxene and amphibole.

Sample(685)	Pl 1	Pl 2	Cpx	Hbl*
SiO2	44.21	46.01	51.15	46.08
TiO2	0.04	0.03	0.12	0.99
Al2O3	35.68	34.94	0.42	7.94
Fe2O3^	0.00	0.00	0.00	20.30
FeO"	0.12	0.17	15.22	0.00
MnO	0.00	0.00	0.37	0.20
MgO	0.11	0.24	9.24	9.34
CaO	19.11	18.17	23.35	12.01
Na2O	0.62	1.36	0.13	1.13
K2O	0.01	0.06	0.01	0.88
Total	99.90	100.98	100.01	98.86

Formula calculated based on 32 oxygens for plagioclase 6 oxygens for pyroxene.

Si	8.18	8.40	1.97	6.91
Ti	0.00	0.00	0.00	0.00
Al	7.78	7.52	0.02	1.40
Fe^{3+}	0.00	0.00	0.04	2.55
Fe^{2+}	0.02	0.03	0.45	0.00
Mn	0.00	0.00	0.01	0.03
Mg	0.03	0.06	0.53	2.09
Ca	3.79	3.56	0.96	1.93
Na	0.22	0.48	0.01	0.33
K	0.00	0.01	0.00	0.17
An	94.36	87.74		

* : Magnesio-hornblende(Leake, 1978).

^ : Fe^{3+} is calculated according to Drop(1987)

" : Fet is assumed as Fe^{2+} in plagioclase

Table 12 : continues

Sample (689)	Pl(1)	Pl(2)	Cpx	Hbl*
SiO2	56.72	44.88	53.22	40.01
TiO2	0.02	0.04	0.07	0.45
Al2O3	27.97	34.47	0.83	14.26
Fe2O3	0.00	0.00	0.70	14.13
FeO	0.17	0.14	7.27	0.00
MnO	0.00	0.00	0.24	0.26
MgO	0.00	0.09	13.11	10.72
CaO	9.98	18.78	24.32	12.24
Na2O	5.79	0.83	0.56	2.89
K2O	0.04	0.03	0.00	0.46
Total	100.69	99.26	100.32	95.42

Formula based on 32 oxygens for plagioclase, 6 for pyroxene and 23 for amphiboles.

Si	10.10	8.34	1.98	6.12
Ti	0.00	0.00	0.00	0.05
Al	5.87	7.55	0.04	2.57
Fe^{3+}	0.00	0.00	0.02	1.81
Fe^{2+}	0.02	0.02	0.23	0.00
Mn	0.00	0.00	0.01	0.03
Mg	0.00	0.02	0.73	2.44
Ca	1.90	3.74	0.97	2.01
Na	2.00	0.30	0.04	0.85
K	0.01	0.01	0.00	0.09
An	48.59	92.34		

* : Magnesio-hastingsite (Leake, 1978)

Table 13: Representative analyses of amphiboles

Sample(548)	Tr(1)	Tr(2)	Act	Hrb[1]
SiO2	56.61	57.52	56.52	53.36
TiO2	0.00	0.05	0.03	0.36
Al2O3	0.45	0.40	1.23	4.25
FeO	3.43	3.34	4.56 Fe2O3*	4.82
MnO	0.16	0.09	0.18	1.19
MgO	22.84	22.93	23.00	21.36
CaO	11.42	11.76	10.35	11.76
Na2O	0.17	0.19	0.32	0.96
K2O	0.09	0.04	0.03	0.00
Cr2O3	0.22	0.08	0.21	0.10
Total	95.38	96.4	96.43	98.16
Formula calculated on the basis of 23 oxygens				
Si	7.94	7.96	7.86	7.45
Ti	0.00	0.00	0.00	0.04
Al	0.07	0.07	0.20	0.70
Fe^{2+}	0.40	0.39	0.53 Fe^{3+}	0.56
Mn	0.02	0.01	0.02	0.02
Mg	4.78	4.73	4.77	4.45
Ca	1.72	1.74	1.54	1.76
Na	0.05	0.05	0.09	0.26
K	0.02	0.01	0.01	0.00
Cr	0.02	0.01	0.02	0.01

1 : Actinolitic Hornblende (Leake, 1978)

* : Fe^{3+} is calculated according to Drop,1987.

Table 13: Cont.

Sample (527)	Hbl[1]	Tr	Hbl[2]
SiO2	53.36	54.63	47.73
TiO2	0.36	0.06	0.58
Al2O3	4.25	1.77	6.96
Fe2O3*	0.00	2.92	6.29
FeO	4.82	2.55	8.04
MnO	0.19	0.08	0.65
MgO	21.36	20.79	13.18
CaO	11.76	11.72	11.08
Na2O	0.96	0.53	0.58
K2O	0.00	0.02	0.23
Cr2O3	0.10	0.42	0.14
Total	97.16	95.49	95.45
Formula calculated on the basis of 23 oxygens			
Si	7.45	7.73	7.07
Ti	0.04	0.01	0.06
Al	0.70	0.29	1.22
Fe^{3+}	0.00	0.31	0.69
Fe^{2+}	0.56	0.30	0.98
Mn	0.02	0.01	0.08
Mg	4.45	4.38	2.91
Ca	1.76	1.78	1.76
Na	0.26	0.15	0.17
K	0.00	0.00	0.04
Cr	0.01	0.05	0.02

[1] : Actinolitic hornblende , [2] : Magnesio-hornblende(Leake, 1978)

* : Fe^{3+} is calculated according to Drop,1987.

III.1.2.4 Marble

This is poor to well bedded depending on the extent of recrystallisation. Bedding thickness varies from 5 cm to around 1 m. Various siliceous, pelitic layers and local lenses or thin (~5 cm thickness) bands of calc-silicates occur. Calcite (95%) is the main rock forming mineral in the marble and accompanies diopside(35%), orthoclase (10%), quartz (10%) scapolite (5%) and plagioclase (5%) in the impure marble.

In addition to the calcite, 0.8 to 0.15 mm, the semipelitic and siliceous varieties contain diopside, 0.5 to 0.08 mm, displaying polysynthetic twinning and partly altered to chlorite. Cloudy orthoclase, 0.8 to 0.3 mm and quartz are present. Plagioclase often shows albite twinning. Scapolite, accessory sphene, zircon and opaque iron ore also present in granoblastic texture.

Quartzite occurs within the marble and semipelites as lenses, laminae or beds. Metachert is seen especially towards the top of the Gobektepe Formation. The quartzite is layered, 2 mm to 24 cm with quartz as the main constituent with minor amounts of chlorite, calcite, sericite, opaque iron ore, apatite and plagioclase in a granoblastic texture. Some semipelite layers also occur.

III.2 CONTACT METAMORPHIC ROCKS

These are best developed in the calcerous xenoliths within the igneous rocks. The main minerals are hedenbergite-diopside, 0.2 to 1.1 mm, showing multiple twinning; wollastonite, 0.5 to 2.0 mm; albite twinned plagioclase(An_{72}), 0.05 to 0.12 mm, has albite twinning; orthoclase, 0.15 to 0.55 mm; corundum, 0.03 to 0.1 mm; garnet and hercynite in the hornfelsic texture.

The semipelitic rocks next to the granitoids also suffered from contact metamorphism. The main constituents in these rocks are light brown to reddish biotite, 0.3-0.8 mm; cordierite which is considerably altered to sericite, biotite, chlorite and opaque iron ore and is 0.27 to 2.4 mm; andesine (~43 % An) with albite twinning, 0.7-0.9 mm and orthoclase, 0.6-0.9mm.

The chemical composition of pyroxenes, feldspars ,corundum, spinel , biotites and tourmaline are given in Tables 14 and 15.

III.2.1 Paragneissic granite

This is a massive, fine to medium grained rock including pelitic inclusions and, calcareous xenoliths, all intruded by granite. Major constituents are quartz(35%), cordierite(25%), biotite(15%), plagioclase(10%) and orthoclase(10%) in granoblastic texture.

It consists of quartz, 0.1 to 0.55 mm; cordierite being 0.3 to 4.2 mm and replaced by muscovite, biotite and sillimanite. The plagioclase, 0.25 to 1.6 mm, with albite twinning and myrmekitic texture has a reversely zoned structure with marginal andesine, and central oligoclase. The light brown to reddish biotite is replaced by sillimanite and muscovite and has zircon

inclusions. Orthoclase, 0.4 to 1.9 mm, containing biotite, quartz and sillimanite as inclusions, is altered to sericite-muscovite. A little garnet is also present. Representative analyses of feldspars, garnet, biotite and cordierite are given in Tables 16 and 17. The calcareous xenolith contains diopside, anorthite which are given in Table 17, and sphene.

The compositions of garnet and biotite in the paragneissic granite (Table 17) are suitable to calculate their last equilibrated temperature so that by using Ferry and Spear(1978)'s calibration 533±50°C temperature is determined at 4 kb. The two feldspars geothermometer(Haselton et al., 1983) also gives almost same result, 526°C, for the same pressure(data in Table 16, Or and Pl 3).

A variety with pinitised cordierite located at 92437 lat. and 85729 long. contains quartz(40%), 0.1 to 0.4 mm, showing undulose extinction; plagioclase with albite twinning(30%), 0.3 to 2 mm; cordierite(15%), 0.3 to 1 mm, was replaced by pinite; orthoclase(10%), 0.2 to 0.55 mm; brown biotite (5%), 0.1 to 0.4 mm, including zircon with pleochroic halo ; minor garnet that was replaced by cordierite; sillimanite and opaque iron ore in a granoblastic texture. The analyses of garnet, plagioclase and biotite are presented in Table 18.

As the composition of the biotite is not suitable for Ferry and Spear(1978)'s garnet-biotite geothermometer due to its high Al^{VI} content, Perchuk and Lavrent'eva (1983)'s calibration with Aranovich et al.'s(1988) correction for Ca-Mg and Fe-Mg isomorphism in garnet and aluminium content in biotite gave 506±14°C as the temperature of equilibrium for garnet and biotite at the same pressure, 4 kb.

Table 14: The chemical compositions of the contact metamorphic clinopyroxene, feldspars, corundum and spinel.

Sample	Di(259)	Pl(259)	Or(259)	Crn(691)	Hc(691)	Hd(245)
SiO2	50.87	48.83	63.57	0.11	0.04	48.22
TiO2	0.09	0.00	0.08	0.06	0.09	0.01
Al2O3	0.71	31.97	18.52	100.17	56.59	0.11
Fe2O3*	1.72	0.00	0.00	0.43	3.43	0.64
FeO	12.73	0.06	0.08	0.00	41.17	23.79
MnO	0.67	0.00	0.00	0.01	0.25	3.05
MgO	8.85	0.11	0.08	0.11	1.30	0.82
CaO	23.71	14.55	0.31	0.00	0.01	22.11
Na2O	0.34	2.96	0.67	-	-	0.37
K2O	0.04	0.10	15.36	-	-	-
Cr2O3	0.00	-	-	0.10	0.29	-
Total	99.73	98.58	98.67	100.99	103.17	99.13

Formula based on 6 oxygens for pyroxene and corundum, 32 for feldspars and spinel.

Si	1.97	9.03	11.89	0.00	0.01	1.99
Ti	0.00	0.00	0.01	0.00	0.02	0.00
Al	0.03	6.97	4.08	3.98	15.12	0.00
Fe^{3+}	0.05	0.00	0.00	0.01	0.58	0.02
Fe^{2+}	0.41	0.01	0.01	-	7.73	0.82
Mn	0.02	0.00	0.00		0.05	0.11
Mg	0.51	0.03	0.02	0.01	0.44	0.05
Ca	0.98	2.88	0.06	0.00	0.00	0.98
Na	0.02	1.06	0.24	-	-	0.03
K	0.00	0.02	3.66	-	-	
Cr	0.00	-	-	0.05	0.05	-
An		72.73				

* : Fe2O3 is calculated according to Drop(1987) for spinel and pyroxene; assumed as '0' in plagioclase, and for corundum FeO^t is assumed as Fe2O3.

Table 15: Representative analyses of the semipelitic hornfels feldspar, biotite and tourmaline.

Sample	Pl (294)	Or(294)	Or(564)	Bt(564)	Bt(294)	Tur(294)
SiO2	57.05	64.92	64.74	34.15	34.37	33.5
TiO2	0.03	0.10	0.04	3.95	2.50	0.85
Al2O3	26.91	18.35	18.13	20.35	21.93	33.96
Fe2O3*	0.00	0.00	0.00	2.86	2.69	0.00
FeO	0.04	0.07	0.02	17.55	16.56	7.44
MnO	0.00	0.00	0.00	0.17	0.14	0.02
MgO	0.04	0.00	0.05	7.36	6.95	5.52
CaO	8.93	0.05	0.00	0.07	0.00	1.49
Na2O	6.42	1.57	0.53	0.22	0.34	1.73
K2O	0.27	14.77	15.84	9.69	9.96	0.12
Total	99.69	99.83	99.35	96.37	95.44	84.63

Formula based on 32 oxygens for feldspars 22 oxygens for biotite 24.5 oxygens for tourmaline

Si	10.26	11.98	12.00	5.18	5.23	7.07
Ti	0.00	0.01	0.00	0.45	0.28	0.14
Al	5.70	3.98	3.96	3.63	3.93	4.22
Fe^{3+}	0.00	0.00	0.00	0.36	0.34	0.00
Fe^{2+}	0.06	0.01	0.00	2.23	2.11	1.31
Mn	0.00	0.00	0.00	0.02	0.02	0.00
Mg	0.01	0.00	0.00	1.66	1.57	1.74
Ca	1.72	0.02	0.00	0.01	0.00	0.34
Na	2.24	0.55	0.19	0.07	0.10	0.71
K	0.06	3.46	3.75	1.87	1.93	0.03
An%	42.78	0.00				

* : $Fe^{2+}/(Fe^{2+} + Fe^{3+})$ is assumed 0.86 (Kretz, 1990) for biotite, and Fet is assumed as Fe^{2+}in plagioclase and tourmaline

Table 16: Analyses of the feldspars from paragneissic granite.

Sample (705)	Or	Pl 1(core)	Pl2(rim)	Pl 3
SiO2	64.62	60.99	58.04	58.88
TiO2	0.17	0.00	0.05	0.00
Al2O3	18.60	24.39	26.18	26.22
FeO*	0.12	0.00	0.06	0.00
MnO	0.00	0.00	0.00	0.06
MgO	0.03	0.08	0.14	0.00
CaO	0.10	5.55	7.32	7.75
Na2O	1.52	8.29	7.30	7.24
K2O	14.07	0.24	0.23	0.24
Total	99.23	99.54	99.32	100.39
Formula based on 32 oxygens				
Si	11.93	10.85	10.44	10.47
Ti	0.02	0.00	0.01	0.00
Al	4.05	5.11	5.55	5.50
Fe	0.02	0.00	0.01	0.00
Mn	0.00	0.00	0.00	0.01
Mg	0.01	0.02	0.04	0.00
Ca	0.02	1.06	1.41	1.48
Na	0.54	2.86	2.54	2.50
K	3.31	0.05	0.05	0.05
An	0.49	26.66	35.20	36.67

* : Fet is assumed as Fe^{2+}

Table 17: Chemical compositions of garnet, biotite, and cordierite from the paragneissic granite; and diopside and plagioclase from the calcareous xenolith.

Sample (705)	Grt	Bt	Crd	Di	Pl
SiO2	36.92	34.52	48.39	52.36	43.88
TiO2	0.04	1.87	0.01	0.16	0.04
Al2O3	21.00	20.50	33.28	0.66	36.02
Fe2O3*	0.55	2.92	0.00	0.35	0.00
FeO	33.42	17.93	10.58	8.93	0.04
MnO	5.28	0.10	0.47	0.14	0.00
MgO	2.31	7.58	7.03	12.53	0.09
CaO	1.57	0.00	0.02	24.15	19.47
Na2O	0.00	0.24	0.19	0.18	0.35
K2O	0.00	9.29	0.02	-	0.02
Cr2O3	0.08	0.00	0.00	-	-
Total	101.17	95.107	99.99	99.46	99.91

Formula based on 24 oxygens for garnet 22 for biotite, 18 for cordierite, 6 for pyroxene and 32 for plagioclase.

Si	5.93	5.54	4.96	1.97	8.11
Ti	0.00	0.23	0.00	0.00	0.00
Al	3.98	3.88	4.02	0.03	7.85
Fe^{3+}	0.07	0.39	0.00	0.01	0.00
Fe^{2+}	4.49	2.41	0.91	0.28	0.01
Mn	0.72	0.01	0.04	0.00	0.00
Mg	0.55	1.81	1.07	0.70	0.03
Ca	0.27	0.00	0.00	0.98	3.86
Na	0.00	0.07	0.04	0.01	0.13
K	0.00	1.90	0.00	0.00	0.00
Cr	0.01	0.00	0.00		
An					96.74

* : Fe^{3+} is calculated according to Drop (1987) for garnet, $Fe^{2+}/(Fe^{2+} + Fe^{3+})$ is assumed as 0.86 for biotite(Kretz,1990) and in cordierite and plagioclase, Fe_t is assumed as Fe^{2+}.

Table 18 : Analyses of plagioclase, garnet and biotite from the pinitised variety of the paragneissic granite.

Sample (437)	Pl	Bt	Grt(core)	Grt(rim)
SiO2	58.76	35.81	36.50	37.69
TiO2	0.00	3.61	0.04	0.04
Al2O3	25.18	19.88	20.65	21.34
Fe2O3*	0.00	2.98	1.40	0.00
FeO	0.02	18.35	35.16	36.45
MnO	0.00	0.19	4.10	4.72
MgO	0.13	7.81	1.86	2.01
CaO	7.06	0.00	1.14	1.43
Na2O	7.36	0.17	-	-
K2O	-	0.31	9.54	-
Total	98.82	98.34	100.85	103.68
Formula based on 32 oxygens for feldspars and 22 for biotite.				
Si	10.58	5.31	5.92	5.91
Ti	0.00	0.40	0.00	0.00
Al	5.35	3.47	3.94	3.94
Fe^{3+}	0.00	2.27	0.17	0.00
Fe^{2+}	0.00	0.37	4.75	4.78
Mn	0.00	0.02	0.56	0.62
Mg	0.03	1.72	0.45	0.47
Ca	1.36	0.00	0.20	0.24
Na	2.57	0.05	-	-
K	0.07	1.81	-	-
An	34			

* : Fe^{3+} is determined according to Drop(1987) in garnet, Fe^{2+}/Fet is assumed as 0.86 for biotite (Kretz, 1990), and in plagioclase, Fet is assumed as Fe^{2+}

III.3 POST METAMORPHIC INTRUSIONS

III.3.1 Ekecekdagi gabbro

It is medium to coarse grained and cut by granitic intrusions of the Ortakoy Pluton or by granophyre. Hornblende gabbro is main rock type of this formation containing very rare banded gabbro. The dyke sheets are sometimes seen as in the dam of Bozkir, where the igneous sequence starts with pegmatitic hornblende gabbro which has been intruded by granophyre. It continues with hornblende microgabbro, then hornblende gabbro and granophyre. The dyke sheets end with hornblende microgabbro or pyroxene-free hornblende diorite. The main rock forming minerals are hornblende, plagioclase, diopside and sometimes biotite in a poikilitic texture.

Hornblende is a dominant mineral, pleochroic from yellowish green to bluish and is occasionally altered to calcite and chlorite. Occasionally a diopside relict is seen in the centre of magnesio-hornblende or actinolitic hornblende which replace the pyroxene. The poikilitic texture is dominated by the existence of the large hornblendes which include plagioclase, biotite and very rare quartz. The plagioclase ranges in anorthite content from 75 up to 93 and often shows albite and carlsbad albite combined twinning. It is altered to calcite and epidote. Both plagioclase and hornblende display the results of tension and polygonisation with mortar texture . Minor biotite, hercynite, ilmenite, zircon and apatite are also present. Modal compositions of the Ekecekdagi gabbro and chemical analyses of amphiboles, plagioclases, diopside, and ilmenite are given in Tables 19, 20, 21 and 22.

Table 19 : Modal compositions of the Ekecekdagi gabbro.

Sample	57-F(1000 points)	556(1200 points)	308(1200 points)
Hornblende*	49.2±2.8	48.9±3	46.0±3.0
Clinopyroxene	33.4±3.1	15.7±2.2	10.8±1.9
Plagioclase	17.4±2.2	34.4±2.8	42.6±3.0
Opaque iron ore	0.00	0.8±0.12	0.4±0.06

* : The range of mineral volumes are given with a 95% confidence(Van der plas and Tobi, 1965)

In the granophyre, plagioclase generally shows albite twinning and slight normal zoning is detected from the core of feldspar in which it is 44 % An at the core and 37 % An at the rim. Quartz occurs either in the feldspar sometimes with granophyric texture, or as large phenocrysts. Light green to dark green amphibole, tschermakite (Table 22), and biotite showing strong pleochroism from yellow to brown sporadically occur with opaque iron ore and apatite in a granophyric texture with myrmekite .

The amphibole-plagioclase geothermometer (Blundy and Holland, 1990) was used to determine the crystallization temperature of the Ekecek-dagi gabbro. Two different samples were chosen; one from the dyke sheet (424) and the one from the normal gabbro (377). The dyke sheet yields a lower crystallization temperature, 763± 75 °C, than the normal gabbros, 846°C± 75. Crystallization pressure is assumed as 5 kb for the geothermometer calculations.

Table 20: The chemical compositions of the Ekecekdagi gabbro amphiboles .

Sample	556[2]	307[1]	375(core)[2]	375(rim)[2]	424[2]
SiO2	44.89	48.87	48.43	43.78	46.34
TiO2	0.15	0.64	0.47	2.12	0.22
Al2O3	12.84	5.68	6.56	9.76	10.13
Fe2O3*	1.79	8.00	0.00	1.15	7.73
FeO	7.21	5.52	16.22	15.59	0.00
MnO	0.20	0.20	0.28	0.21	0.09
MgO	15.72	14.71	12.27	11.44	16.80
CaO	11.30	11.23	11.22	10.69	12.50
Na2O	1.67	0.96	0.80	1.26	1.48
K2O	0.16	0.07	0.10	0.22	0.21
Cr2O3	0.00	0.12	0.10	0.09	0.13
Total	96.32	96.00	96.45	96.31	95.63
Formula calculated on the basis of 23 oxygens					
Si	6.52	7.14	7.21	6.60	6.76
Ti	0.02	0.07	0.05	0.24	0.02
Al	2.20	0.98	1.15	1.73	1.74
Fe^{3+}	0.19	0.86	0.00	0.13	0.94
Fe^{2+}	0.85	0.66	2.02	1.96	0.00
Mn	0.02	0.02	0.03	0.03	0.01
Mg	3.40	3.20	2.72	2.56	3.65
Ca	1.76	1.76	1.79	1.73	1.95
Na	0.47	0.27	0.23	0.37	0.42
K	0.03	0.01	0.02	0.04	0.04
Cr	0.00	0.01	0.01	0.01	0.02

[1] : Actinolitic hornblende, [2] : Magnesio-hornblende (Leake, 1978)

* : Fe^{3+} is calculated according to Drop, 1987.

Table 20 continues

Sample	377[1]	377[3]	215[1]	125[1]	424[4]
SiO2	50.30	43.19	50.06	50.46	51.92
TiO2	0.10	1.90	0.24	0.19	0.12
Al2O3	3.70	10.41	5.05	4.28	3.29
Fe2O3*	0.00	12.41	0.61	6.03	3.68
FeO	14.19	0.00	13.94	7.52	7.53
MnO	0.31	0.25	0.36	0.26	0.26
MgO	14.39	14.22	14.64	4.81	16.30
CaO	11.96	11.43	10.87	12.33	11.98
Na2O	0.40	1.94	0.75	0.64	0.40
K2O	0.02	0.56	0.09	0.07	0.04
Cr2O3	0.05	0.00	0.01	0.06	0.02
Total	95.43	96.38	96.78	96.65	95.54
Formula calculated on the basis of 23 oxygens					
Si	7.45	6.44	7.35	7.33	7.55
Ti	0.01	0.21	0.03	0.02	0.01
Al	0.65	1.83	0.87	0.73	0.56
Fe^{3+}	0.00	1.55	0.07	0.65	0.40
Fe^{2+}	1.76	0.00	1.78	0.90	0.91
Mn	0.04	0.03	0.04	0.03	0.03
Mg	3.18	3.16	3.20	3.25	3.53
Ca	1.90	1.83	1.71	1.92	1.87
Na	0.11	0.56	0.21	0.18	0.11
K	0.00	0.11	0.02	0.01	0.01
Cr	0.18	0.00	0.00	0.01	0.00

[3] : Magnesio-hastingsitic-hornblende, [4] : Actinolite (Leake , 1978)

* : Fe^{3+} is calculated according to Drop, 1987.

Table 21 : Representative analyses of the Ekecekdagi gabbro plagioclases .

Sample	215	424	377
SiO2	44.12	46.12	48.57
TiO2	0.00	0.05	0.03
Al2O3	35.32	33.87	31.57
FeO*	0.08	0.24	0.51
MnO	0.07	0.04	0.09
MgO	0.26	0.16	0.20
CaO	18.70	16.92	15.55
Na2O	0.78	1.85	2.65
K2O	0.00	0.05	0.12
Total	99.41	99.30	99.30
Formula calculated on the basis of 32 oxygens			
Si	8.21	8.54	8.97
Ti	0.00	0.01	0.00
Al	7.74	7.39	6.87
Fe^{2+}	0.01	0.04	0.08
Mn	0.01	0.01	0.01
Mg	0.07	0.04	0.05
Ca	3.72	3.35	3.08
Na	0.28	0.66	0.95
K	0.00	0.01	0.03
An	92.96	83.24	75.94

* : FeO^t is assumed as Fe^{2+}

Table 22: Analyses of the gabbro pyroxene and ilmenite, and granophyre hornblende in the Ekecekdagi gabbro .

Sample	215(di)	424(di)	307(ilm)	423(hbl)^
SiO2	51.01	52.99	0.18	40.00
TiO2	0.23	0.08	52.57	0.67
Al2O3	1.49	0.46	0.04	11.64
Fe2O3*	1.74	0.00	0.00	15.75
FeO	9.07	7.18	43.36	8.65
MnO	0.39	0.26	4.33	0.57
MgO	12.90	14.31	0.25	6.32
CaO	21.76	23.53	0.12	9.70
Na2O	0.20	0.19	0.00	1.68
K2O	0.01	0.00	0.00	0.22
Cr2O3	0.16	0.00	0.16	0.02
Total	99.08	99.00	101.01	95.22
Formula calculated on the basis of 6 oxygens for pyroxene and ilmenite.				
Si	1.94	1.98	0.01	6.22
Ti	0.01	0.00	1.97	0.08
Al	0.07	0.00	0.00	2.13
Fe^{3+}	0.05	0.00	0.00	1.77
Fe^{2+}	0.29	0.23	1.81	1.08
Mn	0.01	0.01	0.18	0.07
Mg	0.73	0.78	0.02	1.46
Ca	0.89	0.94	0.01	1.62
Na	0.01	0.01	0.00	0.50
K	0.00	0.00	0.00	0.04
Cr	0.01	0.00	0.00	0.00

*: Fe^{3+} is calculated according to Drop, 1987.

^ : Tschermakite (Leake, 1978)

III.3.2 Hornblende diorite

This is mainly made of hornblende diorite, quartz-diorite and rare hornblende gabbro cut by diorite-porphyry, pyroxene-hornblendite, microdiorite and granitoid intrusions. The main minerals are plagioclase, hornblende, quartz and sometimes biotite in a hypidiomorphic granular or poikilitic texture. Modal compositions of hornblende diorite are given in Table 23. Late quartz, feldspars and epidote fill miarolitic cavities. Between marble and the hornblende diorite, narrow metasomatic zones developed, either as haematite bands (few cm thick), or Ca-silicate mineral associations, garnet, tremolite and diopside. The hornblende diorite is much smaller and more dark coloured than the Ekecekdagi gabbro and has more geochemical and petrographic variation and occupies lower topographic levels. Some intrusions have plagioclase with high anorthite content; An_{81}, (Table 24, sample 600), whereas others are lower e.g. sample 585 (Table 24),An_{30}. Granitoids are usually near the hornblende diorite.

Table 23: Modal compositions of the hornblende diorite.

Minerals*	48(1200 points)	388(1000 points)	371(1200 points)
Plagioclase	54.8±3.2	32.1±3.0	49.7±3.0
Hornblende	20.4±2.3	67.3±3.0	15.4±2.2
Quartz	9.8±1.2	0.3	12.5±2.0
Ortoclase	0.0	0.0	0.0
Microcline	2.3	0.0	0.0
Biotite	12.0±2.0	0.0	22.3±2.5
Sphene	0.0	0.3	0.0

* : The range of mineral volumes are given with a 95% confidence(Van der plas and Tobi, 1965)

The hornblende, 0.02 to 5.25 mm, has strong pleochroism from light to dark green, sometimes bluish green and is occasionally twinned and zoned with an edenitic- or actinolitic-hornblende core and a magnesio-hastingsitic- or magnesio-hornblende-rich rim(Table 25). As it includes the plagioclase and biotite crystals, a poikilitic texture is present. The light to reddish brown biotite, 0.5 to 2.66 mm, replaces hornblende and commonly altered to chlorite. Alteration of the hornblende produces chlorite, calcite and epidote. The plagioclase is abundantly albite twinned , normally well zoned, and contains the hornblende as inclusions. Saussuritisation of the plagioclase results chlorite, calcite, and epidote. Sphene occurs in the biotite. Cataclasis is sometimes dominant with breaking and twinning of hornblende; inversion of orthoclase to microcline; kinking of biotite, and exhibiting undulose extinction in quartz. Minor zircon and apatite are also present.

The chemical compositions of plagioclase and hornblende rims enable the crystallisation temperature to be calculated using the Blundy and Holland's (1990) amphibole-plagioclase geothermometer. Almost the same two temperatures,839 and 849±75 ^{o}C , were determined from two different samples, 605 and 388, at 5 kb assumed pressure.

The chemical compositions of plagioclases and amphiboles are given in Tables 24 and 25.

III.3.3 Hornblendite

This is coarse grained (approximately 1cm) and shows transition to the hornblende diorite. The main minerals are hornblende, chiefly edenitic-hornblende and some magnesian hornblende, that are partly altered to chlorite which is associated with the muscovite and hercynite forming patches in the host mineral. Minor anorthite (An_{91}), haematite and ilmenite are present with a granular or poikilitic texture.

The chemical compositions of amphiboles and spinel are given in Table 26.

Table 24: Analyses of plagioclases in the hornblende diorite.

Sample	388(rim)	388(core)	585(1)	585(2)
SiO2	55.56	44.92	60.29	56.43
TiO2	0.30	0.00	0.04	0.00
Al2O3	27.66	33.95	24.37	27.02
FeO*	0.23	0.31	0.41	0.44
MnO	0.02	0.01	0.02	0.00
MgO	0.07	0.17	0.05	0.09
CaO	9.83	17.90	6.13	9.44
Na2O	6.00	1.52	7.00	5.89
K2O	0.26	0.15	1.40	0.55
Total	99.66	98.93	99.71	99.86
Formula based on 32 oxygens				
Si	10.04	8.39	10.81	10.18
Ti	0.00	0.00	0.01	0.00
Al	5.89	7.48	5.15	5.75
Fe^{2+}	0.04	0.05	0.06	0.07
Mn	0.00	0.00	0.00	0.00
Mg	0.02	0.05	0.01	0.02
Ca	1.90	3.58	1.18	1.83
Na	2.10	0.55	2.43	2.06
K	0.06	0.03	0.32	0.13
An	46.79	86.06	30.02	45.52

* : FeO^t is assumed as Fe^{2+}

Table 24 continues

Sample	315	605	600
SiO2	53.53	61.95	46.89
TiO2	0.04	0.00	0.03
Al2O3	26.91	23.39	32.55
FeO*	1.83	0.19	0.77
MnO	0.03	0.00	0.01
MgO	0.14	0.05	0.27
CaO	11.11	5.21	16.57
Na2O	5.42	7.88	2.10
K2O	0.43	0.60	0.03
Total	99.44	99.28	99.22
Formula based on 32 oxygens			
Si	9.84	7.94	8.71
Ti	0.01	0.00	0.00
Al	5.83	3.53	7.13
Fe^{2+}	0.28	0.02	0.12
Mn	0.01	0.00	0.00
Mg	0.04	0.01	0.07
Ca	2.19	0.72	3.30
Na	1.93	1.96	0.76
K	0.10	0.10	0.01
An	51.90	25.90	81.08

* : FeO^t is assumed as FeO

Table 25: Chemical analyses of the hornblende diorite amphiboles

Sample No	605(core)[1]	605(rim)[2]	600[3]	315[4]
SiO2	44.21	43.43	50.06	48.23
TiO2	1.91	1.92	0.18	0.37
Fe2O3*	12.75	11.84	8.11	14.82
FeO	0.00	0.00	7.62	0.00
MnO	0.24	0.13	0.42	0.21
MgO	14.34	14.99	13.49	12.61
CaO	11.26	11.25	11.85	11.78
Na2O	1.64	1.99	0.67	0.84
K2O	0.53	0.55	0.23	0.48
Total	96.44	96.12	96.50	96.25
Formula based on 23 formula for amphiboles				
Si	6.58	6.47	7.31	7.49
Ti	0.21	0.22	0.02	0.04
Al	1.68	1.74	0.67	1.25
Fe^{3+}	1.59	1.47	0.89	1.92
Fe^{2+}	0.00	0.00	0.93	0.00
Mn	0.03	0.02	0.05	0.02
Mg	3.18	3.33	2.99	2.92
Ca	1.79	1.79	1.89	1.96
Na	0.47	0.57	0.19	0.25
K	0.10	0.10	0.04	0.09

1 : Edenitic-hornblende 2 : Magnesio-hastingsitic-hornblende
3 : Actinolitic-hornblende 4 : Tremolitic-hornblende (Leake,1978)
* : Fe^{3+} is calculated according to Drop, 1987.

Table 25 continues

Sample	315[5]	388(core)[3]	388(rim)[6]
SiO2	52.13	50.30	43.75
TiO2	0.09	0.15	0.90
Al2O3	3.09	3.58	9.71
Fe2O3*	3.69	6.78	3.81
FeO	8.71	6.51	0.41
MnO	0.26	0.31	0.40
MgO	15.30	14.10	11.56
CaO	12.33	12.02	11.02
Na2O	0.45	0.84	1.57
K2O	0.15	0.36	0.82
Total	96.2	95.48	94.32
Formula based on 23 oxygens for amphiboles			
Si	7.58	7.42	6.56
Ti	0.01	0.02	0.10
Al	0.53	0.63	1.71
Fe^{3+}	0.40	0.74	1.51
Fe^{2+}	1.05	0.79	0.05
Mn	0.03	0.04	0.05
Mg	3.32	3.10	2.58
Ca	1.92	1.90	1.77
Na	0.13	0.24	0.46
K	0.03	0.07	0.15

5 : Actinolite 6 : Magnesio-hornblende

* : Fe^{3+} is calculated according to Drop, 1987.

Table 26 : Analyses of calcic amphiboles and spinel in hornblendite

Minerals	Hbl[1]	Hbl[2]	Act	Spl
SiO2	43.62	44.06	53.51	0.12
TiO2	1.45	0.53	0.20	-
Al2O3	12.57	11.77	3.16	58.15
Fe2O3*	2.20	1.80	0.00	3.27
FeO	8.08	8.27	11.94	25.98
MnO	0.24	0.07	0.43	0.26
MgO	15.24	15.35	16.36	10.38
CaO	11.00	11.05	11.74	0.02
Na2O	1.61	1.44	0.57	-
K2O	0.28	0.52	0.02	-
Total	96.29	94.86	97.93	98.18
Formula based on 23 oxygens for amphiboles and 32 for spinel.				
Si	6.38	6.51	7.65	0.03
Ti	0.16	0.06	0.02	-
Al	2.17	2.05	0.53	15.18
Fe^{3+}	0.24	0.20	0.00	0.54
Fe^{2+}	0.98	1.02	1.43	4.77
Mn	0.03	0.01	0.05	0.05
Mg	3.32	3.38	3.49	3.43
Ca	1.72	1.75	1.80	0.00
Na	0.46	0.42	0.16	-
K	0.05	0.10	0.01	-

1 : Edenitic hornblende , 2 : Magnesian hornblende(Leake, 1978).

* : Fe^{3+} is calculated according to Drop(1987).

III.3. 4 Biotite-hornblende granitoid

This is intruded into the Ekecekdagi gabbro and the hornblende diorite and cut by its aplite and granophyre. It is the commonest igneous rock in the area of study and ranges from granite to tonalite, and sometimes to quartz-monzonite. The main minerals are quartz, plagioclase, orthoclase, biotite, and hornblende in a hypidiomorphic granular, symplectite or mortar texture.

The plagioclase, 0.16 mm to 2.3 cm but occasionally 5.5 cm in length, is albite and albite-pericline twinned with slight normal zoning. It has myrmekitic texture, contains biotite as inclusions and is altered to the sericite and epidote owing to the saussuritisation. The orthoclase, 0.5 mm to 5cm, is carlsbad twinned and perthitic. The biotite has strong pleochroism from light to dark green, rarely the tones of brown, is 0.12 to 2 mm, and contains zircon and allanite as inclusions. It is altered to chlorite along its cleavages. The hornblende, 0.03 to 1.0 mm, is commonly replaced by biotite and shows strong pleochroism light to dark green sometimes bluish green. Anhedral quartz is 0.1 to 4 mm. Cataclastic movements were widespread with tension gashes, undulose extinction in feldspars, formation of microcline from orthoclase, wrapping of biotite around feldspars and polygonisation of quartz. The modal composition of the granitiod and the chemical compositions of the feldspars, biotite and hornblende are given in Tables 27 and 28.

Table 27 : The modal composition of the biotite-hornblende granitoid.

Sample no	559	367
Quartz*	36.3±2.9	26.6±2.7
Plagioclase	30.4±2.8	37.7±3.0
Orthoclase	21.8±2.5	19.1±2.3
Biotite	8.8±1.5	16.5±2.2
Hornblende	2.7±1	

* : The range of mineral volumes are given with a 95% confidence(Van der plas and Tobi, 1965)

A typical xenolith in the biotite-hornblende granitoid contains plagioclase(40%), hornblende(25%), orthoclase(10%), quartz(10%) and biotite(15) in porphyritic or poikilitic texture. The plagioclase, 1.5 to 0.08 mm, displays albite and albite-pericline twinning and oscillatory zoning with a labradorite, ($An_{50.24}$) rich core and an oligoclase, ($An_{27.82}$)rim. It includes abundant hornblende and biotite as inclusions, and is altered to the sericite and epidote. The hornblende, 0.15 to 0.65 mm, is simply twinned and exhibits strong pleochroism from yellowish to dark green. The brown biotite, 0.05 to 0.6 mm, formed at the edge of the hornblende by replacement. Both biotite and hornblende are altered to chlorite. A cloudy appearance is characteristic of the orthoclase, 2.5 to 3.0 mm. The quartz is 0.2 to 0.8 mm. Accessory zircon and apatite are present.

The analyses of xenolith feldspars, hornblende and biotite in the xenolith are given in Table 29.

III.3.5 Microgranite

This is composed of about 65 % orthoclase, 20 % quartz, 10 % plagioclase and 5 % biotite, allanite, and opaque iron ore in a hypidiomorphic granular texture.

The orthoclase, 0.4 to 1.3 mm, often shows carlsbad twinning and perthitic texture. Albite twinning is seen in the plagioclase which is 0.25 to 1.25 mm. Normal zoning with an oligoclase rich core, An_{22}, and albitic rim, An_5 is present. Both feldspars are altered to clay minerals. Myrmekitic texture is developed between the two feldspars. Minor biotite, 0.1 to 1.1 mm, shows strong pleochroism from light to dark brown and is associated with opaque iron ore. Allanite is also present.

The chemical compositions of microgranite orthoclase, plagioclase, biotite and allanite are given in Table 30.

Table 28: The chemical compositions of the granitoid feldspars, biotites and hornblende.

Sample no	291(pl)	573(bt)	439(bt)	439(pl)	439(or)	573(pl)	573(hbl)[1]
SiO2	57.77	34.64	34.44	62.26	64.47	58.99	42.24
TiO2	0.06	3.44	3.74	0.00	0.03	0.04	1.10
Al2O3	26.39	19.32	17.12	23.26	18.33	25.14	7.36
Fe2O3*	0.00	4.17	4.87	0.00	0.00	0.00	18.45^
FeO	0.09	16.67	19.50	0.04	0.00	0.27	2.69
MnO	0.05	0.21	0.31	0.00	0.08	0.02	1.37
MgO	0.20	6.90	6.15	0.12	0.03	0.00	9.37
CaO	8.06	0.00	0.02	4.95	0.07	6.96	10.50
Na2O	6.86	0.56	0.07	8.87	1.45	7.36	1.56
K2O	0.14	9.15	9.38	0.36	14.47	0.57	0.83
Total	99.62	95.06	95.60	99.86	98.93	99.35	95.50
Formula based on 32 oxygens for feldspars and 22 for biotite.							
Si	10.37	5.32	5.38	11.04	11.95	10.62	6.49
Ti	0.01	0.39	0.44	0.00	0.00	0.00	0.13
Al	5.58	3.50	3.15	4.86	4.01	5.33	1.33
Fe^{3+}	0.00	0.54	0.64	0.00	0.00	0.00	2.04
Fe^{2+}	0.01	2.14	2.55	0.01	0.00	0.04	0.33
Mn	0.01	0.03	0.04	0.00	0.01	0.00	0.18
Mg	0.05	1.58	1.43	0.03	0.01	0.00	2.14
Ca	1.55	0.00	0.00	0.94	0.01	1.34	1.73
Na	2.39	0.17	0.02	3.05	0.52	2.56	0.46
K	0.03	1.79	1.87	0.08	3.42	0.13	0.16
An	39.04			23.09		33.25	

* : $Fe^{2+}/(Fe^{2+} + Fe^{3+})$ is assumed 0.80 for biotite, and FeO^t is assumed as Fe^{2+} for feldspars.

^ : Fe2O3 is calculated according to Drop, 1987.

[1] : Magnesio-hornblende

Table 29: The chemical composition of the xenolith feldspars, hornblende and biotite.

Sample(558)	Pl(core)	Pl(rim)	Or	Hrb	Bt
SiO2	55.69	61.34	65.53	46.47	35.81
TiO2	0.02	0.00	0.00	0.55	3.63
Al2O3	28.07	23.86	18.44	4.84	13.88
Fe2O3*	0.00	0.00	0.00	9.52^	5.00
FeO	0.08	0.09	0.10	12.41	19.96
MnO	0.02	0.00	0.00	0.77	0.42
MgO	0.10	0.09	0.05	9.05	8.50
CaO	10.63	5.82	0.01	11.05	0.02
Na2O	5.71	8.00	2.01	0.90	0.08
K2O	0.18	0.51	13.93	0.40	9.24
Total	100.50	99.71	100.07	95.96	96.53
Formula based on 32 oxygens for feldspars, 23 for biotite and 22 for biotite					
Si	9.98	10.93	11.99	7.11	5.53
Ti	0.00	0.00	0.00	0.06	0.42
Al	5.93	5.01	3.98	0.87	2.53
Fe^{3+}	0.00	0.00	0.00	1.07	0.64
Fe^{2+}	0.01	0.01	0.01	1.55	2.54
Mn	0.00	0.00	0.00	0.10	0.05
Mg	0.02	0.02	0.01	2.06	1.96
Ca	2.04	1.11	0.00	1.81	0.00
Na	1.98	2.76	0.71	0.27	0.02
K	0.04	1.12	3.25	0.08	1.82
An	50.24	27.82			

* : $Fe^{2+}/(Fe^{2+} + Fe^{3+})$ is assumed 0.80 for biotite, and FeO^t is assumed as FeO in feldspars.

^ : Fe^{3+} is calculated according to Drop(1987).

Table 30: The analyses of the microgranite feldspars, biotite and allanite.

Sample(744)	Pl(core)	Pl(rim)	Bt	Or	Ep
SiO2	61.89	67.42	36.76	65.78	27.75
TiO2	0.01	0.06	4.66	0.00	0.45
Al2O3	23.10	20.53	13.23	17.92	11.02
Fe2O3*	0.00	0.00	4.64	0.00	0.00
FeO	0.29	0.08	18.58	0.07	14.94
MnO	0.01	0.00	0.91	0.04	0.23
MgO	0.14	0.20	8.91	0.01	0.67
CaO	4.67	1.19	0.01	0.00	9.61
Na2O	8.69	10.97	0.21	0.59	0.33
K2O	0.35	0.25	9.53	15.94	-
Total	99.15	100.70	97.44	100.35	65.00
Formula based on 32 oxygens for feldspars, 22 for biotite and 12 for epidote.					
Si	11.06	11.73	5.63	12.07	3.33
Ti	0.00	0.01	0.54	0.00	0.04
Al	4.87	4.21	2.39	3.87	1.56
Fe^{3+}	0.00	0.00	0.59	0.00	0.00
Fe^{2+}	0.04	0.01	2.38	0.01	1.50
Mn	0.00	0.00	0.12	0.01	0.02
Mg	0.03	0.05	2.03	0.00	0.12
Ca	0.89	0.22	0.00	0.00	1.24
Na	3.01	3.70	0.06	0.21	0.08
K	0.08	0.06	1.86	3.73	-
An	22.36	5.52			

* : FeO^t is assumed as FeO in feldspars and epidote, Fe^{2+}/Fe^t is assumed 0.80 for biotite.

III.3.6 Quartz-alkali syenite

This is mainly a quartz-alkali syenite with minor alkali syenite and alkali granite . The main minerals are albite, orthoclase and plagioclase in hypidiomorphic or allotriomorphic granular texture depending on the relative proportions of plagioclase or else there is mortar texture. Modal compositions are given in Table 31.

Table 31: Modal compositions of the quartz-alkali syenite(634) and alkali syenite(637)

Minerals	634 (800 points)	637(1200 points)
Albite	35.5±3.2	60.6±3
Orthoclase	46.8±3.3	34.2±2.9
Quartz	15.2±2.5	2.2
Chlorite	0.0	2.8
Allanite	0.1	0.2
Sericite	0.8	0.0
Opaque iron ore	1.3	0.0

* : The range of mineral volumes are given with a 95% confidence (Van der plas and Tobi, 1965)

The albite, 0.5 to 3.42 mm, often exhibits albite and carlsbad-albite twinning, and is altered to the sericite. The carlsbad twinning is seen in the orthoclase, 0.2 to 1.33 mm, which often shows perthitic texture. It is altered to clay mineral and the sericite. Minor allanite, opaque iron ore and chlorite are also present. Cataclastic movement caused breakdown and recrystallisation of both feldspars so mortar texture forms.

III.3.7 Vein rocks

III.3.7.1 Aplites

These are formed in the granitoid or at the contact of metamorphic and diorite and can be seen up to ~250 m. in length and 50 cm in thickness (e.g. at lat. 80837 and long. 89387 on the geological map of Ortakoy area). They are composed of quartz, (25%), showing undulose extinction; plagioclase(5%) with albite twinning; orthoclase (65%) that often has perthitic texture; and minor muscovite in anhedral, aplitic, texture.

III.3.7.2 Pegmatites

This is formed in the granitoid (e.g. at 83630 la.95200 lo.), or at the contact of metamorphic and hornblende diorite, and contains spectacular quartz, up to 20 cm in length, orthoclase, tourmaline and sometimes white mica.

III.3.7.3 Tonalite porphyry

This is mainly made of plagioclase(65%), 0.1 to 2.9 mm., shows albite twinning and is altered to sericite; quartz(35%), 0.1 to 2.0, displays undulose extinction; brown biotite (5%),0.05 to 0.65 mm; and green hornblende, 0.45 to 0.9 mm, replaced by biotite with holocrystalline porphyritic texture. The ferromagnesian minerals are altered to the chlorite. Minor sphene and allanite are also present.

III.3.7.4 Quartz

It is possibly formed at the hydrothermal stage as a milky quartz(e.g. at 84.00 lat. and 94750 long.) in accordance with the joint system of the granitoid.

III.3.7.5 Microdiorite

This is mainly made of hornblende (60%), 0.2 to 1.0 mm, showing strong pleochroism from light green to dark green; plagioclase with albite twinning (35%), 0.1 to 0.2 mm; and minor quartz (0.3 to 0.5 mm) and diopside (0.2 to 0.5 mm) in hypidiomorphic granular texture.

III.3.7.6 Granophyre

This consists of quartz, plagioclase(An15), orthoclase, and minor biotite and allanite in granophyric texture.

III.4 NEOGENE FORMATION

III.4.1 Pecenek Formation

III.4.1.1 Tuff

This is made of 30% phenoclasts and 70% groundmass in a porphyritic texture. Plagioclase, 0.25 to 1.4 mm, is a major phenoclast with oscillatory zoning which indicates andesine rich core and rim rich in oligoclase. Strong pleochroism from yellowish to reddish brown is a characteristic of the biotite which is 0.1 to 0.45 mm. Volcanic glass is dominant in the groundmass, therefore, it is a vitric tuff.

Chemical compositions of plagioclases and biotite are presented in Table 32.

III.4.1.1.1 Gravel in the tuff.

This is eroded, transported and deposited volcanic rock made of 45% phenocrysts and 55% groundmass. Hornblende phenocrysts form 30% and are pleochroic from yellowish to greenish brown and 15% of the rock is plagioclase phenocrysts showing albite twinning. The matrix contains 20% hornblende, 20% plagioclase and 15% volcanic glass in a porphyritic texture. This rock is largely volcanic gravel and has been deposited the above tuff as a sediment, almost a gravel (9 cm in diameter).

The analyses of gravel amphibole and plagioclase are given in Table 32.

III.4.1.2 Limestone

Part of the limestone is formed by laminated stromatolitic coatings consisting of alternating layers of micrite and outward growing calcite crystals. Overlying this are micritic sediments containing carbonate and siliceous lithoclasts of igneous and metamorphic rocks and grains of quartz, orthoclase showing perthitic texture, plagioclase with albite twinning and zoned; muscovite and pyroxene. Scattered bioclasts include fragments of gastropod shells. Coated pisolitic grains are present. Tapering and circumgranular cracks are filled with sparry calcite.

The stromatolitic layering is interpreted as representing travertine deposit with calcite precipitated from lake waters. The poorly sorted sediments with coated grains are believed to represent a paleosols formed as the lake dried out.

Table 32: The chemical compositions of plagioclase, biotite from the tuff,(31); and gravel,(700) plagioclase and amphibole.

Sample	Pl,core(31)	Pl,rim(31)	Bt(31)	Hbl(700)[1]	Pl(700)
SiO2	56.13	61.67	37.21	48.61	44.93
TiO2	0.07	0.04	4.92	0.35	0.02
Al2O3	27.49	24.19	13.56	4.54	34.22
Fe2O3*	0.00	0.00	2.97	7.53	0.00
FeO	0.35	0.14	11.89	7.43	0.29
MnO	0.01	0.02	0.23	0.28	0.02
MgO	0.16	0.00	15.03	14.03	0.20
CaO	9.62	5.80	0.04	11.04	18.50
Na2O	6.09	7.82	0.94	0.82	0.97
K2O	0.27	0.79	8.63	0.05	0.00
Cr2O3	-	-	-	0.43	-
Total	100.19	100.47	95.42	95.11	99.15

Formula based on 32 oxygens for plagioclase, 22 for biotite and 23 for amphibole.

Si	10.09	10.91	5.55	7.24	8.36
Ti	0.01	0.01	0.55	0.04	0.00
Al	5.82	5.04	2.38	0.81	7.51
Fe^{3+}	0.00	0.00	0.37	0.83	0.00
Fe^{2+}	0.05	0.02	1.48	0.91	0.04
Mn	0.00	0.00	0.02	0.03	0.00
Mg	0.04	0.00	3.34	3.10	0.05
Ca	1.85	1.10	0.01	1.76	3.69
Na	2.12	2.68	0.27	0.24	0.35
K	0.06	0.17	1.64	0.01	0.00
Cr2O3	-	-	-	0.05	-
An	45.90	27.85			91.34

* : Fe^{3+} is calculated according to Drop(1987) for amphiboles; assumed as 0 for plagioclase; for biotite, it is assumed as 20% of FeO_t.

1 : Magnesio-hornblende (Leake, 1978)

IV GEOCHEMISTRY

IV.1 ANALYTICAL METHODS

The major and trace element analyses were performed by a Philips PW1450 sequential X-ray fluorescence spectrometer with an on line Superbrain microcomputer for data processing at the Department of Geology & Applied Geology, Glasgow University. To determine major elements, fused glass discs were prepared from powdered rock according to the method of Harvey et al. (1973) and using factors to correct for remaining absorbtion-enhancement effects.

The FeO contents of the samples were determined by the method of titration with potassium-dichromate as the X-ray spectrometer gives total iron. Fe2O3 is calculated by subtracting FeO multiplied by 1.1114, from the total iron as Fe2O3.

The amounts of H2O and CO2 were determined by a method of combustion, adsorbtion and gravimetry (Riley, 1958). In some samples, volatile contents were determined by measuring loss on ignition.

Pressed pellets were prepared from powdered rocks to determine trace element according to Leake et al. (1969).

Rare Earth Element analyses were performed at Scottish Reactor Centre, East Kilbride using ICPMS.

IV.2 METASEDIMENTS

IV.2.1 Major and trace elements

The main aims in analysing the sediments are to determine their geochemical characteristics, to find out their geotectonic setting, and to characterize the provenance from which the sediments were derived.

The results exhibit that the compositional variation of the Ortakoy metasediments are quite scattered (Fig. 7). The rocks can be considered as a mixture of some end-members which are clay with c < 5, mg 0.2-0.6, limestone with c about 100, mg 0.9, dolomite with c about 50, mg 1 and the quartzite with c > 5 , mg 0.4-0.8. Ca-silicates can be regarded as a mixture of clay and carbonate. The occurrence of dolomitic marble is highly restricted and shows no transition to calcitic marble or to the other sediments, which suggests that dolomitic marble was not involved to the continuous series of mixture and the conditions of the dolomite formed was probably different than the rest of the Ortakoy sediments.

As there are no agreed chemical limits in the literature between semipelite, psammite and quartzite the boundaries taken were 65 and 80 as the lowest SiO2 wt % content for psammite and quartzite, with less than 65 % SiO2 being semipelite (Tables 33 and 34).

Niggli al-alk was used as an indicator of sheet mineral influence in the original sediments because albite and K-feldspar each has al-alk=0 and the lack of a positive correlation of al-alk with Ca values (Fig. 8) shows that plagioclase is not a major influence on al-alk values. By using al-alk, the clay mineral and detritial mica influence on the composition of the semipelites can be obtained (Senior and Leake, 1978). Therefore, Fig. 9

suggests that K, Fetot (as Fe2O3), Ti, Rb, Zr, and possibly Ba, Ni and Zn were added in sheet minerals, mica and clay minerals. It is not clear if the sheet silicates was the only factor to control the composition of the sediments, but the clay material was probably dominant factor as clay-rich lithology e.g. semipelite contains more trace element than the clay-poor rock group.

Ti shows positive correlation with al-alk so it might be useful in alkali metasomatised metasediments where al-alk will be changed but not Ti (Senior and Leake, 1978). The elements suggested to be largely added to sediments in clay minerals are plotted against TiO2 (Fig. 10) which generally displays better correlation than the plotting against al-alk presumably because of removal of the influence of variable amounts of feldspar. Likewise, Al2O3 shows a positive correlation with TiO2, however no correlation exists between al-alk and Al which suggests that Al was largely added in feldspar. As the feldspar in different quantities in the original sediments might have hindered any possible positive correlation between Al and al-alk, Al2O3 might have been added to the sheet silicates too.

By extrapolating the various plots involving al-alk and TiO2 (Fig.s 9 and 10) towards their extreme limits, it would be possible to determine very approximately the composition of the clay mineral end member which is about 20% Al2O3, 7% Fe2O3t, 4.5% K2O, 0.4% MgO, 0.8% TiO2, 0.1% MnO and by difference 67% SiO2, al-alk 44, mg 0.2, Cr 451, Ni 138, Zn 175, 888 Ba, Rb 192, Ce 104, La 45, Y 37, Ga 25, Zr 304, Sr 2509. This composition accords best with some variety of illite including substantial amount of Si and Fe.

To find out whether the same clay mineral end member added to the sediments in varying proportions or each sedimentary group has its own

characteristic end member, average elemental values of each rock type in this study and in the literature (only shale, psammite and quartzite; Wedephol, 1969) were plotted against al-alk (Fig. 11). The linear trends of these average values indicates that a somewhat similar clay mineral end member was added to metasediments, while the degree of scatter shows that considerable variation also occurs especially in the quartzites and with respect to Ba and Zn. The figure also shows that the simple picture of trace elements controlled by al-alk can be applicable to the general sediments. The more clay material the more trace element content.

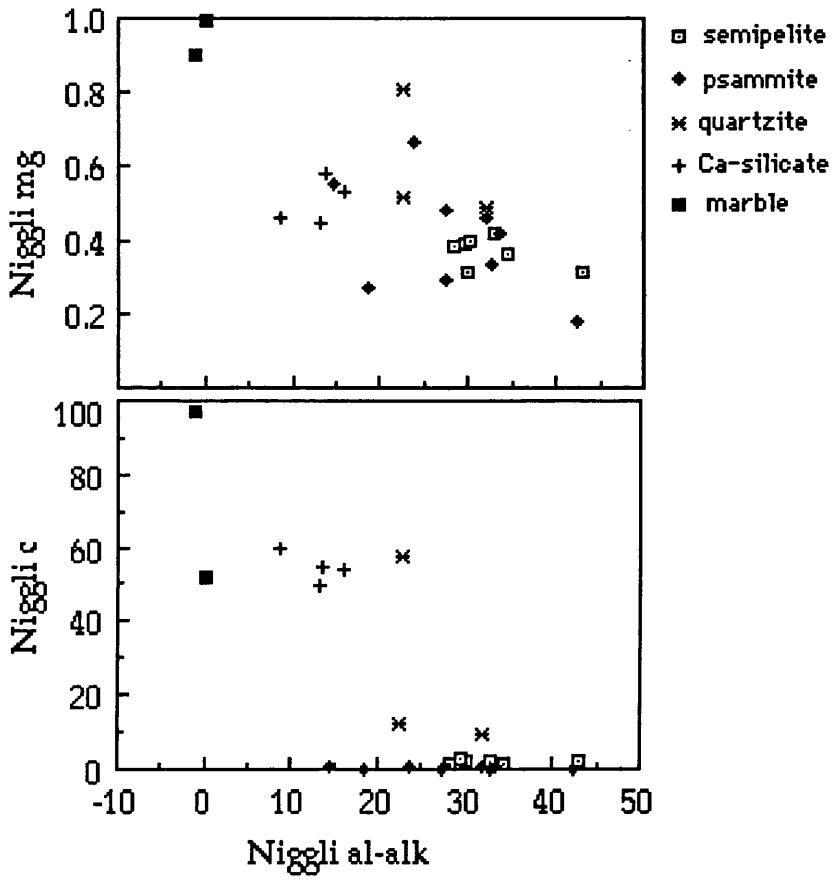

Figure 7: Plots of Niggli mg and c against al-alk.

Table 33 : Major and trace element analyses of the semipelite and psammite

a) Semipelite

Sample No	505	522	506	541	502	529	508	Mean	σn
SiO2	60.47	61.41	61.99	62.11	63.16	63.90	64.34	62.48	1.28
TiO2	0.68	0.79	0.75	0.71	0.74	0.81	0.56	0.72	0.08
Al2O3	19.36	17.64	18.32	16.98	19.47	17.86	16.55	18.02	1.03
Fe2O3	3.23	3.28	4.15	4.44	3.69	5.90	3.62	4.04	0.86
FeO	3.02	2.76	1.27	2.04	1.67	0.50	1.34	1.80	0.82
MnO	0.02	0.04	0.02	0.06	0.07	0.06	0.02	0.04	0.02
MgO	1.85	1.46	1.87	2.48	1.28	1.82	1.67	1.77	0.35
CaO	0.37	0.48	0.45	0.50	0.36	0.32	0.60	0.44	0.09
Na2O	0.76	1.80	1.09	0.64	0.22	1.72	1.51	1.11	0.55
K2O	4.32	3.35	4.71	3.33	3.78	4.01	3.52	3.86	0.48
P2O5	0.11	0.02	0.10	0.09	0.05	0.07	0.11	0.08	0.03
CO2	1.59	1.90	1.43	1.71	1.06	1.33	1.55	1.51	0.25
H2O	4.20	4.66	3.85	4.81	4.25	2.20	4.03	4.00	0.80
Total	99.98	99.59	100.00	99.90	99.80	100.50	99.42		
Zr	194	228	203	234	207	238	175	211	21
Y	20	15	16	25	22	17	20	19	3
Sr	57	114	37	60	49	75	54	64	23
U	4	3	3	3	6	5	4	4	1
Rb	182	141	184	156	165	192	150	167	18
Th	24	10	20	18	22	14	20	18	5
Pb	16	15	18	22	26	21	13	19	4
Ga	23	20	22	20	23	22	20	21	1
Zn	93	78	108	79	91	78	73	86	11
Cu	29	29	21	30	13	37	12	24	9
Ni	63	89	61	138	55	28	76	73	32
Co	12	19	14	14	15	12	11	14	2
Cr	268	293	217	405	149	212	393	277	88
Ce	65	48	54	63	57	57	49	56	6
Ba	570	428	611	565	542	483	503	529	57
La	32	23	26	25	28	27	24	26	3.0

Mean : Arithmetical mean
σn : Standard deviation

Coordinates of the semipelites

505	83425-86140	541	85350-90800
522	86150-91512	502	83425-86140
506	83425-86140	529	86010-93325
508	83375-86100		

b) psammite

Sample No	504	272	278	516	517	686	525	514
SiO2	65.09	65.50	67.17	69.44	70.17	70.67	72.31	74.24
TiO2	0.62	0.54	0.61	0.35	0.29	0.68	0.79	0.48
Al2O3	15.66	15.87	14.40	15.26	12.66	13.58	14.90	12.80
Fe2O3	2.96	2.72	2.72	1.35	0.66	1.51	2.69	1.50
FeO	1.33	2.56	2.17	1.16	1.25	3.38	0.98	1.58
MnO	0.05	0.07	0.07	0.04	0.05	0.10	0.09	0.04
MgO	1.41	2.27	1.85	1.23	1.26	1.96	0.42	1.50
CaO	2.31	0.64	0.58	1.75	4.18	0.21	0.45	0.26
Na2O	1.50	1.11	1.08	5.19	3.46	0.49	1.10	1.23
K2O	3.96	3.28	3.26	1.82	1.87	2.71	2.07	3.16
P2O5	0.07	0.11	0.03	0.10	0.11	0.04	0.06	0.04
CO2	2.11	1.73	3.49	0.46	1.82	1.67	1.57	0.70
H2O	2.93	3.05	2.59	2.05	2.20	1.85	2.58	2.45
Total	100.00	99.45	100.02	100.20	99.98	98.85	100.01	99.98
Zr	226	167	209	218	304	224	268	154
Y	19	20	19	30	28	21	24	14
Sr	127	64	72	291	404	81	78	51
U	5	6	4	2	1	0	4	2
Rb	172	154	144	47	78	117	81	121
Th	20	16	19	18	25	10	18	12
Pb	25	18	21	15	15	8	22	21
Ga	21	19	19	18	14	14	19	14
Zn	76	85	97	48	32	74	54	50
Cu	17	25	15	1	5	3	9	16
Ni	38	92	66	7	5	34	45	36
Co	13	11	14	2	3	12	9	5
Cr	94	255	313	58	113	163	128	389
Ce	58	74	73	67	73	55	71	40
Ba	502	730	695	230	269	480	369	458
La	30	18	24	31	30	24	35	21

Table 33 b: cont.

Sample No	511	676	534	512	539	Mean	σn
SiO2	75.38	76.34	77.75	77.98	79.27	72.41	4.64
TiO2	0.47	0.09	0.25	0.42	0.25	0.45	0.19
Al2O3	13.53	14.02	9.39	9.98	10.79	13.29	2.03
Fe2O3	2.19	0.30	1.91	1.48	1.50	1.81	0.79
FeO	0.63	0.27	3.25	0.31	0.74	1.51	1.00
MnO	0.01	0.0	0.04	0.03	0.06	0.05	0.03
MgO	0.73	0.62	1.05	0.37	1.0	1.20	0.57
CaO	0.49	0.19	1.45	0.59	0.23	1.02	1.11
Na2O	1.26	3.47	1.98	1.75	1.35	1.92	1.27
K2O	2.95	2.24	1.16	1.83	1.76	2.47	0.78
P2O5	0.02	0.08	0.01	0.01	0.02	0.05	0.03
CO2	0.27	0.14	0.31	1.06	0.27	1.20	0.94
H2O	2.10	2.18	1.50	3.98	2.50	2.46	0.60
Total	100.03	99.94	100.05	99.79	99.74		
Zr	147	85	179	199	132	193	56
Y	16	12	16	17	16	19	5
Sr	98	114	55	105	49	122	101
U	0	0	6	0	2	2	2
Rb	132	123	163	64	80	113	38
Th	17	1	20	15	10	15	6
Pb	15	19	14	10	12	17	5
Ga	13	9	25	11	11	16	4
Zn	61	9	76	33	37	56	24
Cu	24	0	28	19	3	13	9
Ni	63	4	36	41	11	37	25
Co	10	8	13	7	2	8	4
Cr	297	231	157	451	190	218	114
Ce	41	13	54	50	104	59	21
Ba	435	344	781	224	263	445	183
La	23	1	24	28	19	24	8

Mean : Arithmetical mean
σn : Standard deviation

Coordinates of the psammites

504	83425-86140	514	83375-86100
272	85275-87750	511	83425-86140
278	85275-87750	676	84675-87587
516	83375-86100	534	85125-93225
517	83425-86140	512	83375-86100
686	86625-87735	539	85275-87750
525	86150-91512		

Table 34 : Analyses of the quartzites, carbonates and Ca-silicates.

a) Quartzites(540, 14, 527) and Carbonates

							Marble(Dolom.)	Marb(Calcite)
Sample No	540	14	527	Mean	σn		598	747
SiO2	80.37	82.01	87.58	83.32	3.08		0.11	2.22
TiO2	0.26	0.07	0.30	0.21	0.10		0.03	0.05
Al2O3	9.70	4.20	4.36	6.09	2.60		1.2	0.07
Fe2O3	1.47	0.25	1.19	0.97	0.52		0.69	0.0
FeO	0.5	0.16	0.80	0.49	0.26		0.19	0.14
MnO	0.04	0.07	0.09	0.07	0.02		0.03	0.02
MgO	1.09	0.92	1.01	1.01	0.07		21.57	0.68
CaO	1.50	5.50	0.57	2.52	2.14		32.82	54.19
Na2O	2.04	0.0	0.40	0.81	0.88		0.27	0.65
K2O	1.20	0.25	0.07	0.51	0.49		0.18	0.05
P2O5	0.01	0.01	0.01	0.01	0.0		0.01	0.03
CO2	0.32	3.81	0.76	1.63	1.55	L.O.I.	43.00	41.90
H2O	1.60	2.50	2.85	2.32	0.53			
Total	100.10	99.75	99.99				100.10	100.26
Zr	136	44	138	106	44		47	5
Y	14	10	13	12	2		8	10
Sr	142	26	66	78	48		154	179
U	0	0	1	0	0		0	0
Rb	57	15	2	25	24		6	1
Th	9	5	10	8	2		8	7
Pb	12	5	4	7	4		3	5
Ga	10	6	5	7	2		1	0
Zn	36	10	19	22	11		0	1
Cu	8	0	3	4	3		0	8
Ni	4	7	33	15	13		2	5
Co	2	1	2	2	1		0	0
Cr	15	46	141	67	54		0	0
Ce	38	10	17	22	12		0	0
Ba	223	131	150	168	40		18	2
La	18	5	1	8	7		7	6

Mean : Arithmetical mean
σn : Standard deviation

Coordinates of the quartzites and carbonates

540	85275-87750	598	85650-93375
14	85562-93325	747	87825-88137
527	83375-86100		

b) Ca-silicates

Sample No	549	515	738	800	Mean	σn
SiO2	41.67	43.50	47.29	47.33	44.94	2.45
TiO2	0.51	0.57	0.55	0.63	0.56	0.04
Al2O3	12.00	15.63	14.28	14.76	14.17	1.34
Fe2O3	1.47	2.63	1.07	3.49	2.16	0.96
FeO	3.57	3.87	3.66	0.43	2.88	1.42
MnO	0.13	0.15	0.11	0.02	0.1	0.05
MgO	2.32	3.93	3.58	1.67	2.87	0.92
CaO	24.89	23.79	22.27	16.70	21.91	3.15
Na2O	1.62	0.90	1.53	1.94	1.49	0.40
K2O	2.56	1.24	1.43	3.26	2.12	0.83
P2O5	0.11	0.11	0.10	0.13	0.11	0.01
CO2	0.0	0.0	0.0	7.19		
H2O	0.0	0.0	0.0	2.46		
L.O.I.	9.10	3.23	4.14			
Total	99.95	99.55	100.01	100.01		
Zr	118	113	119	128	119	5
Y	22	28	37	17	26	7
Sr	555	711	939	2509	1178	780
U	0	2	0	5	2	2
Rb	89	52	49	145	84	39
Th	11	15	14	22	15	4
Pb	12	11	18	13	13	3
Ga	14	24	20	21	20	4
Zn	54	130	175	73	108	48
Cu	31	25	7	30	23	10
Ni	20	58	40	35	38	14
Co	9	20	10	10	12	5
Cr	78	142	129	119	117	24
Ce	29	66	62	58	54	15
Ba	272	440	656	888	564	231
La	26	35	45	28	33	7

Mean : Arithmetical mean
σn : Standard deviation

Coordinates of the Ca-silicates

549	85212-88800
515	83375-86100
738	85600-87850
800	85050-90725

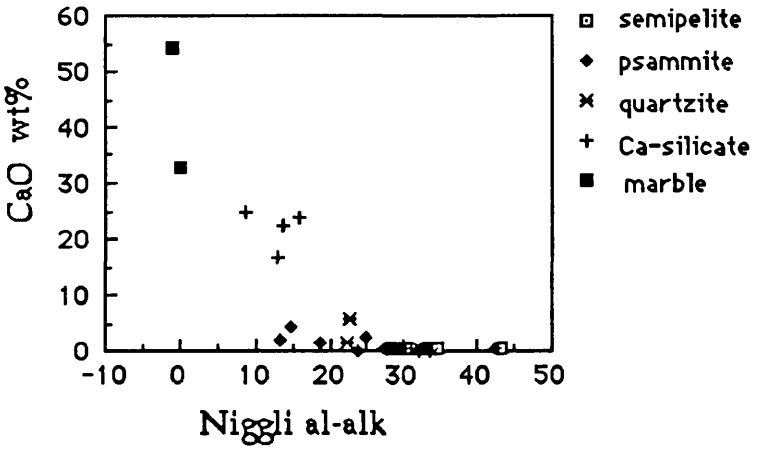

Figure 8 : The relation of CaO with Niggli al-alk.

The quartzites depart, both in the Ortakoy average and the quartzite average, the most from the general trend and this indicates different conditions of deposition from the other sediments perhaps more rapid deposition which did not allow adequate time for absorption of various elements from sea waters and equilibrium was not reached in the way that the remaining lithologies achieved (Senior and Leake, 1978). To keep the general trend of quartzite in Zr al-alk plotting (Fig. 11) is in consistency with the lack of detritial zircon in the unit. The plotting Zr and TiO2 (Fig. 10) confirms this case with the Zr values following the general trend, indicating that Zr was largely associated with the clay minerals.

CaO correlates with Sr in the semipelite and psammite while Ca-silicates shows a negative correlation between these elements (Fig.s 12 and 13). As pointed out before, there is a negative correlation of c and al-alk in the Ortakoy sediments, indicating that Ca and Sr were not originally added to the sheet silicates but probably with carbonate and/or feldspar. In Ca-silicates, there is a positive correlation of K and Sr (Fig. 14), indicating that

these two elements were probably added in K-feldspar and/or the amphibole.

The calcitic marble has low Fe2O3/MnO ratio, 23 and is similar to the average ratio (29 and 20.2) of Dalradian marble which was suggested to form in shallow water(Senior and Leake, 1978; Wilson and Leake, 1972). The close association of the marble with the quartzite is in a good agreement with this suggestion. Low Mn contents (<300) and Sr/Ca ratios ($<10^{-3}$) indicates that the carbonates were not altered during the diagenesis or metamorphism according to the the criteria of Veizer et al.,1989 .

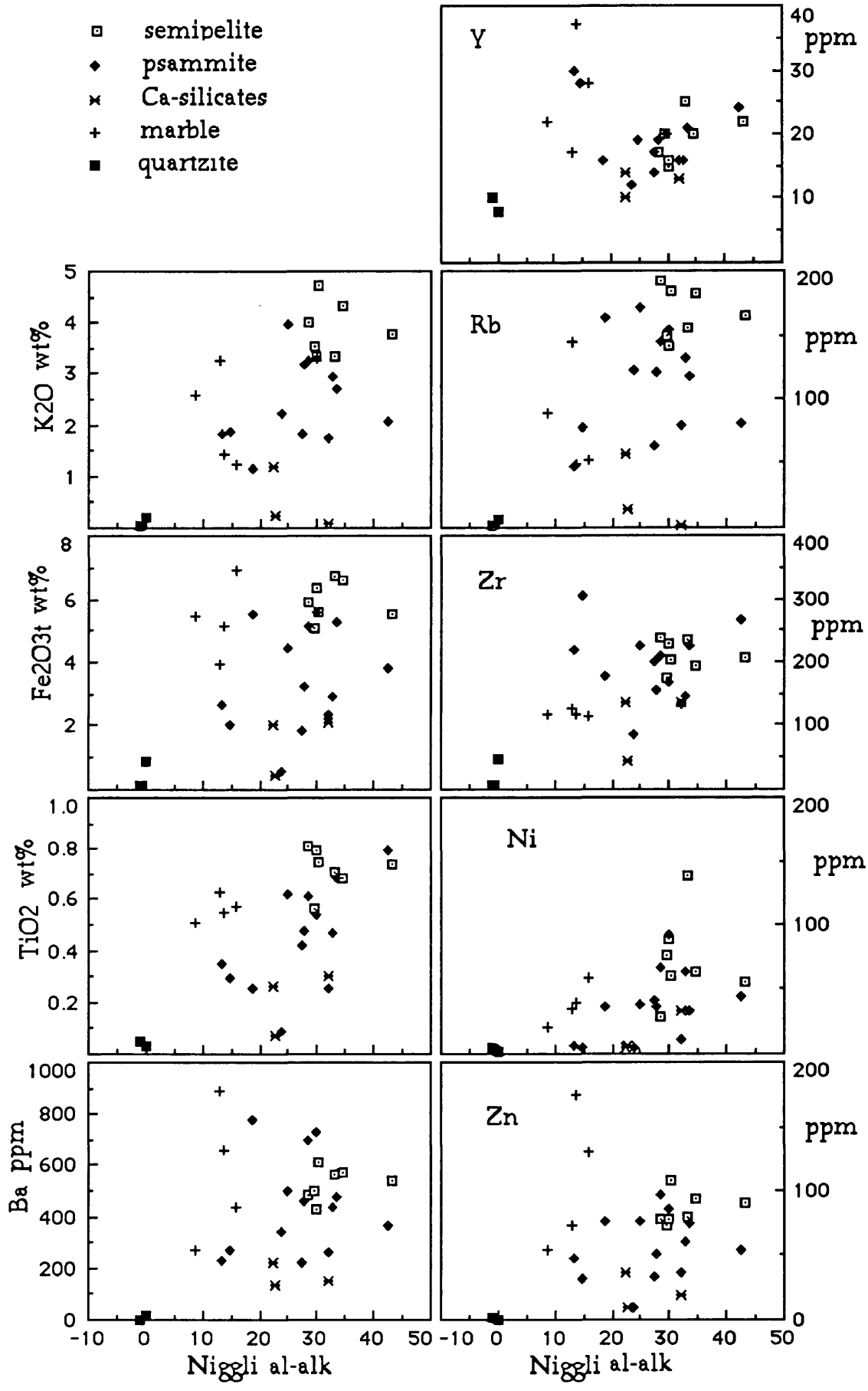

Figure 9 : Plotting K2O, Fe2O3t, TiO2, Ba, Y, Rb, Zr, Ni and Zn against Niggli al-alk.

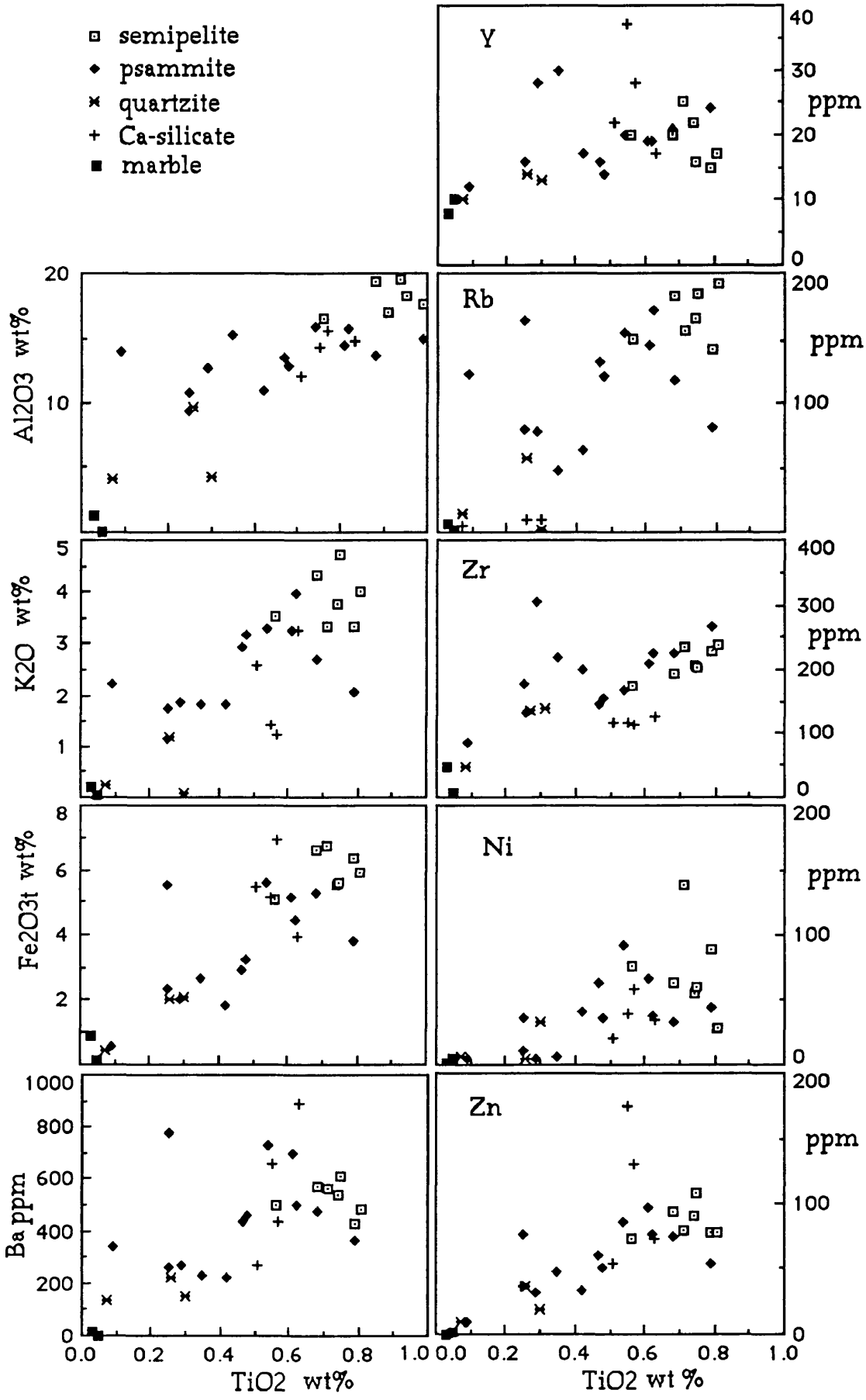

Figure 10: Plotting Al2O3, K2O, Fe2O3t, Ba, Y, Rb, Zr, Ni and Zn against TiO2.

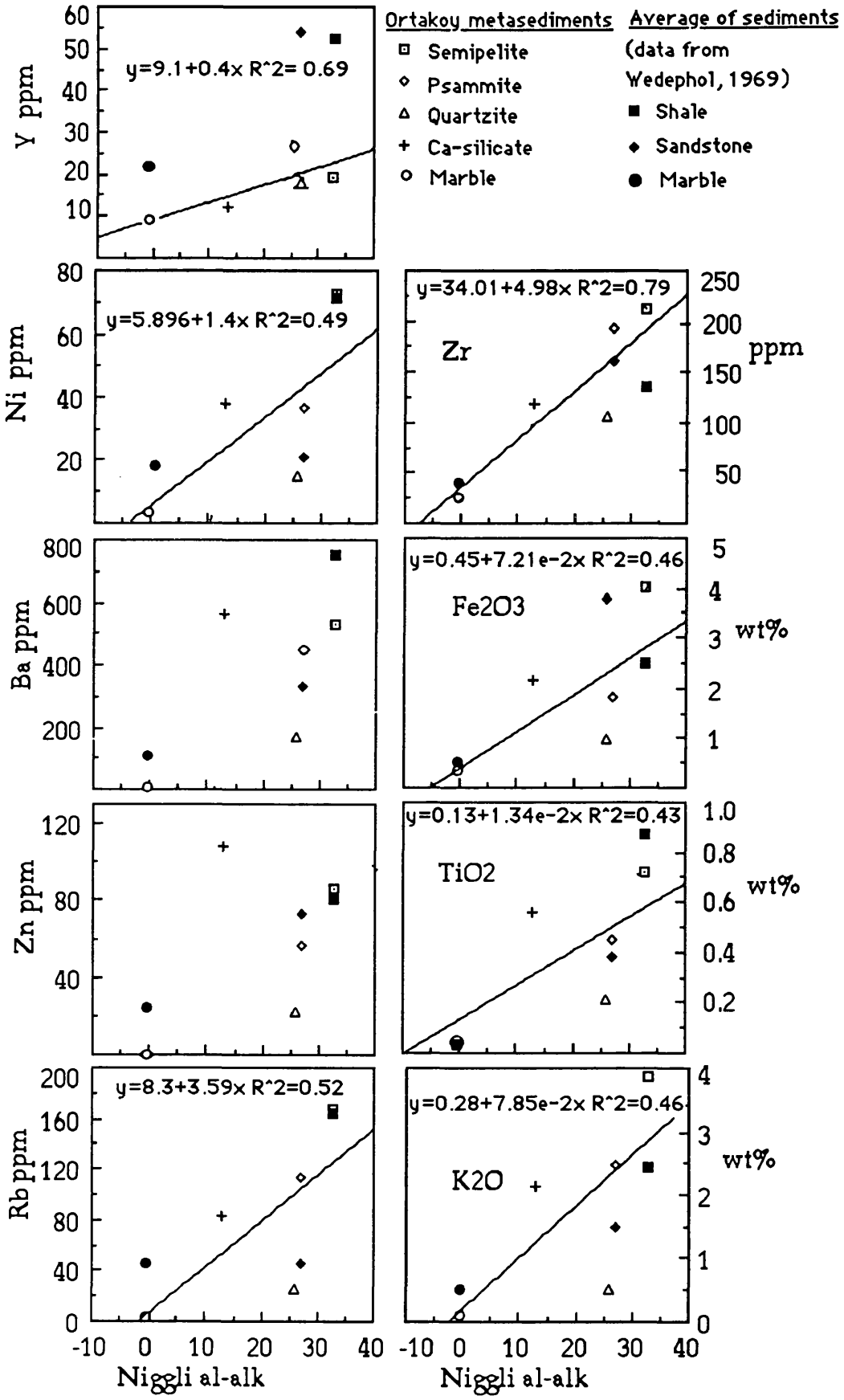

Figure 11: Plots of al-alk against various elements* for average Ortakoy semipelites, psammite, quartzite, marble and average shale, sandstone and marble.

* : The averages of elements taken for this diagram belong to the largest statistical population (data from Wedephol, 1969).

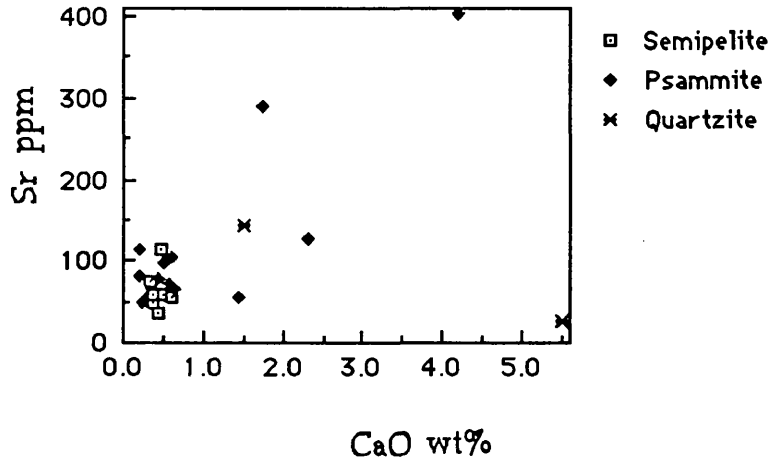

Figure 12: CaO-Sr relation in semipelite, psammite and quartzite.

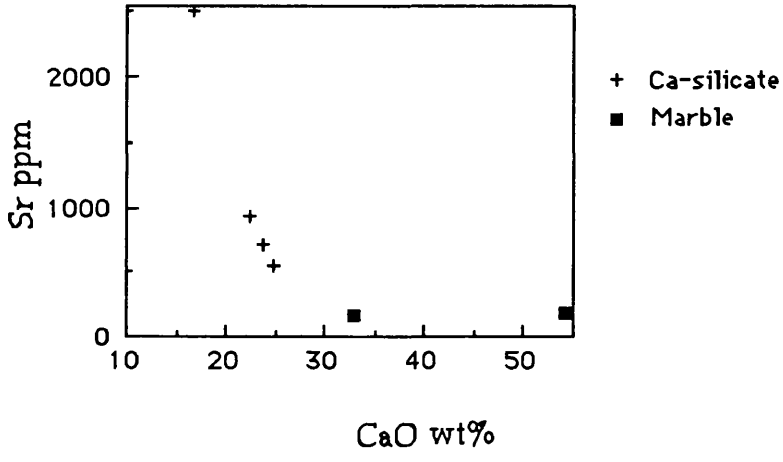

Figure 13: Plotting CaO-Sr in Ca-silicates and marbles

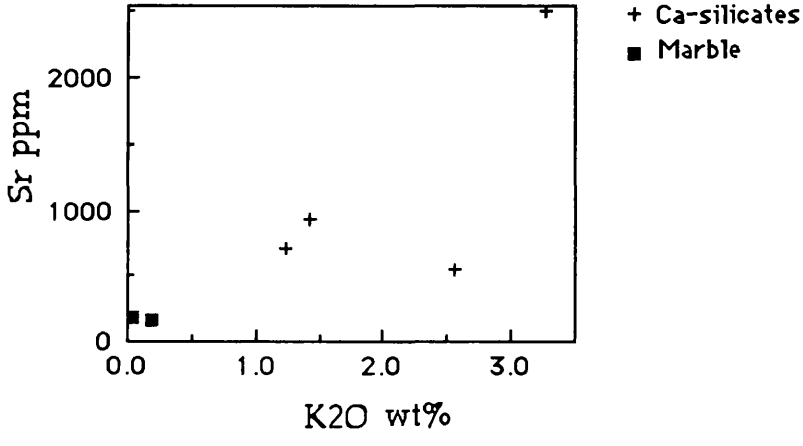

Figure 14: The relation of K2O and Sr in Ca-silicates and marbles.

Excluding dolomite, Ni shows a positive correlation with Cr and with MgO+Fetot (Fig.s 15 and 16). Cr in psammites has a different slope of correlation with MgO+Fetot (Fig. 17) which again suggests that the conditions controlling the absorbtion of Cr in sandstones significantly differ from these involved in semipelites.

Al2O3 shows a positive correlation with Ga (Fig. 18) due to having similar ionic radii and charges.

In general K shows a positive correlation with Rb in Fig. 19. Only one sample of psammite has high Rb content which an analytical error is likely. Ba also correlates well with K2O (Fig. 20)in which suggests that both Rb and Ba were substantially added to the sediments in illite, in mica, and K-feldspar.

The averages ratios of K/Rb in the semipelite, psammite and quartzite are almost same(231, 233 and 242), and comparable with a standard continental crustal value (230, Shaw, 1968). In Ortakoy Ca-silicate and marble, K/Rb ratio are quite high, 260 and 400. The sample 800 differs from the others Ca-silicates with comparatively high Fe2O3/Mn, and low K/Rb values. Likewise, this sample contains high K, Na, Ti and low Ca, Mg, and FeO similar to the semipelite, psammite and quartzite. Therefore, it was largely formed by processes of detritial sedimentation. The rest of Ca-silicates samples might have been dominantly formed by chemical precipitation as they have high Ca, low K content if the carbonate was assumed to formed by chemical precipitation.

Y has positive correlation with TiO2(Fig. 10), P2O5 and Zr (Fig. 21), except Ca-silicates but poorer correlation exists with al-alk which indicates

that Y was probably added in apatite, zircon and only partly in clay minerals and mica.

Niggli mg in metasediments increases from semipelite to psammite to carbonate, while al-alk decreases simultaneously (Fig. 22).

Na2O has a negative correlation with al-alk(Fig. 23) which indicates the presence of detritial sodic plagioclase in metasediments. Low-moderate Na values, 1.11 in the semipelite and 1.92 in the psammite, indicating that Ortakoy gneisses were probably derived relatively mature sediments (Floyd et al., 1989).

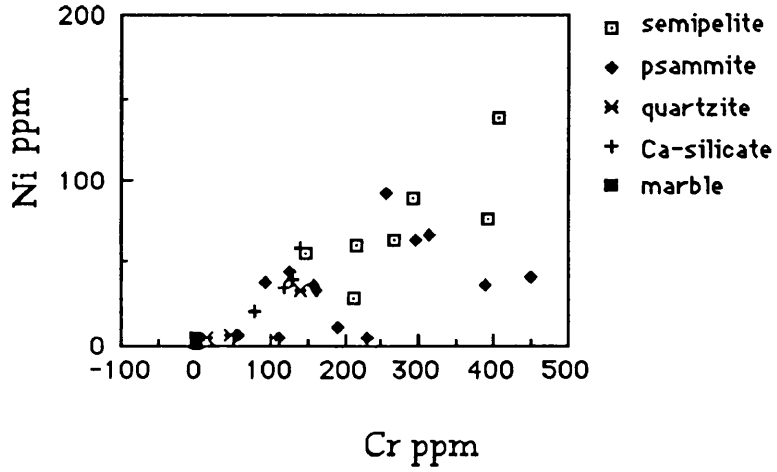

Figure 15: Plot of Ni and Cr

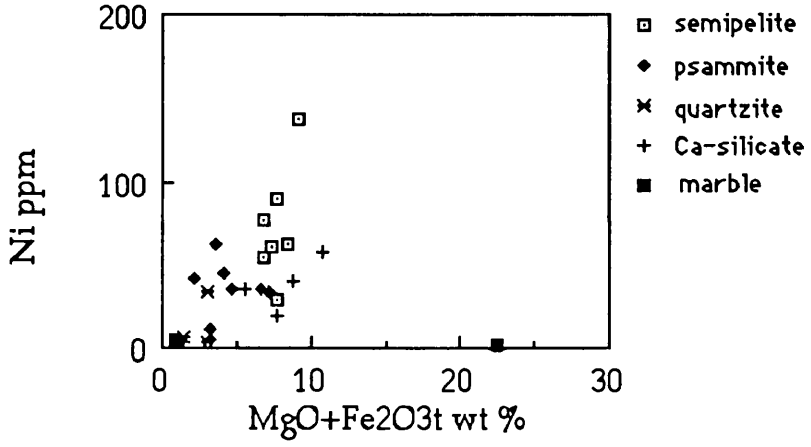

Figure 16: Plot of Ni with MgO+Fe2O3t

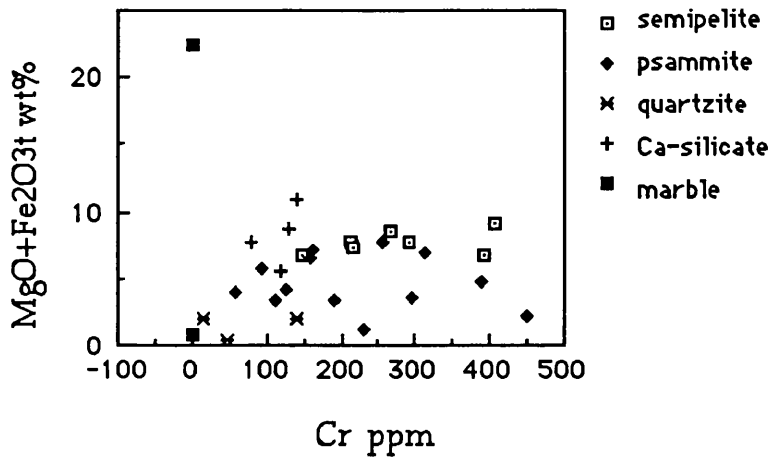

Figure 17: Cr and MgO+Fe2O3t variation in metasediments

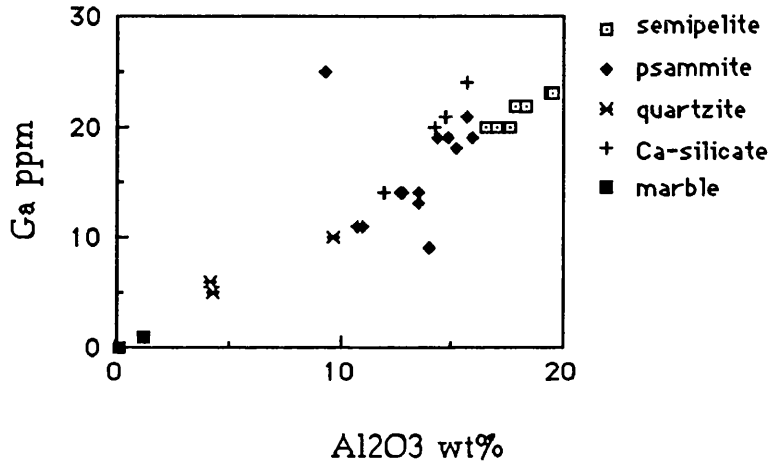

Figure 18: Plotting Ga and Al2O3.

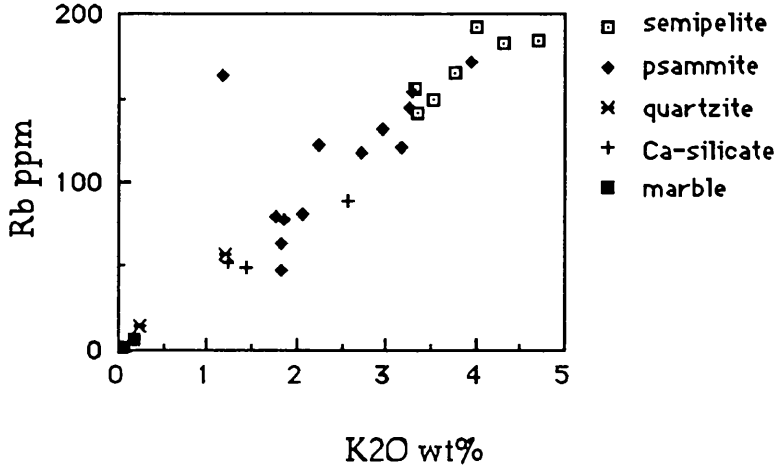

Figure 19 : Plot of Rb against K2O

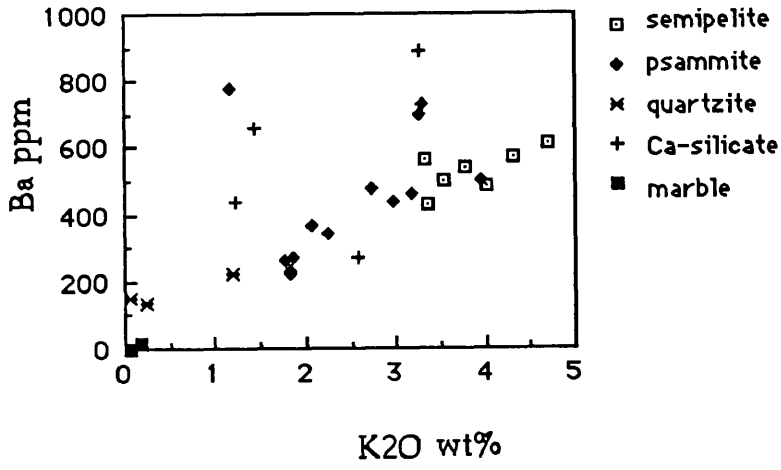

Figure 20 : Plot of Ba against K2O

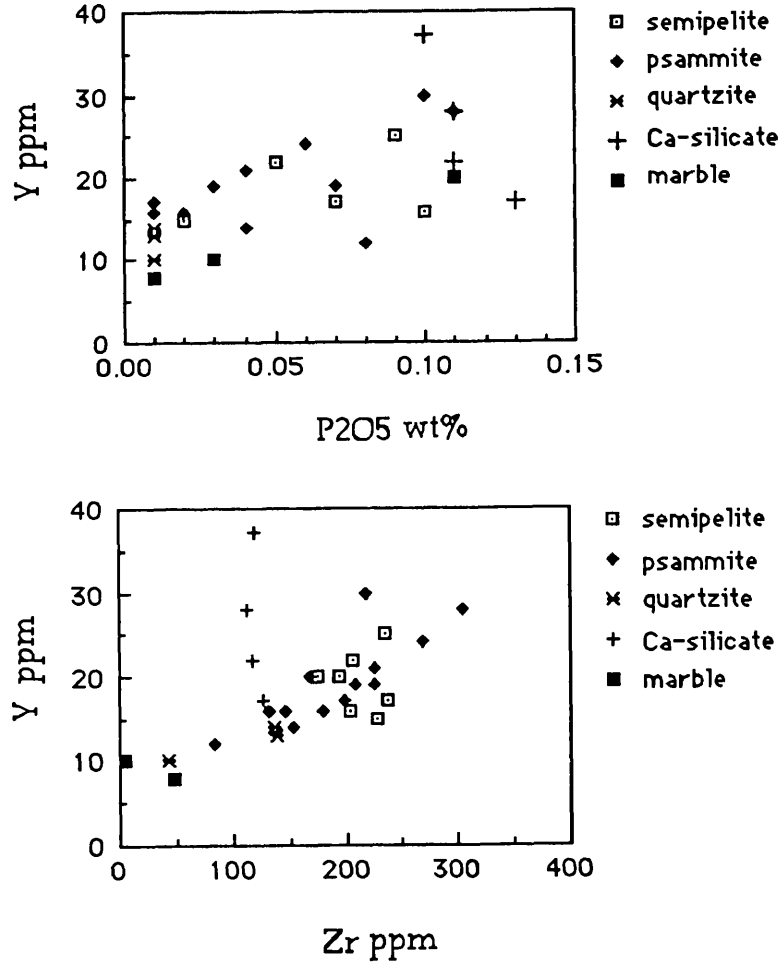

Figure 21: Plots of Y against P2O5 and Zr

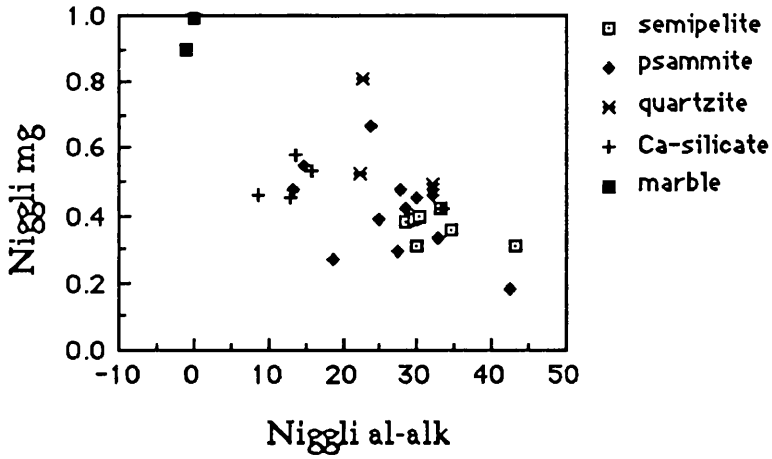

Figure 22: Niggli mg and al-alk variation in metasediments

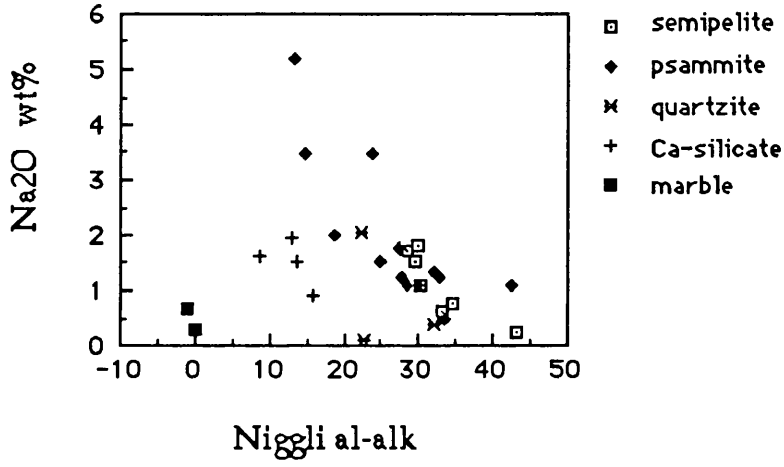

Figure 23 : Plotting Na2O- al-alk in metasediments.

Nesbitt and Young (1982) proposed a "chemical index of alteration" (CIA) using molecular proportions where

CIA= [Al2O3 / (Al2O3+CaO^+Na2O+K2O)] x 100 and where CaO^ represents CaO in the silicates only. The intensity of weathering in the source areas can be can be compared by using CIA. A weighted average CIA in semipelite and psammite are 72 and 63 in the range of 75-82 and 57-80, respectively (Fig. 24). These values are much higher than the CIA for fresh feldspar (50) and granite, 45-55. Therefore, the bulk detritus from which the Ortakoy sediments were derived had suffered relatively moderate chemical weathering before deposition.

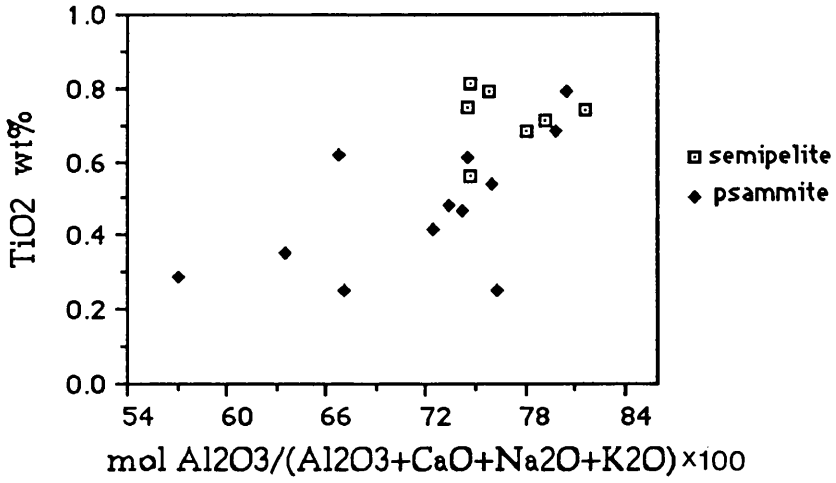

Figure 24: Diagram showing the relation of TiO2 with mol Al2O3/(Al2O3+CaO+Na2O+K2O)

IV.2.2 Tectonic setting

Bhatia(1983) showed that the chemical composition and tectonic setting of sandstones was related with a progressive decrease in Fe2O3+MgO, TiO2, Al2O3/SiO2 and an increase in K2O/Na2O and Al2O3/(CaO+Na2O) in sandstones from oceanic island arc to continental island arc to active continental margins to passive margins. The ratio Al2O3/SiO2 gives an indication of the quartz enrichment in sandstones. The ratio K2O/Na2O is a measure of the K-feldspar and mica versus plagioclase content in the rock and the Al2O3/(CaO+Na2O) parameter is a ratio of the most immobile to the most mobile elements. Ti, Fe and Mg are also relatively immobile. Bhatia(1983) developed some discrimination diagram based on these informations. The attempt of application of the Ortakoy sediments to these classification was conducted and no clear discrimination was achieved e.g. Fig. 25, because of variable enrichments on these parameters. Fig. 25 confirms that sheet silicates in the original sediments was probably dominant factor on controlling of the chemical composition of the sediments. The more clay rich material the higher elements.

Bhatia(1983) developed some geochemical multi-element discrimination functions and used plots of them to identify the tectonic settings of sandstones. In this discrimination, continental arc setting that comprises sedimentary basins formed either on a well developed continental crust or on thin continental margin, and the oceanic island arc represent convergent plate margins. The active continental margin setting includes continental margins of Andean type and strike slip types. Sediments are substantially derived from granite-gneisses and siliceous volcanics of the uplifted basement. The passive margin tectonic setting comprises rifted continental margins of the Atlantic type developed along the edges of continents. Ortakoy metasediments are plotted similarly and match best with an a active continental margins (Fig. 26), with a few samples are found in or near to the field of continental island arcs.

Bhatia and Crook(1986) discriminated tectonic setting of greywackes, sandstones of wide mineralogical range, by using some graph of trace elements such as La, Ce, Th, Zr and Co, which are immobile due to their relatively low mobility during sedimentary process and their low residence times in sea water(Holland, 1978). In Fig. 27, 52% of Ortakoy semipelites, psammites and quartzites (as total sample number) fell on the active continental margin while 26% of that fell on Continental island arc and 13% of that on passive margin.

As a result, the Ortakoy semipelite, psammite and quartzite were probably largely deposited in an Andean type thick continental margins, thick continental crust made of rocks of older fold belts, and minor in continental island arcs where continental fragments detached from the mainland.

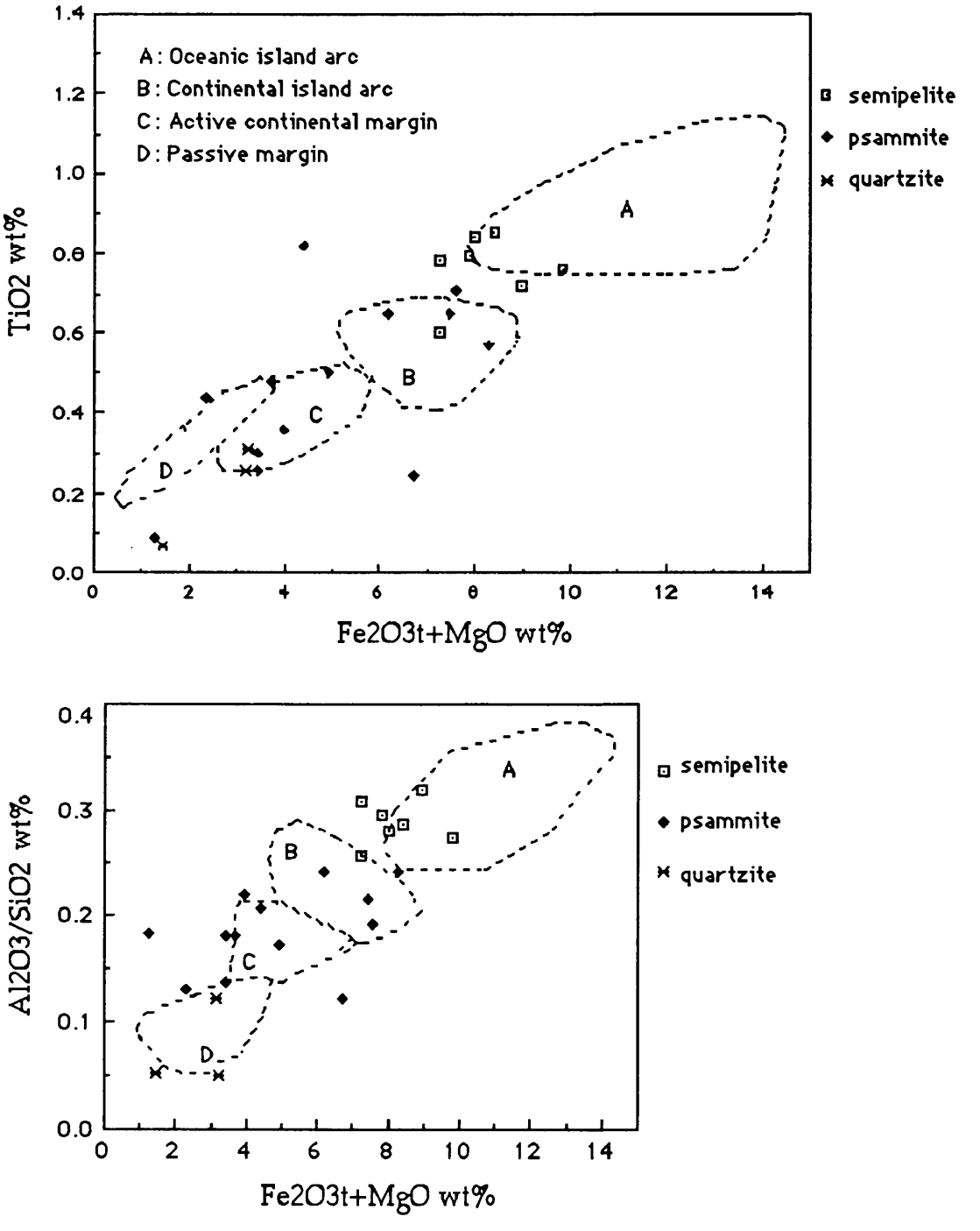

Figure 25: Tectonic setting of the Ortakoy semipelite, psammite and quartzites (Fields after Bhatia, 1983)

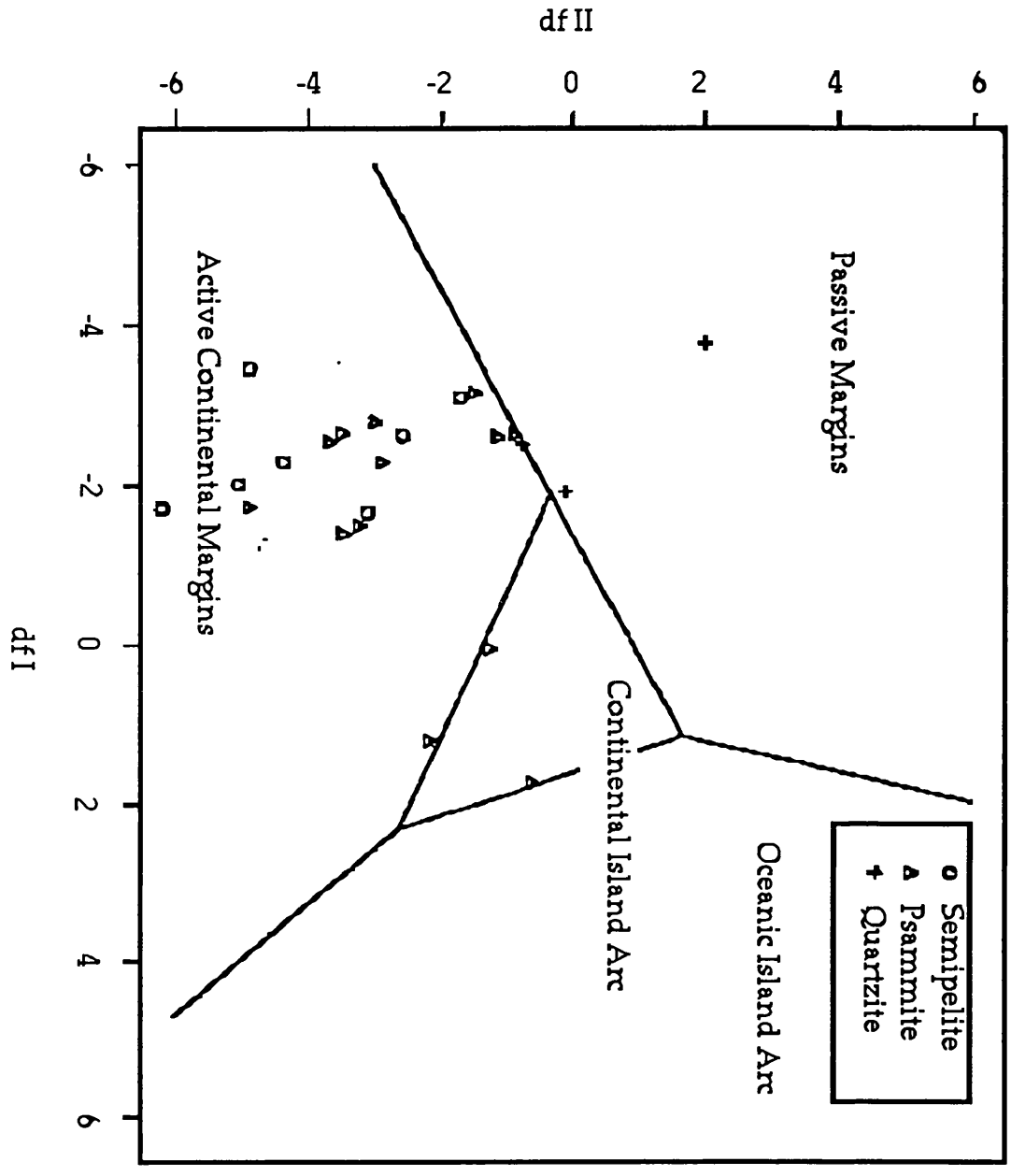

Figure 26: Diagram showing tectonic setting of the Ortakoy semipelite, psammite and quartzite (fields after Bhatia, 1983).

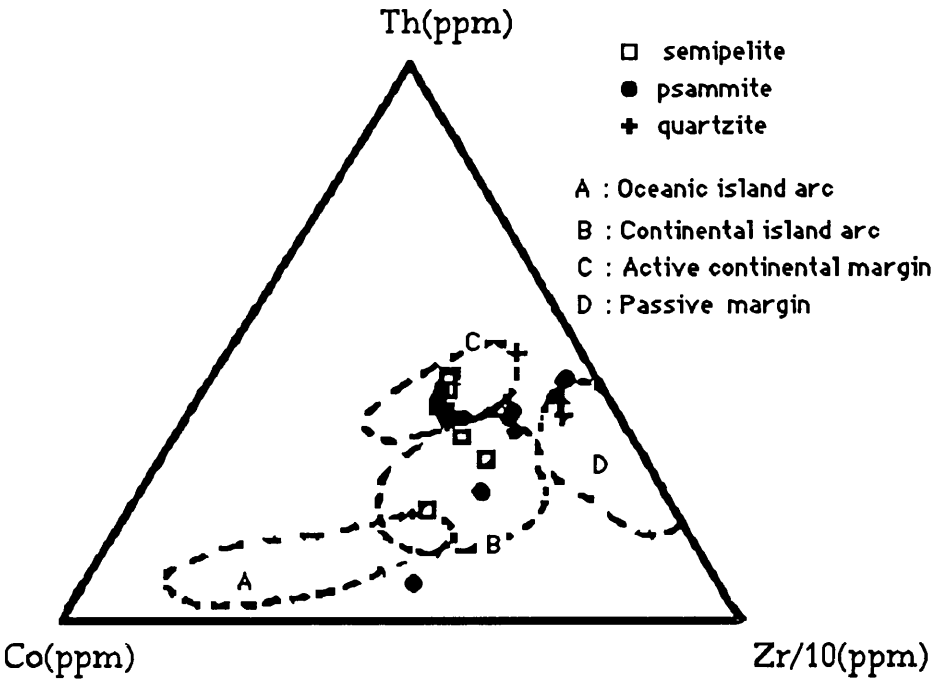

Figure 27: Th-Co-Zr/10 plotting to discriminate tectonic setting of the Ortakoy semipelite, psammite and quartzite (fields after Bhatia & Crook, 1986)

IV.2.3 Chemical discrimination of provenance

Trace elements include the REE, Zr, Ti, Y, Hf, and U can be considered useful in determining the source of sediments as they have intermediate ionic potential and low ocean residence times (Holland, 1978; Henderson, 1982). They are readily incorporated into sediments and also give some indication about the source composition(Taylor and McLennan, 1985). In Fig. 28, Ortakoy semipelite, psammite and quartzite fell an igneous differentiated trend with a ratio of 230 with magmatic trend. This figure suggests that Ortakoy semipelite, psammite and quartzite were derived from a series of igneous rocks ranging from mainly acidic to intermediate composition. The Fig. 29 supports acidic source for Ortakoy sediments, however some semipelites contain high Ni-Cr values (Fig. 30), suggesting some mafic-ultramafic contribution to the Ortakoy pelites. The Ni/Co ratio

varies between 0.5 and 9.8 in the semipelite and psammite, 2 and 16 in the quartzite, probably due to variable degrees of chemical weathering in the mafic-ultramafic source rocks that would tend to selectively enrich in Ni and Co, weathering products. Average Th in Ortakoy semipelite and psammite grouped together (16.9) is similar or higher than the values in Narryer gneisses (11 to 15, Maas and McCulloch, 1991) that were suggested to derive dominantly from K-rich granitic sources , Western Australia. Similarly, this high Th value is consistent with a potassic granite source for Ortakoy semipelite, psammite, and probably quartzite due to its rich Th content (8.0). Thorium/Uranium ratios in the semipelite, psammite and quartzite change from 2.66 to 25, probably because of poor XRF sensitivity at low abundances, possible U mobilisation during the metamorphism and recent weathering.

In Fig. 31, the samples of Ortakoy semipelite, psammite and quartzite are found on quartzose, intermediate and felsic source. Probably weathering was effective on the composition of the Ortakoy sediments, CIA is above 60 indicating relatively moderate chemical weathering and variable U/Th ratios, and caused the scarcity on this diagram but also minor contributions from dominantly intermediate and basic-ultrabasic rocks to the Ortakoy sediments are likely.

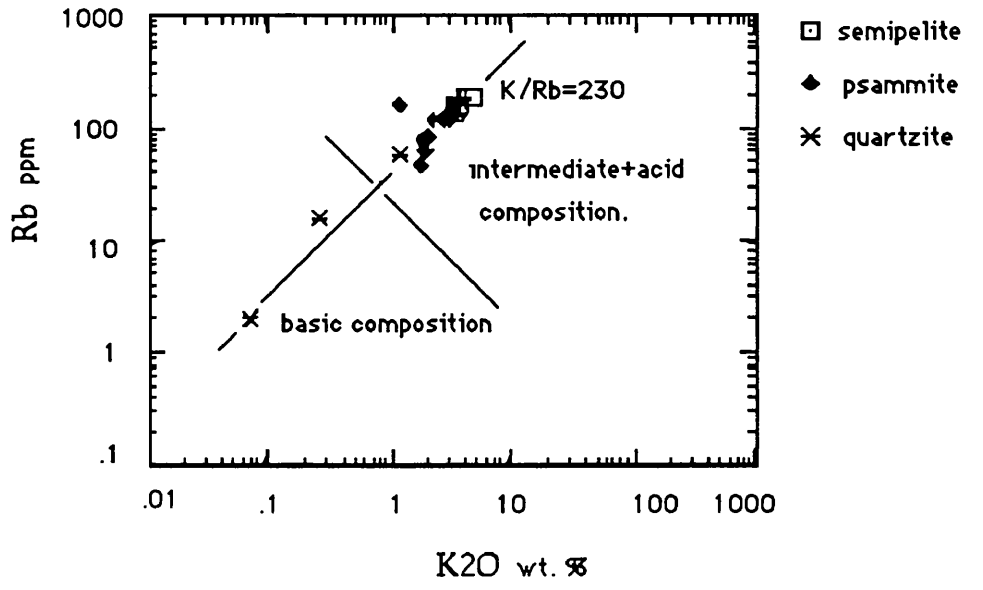

Figure 28: Relation of K2O with Rb (main trend of Shaw, 1968)

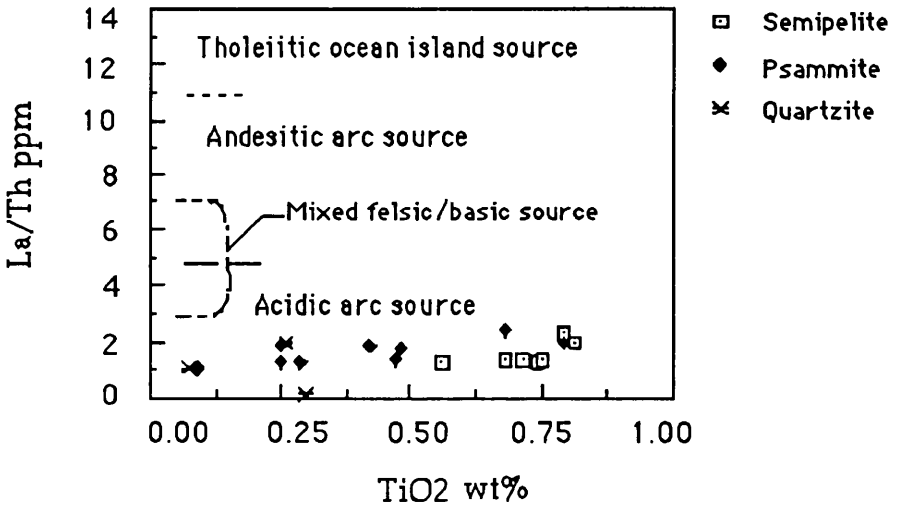

Figure 29 : Plot of TiO2-La/Th showing the source of the Ortakoy semipelite, psammite and quartzite. (data from Bhatia &Taylor, 1981; McLennan et al.,1984; Taylor &McLennan, 1985)

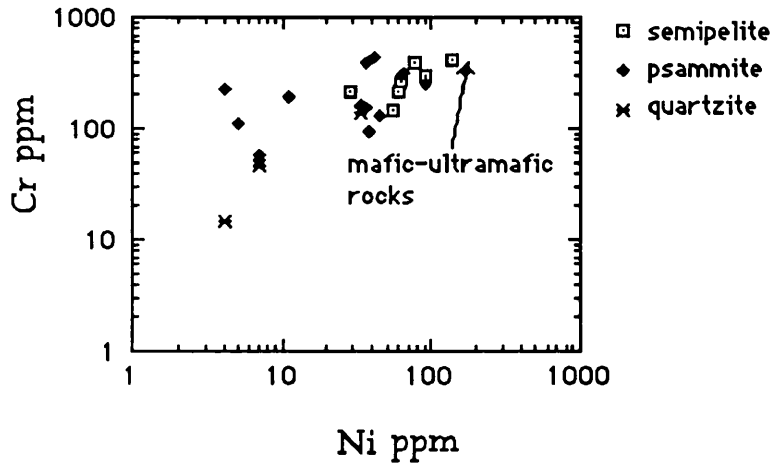

Figure 30 : Cr-Ni plotting of the Ortakoy semipelite, psammite and quartzite.

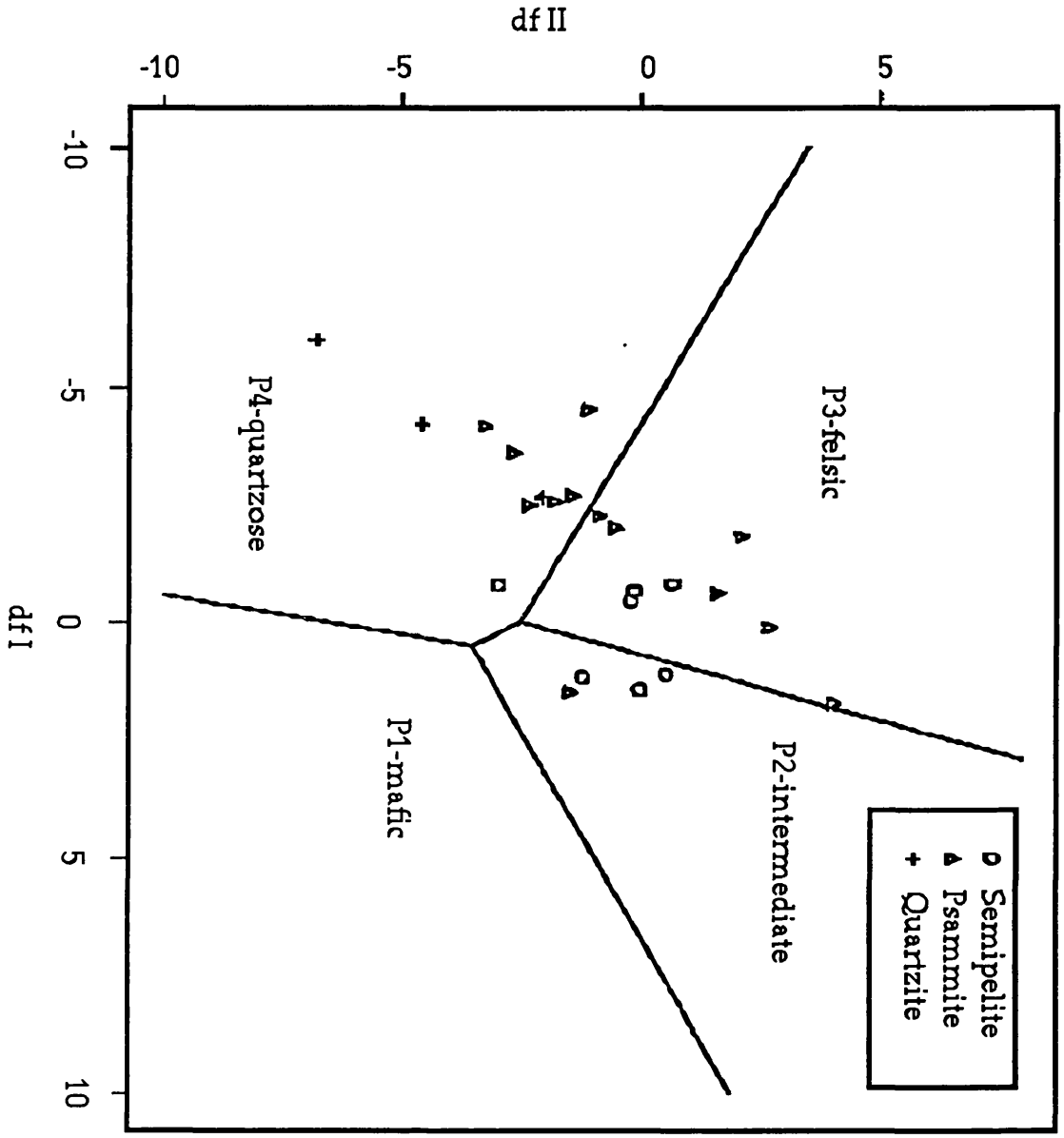

Figure 31: Diagram showing the source of the Ortakoy semipelite, psammite and quartzite. (Fields after Roser & Korsch, 1988)

IV.2.4 REE Analyses

Three representative samples of psammite were analysed to determine their REE content. The samples would not go completely into the solution, despite being treated by acid several times. The relicts contained tourmaline as determined by means of XRD. In Fig. 32, the REE pattern of psammite and tourmaline are given altogether.

Ortakoy psammite are characterised by LREE enrichment(La/Lu= 36-49), fractionated HREE (Gd/Yb= 6.6 to 8.6) and slight negative Eu anomaly. If the the tourmaline had been dissolved with the rest of the samples into the solution it would be likely to have a less fractionated HREE pattern with distinct negative Eu anomaly. The presence of Eu-depletion may be interpreted as reflecting shallow, intracrustal differentiation resulting in Eu depletion in the upper crust, associated with the production of granitic rocks(McLennan, 1989). These intracrustal processes can include both partial melting where plagioclase is a residual phase or fractional crystallisation where plagioclase is a fractionating phase (Hanson, 1980, 1989). On the basis of petrographic, geochemical, and isotopic data, several major source components for sediments deposited at active continental margins were suggested (McLennan et al.,1990). One source is old upper crust which is made up either old igneous /metamorphic terrains or old, recycled sedimentary rocks. Such sources are likely to have flat HREE pattern which is probably characteristic for average, or typical upper continental upper crust. A second major source is a young component derived from island arc or continental arc material. At shallow depth (e.g. within the field of plagioclase stability), igneous rocks which has not undergone significant crystal fractionation will show less fractionated REE patterns with no Eu-anomalies. A third possible source is fractionated felsic volcanics and

plutonic rocks which might be incorporated into sediments during explosive volcanism or , more likely, when the arc is matured and dissected to expose plutonic root zones. They are likely to exhibit different REE patterns but in general will have negative Eu-anomaly as plagioclase removed during their igneous history (McLennan et al., 1990). The REE pattern of Ortakoy psammite which has depleted HREE with slight Eu-anomaly probably represents the source rocks of fractionated felsic volcanics and plutonics. Such HREE depletion is probably the signature of either garnet fractionation sometime in the igneous history of the provenance or a reflection of the mantle source REE pattern (McLennan, 1989). In Archean greenstone belts, similar patterns without Eu-anomalies occurs and interpreted as showing the sediments being derived from Na-rich granitic and felsic volcanic rocks (Fig. 33).

Finally, the Ortakoy psammites were probably derived from acidic plutonic and volcanic rocks which might have been fractionated since the psammites pattern have negative Eu-anomaly.

IV.2.5 Conclusions

It has been shown that K, Fe+3, Ti, Rb, Zr and possibly Ba, Ni and Zn were probably added in sheet silicates. This is supported by plotting against TiO2 which shows better correlation than that against al-alk due to removing the influence of any alkali variation and variation in feldspar abundance.

Ca and Sr were added in carbonate and/or feldspar and, Y added mainly in apatite and zircon in the original sediments that contains detritial sodic plagioclase. Al were also largely added in feldspar and possibly in clay materials.

The linear correlation of the average values of those elements against average al-alk shows that a similar clay mineral end member, illite with substantial Si and Fe, was added to all Ortakoy sediments in various proportions. The sheet silicates were probably the dominant factor controlling the composition of the sediments and this may be applicable to the general sediments.

The quartzite has lower average values in Fe, Ti, K, Zr, Rb, Zn, Ba and Ni than the rest of the sediments because of probably being deposited rapidly, which did not allow enough time for absorbtion of various elements from sea-water.

The carbonates were not altered after the deposition since they have low Mn and Sr/Ca ratios. Both physical and chemical precipitation were effectual at the forming of Ca-silicates.

Finally, the metasediments were largely derived from non mafic source, particularly acidic igneous and volcanic rocks (probably fractionated) with possible minor basic-ultrabasic contributions and deposited in an Andean type continental margin environment. Some of the sediments might have been deposited in an continental island arc. The source of the sediments probably suffered from moderate chemical weathering as their CIA are about 68 (average of semipelite and psammite)

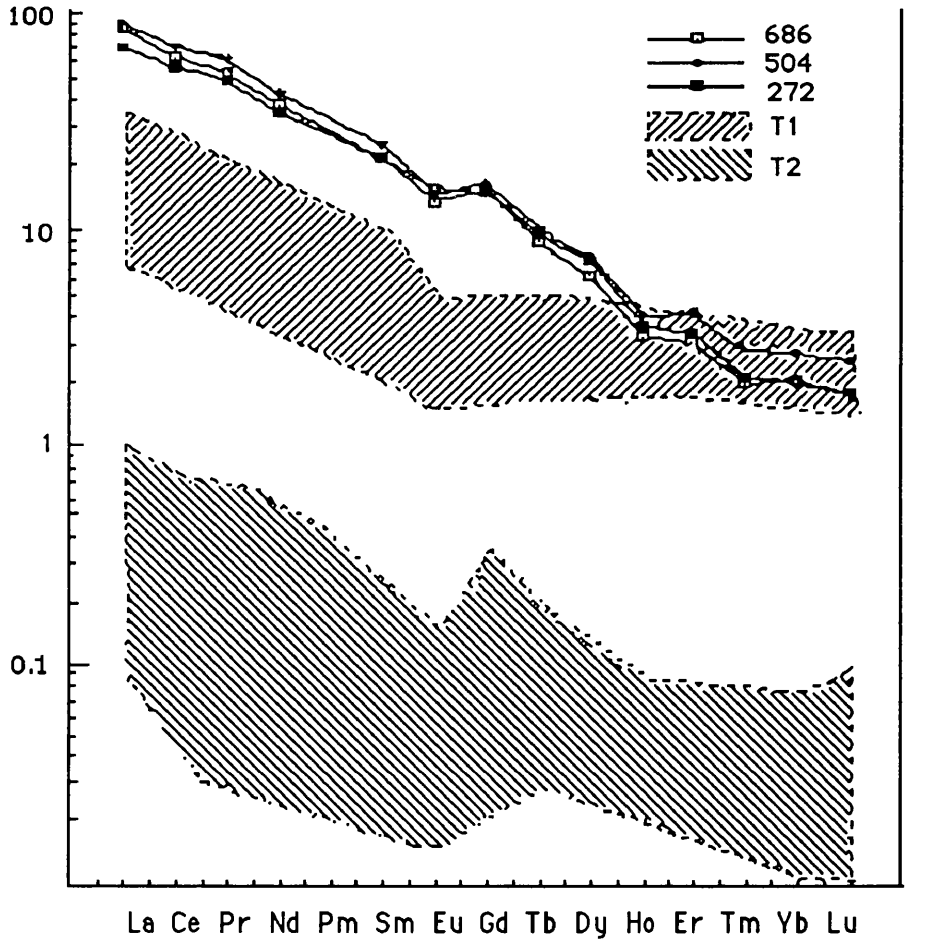

Figure 32: Chondrite normalised (Boynton, 1984) Rare Earth Element analyses of the Ortakoy psammite. REE analyses of tourmaline (T1 and T2) are also given to take account for tourmaline omission from the the psammite. T1 : Data from Jollif et al.,1987; King et al., 1988 (within T1 area), T2: Jollif et al., 1987.

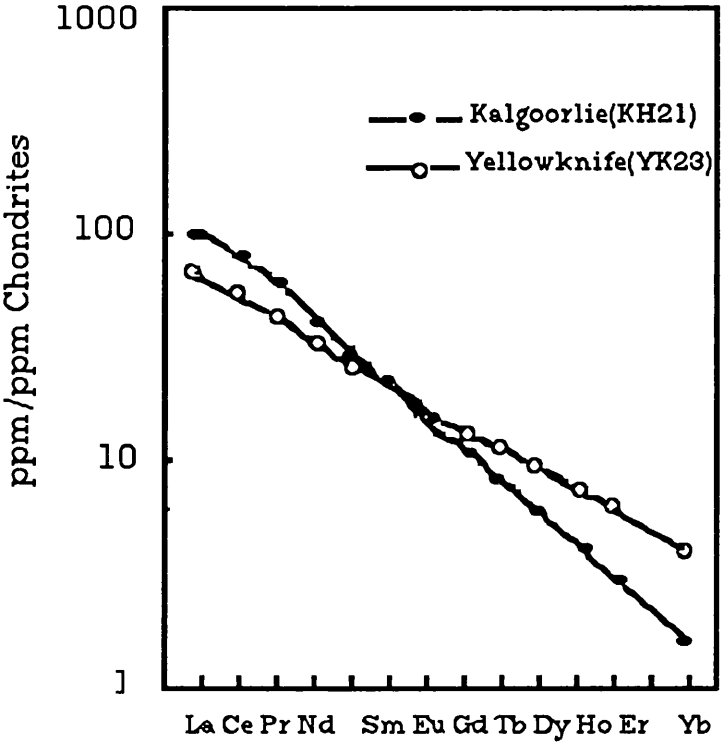

Figure 33: Chondrite normalized REE diagram for greywacke-shale turbidites from Archean greenstone belts. Data from Wildeman and Condie (1973), Nance and Taylor (1977), Bavinton and Taylor (1980), Jenner et al. (1981), McLennan et al. (1983).

IV.3 AMPHIBOLITE

IV.3.1 Major and Trace Elements

Table 35 lists the results of major and trace chemical analyses of the Ortakoy amphibolites. These plot in and around the igneous trend of Shaw(1968) while in Leake (1964)'s amphiboli[te]discrimination diagram, they are situated where the fields of pelite-limestone mixtures and igneous rocks overlap (Fig.s 34 and 35). The amphibolites usually have diopside and hypersthene in their norms and are mainly andesitic but with some basaltic compositions (Fig.s 36 and 37). Fig. 38 shows their subalkaline character in a plot of total alkali versus silica. The amphibolites mainly fall in the calc-alkaline field in Fig. 39 which is a plot of SiO2 versus FeO (total)/MgO.

The good correlation between Zr and Y and lack of a positive correlation between P2O5 and Y (Fig. 40) suggest that Y was largely held in zircon rather than apatite. Al and Ni do not show any clear correlation with Ga and Cr in Fig.s 41 and 42 due to insufficient samples albeit these elements have similiar chemical features such as ionic radii and ionic charge.

Major and trace elements of the amphibolites were plotted against Niggli mg (Fig.s 43 and 44) to find if fractional crystallisation was involved in the petrogenesis of the amphibolites. Niggli mg has variable possible negative correlations with P2O5, Cu, Sr, Ba, Ni and Cr, and positive correlation with MnO,Zn, Pb. Therefore, it is unlikely that the amphibolites were formed by fractional-crystallisation However the number of samples makes this tentative.

Pearce and Cann (1973) show that immobile elements must be considered important in establishing the tectonic setting of the basic rocks as these elements are least affected by alteration and metamorphism. Accordingly, Fig. 45 which is a binary plot of Zr and Zr/Y, shows that the geotectonic setting of the Ortakoy amphibolites is that of within plate basalts

IV.3.2 REE Analyses

Two samples of the Ortakoy amphibolites were analysed and their chondrite normalized REE patterns are shown in Fig. 46. They are marked by LREE enrichment (La/Lu : 6.5 - 11.84) with slightly fractionated HREE (Gd/Lu : 1.9 - 2.3) which is typical for continental basalt. This LREE element enrichment also indicates a garnet-bearing source rock. They show a negative Eu anomaly, which is indicative of plagioclase removal.

IV.3.3 Conclusions

The Ortakoy amphibolites represent andesitic or basaltic rocks which have subalkaline and calc-alkaline character and are derived from a garnet-bearing source. They also have within plate geochemical features consistent with a continental derivation.

Table 35 : Major and minor chemical analyses of the Ortakoy amphibolites

Sample No	684	689	690	685	Mean	σn
SiO2	50.32	55.41	59.84	57.62	55.80	3.53
TiO2	0.6	0.6	0.78	0.78	0.69	0.09
Al2O3	17.98	17.01	11.78	16.77	15.88	2.41
Fe2O3	1.64	1.17	1.30	1.12	1.31	0.20
FeO	8.16	5.36	5.80	4.72	6.01	1.30
MnO	0.12	0.12	0.13	0.1	0.11	0.01
MgO	5.05	3.11	4.73	2.70	3.89	1.00
CaO	10.3	12.14	11.84	12.67	11.74	0.88
Na2O	1.91	1.49	1.31	1.83	1.63	0.24
K2O	0.93	0.4	0.43	0.05	0.45	0.31
P2O5	0.09	0.07	0.02	0.12	0.07	0.04
CO2	0.35	0.72	0.37	0.1	0.38	0.22
H2O	2.50	2.45	1.68	1.19	2.21	0.38
Total	99.95	100.05	100.01	99.77		
Zr	92	162	124	170	137	31
Y	20	28	28	33	27	5
Sr	276	867	234	732	527	277
U	0	0	0	1	0	0
Rb	39	6	9	20	18	13
Th	5	15	7	12	10	4
Pb	15	7	15	5	10	5
Ga	16	24	16	24	20	4
Zn	97	80	109	83	92	12
Cu	5	5	1	8	5	3
Ni	20	76	7	67	42	30
Co	41	27	11	19	24	11
Cr	100	257	106	169	158	63
Ce	22	70	37	63	48	19
Ba	182	514	57	351	276	173
La	11	30	18	31	22	8

Mineralogical composition and coordinates of the samples

684 hbl+pl+bt	87512-87887
689 hbl+ pl+ di+ sp	85650-88550
690 hbl+ qtz+ pl+ di	85655-88560
685 pl + hbl+ qtz+ sp	85825-87875

Mean : Arithmetical mean

σn : Standard deviation

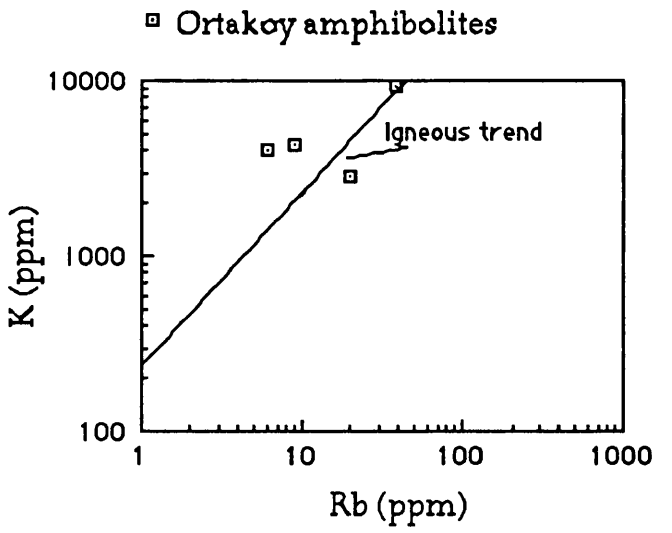

Figure 34: Plot of K versus Rb (igneous trend from Shaw, 1968)

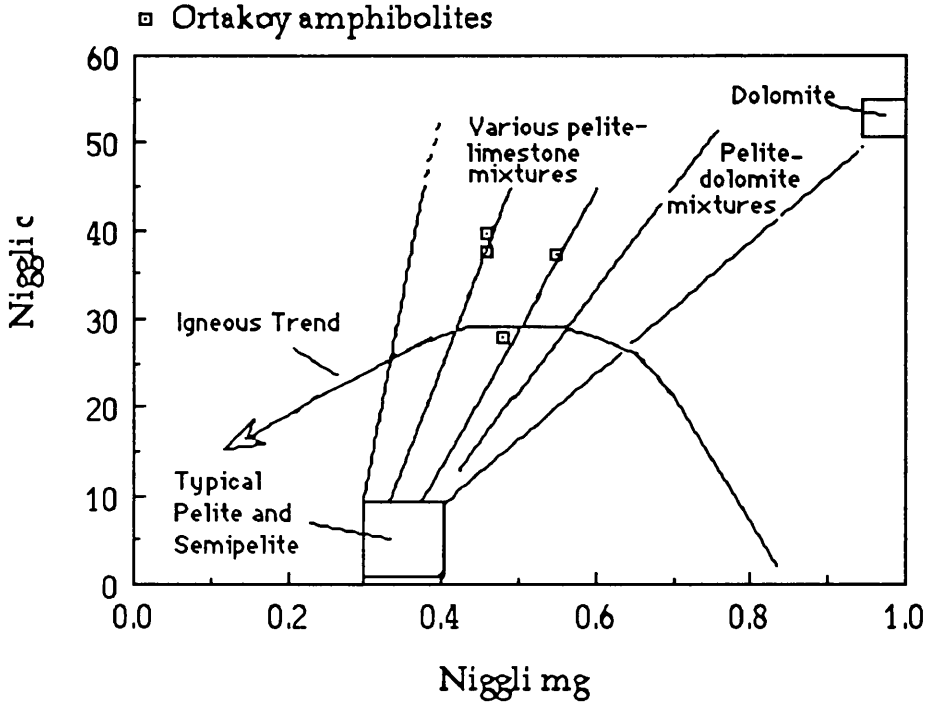

Figure 35: Niggli c-mg variation in the amphibolites (after Leake, 1964).

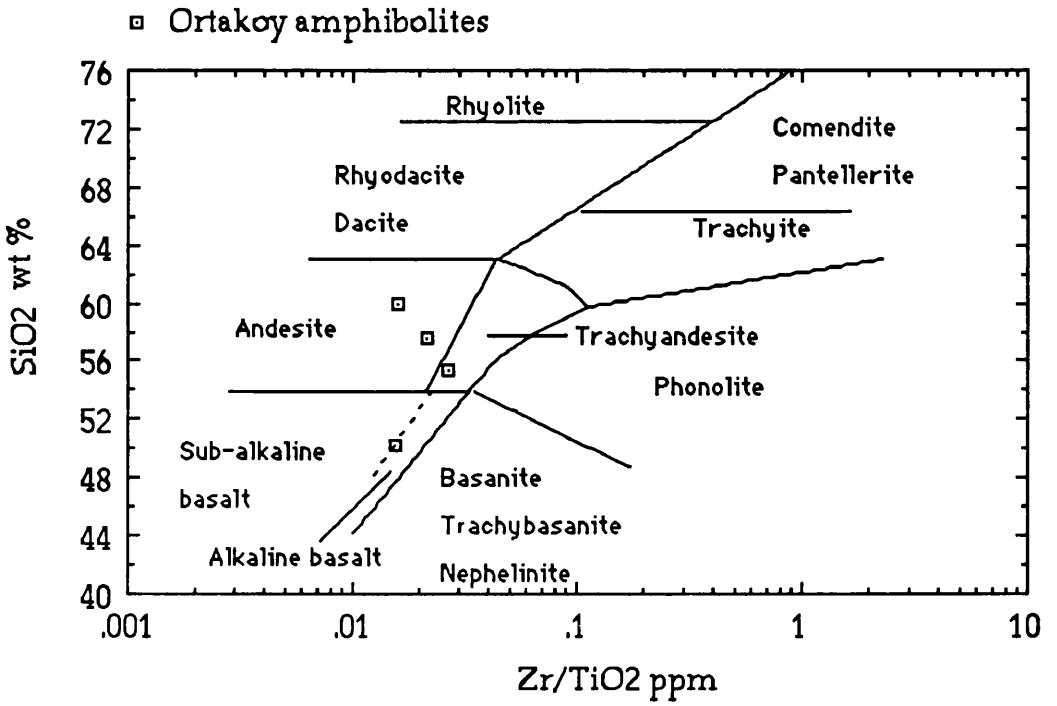

Figure 36: Classification of the amphibolites according to Zr/TiO2 and SiO2 parameters, after Winchester & Floyd(1977).

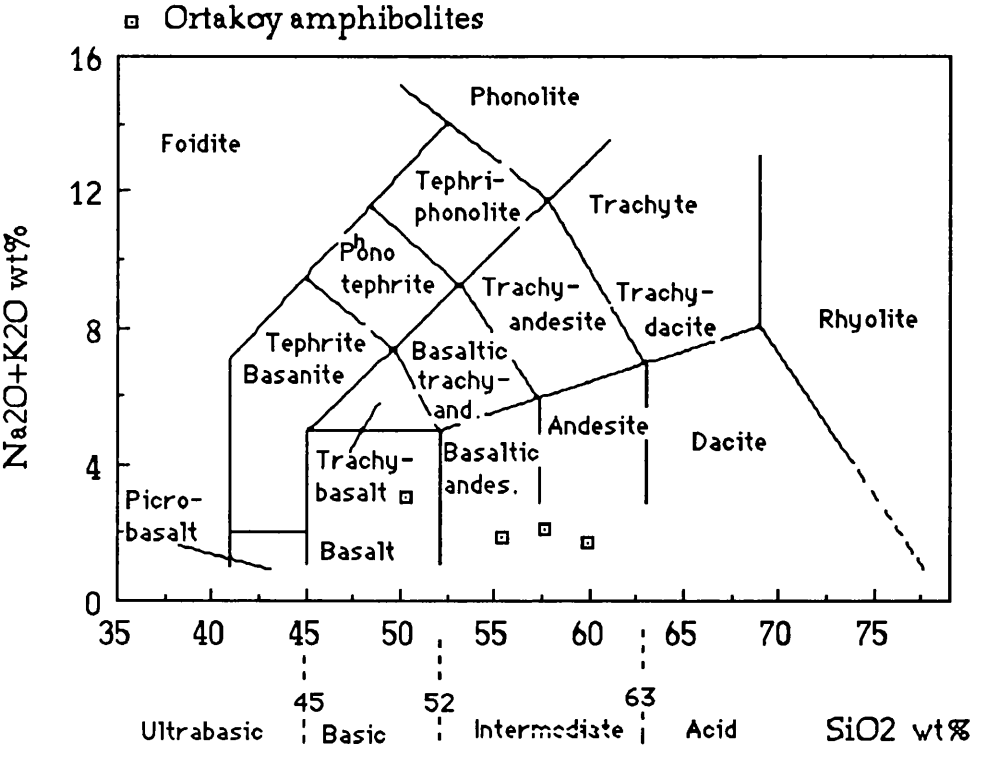

Figure 37: SiO2 versus Na2O+K2O, showing original rock groups of the amphibolites (after Le Bas et al., 1986).

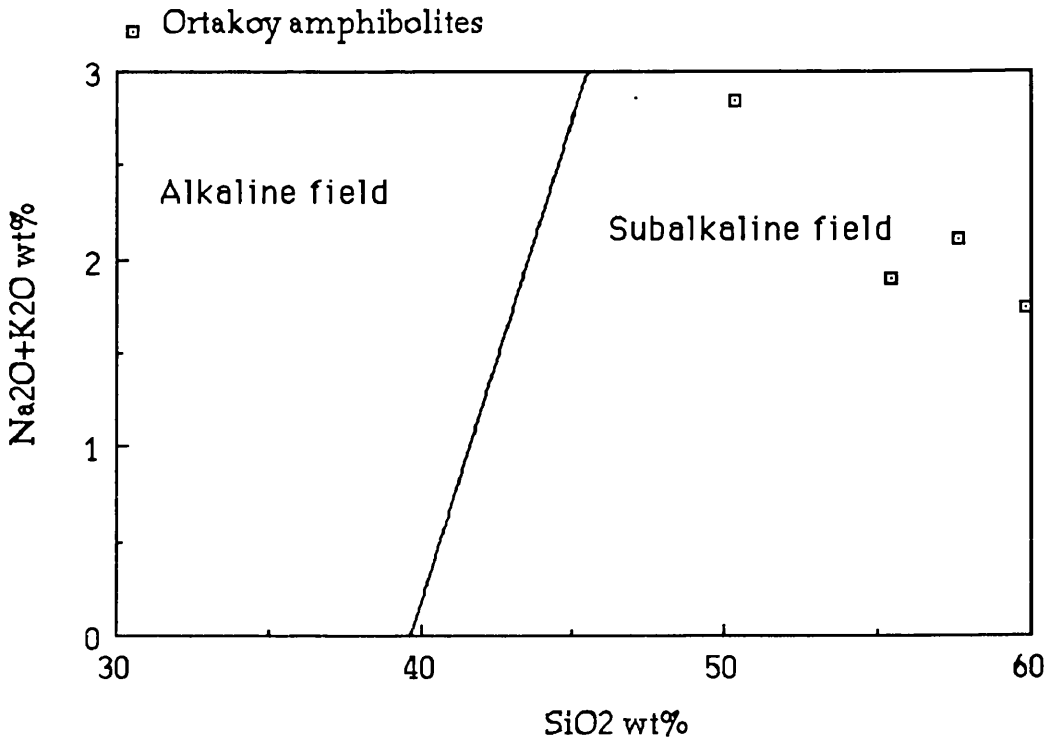

Figure 38: Alkali-silica variation in the amphibolites. (Fields after Irvine & Baragar, 1971)

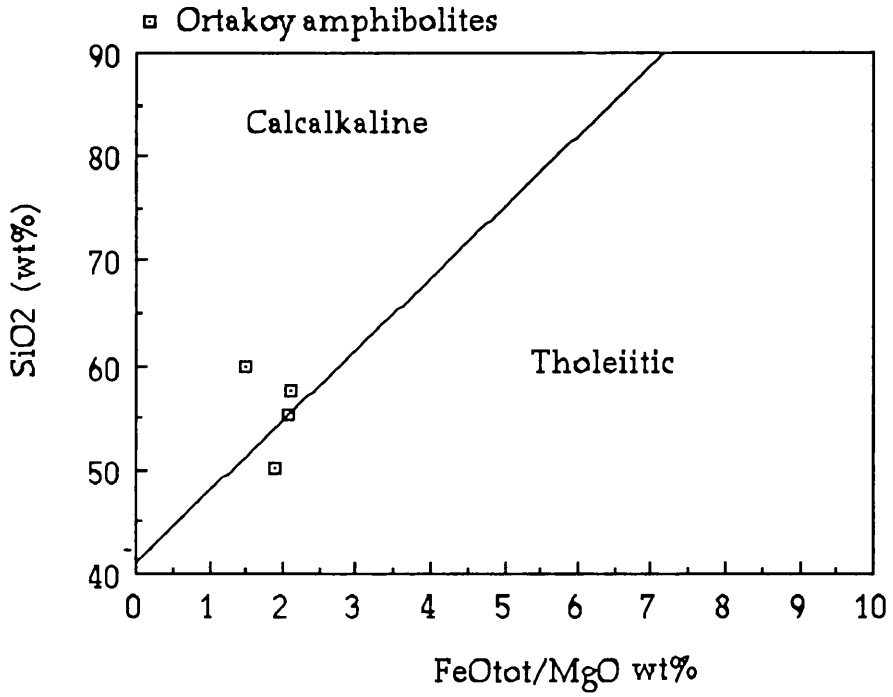

Figure 39: Plot of SiO2 versus FeOtot/MgO, showing calcalkaline character in the Ortakoy amphibolites, after Miyashiro(1974).

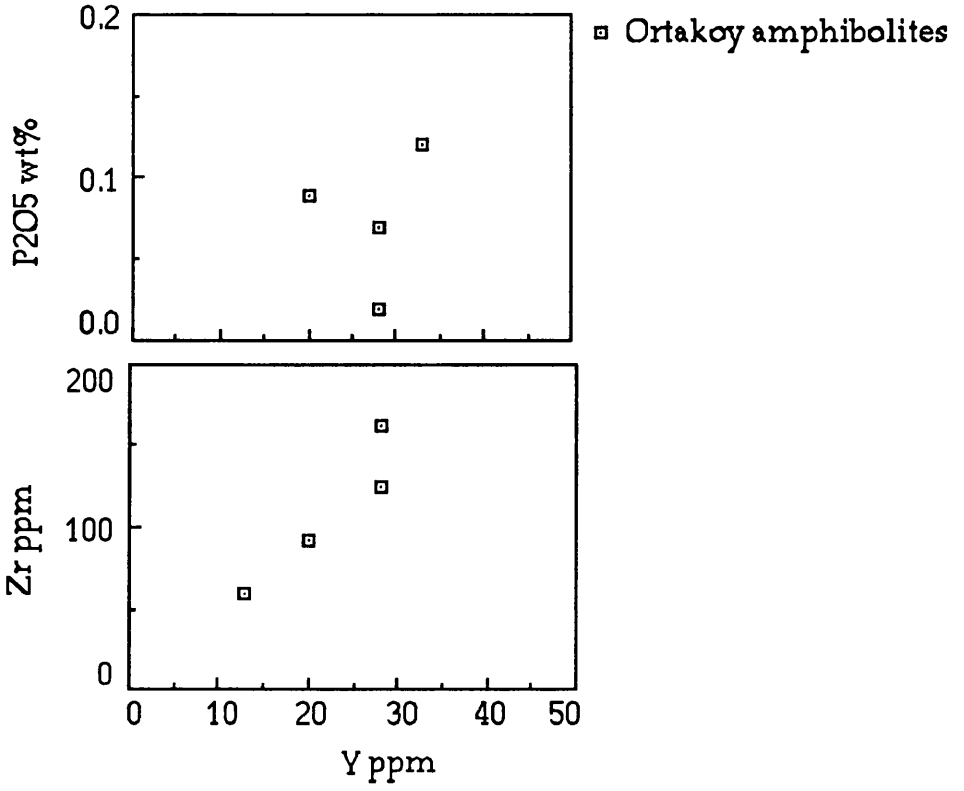

Figure 40: P2O5, Zr and Y variation in the amphibolites

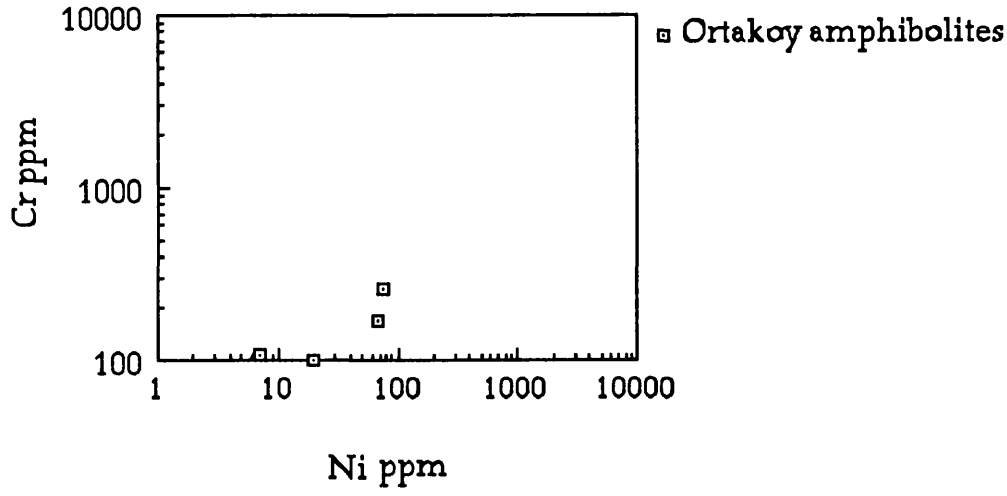

Figure 41: Plot of Cr against Ni.

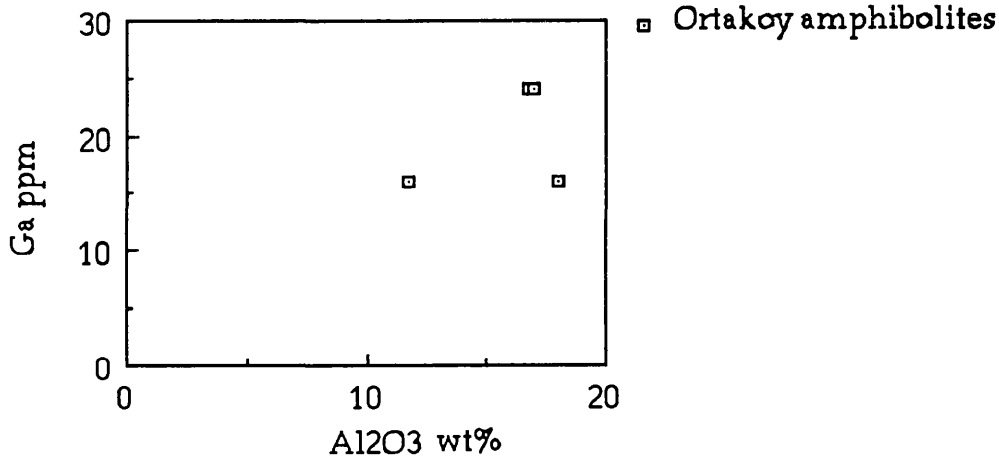

Figure 42: Plotting Ga versus Al2O3.

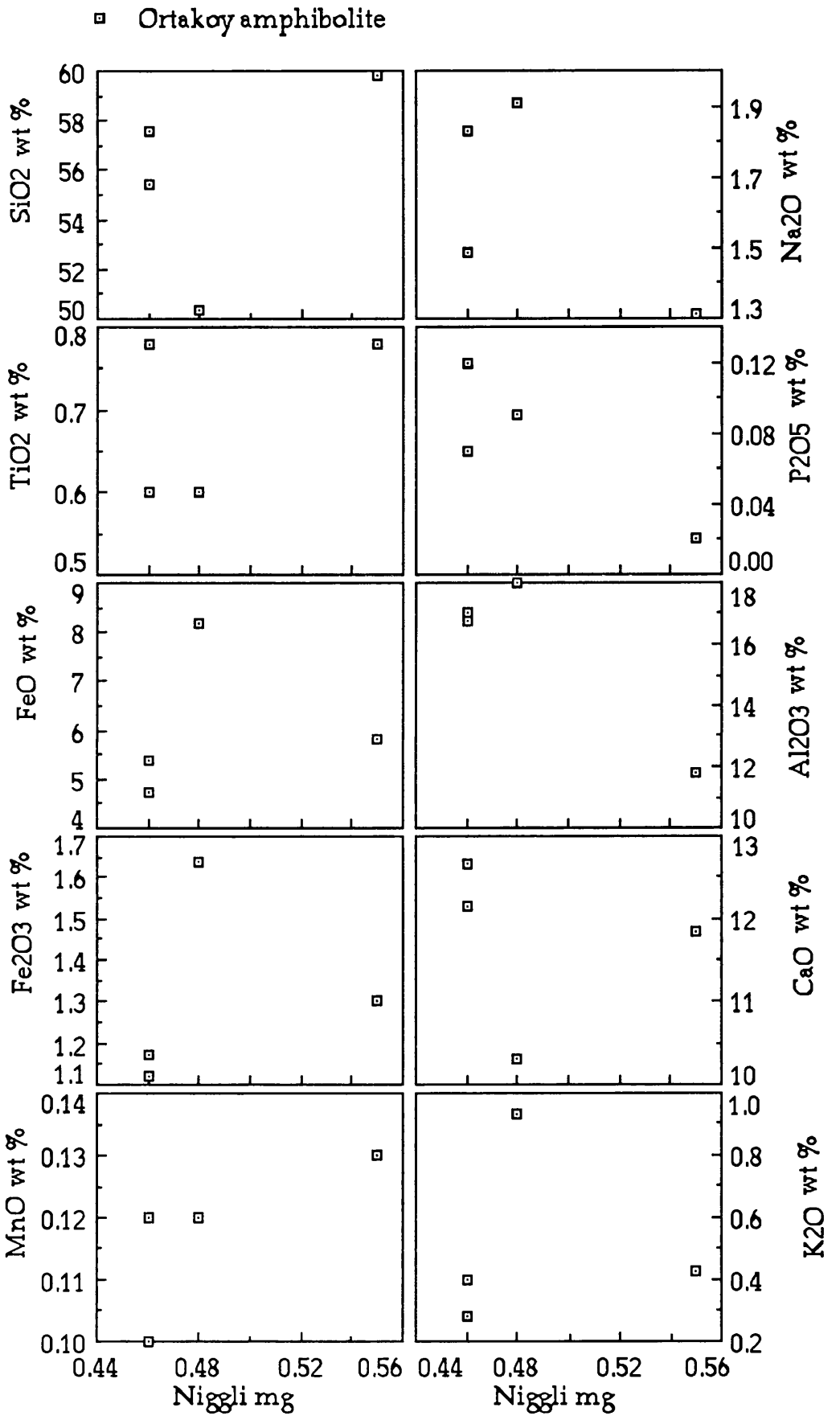

Figure 43: Plots of major oxides versus Niggli mg.

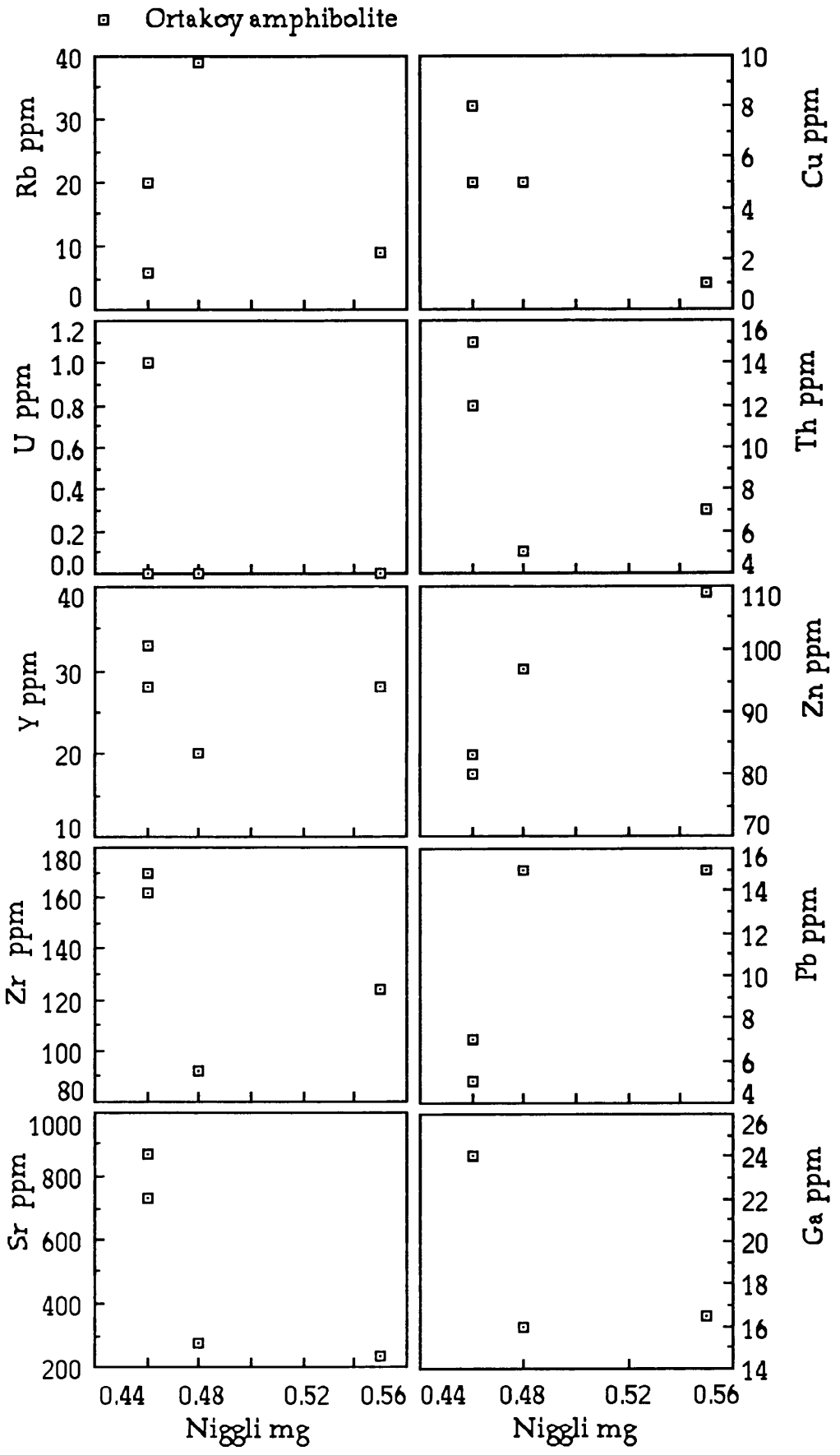

Figure 44 : Trace elements versus Niggli mg

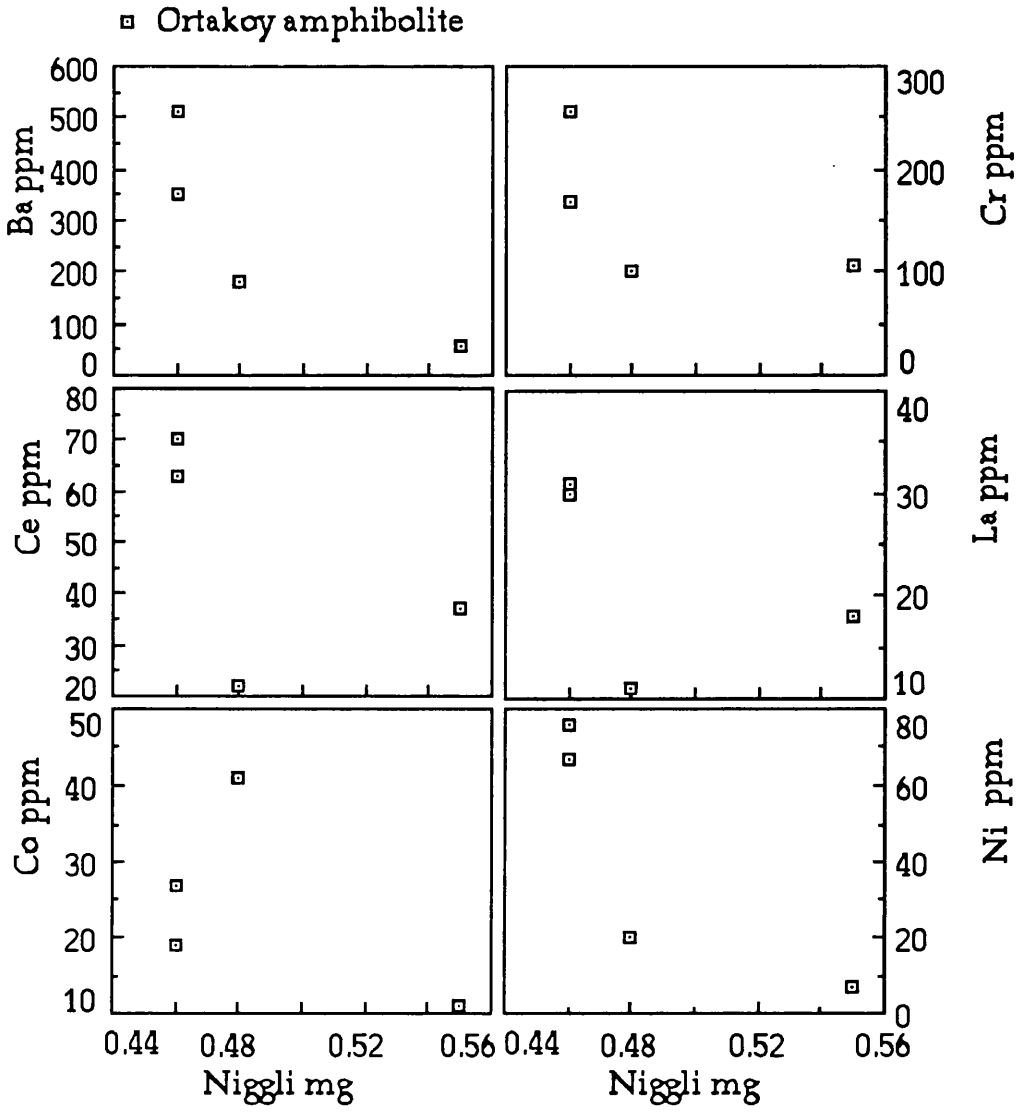
Ortakoy amphibolite
Ba ppm
600
500
400
300
200
100
0
Cr ppm
300
200
100
0
Ce ppm
80
70
60
50
40
30
20
La ppm
40
30
20
10
Co ppm
50
40
30
20
10
Ni ppm
80
60
40
20
0
0.44
0.48
0.52
0.56
Niggli mg
Niggli mg

Fig. 44: cont.

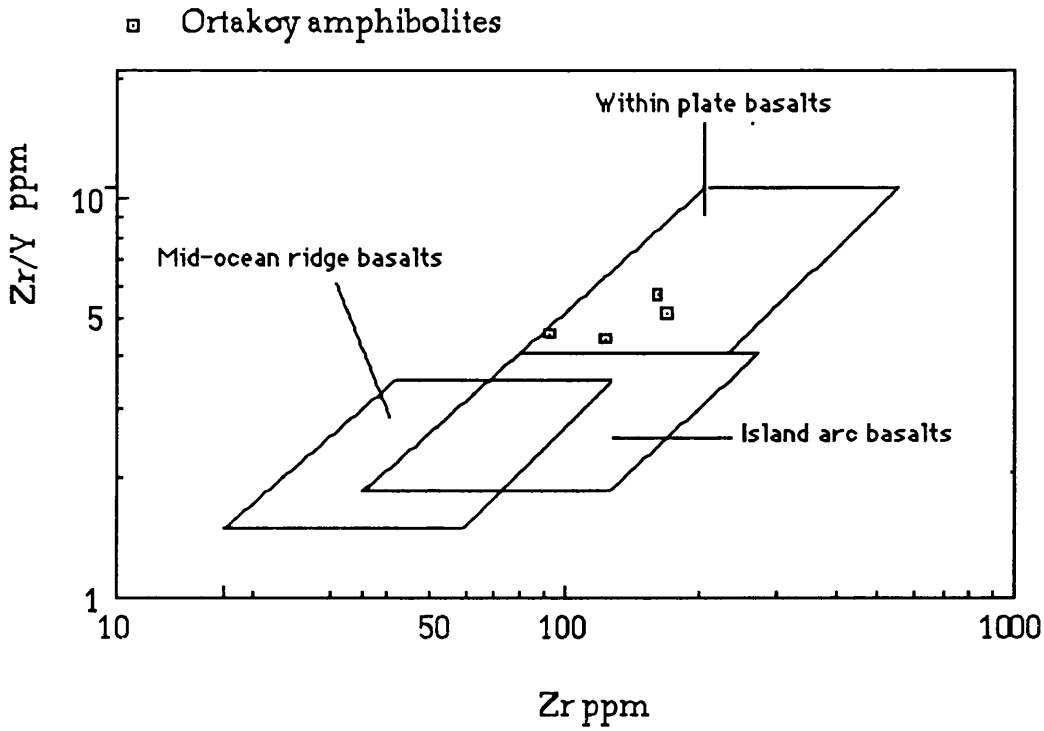

Figure 45: Zr/Y versus Zr plotting, fields after Pearce & Cann(1973).

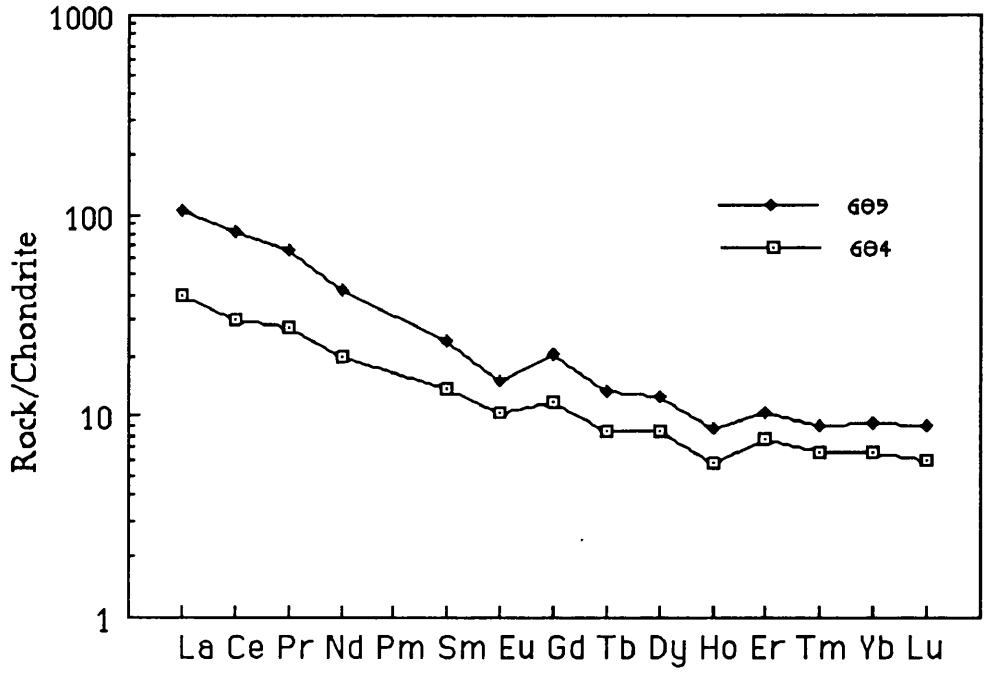

Figure 46: Chondrite normalized (Boynton, 1984) REE analyses of the Ortakoy amphibolites

IV.4 PARAGNEISSIC GRANITE

IV.4.1 Major and trace elements

The chemical compositions of a paragneissic granite produced by the heating and partial melting of semipelitic material by the intrusion of the Ortakoy diorite and, or the Ekecekdagi gabbro, is given in Table 36 together with analyses of inclusions of pelitic material which resisted melting because of their higher melting temperature due to their aluminous-rich and silica-poor nature. The abundant sillimanite, biotite and cordierite shows these inclusions to be clearly pelitic in origin and the existence of sillimanite+biotite+cordierite in the peraluminous anatectic granite shows that this is formed from a paragneiss.

The pelitic inclusions record a temperature based on the garnet-biotite exchange thermometer of Ferry and Spear's (1978) of 681± 50°C but probably exceeded this temperature and a pressure of 4.17± 0.29 kb determined from the compositions of garnet, biotite, sillimanite and cordierite using Holland and Powell's (1990) updated thermodynamic dataset. The inclusion compositions are typical of an originally clay-rich sediment with high contents of elements typically associated with clay minerals namely Al2O3, TiO2, FeO, MnO, MgO,Na2O, K2O and impoverished in SiO2.

The paragneissic granite formed from semipelite because of its gradational nature with metasediment.

IV.4.2 Conclusions

The paragneissic granite was formed from semipelite by the heating and partial melting induced by Ortakoy diorite and, or the Ekecekdagi gabbro at temperature of at least 681±59°C and 4.17±0.29 pressure. The anatectic, peraluminous granite contains inclusions of pelitic material which have higher K2O and Rb contents than the semipelite and granite. These inclusions resisted melting due to their aluminium-rich and silica-poor compositions.

Table 36: Major and minor chemical analyses of the inclusions and paragneissic granite and semipelite.

	(inclusions)					(705)	(Average)	
Sample No	340	711	708	Mean	σn	Paragneissic granite	Semipelite	σn
SiO2	49.17	51.62	50.91	50.57	1.03	69.79	62.48	1.38
TiO2	1.11	0.92	0.98	1.0	0.08	0.6	0.72	0.08
Al2O3	25.32	22.79	23.59	23.9	1.06	14.57	18.02	1.11
Fe2O3	4.9	3.0	3.21	3.7	0.85	0.93	4.04	0.93
FeO	5.46	5.91	5.68	5.68	0.18	3.6	1.73	1.01
MnO	0.19	0.25	0.24	0.23	0.03	0.09	0.04	0.02
MgO	3.05	2.51	2.62	2.73	0.23	1.76	1.77	0.38
CaO	1.05	1.23	1.22	1.17	0.1	1.26	0.44	0.09
Na2O	1.59	2.81	2.91	2.44	0.60	2.5	1.11	0.60
K2O	4.95	5.62	5.24	5.27	0.27	3.48	3.86	0.52
P2O5	0.1	0.08	0.07	0.08	0.01	0.12	0.08	0.03
CO2	0.27	0.28	0.28	0.28	0.00	0.0		
H2O	2.95	2.90	2.85	2.90	0.04	1.28		
Total	100.11	99.92	99.8			99.98		
Zr	188	153	171	171	14	175	211	23
Y	25	41	30	32	7	27	19	4
Sr	179	246	235	220	29	150	63	25
U	6	0	1	2	3	0.0	4	1
Rb	180	192	175	182	7	118	167	19
Th	26	14	16	18	5	9	18	5
Pb	31	40	40	37	4	25	18	5
Ga	34	28	32	31	2	17	21	1
Zn	137	127	123	129	6	72	85	12
Cu	28	39	32	33	4	23	24	9
Ni	40	45	50	45	4	33	72	34
Co	26	19	21	22	3	12	13	3
Cr	183	154	205	181	21	85	276	95
Ce	109	74	55	79	22	33	56	6
Ba	1238	1837	1873	1649	291	572	528	62
La	58	41	45	48	7	19	26	3

Mineralogical compositions of the samples

340 sil+bi+pl+crd+or+chl+qtz+gt
711 crd+sil+bi+gt
708 bi+sil+crd+gar+mus+chl

705 qtz+crd+bi+pl+or+gt(paragneissic granite).

Coordinations of the paragneissic granite and pelitic inclusions: 93000-86600

Mean: Arithmetical mean
σn: Standard deviation

IV.5 POST METAMORPHIC INTRUSIONS

IV.5.1 Ekecekdagi gabbro

IV.5.1.1 Major and trace elements

The results of chemical analyses of Ekecekdagi gabbro, "EG", and granophyres are presented in Tables 37 and 38. They are subalkaline and tholeiitic in composition (Figs. 47 and 48a-b) and have high CaO (~12-18%) low alkalis (Na2O 0.44-1.8 , K2O 0-0.22 %) when compared with average low K olivine-tholeiite which is equivalent of EG in Wilkinson's(1986) classification. Harker diagrams of EG, in which various degree of positive correlation with Na2O, Zr, Y, Cr, Zn and negative correlation with FeO, Fe2O3 against SiO2 exist are shown in Fig. 49. The rest of major oxides and trace elements display no clear trend. Some gabbro samples contain quite high Ba (> 300 ppm) which an analytical error is likely.

Niggli mg has positive correlation with CaO, Cr and Ni and negative correlation with TiO2, Al2O3, FeO, MnO, Ga and Zn (Fig. 50). In general trend of the diagram, a gap occurs between sample 345, ultrabasic rock and the rest of the samples. It is probably due to insufficient sampling or scarce occurence of this kind rock in the formation.

Y correlates well with Zr and P2O5 (Fig. 51) due to substantially being concentrated in zircon and apatite.

Several veins of successive hornblende gabbro, hornblende microgabbro and granophyre, as mentioned in the petrography chapter were determined from the Bozkir Dam cutting. Major oxides and trace elements plotted (Fig. 52) against the known intrusion order gives the chemical variation during the intrusion sequence. There is a clear alternation of acid and basic magma pulses and the third basic intrusion,

hornblende gabbro has the lowest Al2O3, Na2O, Ga, Sr and the highest MgO, Ni, Cr and Cu indicating that the basic magma initially became more basic with time such as occurs with progressive partial melting of the mantle but later became less basic. In the granophyres, the second pulse possesses higher SiO2, CaO, FeO, Cr and Cu and lower Fe2O3, K2O, Ga, Pb, Rb, Ba, Zn, Ce than the first one.

Mantle normalised EG pattern is shown in Fig. 53 with mantle normalised Upper Crust, "UC", and Lower Crust, "LC". Clearly, close similarity is seen between the patterns of EG and LC though EG was depleted relatively in K, La, Sr, Zr, Ti and particularly Ce. The concentration of elements in UC, as expected are generally higher than that in EG apart from Ti what is much the same in both EG and UC.

The fractionation is evaluated graphically by using methods described by Cox et al.(1979). Fig. 54 suggests that the compositions of the anorthite and diopside were controlled by fractionation.

The fractionation was tested with linear least-squares mass balance computer calculations (Table 39) using an XLFRAC computer program (Stormer&Nicholls, 1978) with the bulk chemical analyses of hornblende gabbros which are ones of the most primitive and evolved samples, and microprobe analyses of diopside and anorthite as initial phases. The sum of the squares of the residuals is larger than 1 (28.38), indicating negative result. This is probably because of that the assumed initial composition may have cumulative character and hence it may not represent the original magma composition.

Most models for the formation of tholeiites assume about 20-30 % melting of upper mantle peridotite (Cullers&Graf, 1984). Tholeiitic basalts can also be produced by a low pressure and H2O rich volatiles while high

pressure and CO2 rich volatiles produce alkali basalts (Yoder, 1976). Similarly, EG may be formed by a higher degree of melting, a lower pressure, or a high H2O/CO2 ratio, and possibly coupled by fractional crystallisation of diopside and anorthite.

The granophyre considered to be situated almost at the top of the EG might have been formed by continuous differentiation from Ekecekdagi basic magma. As Naslund(1983) showed experimentally for granophyre to originate by differentiation would require the magma to change through a series of major element compositions which is immiscible. The high P, La, Sr, Ce and Zr contents of granophyre do not show this since these elements would show enrichment in the more mafic liquid (Watson, 1976). For the granophyre in EG to originate by partial melting of the metasediments of Seksenusagi and Gobektepe formations it seems necessary for the K2O to be higher than the observed average of 0.29±0.23%.

IV.5.1.2 REE analyses

Three samples of EG , one of which is ultrabasic (345) were analysed and results are shown in Fig. 55. Basic rocks are characterised by LREE enrichment (La/Lu ~2-6) while the ultrabasic sample, 345 shows slight LREE depletion (La/Lu 0.5). HREE in both group show almost no fractionation (Gd/Lu~1). Samples 552 and 345 exhibit positive Eu anomalies, indicating accumulation of plagioclase crystals. The most noticeable features are low Ce and high La/Ce ratios in the samples. In the oceans, the shelf waters have normal La/Ce ratios(Humphris, 1984), but the La/Ce are high in the open ocean because of Ce removal preferential to the other Lanthanides(Brookins, 1989). Therefore, this large La/Ce ratio in EG is probably due to sea-water affect on EG, which could have influenced the Ce.

IV.5.1.3 Conclusions

Fractional crystallisation of diopside and anorthite can be responsible for main chemical variations in EG, which are depletion of CaO, MgO and Ni and enrichment of SiO2, TiO2, Al2O3, FeO, MnO, Na2O, Ga and Zn

It has been suggested that EG with tholeiitic character may be formed from a mantle peridotite by a higher degree of melting, a lower pressure, or a high H2O/CO2 ratio. This was possibly coupled by fractional crystallisation of diopside and anorthite.

The granophyre is shown to have genetic relation with neither EG nor the metasediments of Seksenusagi and Gobektepe formations.

Sea-water might have been responsible for the low Ce and high La/Ce ratio in the REE patterns of EG.

Table 37: Major oxides and trace element analyses of the Ekecekdagi gabbro.

Sample No	567	418	424	420	419	425	426
SiO2	48.22	50.31	48.42	48.99	50.50	46.45	49.21
TiO2	0.20	0.34	0.24	0.43	0.42	0.20	0.46
Al2O3	17.34	14.73	7.79	17.85	15.02	15.98	14.20
Fe2O3	1.4	2.19	2.67	2.13	2.16	2.19	2.14
FeO	4.60	5.84	5.25	6.62	6.44	3.97	6.71
MgO	9.17	9.56	16.27	7.76	8.70	12.01	9.98
MnO	0.13	0.12	0.18	0.17	0.17	0.13	0.15
CaO	16.73	13.23	16.82	11.91	12.25	16.35	13.05
Na2O	0.83	1.57	0.30	1.79	1.82	1.00	1.44
K2O	0.02	0.11	0.00	0.12	0.00	0.04	0.07
P2O5	0.03	0.04	0.03	0.05	0.03	0.02	0.06
H2O	1.35	1.60	1.55	1.60	2.35	1.65	2.40
CO2	0.10	0.22	0.37	0.48	0.17	0.21	0.17
Total	100.12	99.86	99.89	99.90	100.03	100.20	100.04
U	3	1	0	0	2	3	3
Th	0	1	0	0	1	0	2
Ce	0	0	0	0	0	0	0
La	2	0	0	0	2	0	2
Pb	0	3	0	0	10	2	2
Ba	48	121	162	42	422	27	149
Zr	23	19	22	30	23	13	29
Y	10	18	11	14	16	9	15
Sr	100	81	53	85	85	76	96
Rb	6	7	3	5	3	2	6
Ga	9	11	4	12	11	9	12
Zn	46	63	39	52	79	59	72
Cu	21	85	270	56	96	52	58
Ni	78	87	195	44	51	110	104
Co	29	39	56	34	31	40	40
Cr	269	459	610	302	369	381	505

Table 37. cont.

Sample No	215	307	60	57	212	552	554
SiO2	45.32	48.80	46.95	47.33	46.71	45.10	45.78
TiO2	0.34	0.24	0.47	0.21	0.42	0.32	0.32
Al2O3	16.54	18.55	16.37	10.08	17.78	18.11	17.12
Fe2O3	2.15	1.83	1.59	2.02	1.78	2.21	2.62
FeO	7.85	4.83	9.31	4.38	8.00	7.38	6.62
MgO	9.83	6.85	8.80	12.96	8.37	9.36	8.75
MnO	0.20	0.11	0.21	0.10	0.18	0.18	0.14
CaO	14.14	14.68	12.71	18.81	13.04	14.37	16.05
Na2O	0.78	1.36	1.17	1.52	1.35	0.82	0.44
K2O	0.01	0.03	0.03	0.01	0.22	0.02	0.02
P2O5	0.03	0.03	0.03	0.03	0.03	0.02	0.02
H2O	2.50	2.58	2.21	1.98	1.97	1.91	1.18
CO2	0.18	0.30	0.15	0.35	0.14	0.15	0.23
Total	99.87	100.19	100.00	99.78	99.99	99.95	99.29
U	1	1	2	3	2	0	0
Th	0	0	0	2	3	0	0
Ce	0	0	0	0	0	0	0
La	0	2	0	0	2	0	0
Pb	0	3	0	11	6	0	0
Ba	18	44	353	483	31	12	19
Zr	19	15	13	14	18	17	21
Y	8	10	12	8	12	0	9
Sr	71	103	80	61	80	68	69
Rb	3	5	2	5	14	3	4
Ga	10	11	12	6	12	11	12
Zn	47	48	70	34	66	42	42
Cu	36	20	43	225	22	76	118
Ni	35	52	57	116	46	46	59
Co	46	34	43	48	41	44	44
Cr	216	275	302	464	117	197	262

Table 37. cont.

Sample No	556	308	345	Mean	σn
SiO2	46.52	47.71	42.70	47.35	1.94
TiO2	0.22	1.00	0.87	0.39	0.22
Al2O3	17.09	15.72	17.74	15.76	2.79
Fe2O3	2.14	2.25	3.37	2.17	0.43
FeO	7.06	6.23	13.21	6.72	2.12
MgO	9.37	9.22	5.67	9.57	2.33
MnO	0.20	0.13	0.25	0.16	0.04
CaO	15.40	14.74	12.44	14.51	1.89
Na2O	0.58	0.81	1.32	1.11	0.45
K2O	0.01	0.11	0.30	0.07	0.08
P2O5	0.02	0.16	0.07	0.04	0.03
H2O	1.25	1.55	1.80	1.85	0.43
CO2	0.21	0.38	0.13	0.23	0.10
Total	100.07	100.01	99.87		
U	2	0	2	1	1
Th	0	1	0	1	1
Ce	0	0	0	0	0
La	2	1	0	1	1
Pb	2	4	7	3	3
Ba	18	46	81	122	146
Zr	15	26	27	20	5
Y	8	14	21	11	5
Sr	76	99	115	82	16
Rb	8	0	6	5	3
Ga	11	10	20	11	3
Zn	60	42	105	57	17
Cu	70	85	17	79	70
Ni	55	56	12	71	41
Co	38	52	47	42	7
Cr	224	252	93	312	133

Mean : Arithmetical mean
σn : Standard deviation

Mineralogiocal composition and coordinates of the samples

567	pl+hbl+di	91225-94487	57	hbl+pl+di	86725-97625
418	pl+hbl	91225-94487	212	hbl+pl+di	77637-93500
424	hbl+pl+di	91225-94487	552	hbl+pl+di+mag	77650-92425
420	hbl+pl+qtz	91225-94487	554	hbl+pl+di+mag	77750-90762
419	hbl+pl	91225-94487	556	hbl+pl+di+mag	77587-93800
425	hbl+pl+di	91225-94487	308	hbl+pl+di	95225-89325
426	hbl+pl	91225-94487	345	hbl+pl+mag	92925-87962
215	hbl+pl+di	77475-92525			
307	pl+hbl+di	92700-92925			
60	pl+hbl	86725-97625			

Table 38: Chemical analyses of the granophyres.

Sample No	427	428	568	Mean	σn
SiO2	73.62	74.12	74.25	74.00	0.27
TiO2	0.24	0.20	0.24	0.23	0.02
Al2O3	13.35	13.35	13.06	13.25	0.14
Fe2O3	2.99	2.37	1.27	2.21	0.71
FeO	0.75	0.64	1.05	0.81	0.17
MgO	0.65	0.51	0.52	0.56	0.06
MnO	0.04	0.01	0.04	0.03	0.01
CaO	3.15	2.89	3.84	3.29	0.40
Na2O	3.43	3.52	3.99	3.65	0.24
K2O	0.38	0.47	0.03	0.29	0.19
P2O5	0.06	0.06	0.06	0.06	0.00
H2O	1.20	1.50	1.46	1.39	0.13
CO2	0.09	0.30	0.20	0.19	0.09
Total	99.95	99.94	100.01		
U	0	1	1	1	0
Th	1	2	1	1	0
Ce	8	11	8	9	1
La	5	3	0	3	2
Pb	6	6	1	4	2
Ba	100	88	58	82	18
Zr	70	71	67	69	2
Y	39	25	41	35	7
Sr	107	118	104	110	6
U	0	1	1	1	0
Rb	24	15	3	14	9
Pb	6	6	1	4	2
Ga	14	14	12	13	1
Zn	38	42	13	31	13
Cu	16	5	11	11	5
Ni	3	6	4	4	1
Co	2	0	2	1	1
Cr	34	26	106	55	36

σn : Standard deviation

Mean: Arithmetical mean

Coordinates of the samples: 91225-94487

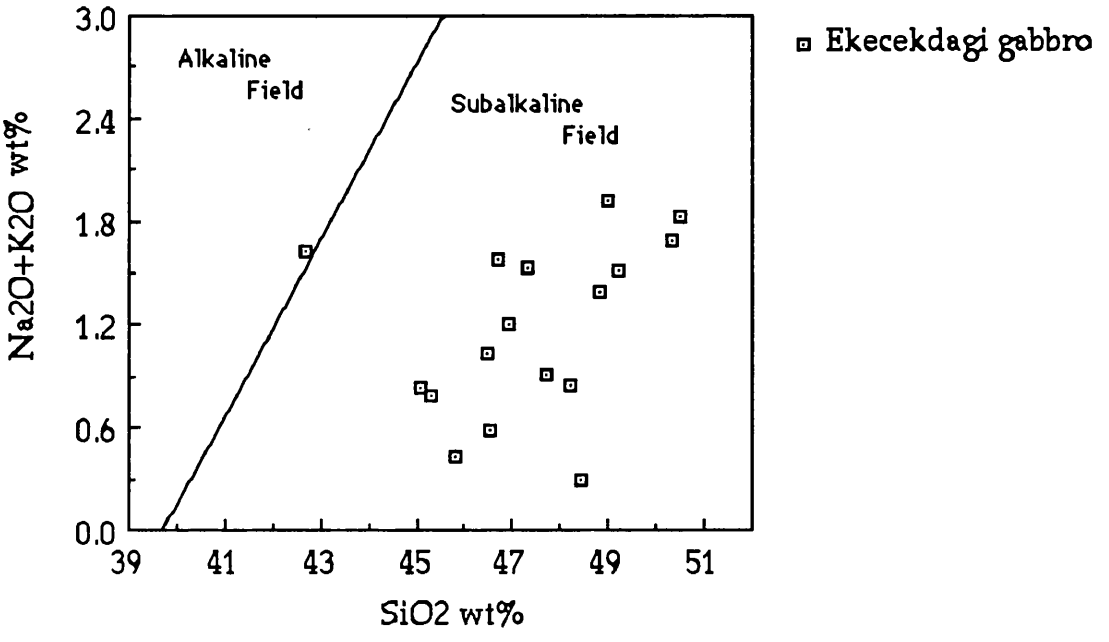

Figure 47: Plot showing subalkaline behaviour of the Ekecekdagi gabbro (Fields after Irvine & Baragar, 1971)

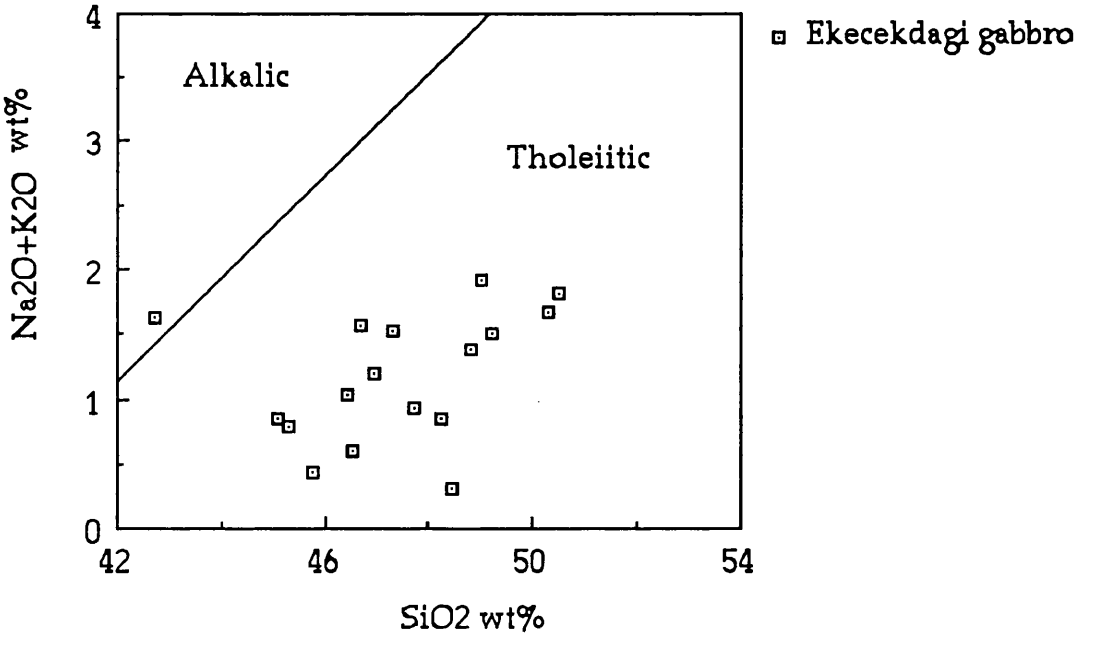

Figure 48-a: Plotting alkali versus silica. Fields as defined by Macdonald and Katsura (1964).

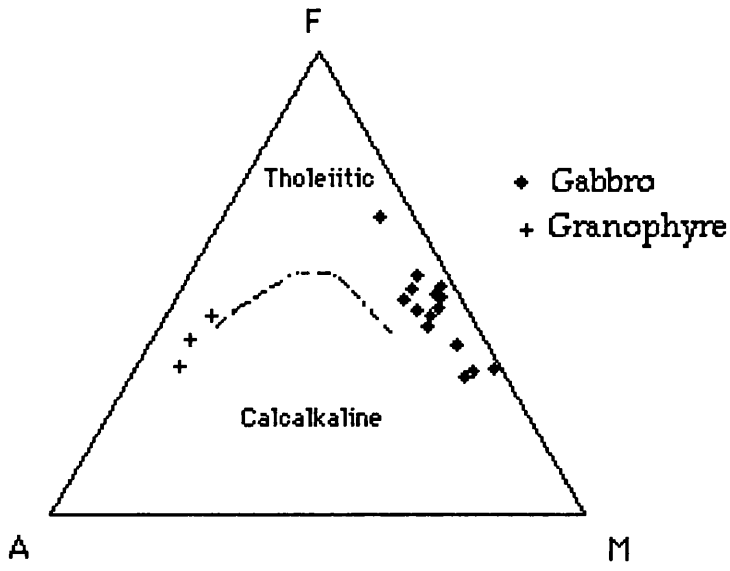

Figure 48-b: AFM plotting of the Ekecekdagi gabbro and granophyre (fields after Irvine & Baragar, 1971).

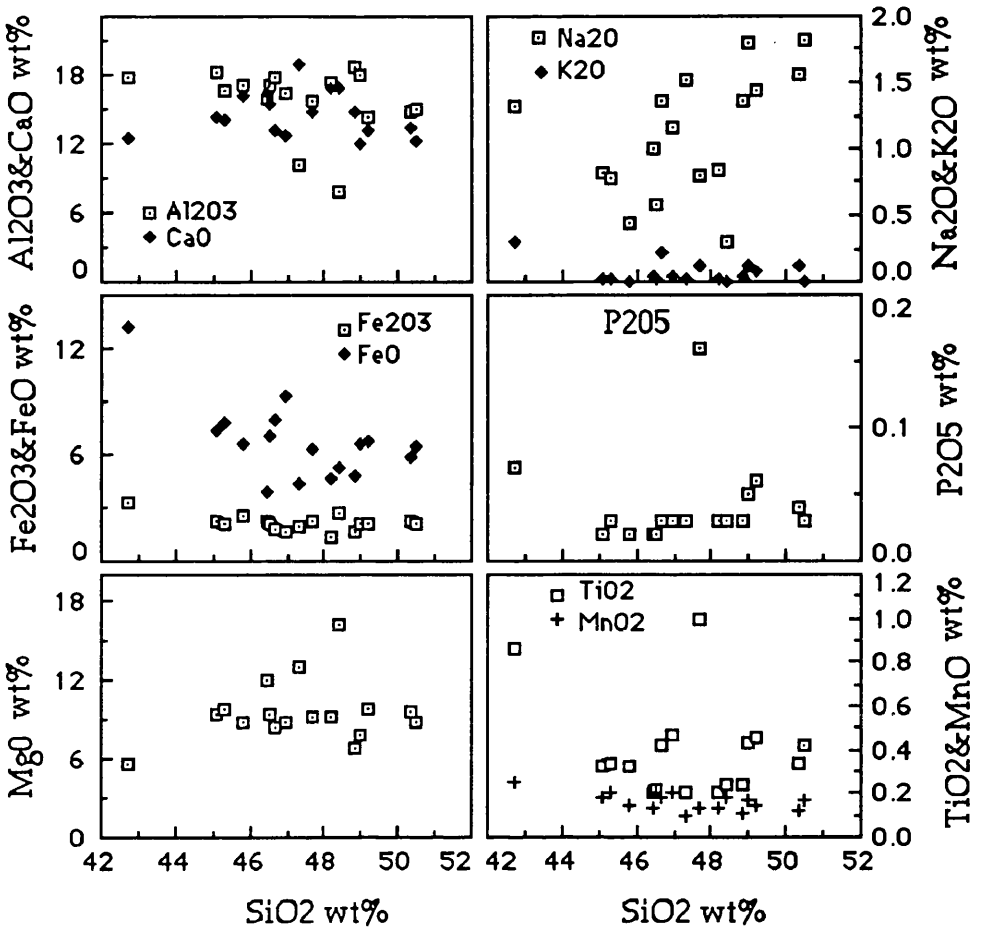

Figure 49: Harker diagrams of the Ekecekdagi gabbro

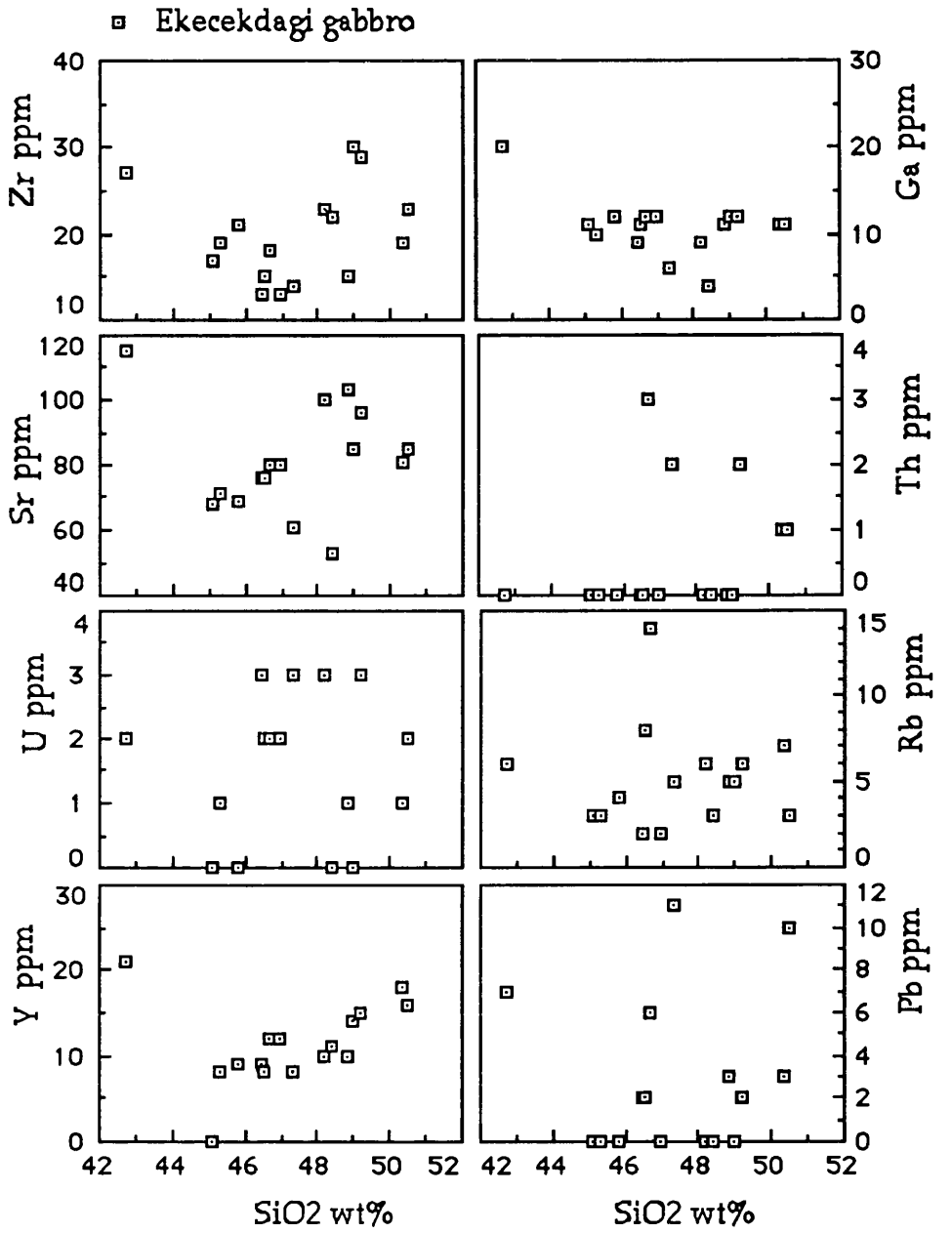
Ekecekdagi gabbro
Zr ppm
Ga ppm
Sr ppm
Th ppm
U ppm
Rb ppm
Y ppm
Pb ppm
SiO2 wt%
SiO2 wt%

Fig. 49. cont.

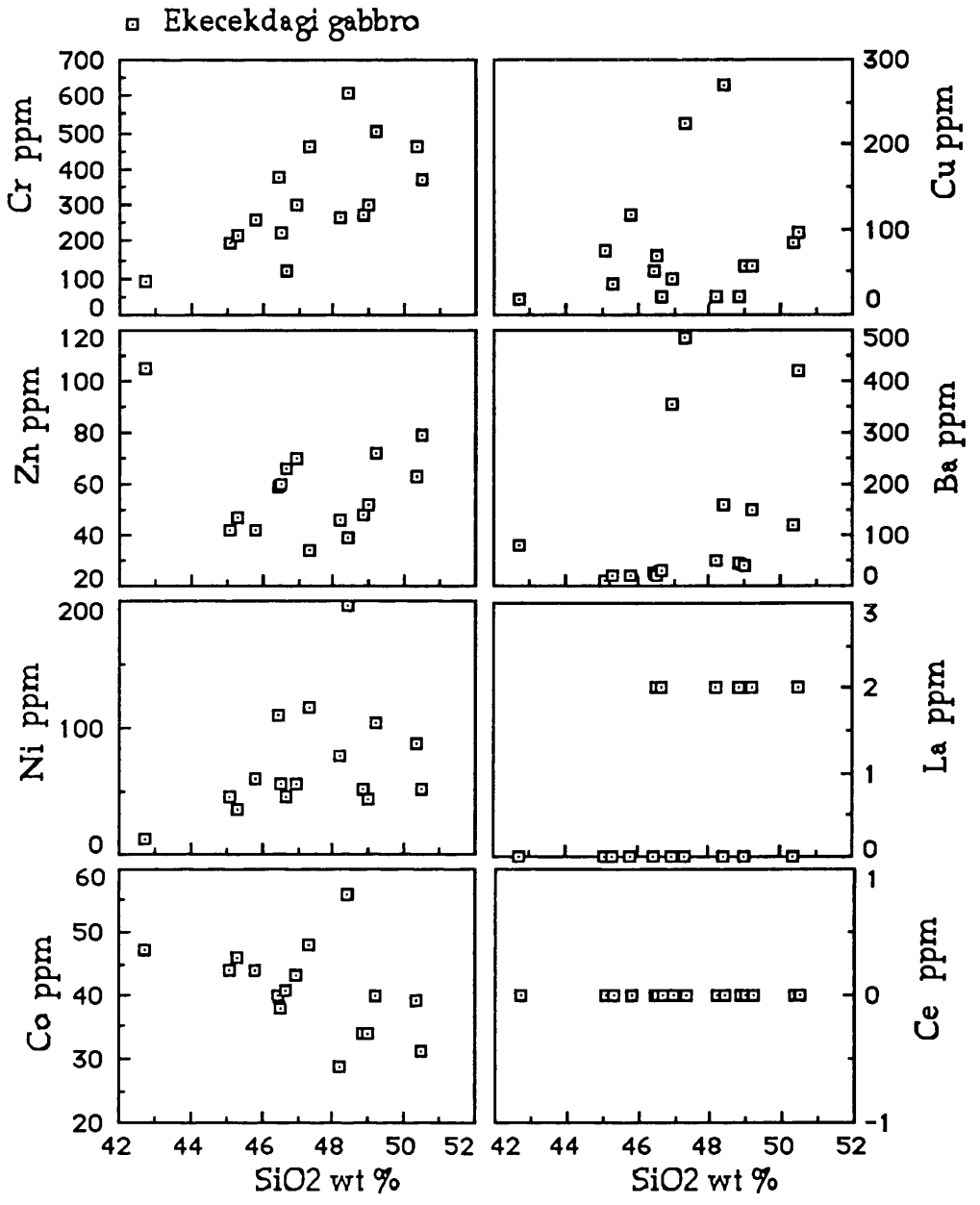
Ekecekdagi gabbro
Cr ppm
Cu ppm
Zn ppm
Ba ppm
Ni ppm
La ppm
Co ppm
Ce ppm
SiO2 wt %
SiO2 wt %

Fig. 49. cont.

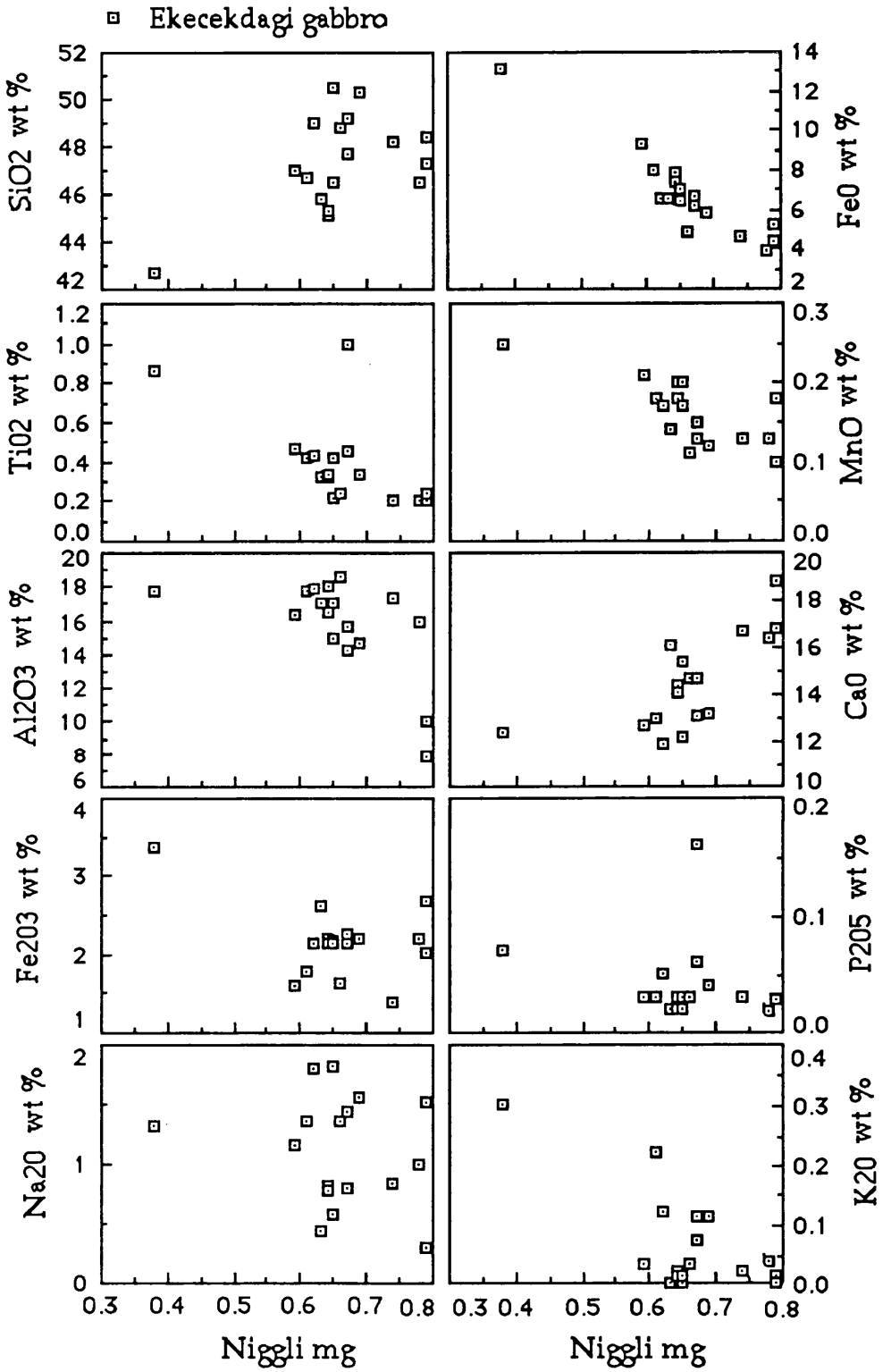

Figure 50: Plots of major oxides and trace elements versus Niggli mg.

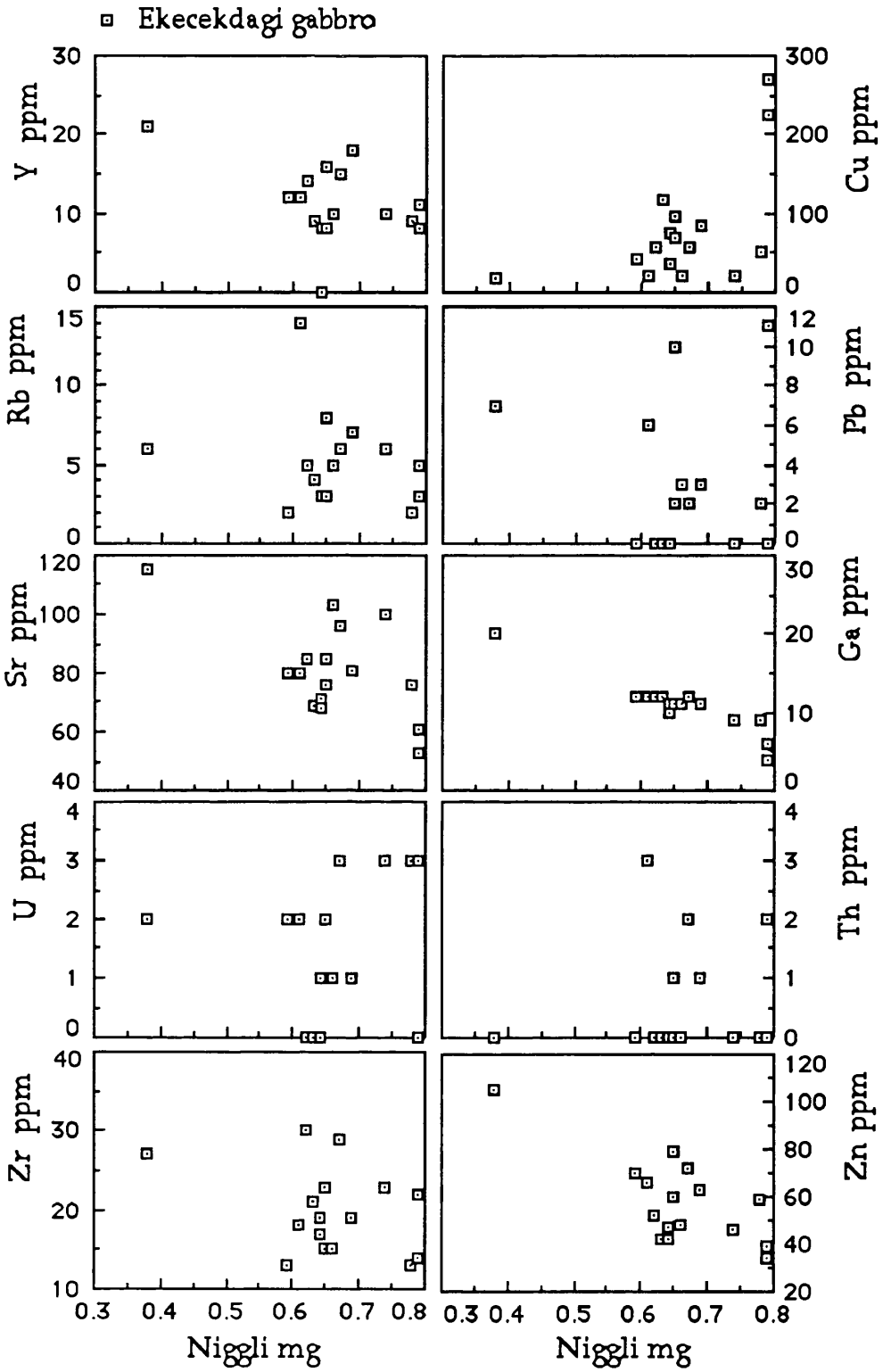
Ekecekdagi gabbro
Y ppm
Cu ppm
Rb ppm
Pb ppm
Sr ppm
Ga ppm
U ppm
Th ppm
Zr ppm
Zn ppm
Niggli mg
Niggli mg

Fig. 50: cont.

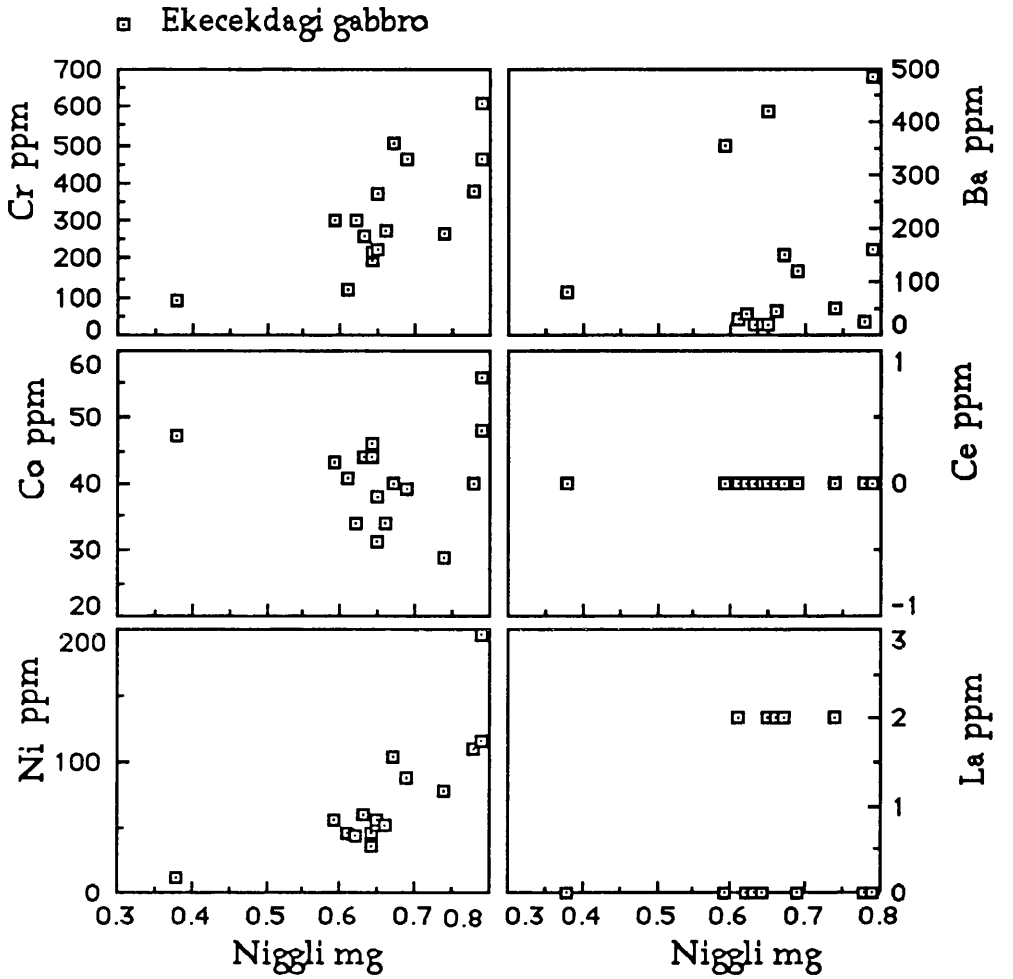
Ekecekdagi gabbro
Cr ppm
Ba ppm
Co ppm
Ce ppm
Ni ppm
La ppm
Niggli mg
Niggli mg

Fig. 50: cont.

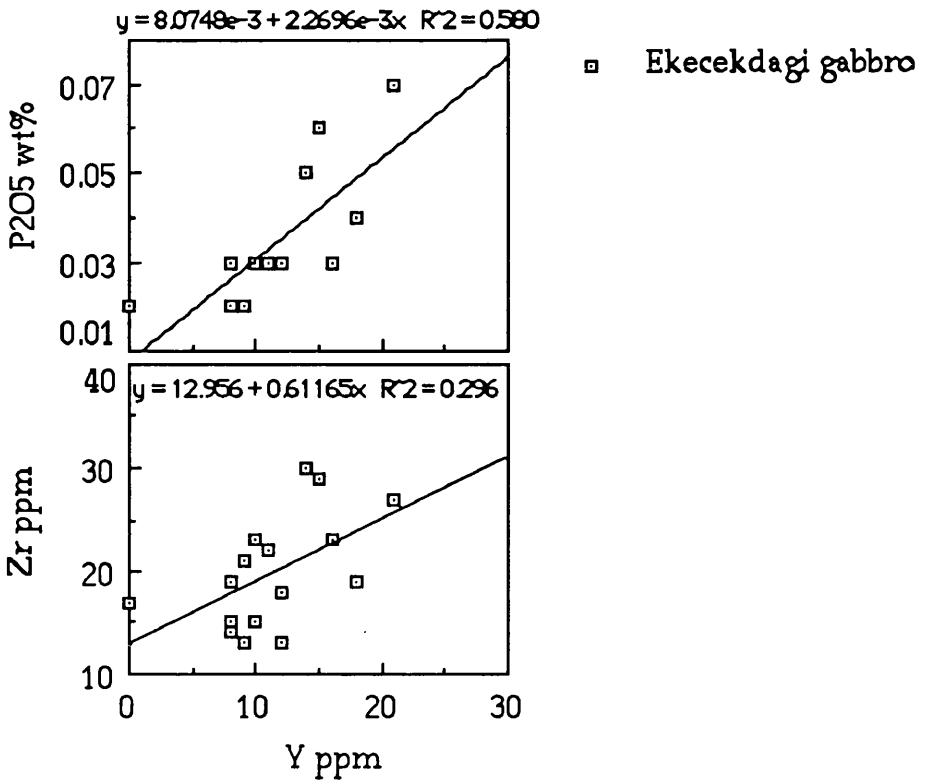

Figure 51: Zr and P2O5 versus Y.

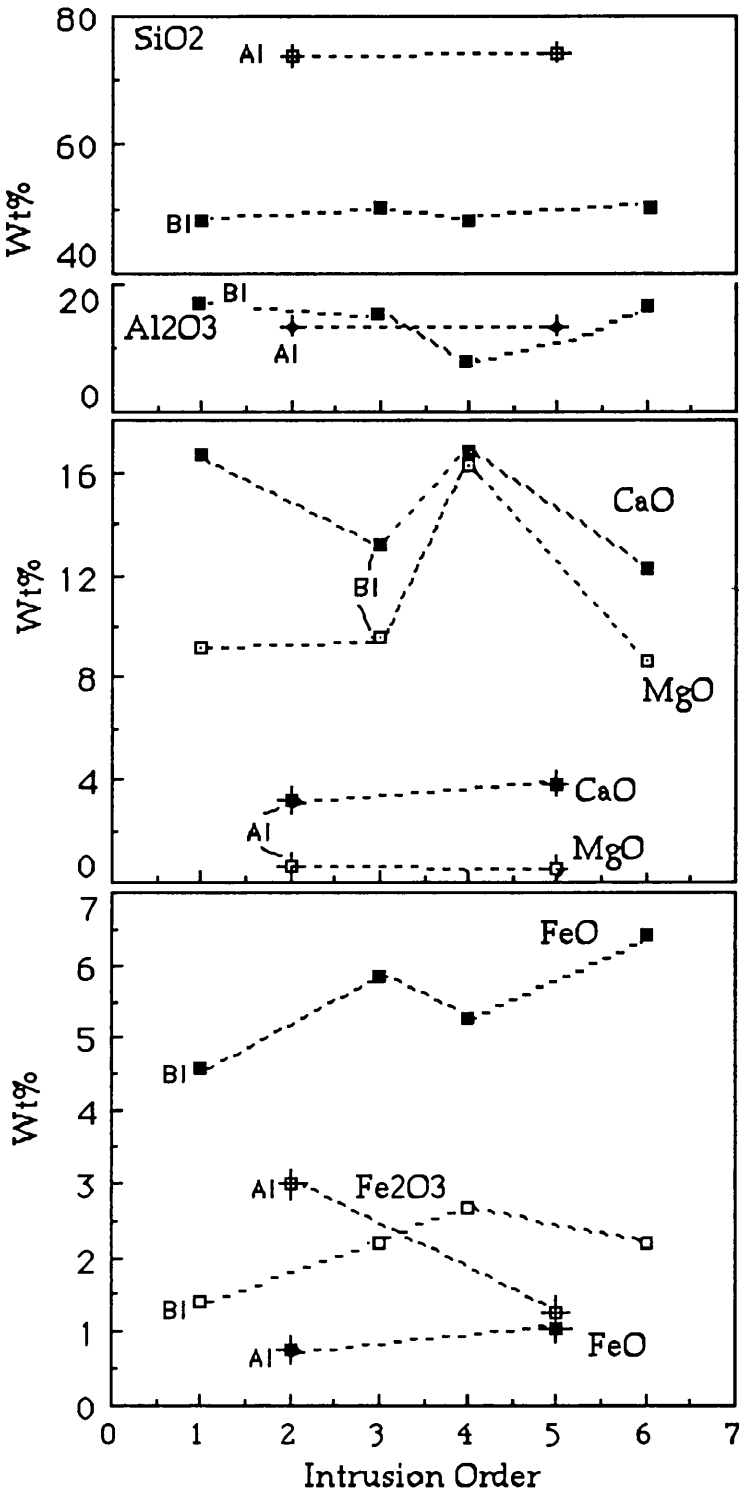

Figure 52: Major oxides and trace elements versus intrusion order.

AI: Acidic intrusion, BI: Basic intrusion.

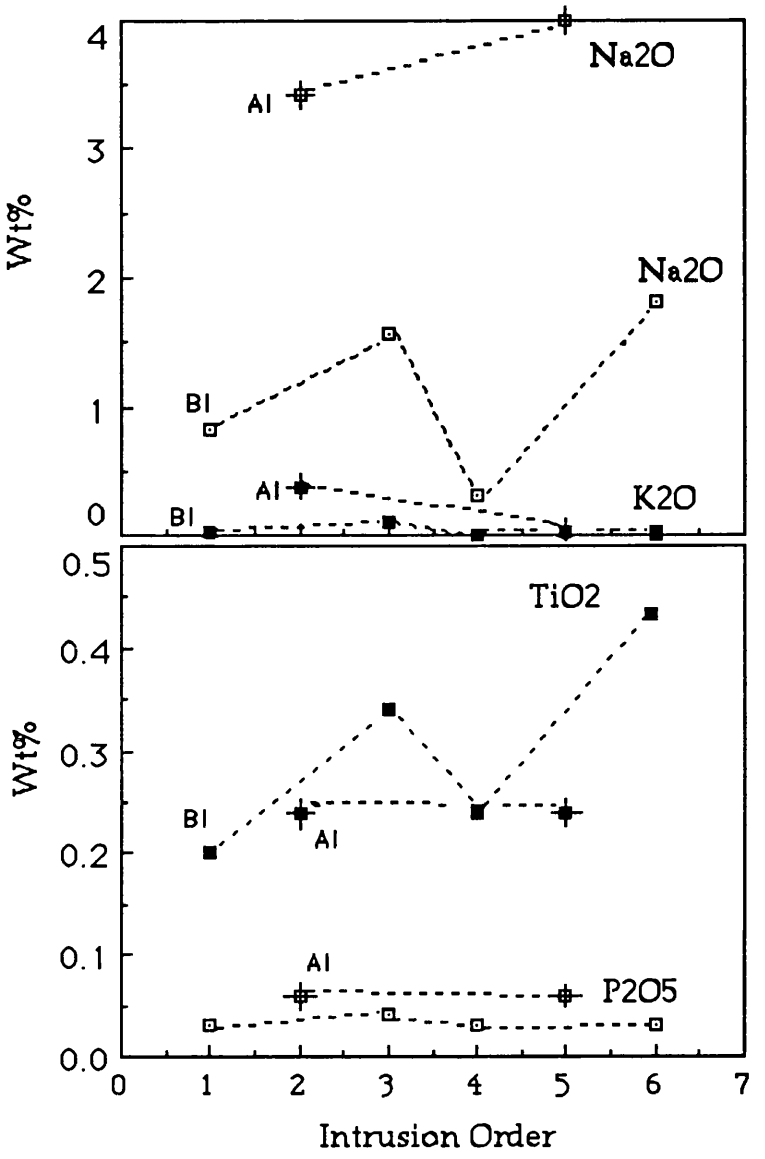
Na2O
Al
Na2O
Bl
Al
K2O
Bl
Wt%
TiO2
Bl
Al
Al
P2O5
Wt%
Intrusion Order

Fig. 52: Cont.

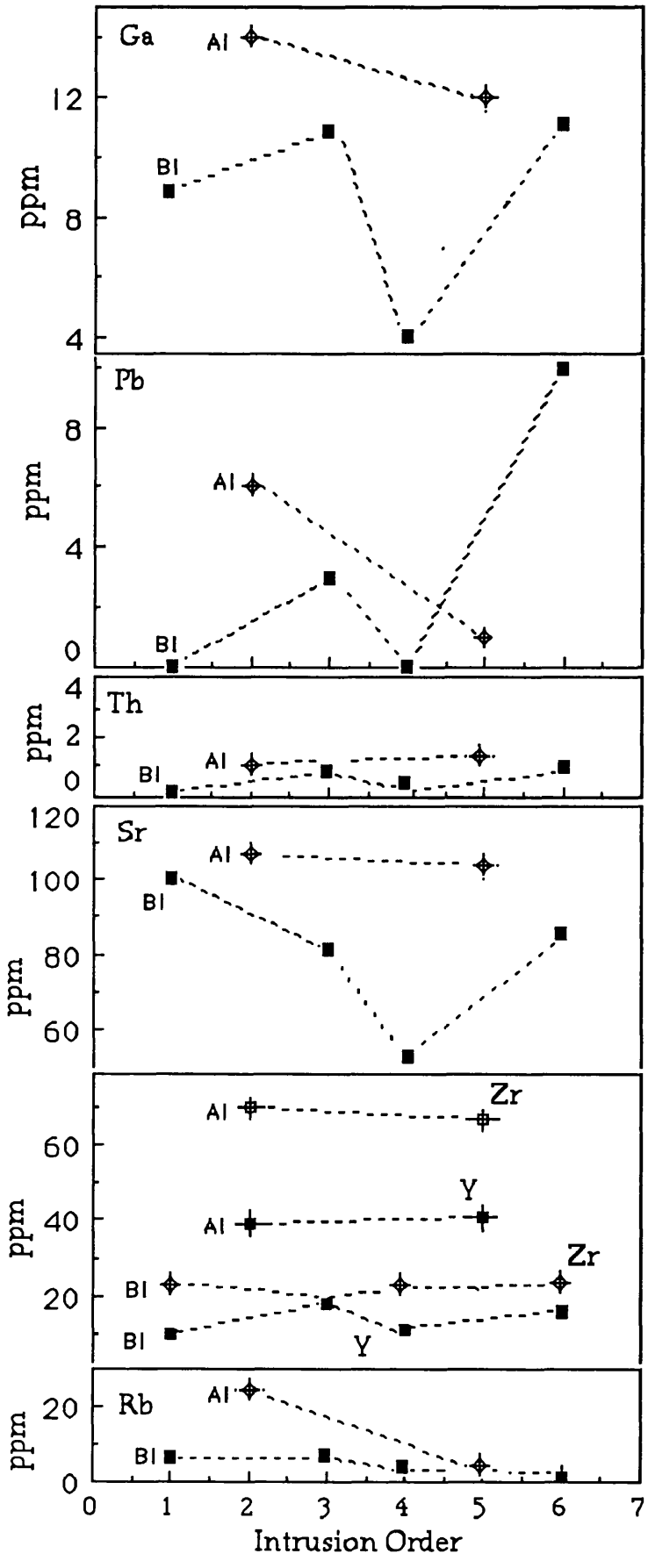
Ga
Al
Bl
12
8
4
ppm
Pb
8
4
0
Th
2
0
Sr
120
100
80
60
Zr
Y
Zr
Y
40
20
Rb
0
1
2
3
4
5
6
7
Intrusion Order

Fig. 52: Cont.

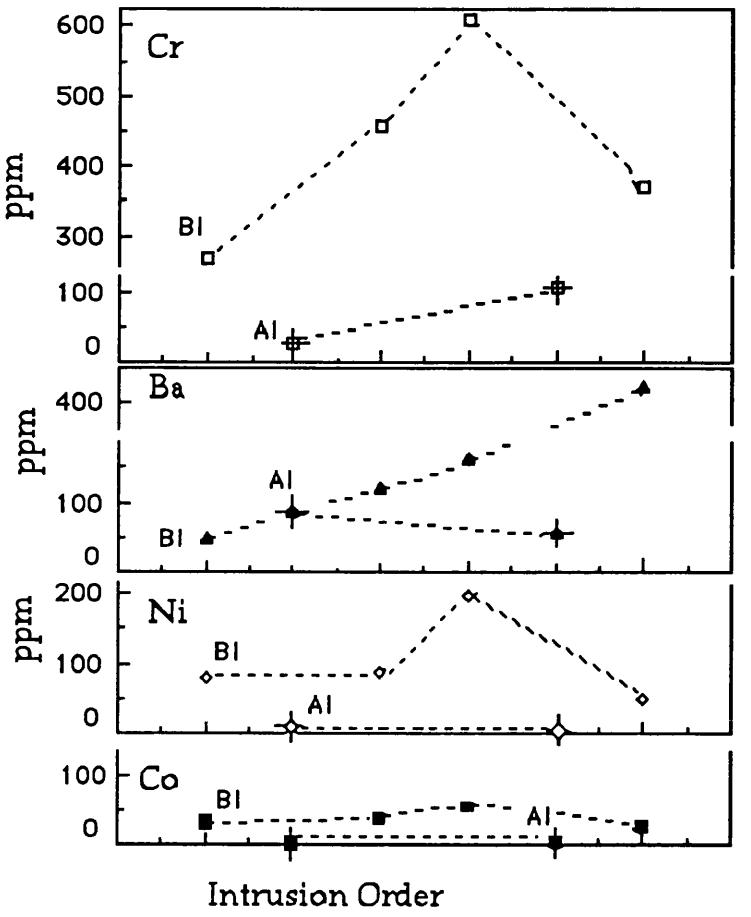
Cr
ppm
600
500
400
300
100
0
Bl
Al
Ba
ppm
400
100
0
Al
Bl
Ni
ppm
200
100
0
Bl
Al
Co
100
0
Bl
Al
Intrusion Order

Fig. 52: Cont.

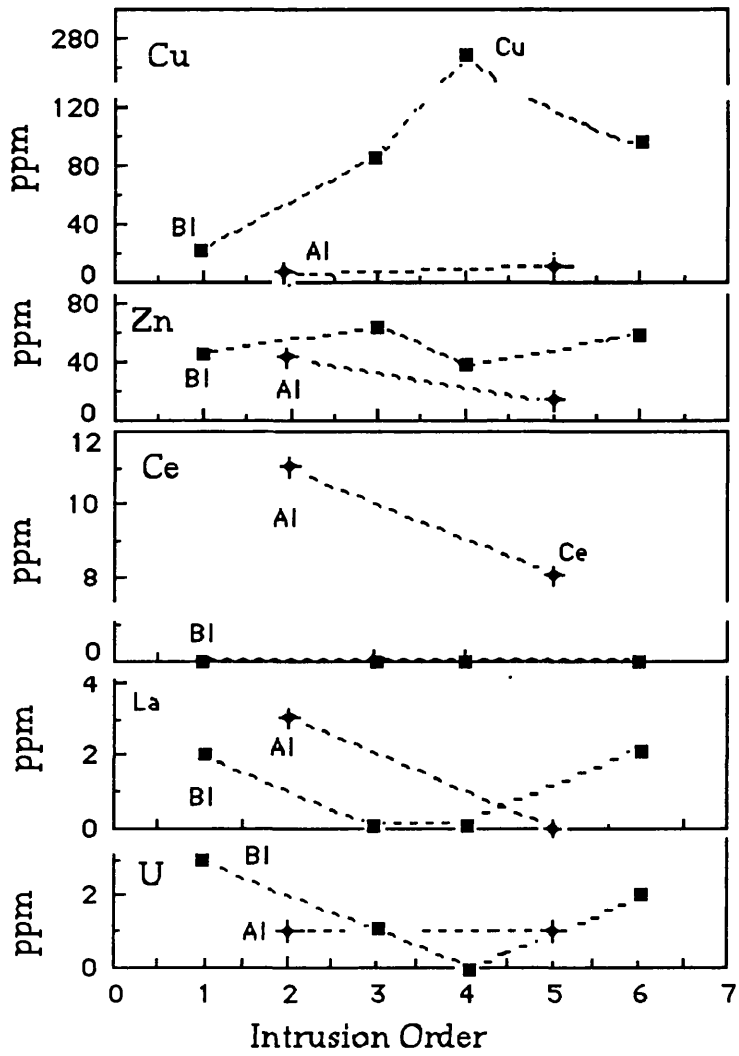
Cu
Cu
BI
AI
280
120
80
40
0
ppm
Zn
BI
AI
80
40
0
ppm
Ce
AI
Ce
BI
12
10
8
0
ppm
La
AI
BI
4
2
0
ppm
U
BI
AI
2
0
ppm
0
1
2
3
4
5
6
7
Intrusion Order

Fig. 52: Cont.

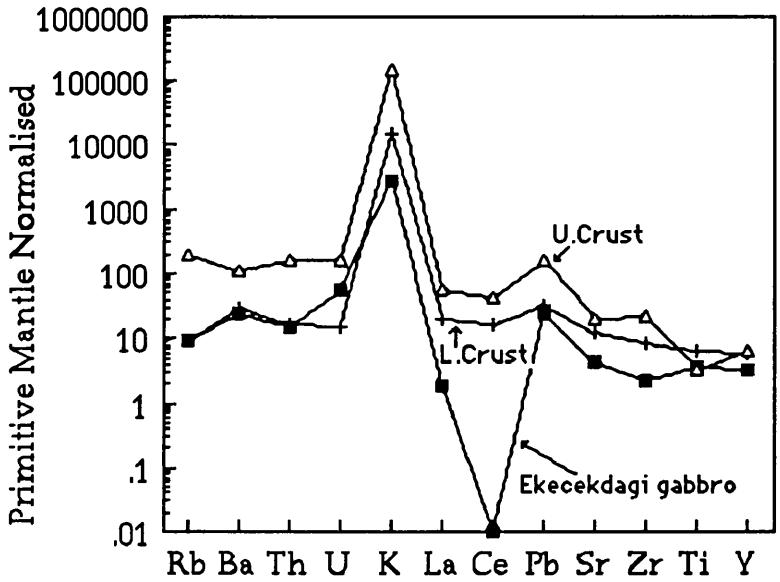

Figure 53: Primitive mantle normalised the Ekecekdagi gabbro, Upper Crust and Lower Crust. Mantle and Crust values are from Taylor & Mclennan, 1985.

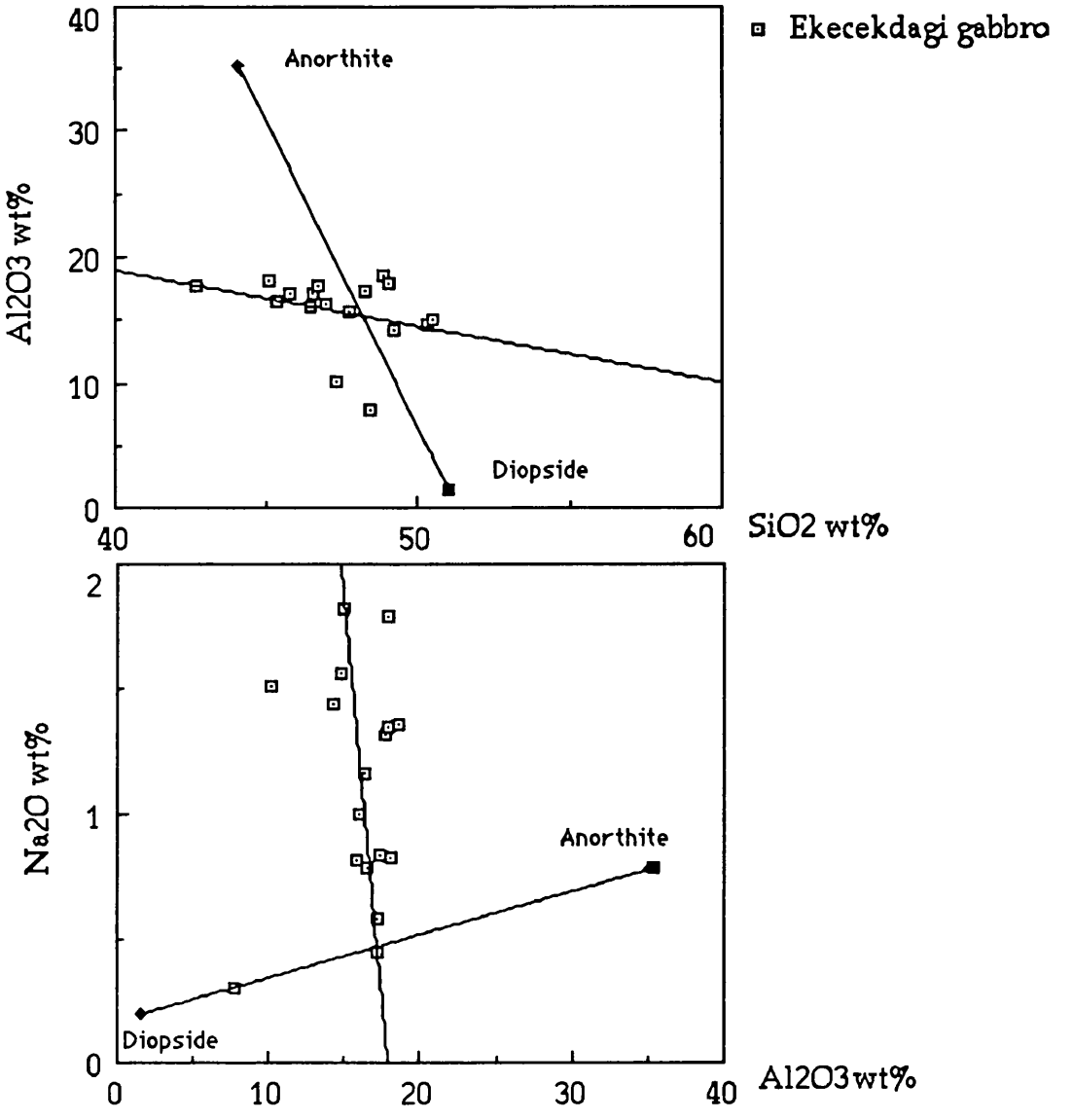

Figure 54: Graphical evaluation of fractionation, Al2O3 vs SiO2 and Na2O vs Al2O3. Mineral compositions are approximated.

Table 39: The results of the fractional crystallization test.

recalculated analyses (wt.percent. basis)

Comp.	initial(215)	final(418)	Di	An
SiO2	46.21	51.03	51.12	44.41
TiO2	0.35	0.35	0.23	0.00
Al2O3	16.87	14.94	1.49	35.55
Fe*2O3	11.09	8.70	11.84	0.09
MnO	0.21	0.12	0.39	0.07
MgO	10.02	9.70	12.93	0.26
CaO	14.42	13.42	21.80	18.83
Na2O	0.79	1.59	0.20	0.79
K2O	0.01	0.11	0.01	0.00
P2O5	0.03	0.04	0.00	0.00
H2O	0.00	0.00	0.00	0.00
CO2	0.00	0.00	0.00	0.00
S%	0.00	0.00	0.00	0.00
Cr2O3	0.00	0.00	0.00	0.00
NiO	0.00	0.00	0.00	0.00

coefficients of transformed eqns.

results: differentiating from # 215 to # 418

	bulk comp. of added or subtr.matl.	obs.diff., between magmas	calc.diff. between magmas	obs.-calc. (residuals)
SiO2	47.43	4.819	0.832	3.987
TiO2	0.10	0.001	0.057	-0.056
Al2O3	20.23	-1.927	-1.220	-0.707
Fe*2O3	5.38	-2.388	0.768	-3.156
MnO	0.21	-0.089	-0.021	-0.067
MgO	5.96	-0.324	0.863	-1.186
CaO	20.16	-0.999	-1.557	0.558
Na2O	0.52	0.797	0.246	0.550
K2O	0.00	0.099	0.024	0.075
P2O5	0.00	0.010	0.009	0.001
H2O	0.00	0.000	0.000	0.000
CO2	0.00	0.000	0.000	0.000
S%	0.00	0.000	0.000	0.000
Cr2O3	0.00	0.000	0.000	0.000
NiO	0.00	0.000	0.000	0.000
total				0.000

sum of the squares of the residuals = 28.3872

phase name	amount as wt.pct. of init.magma	amount as wt.pct. of all phases	amount as wt.pct. of added phs.	amount as wt.pct. of subtrd.phs
Diopside	-10.39	45.00	0.00	45.00
Anorthite	-12.70	55.00	0.00	55.00
totals rel. to initial magma =			0.00	23.10

* : Fetot as Fe2O3

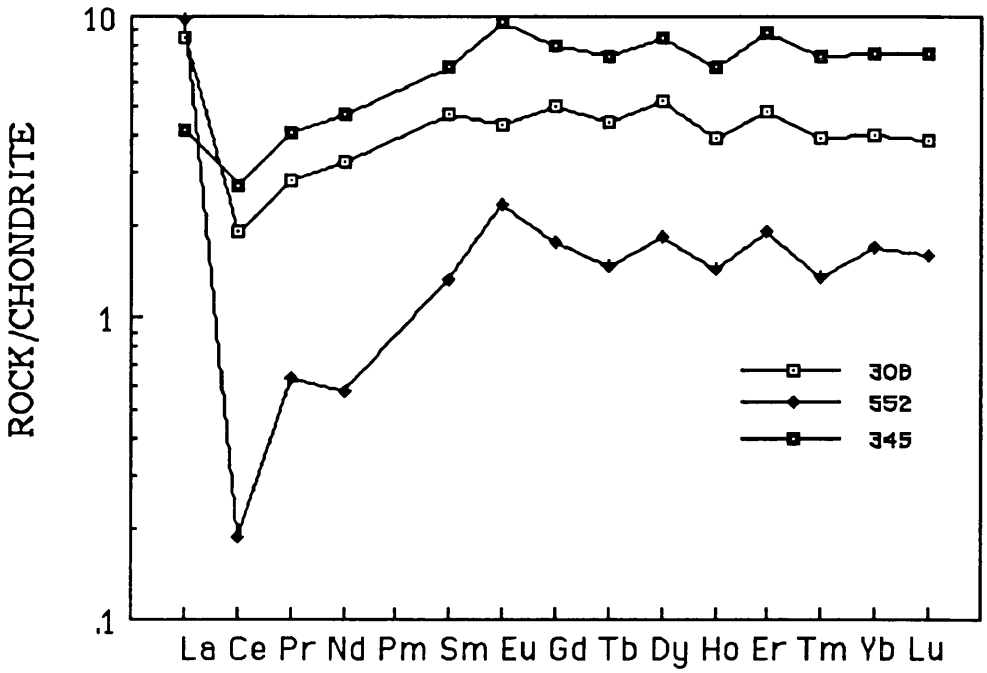

Figure 55: Chondrite normalised (Boynton, 1984) REE pattern of the Ekecekdagi gabbro.

IV.5.2 Hornblende diorite and hornblendite

IV.5.2.1 Major and trace elements

Chemical analyses of hornblende diorites, which just range into the gabbro field based on the plagioclase compositional limit of An_{50} are given in Table 40 together with one hornblendite. There is gradation between hornblende diorite and gabbro in the field with small, rare patches of hornblendite in the hornblende diorite. The hornblende diorites show variation, between 48.88 and 61.55%, in SiO2 (Table 40) and predominantly plot across the quartz-diorite / quartz-gabbro to monzogabbro / monzodiorite fields of Debon and Le Fort (1982) (Fig. 56). The hornblende diorites fall in the subalkaline field while the hornblendite is found in the alkaline field in Fig. 57. Alkali (Na2O+K2O) exceeds CaO at ~60% SiO2(Fig. 58) and so the suite is calcalkaline (55-61% SiO2, Peacock, 1931). However, using both Irvine and Baragar(1971) and Miyashiro's(1974) plots, the samples straddle the tholeiitic and calcalkaline fields (Figs. 59 and 60).

Many diorites have substantial K contents but the present diorites, which average 1.83% K2O do not have enough K2O to be classified as High-K diorites according to Gulson et al.(1972). As compared with the average diorite of Le Maitre(1976), Ortakoy diorites have higher FeO, MgO, CaO, K2O lesser SiO2, TiO2, Fe2O3, Na2O, P2O5 and similar Al2O3 and MnO contents(Table 40). This K2O-enrichment and Na2O-depletion in hornblende diorites might be considered to be explained by contamination with metasediments which contain relatively higher K2O (3.86% in semipelite and 2.47 % in psammite) and lower Na2O (1.1% in semipelites and 1.92 in psammites). However, as metasediments contain high SiO2 (62.48% average in semipelite and 72.41% in psammite), the hornblende diorite would be expected to have higher silica content owing to the

contamination. The low silica of the hornblende diorites precludes this contamination process. The Ortakoy diorites have similar SiO2, TiO2, Fe2O3, FeO, MnO, CaO contents to pyroxene mica diorites and hornblende diorites (Table 40) of Appinite suites (Wright&Bowes, 1979). As a whole, the chemical characteristics of the Ortakoy diorites show a tendency towards the pyroxene mica diorite and hornblende diorites-appinite suites rather than that of the average diorites of Le Maitre(1976).

Major oxide and trace elements show regular variation trends on Harker diagrams (Fig. 61). Usually, the hornblendite plots at the low SiO2, high MgO end of the hornblende diorite trends on the Harker diagrams, suggesting fractional crystallisation with early separation of the hornblendite. This is consistent with Figs. 62 and 63 which show that Niggli mg has a positive correlation with FeO, CaO, Th, Rb, Ni, Co and negative correlation with SiO2, Al2O3, TiO2, P2O5, Na2O and Zr.

A mantle normalised hornblende diorite pattern is shown in Fig. 64 and compared with Taylor and McLennan's(1985) Upper and Lower Crustal patterns. Elements in the hornblende diorite (particularly K) show a close similarity to these patterns with a tendency to be nearer to the Upper Crustal one, although they occur between Upper and Lower Crustal patterns. Clearly, Ti was relatively enriched in the hornblende diorites and exceeded the average of the Upper Crustal value.

IV.5.2.2 REE analyses

Two samples of the hornblende diorites were analysed for REE and their chondrite normalized patterns are shown in Fig. 65. The concentration of all REE seems to be increasing with increasing SiO2. LREE enrichment (La/Lu 7.5-9.1) and HREE fractionation (Gd/Lu 2.09-2.3) are characteristics in these samples with slight negative Eu anomaly, possibly indicating some previous plagioclase fractionation. The whole pattern is typical of a basic magma of within continent type with moderate LREE enrichment.

Mafic rocks accompanying granitoid suites are considered as magmatic precursors(Didier, 1973). The amphibolites melting at crustal conditions might form andesitic magmas (Pichler&Zeil, 1972) and the injection of basalt magma into the lower crust can account for this melting(Burnham, 1979; Huppert&Sparks, 1988). In this regard, the quartz-diorite melt could be formed from amphibolite by injection of a basalt magma at 1200° C (Burnham, 1979). Amphibole would be separated from basalt magma under hydrous conditions(Cawthorn&O'Hara, 1976) and makes crystal fractionation to be plausible mechanism forming diorite. Similarly, appinites were suggested being formed by differentiation of basic magma(Wright&Bowes, 1979) or by hornblende accumulation from hydrous andesite or basalt magma (Groome&Hall, 1974). Spatial association of the Ortakoy diorites with hornblendite, and the similarity in chemical compositions of the Ortakoy and Scottish appinite diorites suggest a similar petrogenetic process. The steep REE pattern of the Ortakoy diorite may support the hornblende fractionation as shown by Frey et al. (1978) although such patterns are widely accepted as indicating residual garnet during melting. Moreover, the fractionation of hornblende is evident in the thin

sections of the hornblende diorites with an edenitic- or actinolitic-hornblende core and a magnesio-hastingsitic- or magnesio-hornblende-rich rim(see petrography chap.). Plagioclase is likely to accompany hornblende fractionation and the negative Eu anomalies in the REE pattern of the hornblende diorites would require early separation and removal of plagioclase.

The fractional crystallization was tested with linear mass-balance calculations on XLFRAC computer program(Stormer&Nicholls, 1978) by using the chemical analyses of the hornblendite and hornblende diorite, initial and final compositions of magma (Table 42). The microprobe analyses of the hornblende, anorthite, and spinel in the hornblendite were taken as initial phases. The sum of the squares of the residuals is however rather large (40), which suggests that the fractionation of these phases in the hornblendite to produce the Ortakoy diorites are unlikely. Hence, it is likely that the hornblende diorites were formed by melting of a garnet-bearing source at crustal conditions, possibly coupled with fractional crystallisation of hornblende, anorthite and spinel.

IV.5.2.3 Conclusions

The hornblende diorites are subalkaline and tend to be calcalkaline to tholeiitic in composition.

They are relatively enriched in FeO, MgO, CaO, K2O and depleted in SiO2, TiO2, Fe2O3, Na2O and P2O5 with respect to the average diorite of Le Maitre(1976). There seems to be no relationship between the variation of the major oxides and the contamination of the hornblende diorites by metasediments. The Ortakoy diorites tend to be appinitic having similar SiO2, TiO2, Fe2O3, FeO, MnO and CaO contents to typical appinite diorite (Wright&Bowes, 1979).

Primitive mantle normalised pattern of the Ortakoy diorites shows similarity to that of Upper Crust .

The hornblende diorites were suggested to be formed by melting of a garnet-bearing source at crustal conditions. This was possibly coupled with fractional crystallisation of hornblende, anorthite and spinel, which is supported by zoning in hornblende and feldspar in thin section, and by the transition between hornblende diorite and hornblendite in the field.

Table 40: Major and minor chemical analyses of the hornblende diorites with hornblendite and average compositions of diorite of Le Maitre(1976) and diorite of Appinites.

Sample No	371	446	128	317	384	290	315	369
SiO2	54.68	59.99	52.80	55.56	48.88	54.15	53.11	61.55
TiO2	0.85	0.64	0.59	0.58	0.56	0.78	0.45	0.44
Al2O3	20.57	15.56	18.22	18.42	12.71	18.30	15.35	17.37
Fe2O3	6.26	1.70	1.34	1.25	2.02	2.69	2.08	1.45
FeO	0.57	6.22	5.36	6.03	8.30	6.36	5.22	3.21
MgO	2.66	2.47	3.40	3.84	9.13	3.28	6.30	2.04
MnO	0.11	0.14	0.14	0.10	0.19	0.19	0.14	0.11
CaO	7.72	8.05	9.18	7.24	12.52	7.32	9.01	4.69
Na2O	2.84	2.73	3.35	2.30	1.63	3.14	3.04	3.79
K2O	1.36	0.44	3.25	2.17	0.68	1.63	3.05	3.15
P2O5	0.17	0.09	0.14	0.11	0.08	0.21	0.09	0.15
H2O	2.10	1.85	1.50	2.13	2.48	1.90	1.92	1.90
CO2	0.15	0.10	0.65	0.17	0.81	0.10	0.14	0.09
Total	100.04	99.98	99.92	99.90	99.99	100.05	99.90	99.94
U	2	2	3	4	3	3	3	2
Th	3	0	12	8	7	0	4	8
Ce	32	0	56	33	20	53	32	51
La	16	0	23	11	7	25	19	26
Pb	17	10	19	20	5	13	12	25
Ba	414	100	675	406	111	626	862	691
Zr	209	25	144	87	32	129	54	176
Y	16	28	30	15	17	33	15	22
Sr	300	144	274	212	214	304	379	235
Rb	52	17	94	97	22	51	93	94
Ga	22	15	18	18	11	18	13	16
Zn	89	57	80	62	90	109	60	70
Cu	26	7	10	27	2	5	22	16
Ni	24	3	15	16	55	6	33	12
Co	18	13	13	24	41	17	24	11
Cr	126	51	70	47	368	112	289	49

Table 40: cont.

					Ortakoy dio.		Appinite^	Gen.Dio*.	
Sample No	38	48	714	388	Mean	σn	Mean	Mean	Hornbldt.
SiO2	57.65	56.87	50.17	51.29	54.72	3.67	55.36	57.48	40.29
TiO2	0.55	0.61	0.78	0.69	0.63	0.12	0.92	0.95	0.33
Al2O3	16.18	16.87	17.33	12.94	16.65	2.18	15.75	16.67	12.86
Fe2O3	1.32	0.97	1.95	1.52	2.05	1.35	1.77	2.50	4.09
FeO	5.32	6.17	7.80	8.56	5.76	2.11	5.48	4.92	8.02
MgO	2.85	3.89	4.87	8.90	4.47	2.31	5.87	3.71	19.51
MnO	0.16	0.12	0.13	0.12	0.14	0.03	0.15	0.12	0.22
CaO	5.75	7.50	10.43	11.62	8.42	2.18	7.15	6.58	7.95
Na2O	5.22	2.66	2.92	1.61	2.94	0.92	2.81	3.54	1.04
K2O	3.27	2.02	0.40	0.59	1.83	1.10	2.25	1.76	0.31
P2O5	0.19	0.13	0.08	0.06	0.12	0.05	0.21	0.29	0.03
H2O	1.42	1.90	2.40	1.85	1.95	0.29	1.72	1.15->H20+	
CO2	0.22	0.24	0.70	0.10	0.29	0.25	0.57	0.21->H20-	5.36
								0.10->CO2	(LOI)
Total	100.10	99.95	99.96	99.85					
U	1	3	0	0	2	1			
Th	0	6	3	6	5	4	16		
Ce	42	36	55	15	35	17	29		
La	21	26	20	11	17	8	18		
Pb	8	19	7	4	13	6	16		
Ba	590	368	90	116	421	259	529		
Zr	110	106	75	51	100	55	173		
Y	18	22	19	28	22	6	-		
Sr	256	229	247	266	255	56	433		
Rb	72	77	1	0	56	36	64		
Ga	18	18	16	13	16	3	20		
Zn	74	84	53	91	77	16	75		
Cu	5	14	0	1	11	9	71		
Ni	8	22	4	54	21	17	71		
Co	17	26	14	49	22	11	31		
Cr	122	136	75	729	181	191	229		

^ : Averages of the pyroxene mica diorites and hornblende diorites, Appinite suite from Loch Lomond-Loch Fyne region, Wright &Bowes(1979)

* : Averages of diorite calculated from 872 samples, Le Maitre(1976).

σn : Standard deviation

Mean: Arithmetical mean

Mineralogical compositions and coordinates of the samples

Sample No	Minerals**	Coordinates	Sample No and Minerals**	Coordinates
371	pl+ hbl+ bt+ qtz	90800-87637	38 pl+hbl+ or	86100-86700
446	pl+ hbl+ qtz+ bt	91762-88150	48 pl+hbl+bt+qtz	88937-96137
128	pl+hbl+ or+qtz+bt	88375-87687	714 pl+hbl	91425-86800
317	pl+bt+hbl+qtz	91350-89162	388 hbl+pl	87825-82975
384	hbl+pl	87070-82725		
290	pl+bt+hbl+qtz	87812-84550		
315	hbl+pl+qtz	91687-90837		
369	pl+hbl+qtz+bt	92250-84925	Hornblendite: hbl+act+an+spl	85250-85762

** : Mineral symbols are from Kretz(1983).

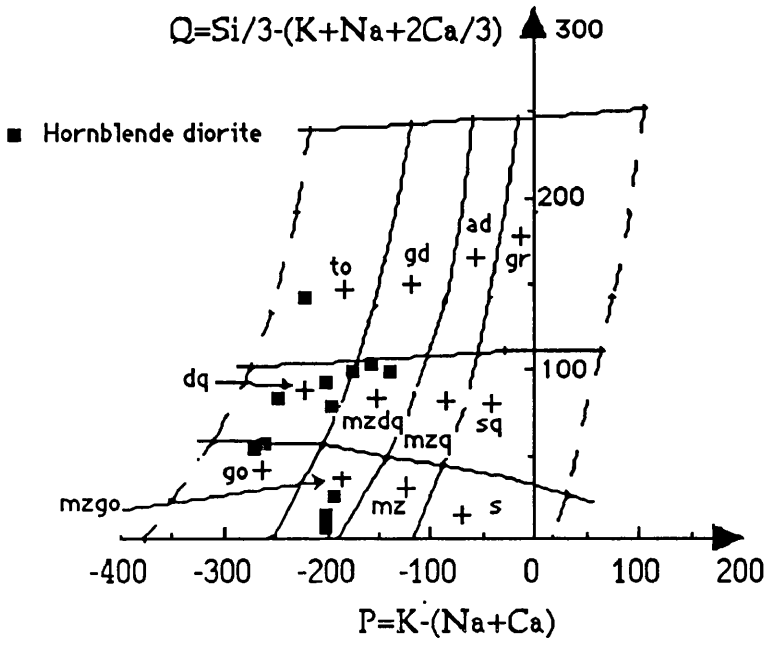

Figure 56: Nomenclature of the hornblende diorites using a Debon and Le Fort(1982) diagram. Its parameters are expressed as gram-atomx10^3 of each element in 100 g of material (see Table 41 for calculation). Crosses represent 12 model compositions for a reference:

gr: granite, ad: adamellite, gd: granodiorite, to: tonalite, sq: quartz-syenite mzq: quartz monzonite, mzdq: quartz monzodiorite, dq: quartz diorite (quartz gabbro-quartz anorthosite), s: syenite, mz: monzonite,

mzgo: monzogabbro, monzodiorite, go: gabbro (diorite-anorthosite)

Table 41: Example calculation of the different parameters for the diagram of Debon and Le Fort(1982).

Column 1: Chemical analysis, in weight percent of metallic oxides. Fe2O3t, total iron as ferric oxide; L.I., loss on ignition. Column2: molecular weight of the different oxides. Column 3; factor obtained by dividing the molecular weight by the number of metallic atoms(cations) in the oxide formula. Column 4: number of millications(10^3 gram-atoms) per 100 grams, obtained by dividing values from column 1 by the corresponding factor of column 3, and then multiplying by 10^3. Column 5: Parameters are calculated from the millicationic value.

	1	2	3	4	5
	Oxide %	Molecular weight	Factor	Millications	Parameters
SiO2	74.16	60.06	60.06	Si=1235	Q=Si/3-(K+Na+2Ca/3)=178
Al2O3	14.89	101.94	50.97	Al=292	P=K-(Na+Ca) =-78
Fe2O3t	0.59	159.70	79.85	Fe3+=7	
FeO	-	71.85	71.85	Fe2+= -	
MnO	0.10	70.93	70.93	Mn= 1	
MgO	0.16	40.32	40.32	Mg= 4	
CaO	0.75	56.08	56.08	Ca= 13	
Na2O	4.49	62.00	31.00	Na=145	
K2O	3.75	94.19	47.10	K =80	
TiO2	0.06	79.90	79.90	Ti = 1	
L.I.	0.59				
Total	99.54				

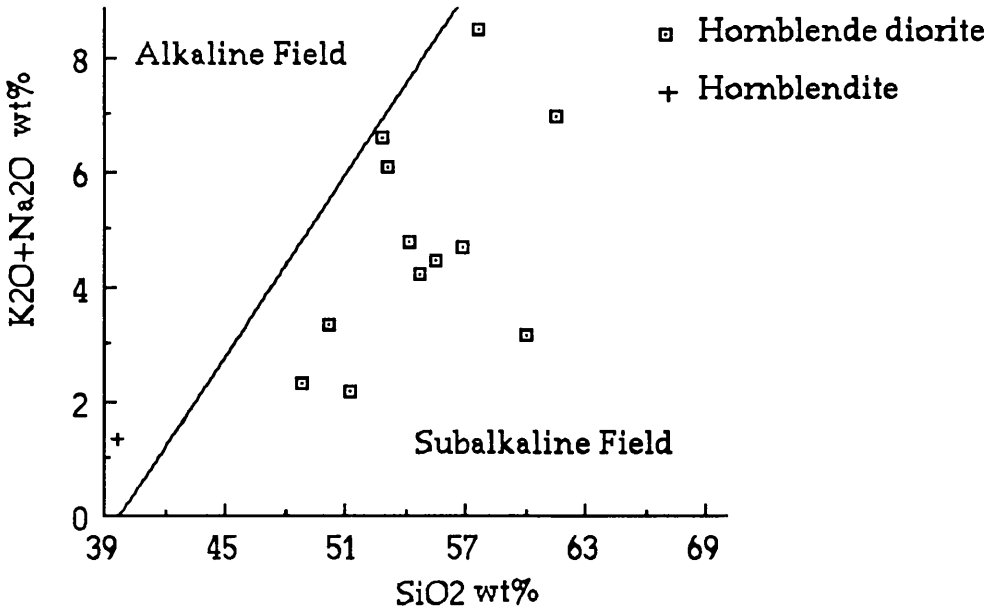

Figure 57: SiO2 versus Na2O+K2O showing subalkaline behaviour of the hornblende diorite and hornblendite (fields after Irvine & Baragar, 1971).

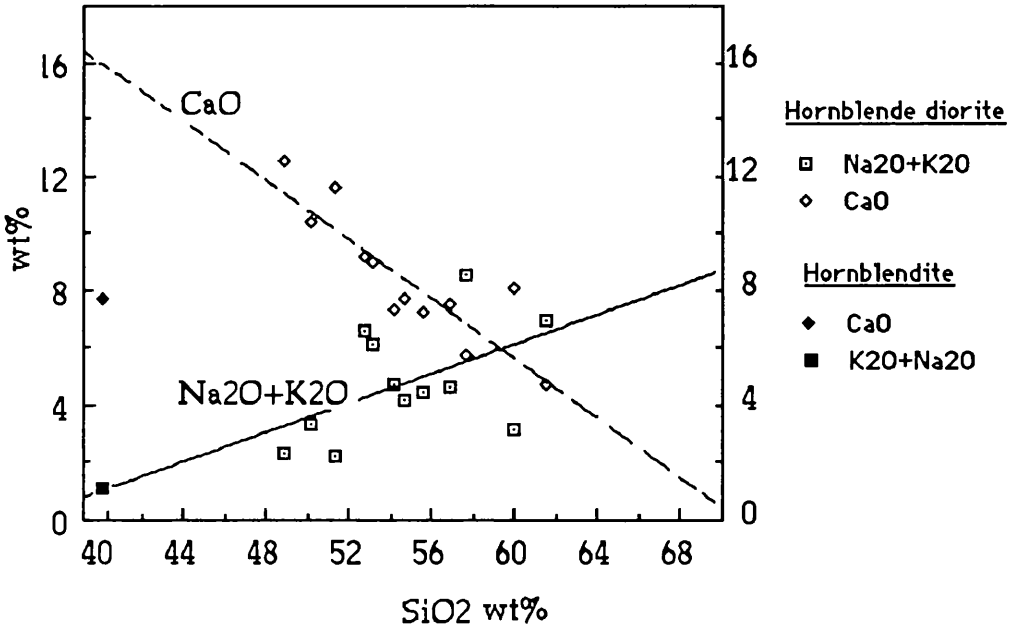

Figure 58: Alkali and CaO versus silica.

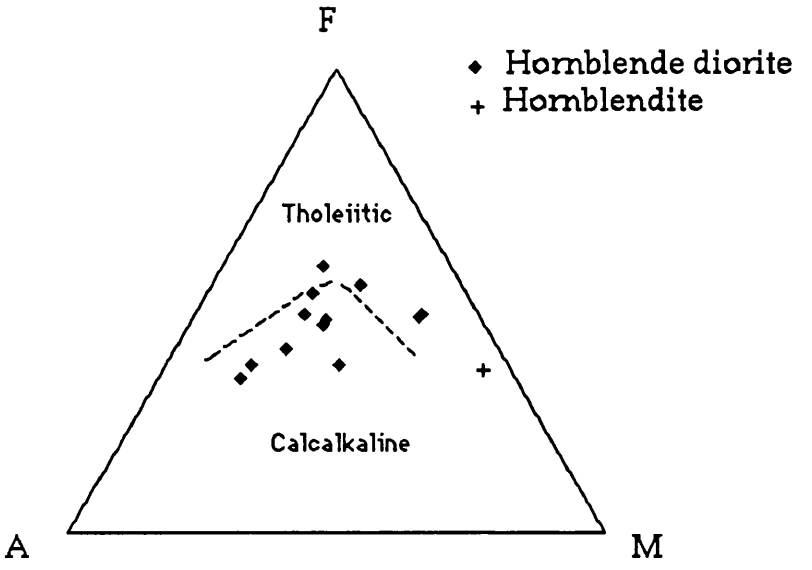

Figure 59: AFM diagram of the hornblende diorites and the hornblendite. Fields after Irvine and Baragar (1971).

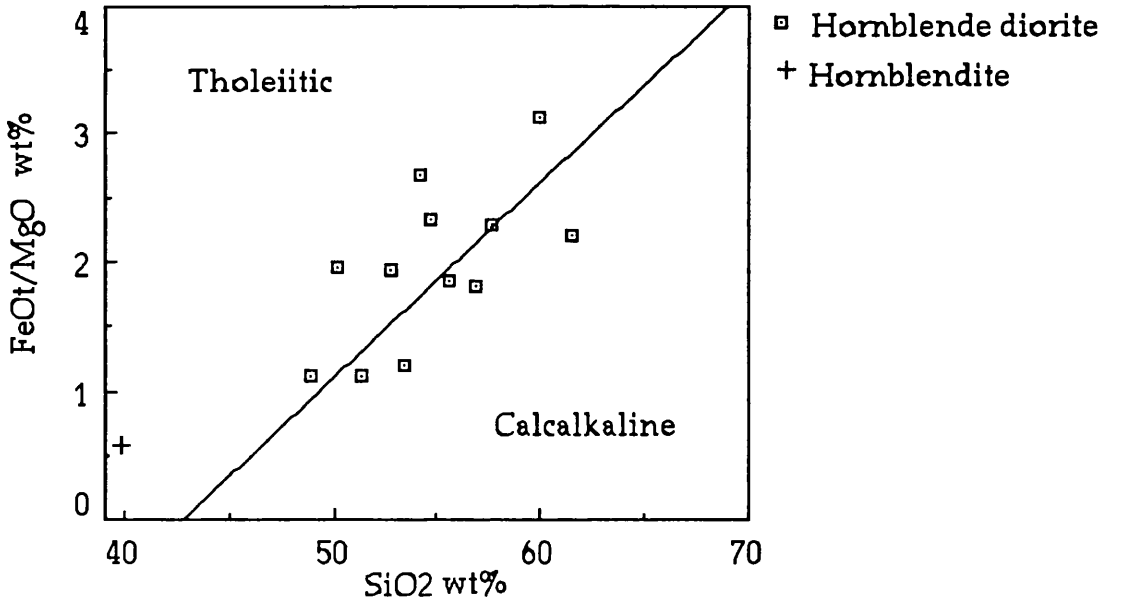

Figure 60: Plot of FeOt/MgO vs SiO2. Tholeiitic-calcalkaline from Miyashiro (1974).

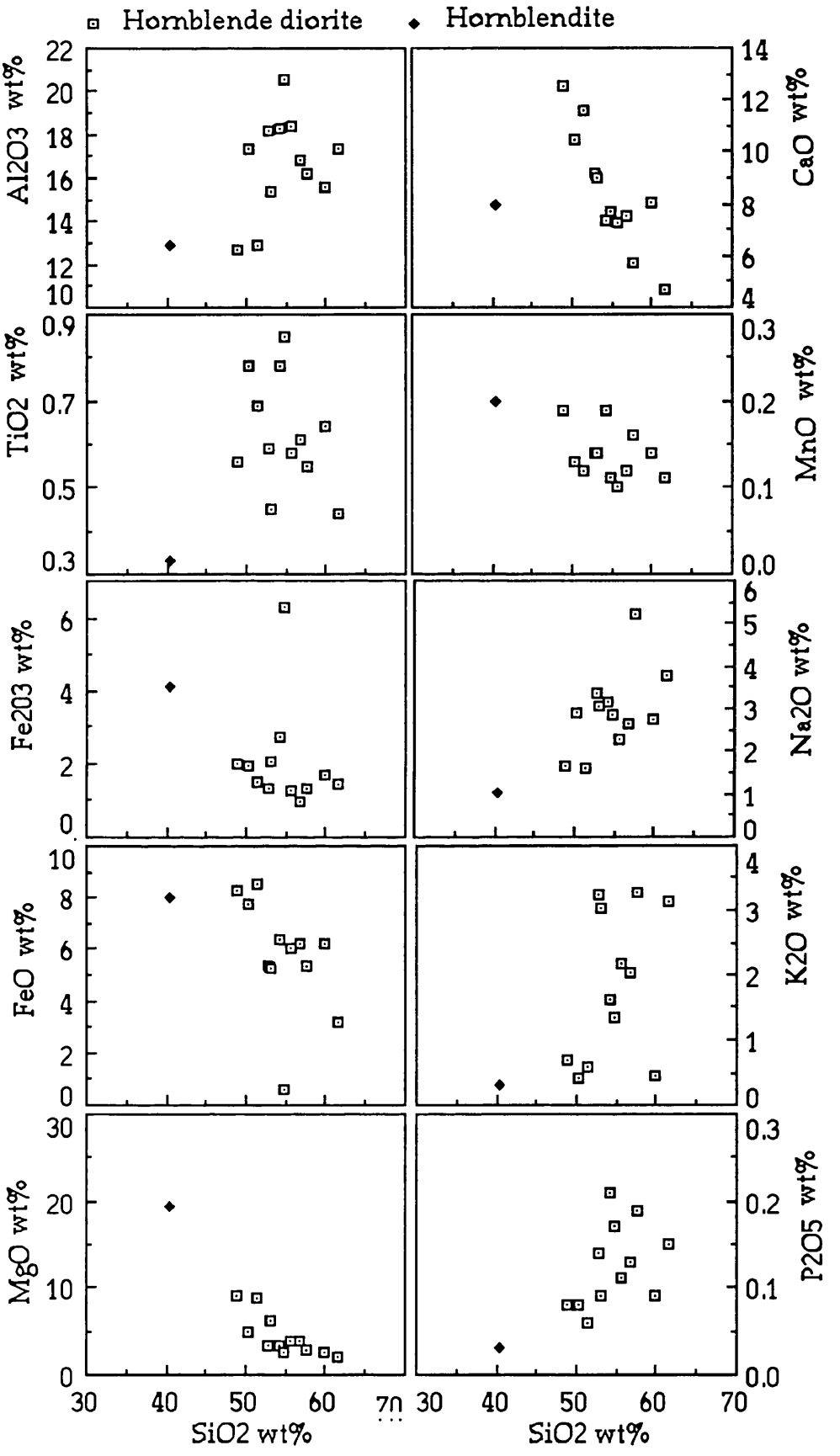

Figure 61: Harker variation diagram of the hornblende diorite and hornblendite.

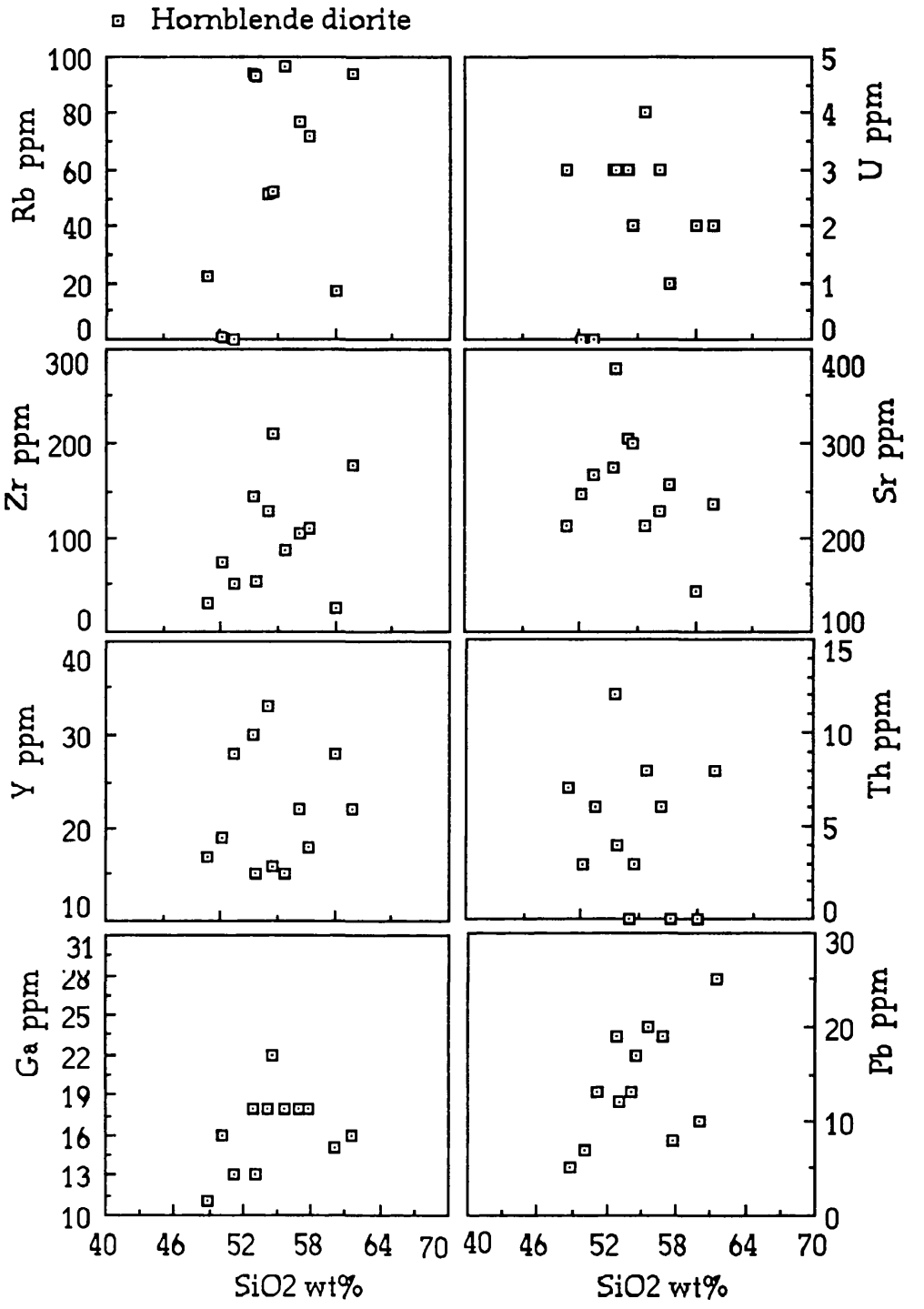
Hornblende diorite
Rb ppm
U ppm
Zr ppm
Sr ppm
Y ppm
Th ppm
Ga ppm
Pb ppm
SiO2 wt%
SiO2 wt%

Fig. 61: Cont.

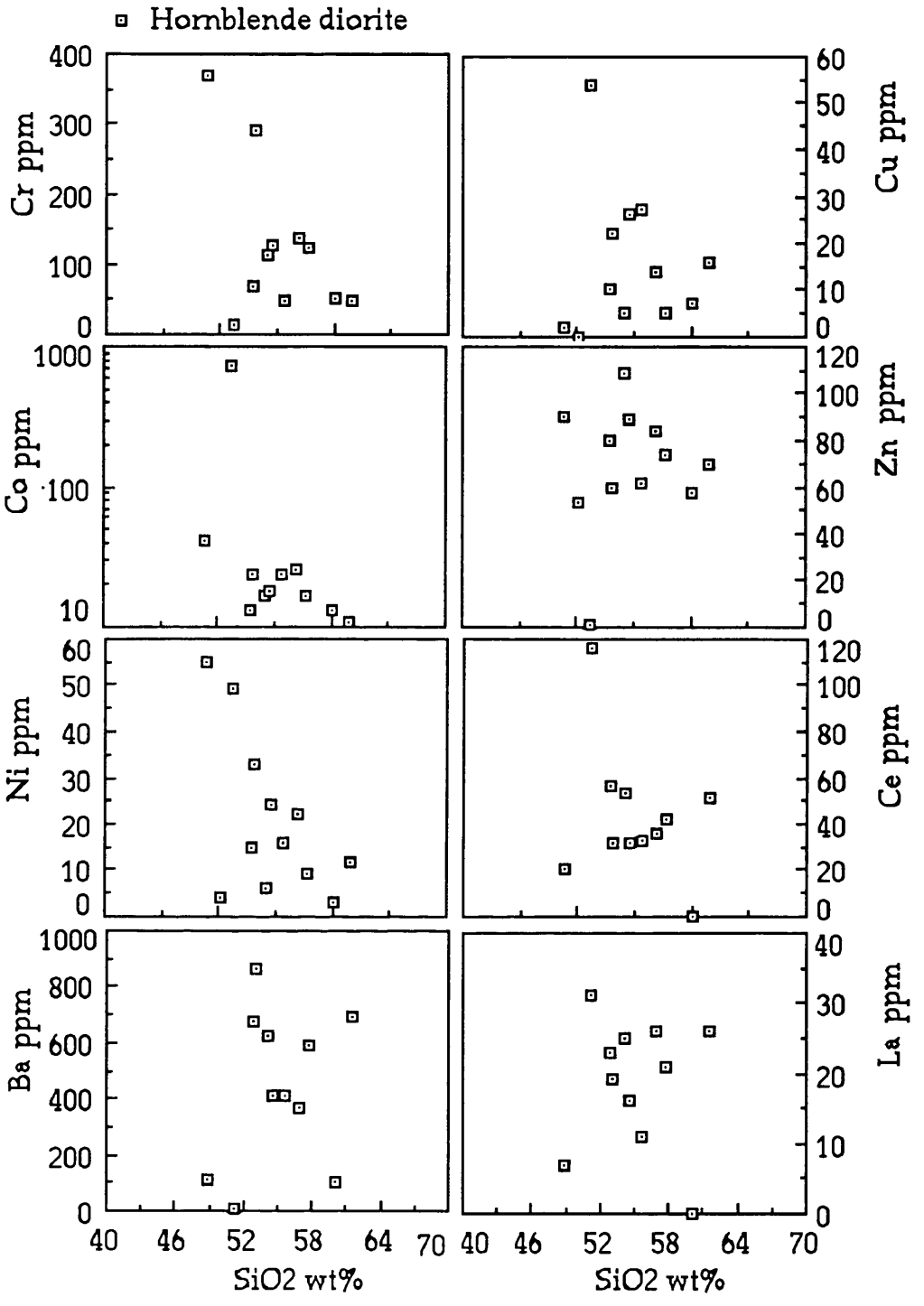
Hornblende diorite
Cr ppm
Cu ppm
Co ppm
Zn ppm
Ni ppm
Ce ppm
Ba ppm
La ppm
SiO2 wt%
SiO2 wt%

Fig. 61: Cont.

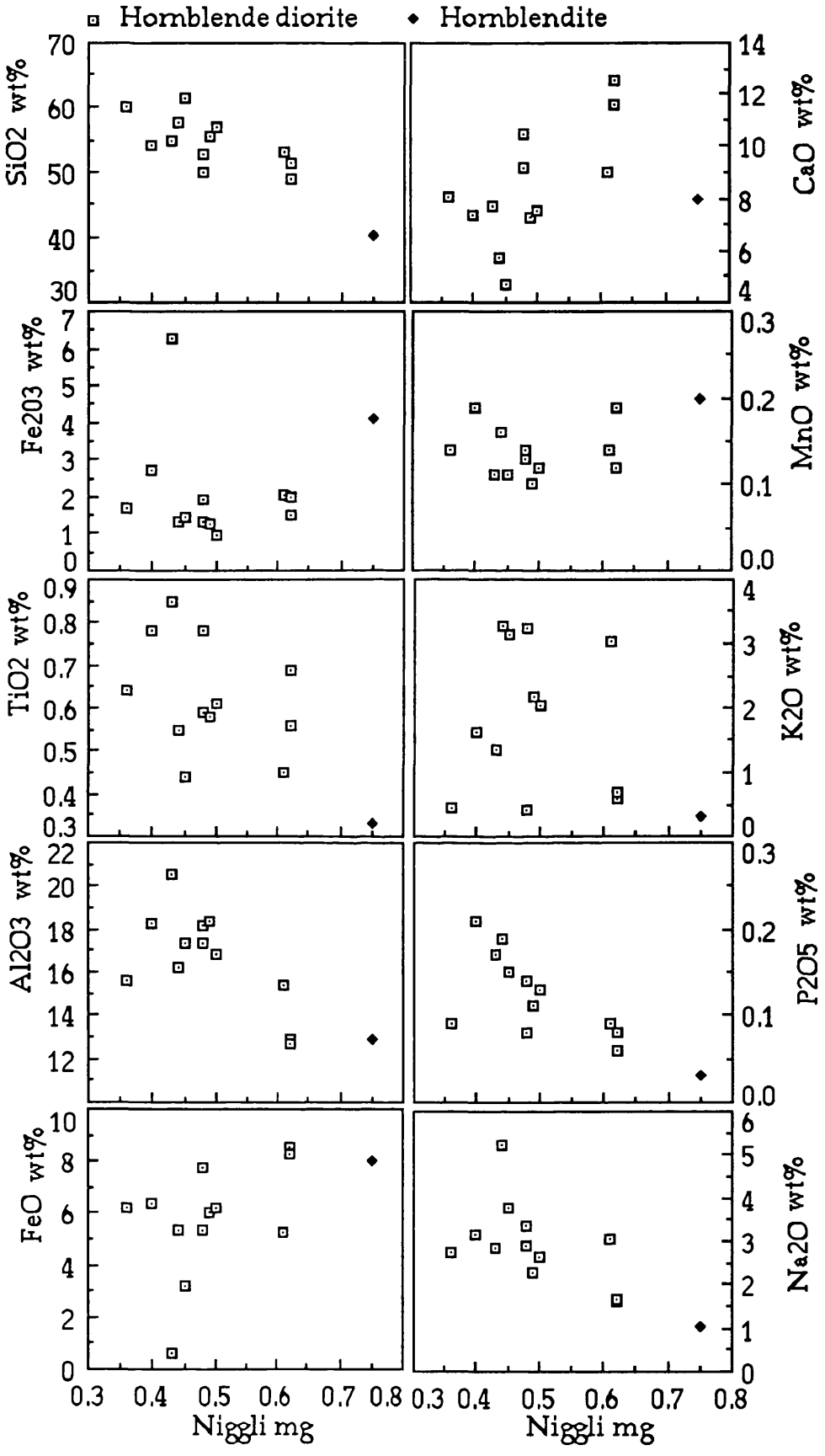

Figure 62: Major oxides vs Niggli mg.

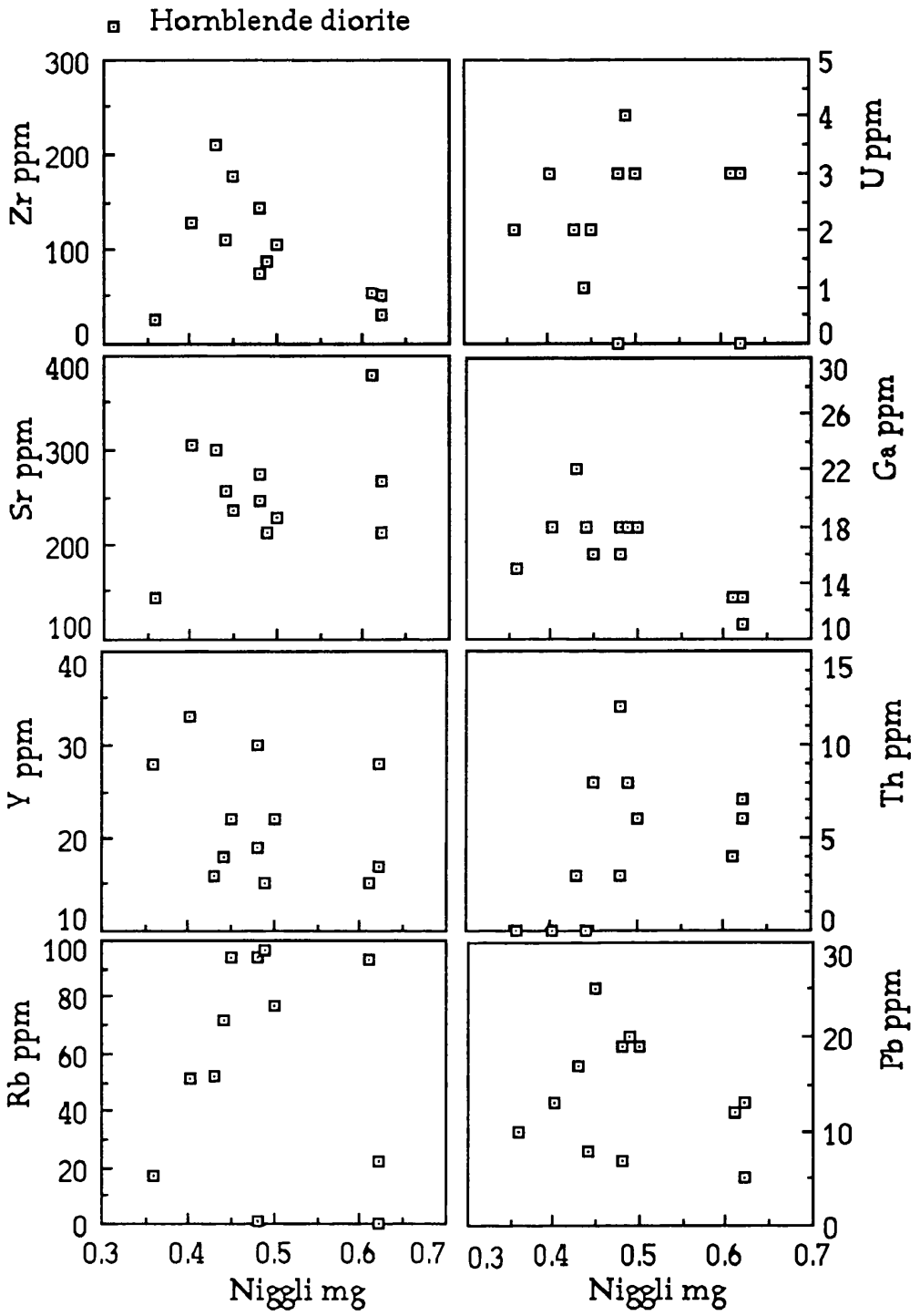

Figure 63: Trace elements versus Niggli mg.

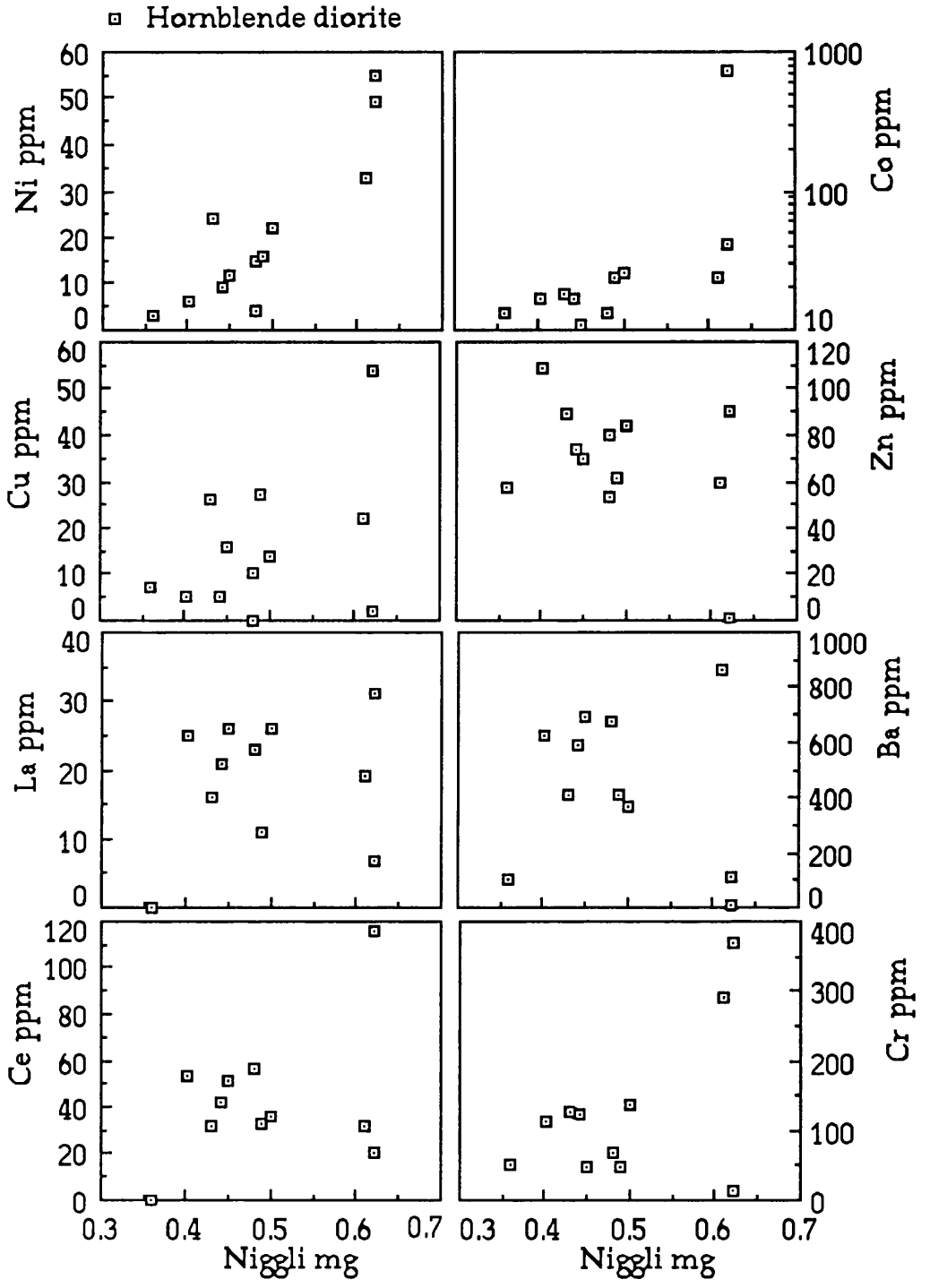
Hornblende diorite
Ni ppm
Co ppm
Cu ppm
Zn ppm
La ppm
Ba ppm
Ce ppm
Cr ppm
Niggli mg
Niggli mg

Fig. 63: Cont.

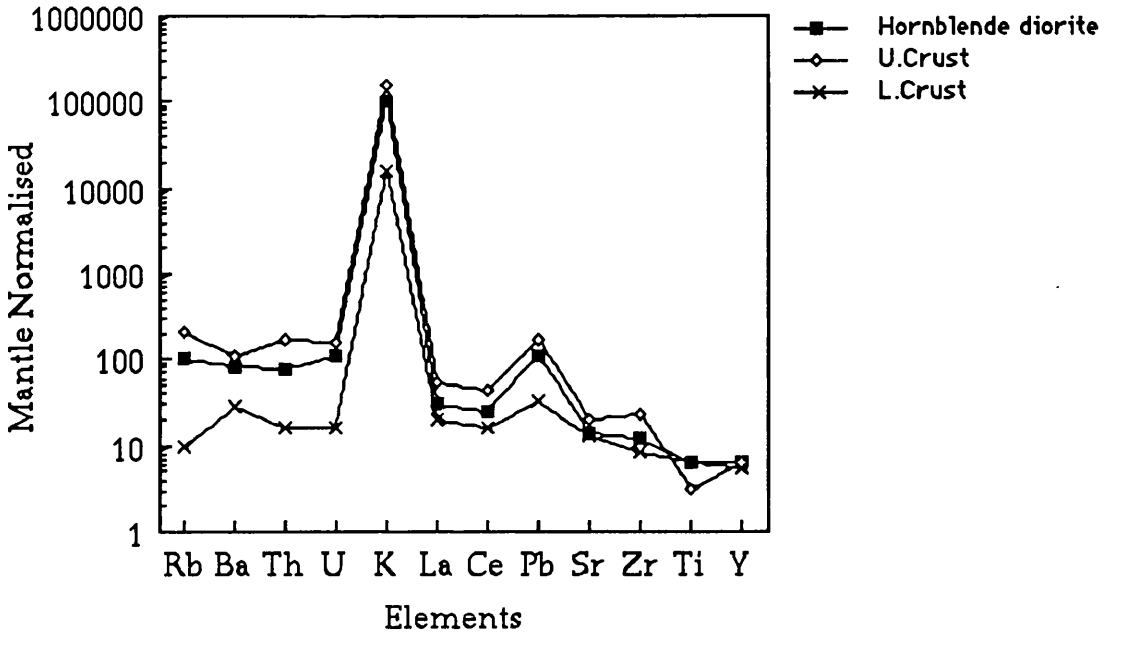

Figure 64: Primitive mantle normalised hornblende diorite, Upper Crust and Lower Crust. Mantle and Crust values are from Taylor and McLennan(1985).

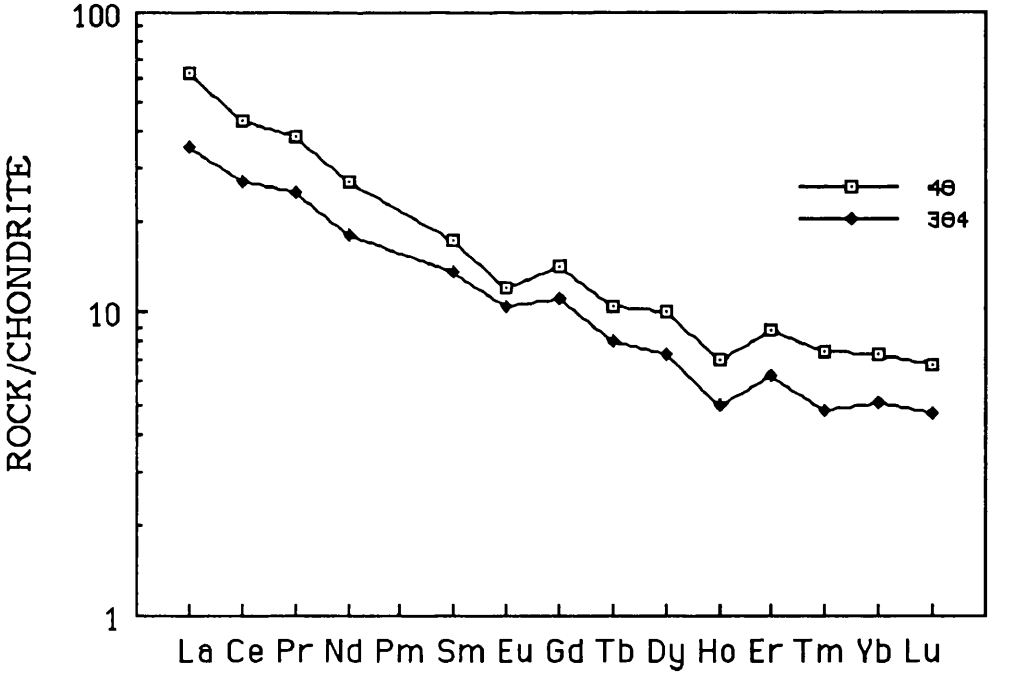

Figure 65: Chondrite normalized (Boynton, 1984) REE pattern of the hornblende diorite.

Table 42: Test of fractionation from the hornblendite to sample 369, hornblende diorite.

Composition:	initial	final	hbl	An	Spl
SiO2	39.93	61.37	46.88	45.22	0.12
TiO2	0.33	0.44	1.49	0.07	0.00
Al2O3	12.75	17.32	12.93	34.63	57.53
Fe*2O3	12.88	5.00	11.50	0.32	31.80
MnO	0.22	0.11	0.25	0.00	0.26
MgO	19.34	2.03	15.68	0.12	10.27
CaO	7.88	4.68	11.32	18.62	0.02
Na2O	1.03	3.78	1.66	0.98	0.00
K2O	0.31	3.14	0.29	0.03	0.00
P2O5	0.03	0.15	0.00	0.00	0.00
H2O	5.31	1.89	0.00	0.00	0.00
CO2	0.00	0.09	0.00	0.00	0.00
S%	0.00	0.00	0.00	0.00	0.00
Cr2O3	0.00	0.00	0.00	0.00	0.00
NiO	0.00	0.00	0.00	0.00	0.00

	bulk comp. of added or subtr.matl.	obs.diff. between magmas	calc.diff. between magmas	obs.-calc. (residuals)
SiO2	40.94	21.435	20.455	0.980
TiO2	1.62	0.112	-1.186	1.298
Al2O3	12.82	4.573	4.501	0.072
Fe*2O3	15.31	-7.879	-10.321	2.442
MnO	0.29	-0.108	-0.184	0.075
MgO	18.06	-17.302	-16.052	-1.250
CaO	9.00	-3.203	-4.330	1.127
Na2O	1.69	2.748	2.145	0.603
K2O	0.31	2.833	2.834	-0.001
P2O5	0.00	0.120	0.150	-0.030
H2O	0.00	-3.418	1.897	-5.315
CO2	0.00	0.090	0.090	0.000
S%	0.00	0.000	0.000	0.000
Cr2O3	0.00	0.000	0.000	0.000
NiO	0.00	0.000	0.000	0.000
total				0.000

sum of the squares of the residuals = 40.0629

phase name	amount as wt.pct. of init.magma	amount as wt.pct. of all phases	amount as wt.pct. of added phases	amount as wt.pct. of subtrd.phases
Hornblende	-109.81	80.24	0.00	92.67
Anorthite	-8.68	6.34	0.00	7.33
Spinel	18.35	13.41	100.00	0.00
totals rel. to initial magma =			18.35	118.49

hrb: hornblende, an: anorthite, spl: spinel
obs.diff: observed difference, wt. pct: weight percentage

* :Fet as Fe2O3

IV.5.3 Granitoids and associated rocks

In this chapter, granitoids with enclaves, microgranites and quartz-alkali syenites will be examined to decipher any possible genetic link with each other using principally chemical analyses.

IV.5.3.1 Granitoids

IV.5.3.1.1 Major and trace elements

The granitoids have substantial variation in composition: SiO2 ranges from 64.13% to 73.43% with an average of 69.11 % while Na2O and K2O vary between 1.84-4.19% and 2.14-4.56%, respectively (Table 43). The ratio of K2O to Na2O is generally >1(1.12 mean) and changes with the proportion of biotite and K-feldspar to albite. CaO, in Ca-plagioclase (hornblende is minor) varies from 1.30% to 4.44% having an average of 2.67. The molar-ratio of Al2O3 to Na2O+K2O+CaO, A/CNK is usually less than 1.1 but also equal to or larger than 1.0 therefore, granitoids are metaluminous to slightly peraluminous in composition(Fig. 66) according to the definition of Shand(1947).

The granitoids, plot in the adamellite and granodiorite field on Debon & Le Fort's (1982) diagram (Fig. 67) and in the biotite+hornblende or biotite granite field in the characteristic minerals diagram (Fig. 68-a). The lineament they define on the classification diagram is characteristic for neither the cafemic nor alumino-cafemic group (Fig. 68-b). But the enclaves follow the cafemic group, which always starts with amphibole and/or pyroxene but often ends with biotite alone or two mica rocks(Debon&Le Fort, 1982). To identify the cafemic or alumino-cafemic subgroup a QBF triangular diagram was used (Fig. 69-a). As the granitoids

plot at the intersection of the light-coloured subalkaline (SALKL) and calkalkaline (CALK) lines (Fig.69-b), they are of either SALKL or CALK in characteristic. Debon and Le Fort (1988) classified igneous rocks into magnesian and ferriferous associations using Mg/(Fe+Mg) versus Fe+Mg+Ti diagram. The dividing line between the two associations passes through the granite, adamellite, granodiorite, tonalite, quartz diorite and gabbro reference points which are average values obtained from 670 plutonic samples from Afganistan (Debon and Le Fort, 1988). Therefore, Fig. 70 shows that the Ortakoy granitoids are relatively enriched in Mg and can be called magnesian associations.

Granitoids plot largely in the high-K field of Peccerillo and Taylor(1976) in a binary diagram of K2O versus SiO2 (Fig. 71). On an AFM ternary diagram (Fig. 72), they show typical calcalkaline character. In a Harker, diagram increase of Al2O3, CaO, TiO2, MgO, FeO, Fe2O3, P2O5, Zn, Ga and decrease of K2O, Th and Rb with decreasing SiO2 suggest fractionation of plagioclase, hornblende and apatite (Fig. 73) and Fig.s 74, 75 and 76 confirm (apart from apatite) these suggestions. Better correlation is seen when the granitoids and the diorites are plotted together (Fig.s 77 and 78) on the Harker diagram than when the granitoid is plotted alone (particularly for CaO , MgO and FeO). The fractionation was tested with linear mass-balance calculations using an XLFRAC computer program (Stormer&Nicholls, 1978) with the chemical composition of the diorite as an initial magma and microprobe analyses of the hornblende and the plagioclase as fractionation phases. and the results are presented in Table 48. The sum of the squares of the residuals is not smaller than 1(10.72) hence the fractionation of the granitoids from the diorite is unlikely.

Granitic rocks are classified into two major groups according to their source by Chappell and White(1974). I-type granitoids are free of normative corundum and are in theory derived by fractional crystallisation or remelting of basaltic parents while S-type granitoids have normative corundum and a metasedimentary source and contain modal cordierite and biotite with or without garnet, Al-silicate polymorphs and muscovite. The average composition of the Ortakoy granitoid is similar to the that of I-type granite from the Lachlan Fold Belt, with only slight differences with low Fe2O3, TiO2, MgO, CaO, Y, Sr, U, Th, Cu, Ce, and higher MnO, Pb and Cr (Fig. 79). Fig. 80 also shows that the granitoid samples largely plot in the I-type field with only a few samples at the edge of the S-field. The hornblende-bearing mineralogy and the existence of igneous xenoliths(enclaves) in the samples are in conformity with an I-type granite. Their slightly peraluminous character is not untypical since almost one half of the I-type granitoids of the Lachlan Fold Belt are weakly peraluminous with a ratio generally less than 1.1(Chappell&White, 1992). This slight Al enrichment in I-type granites may result from small analytical errors or hydrothermal alteration which can lead to the destruction or mobilisation of feldspars and the mobilisation of Na, K, and Ca.

Barbarin (1990) compared the main petrogenetic classifications of granitoids with each other and proposed another classification based on whether the granitoids were derived from the mantle, the crust and/or were hybrid. Granitoids with A/CNK generally less than 1.1 and FeOt/(FeOt+MgO) less than 0.8 are termed "hybrid continental arc groups" (H_{CA}), which were emplaced in a continental margin above an active subduction zone. According to this classification, the granitoids are supposed to have an initial $^{87}Sr/^{86}Sr$ between 0.706 to 0.708. The

counterparts of H_{CA} are the Andino type of Pitcher(1983, 1987), and continental arc granitoids (CAG) of Maniar and Piccoli(1989).

Granites are the most abundant plutonic rock in the crust (Clarke, 1992) and can be produced from various sources by partial melting process (e.g. Tuttle &Bowen, 1958; Helz, 1976; Wyllie, 1983; Ellis&Thompson, 1986; Conrad et al.,1988; Vielzeuf&Halloway, 1988). The amount of melt produced by this process is dependent on P-T-fluid conditions at, and the composition of the source region. The melt becomes mobile with its restite after reaching the critical melt fraction of Van der Moolen and Paterson (1979). Granite magmas must originally contain restite at their source and many of them never completely rid themselves of that component (Chappell&White, 1992). The proportion of the melt and restite varies from granites that are pure magma to those that contain abundant restite. Melt dominated granites can be distinguished from restite-dominated ones by decreasing K/Rb with increasing SiO2(Wyborn et al., 1992). Fig. 81 shows that the Ortakoy granitoids are melt-dominated rather than restite-dominated.

Y/Nb ratio is generally unchanged by crustal assimilation(Eby, 1990), therefore different Y/Nb ratios between granites at similar stages of their magmatic evolutions might have originated from heterogeneous source materials(Sewell et al., 1992). As seen in Fig. 82, the granitoids display two distinct trends; one with decreasing Y/Nb with increasing SiO2, probably as a result of the crystallisation of amphibole and the other with little change of Y/Nb with respect to SiO2 variation. Although, hydrothermal alteration might induce Y/Nb variation by leaching and removing accessory minerals the actual accessory mineral contents of those samples which have lower Y/Nb do not support this suggestion. Hence, the granitoids are likely to

have been derived from heterogeneous sources. The classification peraluminous and metaluminous parameters do not correspond to these differences with A/CNK in these samples varying from 0.96 to 1.12 but showing no correlation with Y/Nb (Fig. 83).

IV.5.3.1.2 Tectonic Setting

Using the multicationic diagram of Fig. 84, the granitoids largely fall into group 2, representing calcalkaline and trondjhemitic rocks in composition, and group 6 which represents syn-collision, anatectic two mica leucogranites. However, the Nb-Y diagram of Pearce et al.,(1984) shows them as Volcanic Arc Granitoids (VAG) and Syn-Collision Granitoids, syn-COLG, (Fig.85). Clear distinction between these two groups is made by a Rb versus Y+Nb diagram(Fig. 86) showing that the granitoids posses VAG character. Fig. 87 shows that the K/Rb ratios in the Ortakoy granitoids are generally less than 320, similar to continental arc granitoids of Peru. The compositions of the Ortakoy granitoids are close to those occuring in normal continental arcs rather than mature or primitive continental arcs (Fig. 88). Low FeOt/MgO ratio in the granitoids (Fig. 89) suggests that the acidic rocks are of unfractionated type according to Whalen et al.(1987). In summary, the unfractionated Ortakoy granitoids agree with a volcanic arc setting which is of continental and normal(not primitive or mature) type.

IV.5.3.1.3 REE analyses

The REE patterns of the granitoids are characterised by a light REE enrichment compared with the heavy REE. This is often interpreted as evidence for residual garnet during the partial melting event (Fig.91). A

moderate negative Eu anomaly (Eu/Eu*: 0.53-0.75) indicates the fractionation of plagioclase out of the magma before the analysed material crystallised. This Eu anomaly could also indicate the presence of residual plagioclase during the granitoid melting event or be a feature inherited from the source materials. Sample 367 exhibits a much more fractionated pattern, particularly in HREE(Gd/Lu: 6.2) than the rest of three samples in which Gd/Lu ranges from 1.8 to 2.5. If all samples have experienced a similar petrological process then the difference in REE pattern might have resulted from heterogeneous source compositions, probably variable amounts of garnet. Therefore, the granitoids could have formed from a garnet and plagioclase-bearing source.

IV.5.3.1.4 Source of the granitoids

The occurrence of migmatites in the metasediments provokes granite forming by partial melting. The slightly peraluminous character of the Ortakoy granitoids with minor metasedimentary xenoliths might suggest a sedimentary source. However, the granodiorite-dominated mineralogical composition and I-type characteristics in the granitoids(hornblende-bearing mineralogy, existence of mafic enclaves etc), suggesting an igneous source precludes this but it is possible that metasediments might have contributed to the granitic magma to a small extent. Barbarin (1990) classification for the Ortakoy granitoids, hybrid continental arc groups, support this view.

Experimental petrology shows that amphibolites and eclogites are suitable sources for the tonalite and granodiorite family (Helz, 1973, 1976; Burnham, 1979; Wyllie, 1984). Mantle peridotite is less likely to produce voluminous granitoid batholiths (Clarke, 1992). REE patterns of the granitoids carry the signature of garnet at their source. Therefore, the

Ortakoy granitoids, originally could have been extracted from a garnet-bearing source (eclogite and/or garnet-amphibolite).

IV.5.3.2 Enclaves

IV.5.3.2.1 Major and trace elements

Although only two enclave samples were analysed (Table 44) they show SiO2 ranging from 54.04 to 58.76 wt% while CaO changes from 4.67% to 7.16% and K2O from 1.51 to 4.37%. These variations reflect modal changes in K-feldspar, biotite and plagioclase. The analyses are metaluminous in composition with A/CNK values between 0.84 and 0.92.

The enclaves are generally much more basic than their host rocks (Fig.s 73 and 77). The grain size in the enclaves is finer than that of the host granitoid, which is interpreted to be important in supporting a magmatic origin for the enclaves(Vernon, 1984). The existence of sharp contacts between the enclaves and the host rocks indicates the lack of reaction (diffusion) between these rocks. Such mafic rocks within intermediate and acidic intrusives are mainly considered as magmatic precursors (e.g. Didier,1973; Bacon,1986; Hill et al., 1986; Zorpi et al., 1989) or else disrupted basic dykes. They are thought to be helpful in identifying any mixing and mingling process between acidic and basic magmas (Zorpi et al., 1991; Holden et al., 1991; Lorenc, 1990; Castro et al., 1990; Lorenc & Saavedra, 1989). The existence of some minerals in the enclaves, viz. poikilitic hornblende and particularly K-feldspar may be related to hybridization (Lorenc, 1990). K-feldspar which occurs in enclaves and is similar to K-feldspar in the host rock was possibly incorporated into the basic magma probably during their injection into the host rock(Hibbard, 1981).

The abundance of hornblende and biotite in the enclaves reflects crystallisation under high P_{H2O} conditions. The ellipsoidal and somewhat elongated shape is dominant in the enclave reflecting reaction during flow in the host magma. The host granite was probably a crystal mush when it came into the contact with the enclave magma melt, hence megacryst development in the enclaves (Eberz & Nicholls, 1988).

The enclaves contain relatively high K and Rb compared to their SiO2 content (Fig.s 71 and 73). This enrichment process results from crystallisation of K-feldspar.

There are two main hypotheses for the origin of enclaves: a) enclaves derived from mafic rocks, synplutonic with their host rock(e.g. Eberz & Nicholls, 1988; Zorpi et al.,1989). b) Mafic magma precursor of the granitic magmatism. For instance, Holden et al.(1987) showed that suites of microdiorite enclaves in two separate granite plutons from Scotland have higher initial $\in_{Nd}$ than their immediately enclosing host granitoid, indicating injection of mantle-derived magmas into the crust as precursors to the production of the host granitoid magma. This is in accord with the petrographic and field evidence.

The enclaves, together with the host rock, underwent plastic deformation during the intrusion's emplacement, and this resulted in an elliptic shape oriented parallel to the granite margin in the marginal zones of intrusion. (Lorenc&Saavedra, 1989).

Two main hybridization mechanisms, leading to enclave-forming in granitoids, were suggested by Zorpi et al.(1991) a) Chemical migration from

felsic to mafic component (e.g. Si, Rb, K) and in the opposite direction loss of Ca and Sr by volatiles and diffusion induce formation of a transition zone between the enclave and host rock. The rate of chemical transfer depends on the chemical contrast and the physical state of both components. The rate is greatest for the fully-molten state, decreases progressively with the crystallisation of the enclaves. Thus, since the size of enclaves controls their cooling rate so the magnitude of chemical exchange increases with enclave size (Barbarin&Didier, 1992) b) Mass-to-mass mixing is performed by disaggregation of a mafic component and its "partial assimilation" by granitic rocks. Mechanical transfer of crystals occurs due to differences in viscosities or active stirring of the two magmas (Barbarin&Didier, 1992). In summary, the Ortakoy granitoids with enclaves might have been involved to mass-to-mass mixing and mechanical transfer (inducing the formation of K-feldspar). Chemical migration is unlikely owing to the existing sharp contact between the mafic component and its host rock.

The modelling of genetic links between the enclaves and their host rock is impossible due to the fact that the enclaves are megacrystic and not homogeneous(Eberz & Nicholls, 1988). The physical appearance, and the chemical (Fig.s 77 and 78) and mineralogical compositions of the enclaves, are close to the that of the diorite so it is likely that the diorites are a possible source from which enclaves were derived.

IV.5.3.3 Microgranite

IV.5.3.3.1 Major and Trace Elements

The microgranites are associated with the granitoids and are peraluminous in composition with K2O/Na2O ranging from 0.98 to 1.71(Table 45). On Debon & Le Fort (1982) diagram, the microgranites plot in the granite and perquartzose granitoids fields (Fig. 67). They are in or close to leucogranite on the characteristic minerals and QBF triangular diagrams (Fig.s 68-a and 69-a).

The microgranites plot on both the high- and low-K field of Peccerillo and Taylor(1976) in Fig.71. The transition between granitoid and microgranite is seen on an AFM diagram with alkali enrichment in the calcalkaline field(Fig. 72). In general, they are coherent to the trends of the granitoids on Harker diagrams (Fig.73, 77 and 78). Na2O and K2O of the microgranite plot on the border between I- and S-type granites in Fig.80. However, because of the lack of Al-rich minerals such as muscovite or garnet and close associations with the granitoids (I-type), it is probable that these are fractionated I-type granites and Fig. 89 may support this. The increase in Rb/Ba in the microgranite indicates pronounced alkali feldspar fractionation(Fig.90). The decrease in Zr+Ce+Y is perhaps due to the separation of zircon and apatite as accessory minerals, depleting the magma in Zr and REE.

The fractionation of microgranite from the granitoid was also tested (Table 49) with same method as for the granitoid (least mass balance calculations) and the sum of the squares is 1.896 making such fractionation unlikely.

In the Pearce et al.(1984) tectonic classification diagram, the microgranites plot in the VAG field with the granitoids(Fig.s 85 and 86). The binary diagram of Rb/Zr versus Nb(Fig.88) agrees with formation in a Normal Continental Arc with the granitoids.

IV.5.3.4 Quartz-alkali syenite

IV.5.3.4.1 Major and trace elements

The mineralogical composition of the analysed samples varies from alkali syenite(637) through quartz-alkali syenite(634) to alkali granite(658). The samples range in SiO2 from 69.18% to 78.73% while K2O/Na2O changes between 0.04 and 1.77(Table 46). A/CNK values in the quartz-alkali syenite are always larger than 1, i.e. they are peraluminous. The terminology on a Debon & Le Fort (1982) diagram (Fig. 67) depends on the relative proportions of albite, quartz and orthoclase. Albite dominated samples have a composition of gabbro/diorite/anorthosite, which shows an important difference between mineralogical and chemical classifications, whereas quartz and K-feldspar dominated samples plot as granodiorite and granite respectively. The quartz-alkali syenites spread over the leuco granite area in the QBF triangular diagram(Fig. 69-a).

The quartz-alkali syenites plot mainly in the high-K field with one sample in the low-K field (Fig.71). On an AFM ternary diagram(Fig. 72), they plot close to the alkaline corner. The quartz-alkali syenites follow different trends from the granitoids for Al2O3, Na2O, K2O, Fe2O3 and Rb, Pb and possibly Nb on Harker diagrams(Fig.s 73, 77 and 78). This precludes the quartz-alkali syenites from being formed from the granitoids by fractionation. The quartz-alkali syenites, which have variable chemical compositions ranging from alkali syenite to alkali granite can be formed from a syenitic magma by crystal fractionation.

With fractionation, the ratio of K/Rb decreases sharply and Y/Nb increases slightly (Fig.s 81 and 82). In the Pearce et al.(1984) diagram of Rb-Y+Nb, the quartz-alkali syenites occur in the VAG field (Fig.s 85 and 86).

IV.5.3.4.2 REE Analysis

The REE pattern of the quartz-alkali syenite (Fig.92) is characterised by light REE enrichment (La/Sm: 4.63) with slightly fractionated HREE (Gd/Lu: 1.91). The existence of moderate negative Eu anomaly (Eu/Sm: 0.42) indicate the fractionation of plagioclase.

IV.5.3.5 Conclusions

The Ortakoy granitoids are metaluminous to slightly peraluminous, high-K (Peccerillo and Taylor,1976), magnesian and possibly cafemic (Debon & Le Fort, 1988), and calcalkaline (Irvine & Baragar, 1971) in character.

Fractionations of various phases viz. feldspars, biotite, hornblende and apatite largely control the chemical variations within the acidic rocks which are of I- and Andino type(Chappell&White, 1974; Pitcher, 1983), continental arc granitoids (Maniar&Piccoli, 1989) and hybrid continental arc groups (Barbarin, 1990). The fractionation test shows that the formation of the granitoid from the diorite via fractional crystallisation of hornblende and plagioclase is unlikely. It is suggested that the granitoids could have been formed from a garnet bearing source (eclogite and/or amphibolite) by partial melting. The metasediments are likely to contribute to the granitic magma.

As K/Rb decreases with increasing SiO2, the granitoids are melt-rich type (Wyborn et al., 1992) that were derived from an heterogeneous source inferred from the different Y/Nb ratios at similar evolution stages of the acidic pluton.

Poikilitic hornblende and K-feldspar in the enclaves, similar to those occur in the host rock, are suggested to be xenocrysts derived from the granitoid. The enclaves possibly belong to the diorite magma and crystallised away from their present host. Mass-to-mass mixing and mechanical transfer are possible hybridization processes altering the chemical compositions of the mafic component and its host.

The microgranite is suggested to have formed in a continental arc setting associated with the granitoids.

The quartz-alkali syenites showing transition to alkali syenite and alkali granite may be formed from a syenitic magma by crystal fractionation

Table 43: Major oxides and trace elements analyses of the granitoids

Sample No	655	573	562	559	437	669
SiO2	71.83	64.13	69.90	68.79	73.43	70.98
TiO2	0.23	0.45	0.31	0.34	0.51	0.22
Al2O3	13.73	16.67	14.45	14.95	13.80	13.65
Fe2O3	0.26	1.89	0.46	0.72	0.57	0.28
FeO	1.88	2.87	1.60	2.64	2.75	2.04
MgO	0.69	1.51	1.00	1.31	1.54	1.24
MnO	0.12	0.11	0.06	0.09	0.08	0.11
CaO	2.08	4.44	1.89	3.02	1.30	2.58
Na2O	3.63	3.69	4.19	2.78	1.84	3.11
K2O	3.44	2.33	4.33	3.72	2.14	4.02
P2O5	0.06	0.18	0.10	0.09	0.08	0.06
H2O	1.35	1.30	1.25	1.40	1.67	1.40
CO2	0.74	0.07	0.19	0.29	0.19	0.49
Total	100.04	99.64	99.73	100.14	99.90	100.18
K2O/Na2O	0.95	0.63	1.03	1.34	1.16	1.29
A/CNK*	1.01	1.0	0.96	1.06	1.79	0.96
U	0	2	3	2	1	0
Th	19	9	18	22	12	15
Ce	47	55	63	62	47	41
La	23	32	31	33	24	19
Pb	49	19	23	27	14	31
Ba	489	1031	630	368	469	262
Zr	128	200	190	137	206	100
Y	11	20	22	22	23	15
Sr	132	321	113	128	146	116
Rb	244	75	184	156	66	190
Ga	12	18	18	15	16	12
Zn	35	74	32	51	45	34
Cu	1	0	0	2	7	3
Ni	3	1	6	5	29	6
Co	8	5	3	4	7	11
Cr	21	35	122	19	146	38
S	22	6	0	5	2	23
Nb	12	8	15	9	9	6
K/Rb	141	311	235	238	324	211
Rb/Sr	1.8	0.2	1.6	1.2	0.4	1.6

* : molar-ratio of Al2O3 to CaO+Na2O+K2O

Table 43 cont.

Sample No	367	314	233	203	Mean	σn
SiO2	67.46	66.74	70.97	66.87	69.11	2.68
TiO2	0.40	0.37	0.19	0.33	0.34	0.10
Al2O3	15.41	16.13	14.04	15.43	14.83	1.00
Fe2O3	0.60	0.91	0.35	0.57	0.66	0.45
FeO	2.97	2.70	1.90	2.79	2.41	0.47
MgO	1.67	1.44	0.77	1.41	1.26	0.32
MnO	0.06	0.04	0.07	0.06	0.08	0.03
CaO	2.77	3.41	2.06	3.2	2.67	0.85
Na2O	2.75	3.09	3.43	3.52	3.20	0.62
K2O	3.85	2.97	4.56	4.02	3.54	0.77
P2O5	0.16	0.12	0.07	0.10	0.10	0.04
H2O	1.50	1.65	1.48	1.48	1.45	0.13
CO2	0.19	0.12	0.11	0.20	0.26	0.19
Total	99.79	99.69	100.01	99.98		
K2O/Na2O	1.4	0.96	1.33	1.14	1.12	0.22
A/CNK*	1.12	1.11	0.98	0.97	1.1	0.24
U	3	3	3	0	2	1
Th	5	12	20	11	14	5
Ce	34	46	39	60	49	10
La	17	21	22	34	26	6
Pb	36	30	25	21	28	9
Ba	495	434	293	369	484	209
Zr	135	131	128	132	149	34
Y	16	21	14	0	16	7
Sr	171	159	101	147	153	59
Rb	153	140	192	152	155	51
Ga	17	19	13	15	16	2
Zn	57	52	26	30	44	14
Cu	12	9	5	2	4	4
Ni	19	7	3	3	8	9
Co	10	6	5	7	7	2
Cr	114	131	82	108	82	46
S	4	4	2	4	7	8
Nb	9	3	5	3	8	4
K/Rb	252	212	238	264	242.6	49.2
Rb/Sr	0.9	0.9	1.9	1.0	1.15	0.55

* : molar-ratio of Al2O3 to CaO+Na2O+K2O

σn : Standard deviation

Mean: Arithmetical mean

Mineralogical composition and coordinates of the granitoids analysed

655	pl+qtz+hbl+or+bt"	82200-93150	367	qtz+pl+or+bt	92105-82350
573	pl+qtz+bt+or+hbl	84550-85800	314	qtz+pl+or+bt	91400-91075
562	pl+qtz+or+bt+hbl	81437-94825	233	qtz+pl+or+bt+hbl	80412-87750
559	pl+or+bt+qtz+hbl	78520-93862	203	qtz+pl+or+bt+hbl	77275-95688
437	qtz+pl+ser^+bt	92750-84650			
669	qtz+or+pl+bt+hbl	77262-95812			

^ : sericite

" : mineral symbols are from Kretz(1983)

Table 44: Major oxides and trace elements analyses of the enclaves

Sample No	227	96	Mean	σn
SiO2	58.76	54.04	56.40	2.36
TiO2	0.46	0.60	0.53	0.07
Al2O3	16.76	17.42	17.09	0.33
Fe2O3	1.88	1.5	1.69	0.19
FeO	5.11	7.87	6.49	1.38
MgO	2.75	3.16	2.96	0.21
MnO	0.20	0.26	0.23	0.03
CaO	4.67	7.16	5.91	1.24
Na2O	3.02	3.73	3.38	0.36
K2O	4.37	1.51	2.94	1.43
P2O5	0.09	0.10	0.09	0.01
H2O	1.10	2.46	1.68	0.42
CO2	0.83	0.12	0.47	0.36
Total	100.13	99.57		
K2O/Na2O	1.45	0.40	0.92	0.53
A/CNK*	0.92	0.84	0.88	0.04
U	3	3	3	0
Th	7	4	5	1
Ce	36	40	38	2
La	13	11	12	1
Pb	45	49	47	2
Ba	617	682	650	32
Zr	89	101	95	6
Y	35	33	34	1
Sr	102	348	225	123
Rb	206	158	182	24
Ga	15	16	16	0
Zn	87	91	89	2
Cu	14	15	15	0
Ni	11	14	12	1
Co	11	9	10	1
Cr	53	28	40	12
S	4	10	7	3
Nb	5	4	5	0
K/Rb	212	96	154	58.0
Rb/Sr	2.02	0.4	1.21	8.8

* : molar-ratio of Al2O3 to CaO+Na2O+K2O

σn : Standard deviation

Mean: Arithmetical mean

Mineralogical composition and coordinates of the enclaves

227	pl" +hbl+ort+qtz+bt+ap	79000-89550
96	pl+qtz+hbl+bt	85150-91975

": mineral symbols are from Kretz(1983)

Table 45: Major oxides and trace elements analyses of the microgranites

Sample No	744	746	Mean	σn
SiO2	76.45	76.39	76.42	0.03
TiO2	0.21	0.09	0.15	0.06
Al2O3	13.28	12.66	12.97	0.31
Fe2O3	0.48	0.34	0.41	0.07
FeO	1.45	0.40	0.92	0.52
MgO	0.54	0.10	0.32	0.22
MnO	0.03	0.02	0.02	0.01
CaO	0.15	0.55	0.35	0.20
Na2O	2.04	3.00	2.52	0.48
K2O	2.00	5.12	3.56	1.56
P2O5	1.73	0.00	0.87	0.87
H2O	1.15	1.20	1.17	0.02
CO2	0.29	0.26	0.27	0.01
Total	99.80	100.13		
K2O/Na2O	0.98	1.71	1.34	0.36
A/CNK*	2.29	1.10	1.69	0.59
U	0	0	0	0
Th	12	28	20	8
Ce	31	24	28	3
La	24	14	19	5
Pb	28	59	44	15
Ba	422	70	246	176
Zr	111	49	80	31
Y	17	13	15	2
Sr	98	25	62	36
Rb	180	253	217	36
Ga	12	11	12	0
Zn	31	14	23	8
Cu	3	7	5	2
Ni	4	3	4	0
Co	0	0	0	0
Cr	86	38	62	24
S	0	14	7	7
Nb	19	14	17	2
K/Rb	111	202	156.5	45.5
Rb/Sr	1.8	10.1	5.95	4.15

* : molar-ratio of Al2O3 to CaO+Na2O+K2O

σn : Standard deviation

Mean: Arithmetical mean

Mineralogical composition and coordinates of the microgranite

744	or+qtz+pl+bt	84860-96800
746	or+qtz+pl+bt+ep	85710-97862

Table 46: Major oxides and trace elements analyses of the quartz-alkali syenites

Sample No	634	637	658	Mean	σn
SiO2	71.18	69.18	78.73	73.03	4.11
TiO2	0.17	0.17	0.09	0.17	0.04
Al2O3	16.12	18.45	12.18	15.58	2.59
Fe2O3	1.05	0.01	0.11	0.39	0.47
FeO	0.13	0.20	0.48	0.27	0.15
MgO	0.23	0.36	0.61	0.40	0.16
MnO	0.04	0.03	0.00	0.02	0.02
CaO	0.06	0.00	0.02	0.03	0.03
Na2O	7.08	10.11	2.73	6.64	3.03
K2O	3.26	0.36	4.82	2.81	1.85
P2O5	0.03	0.01	0.02	0.02	0.01
H2O	0.35	0.45	0.31	0.37	0.06
CO2	0.10	0.16	0.10	0.12	0.03
Total	99.8	99.49	100.2		
K2O/Na2O	0.46	0.04	1.77	0.76	0.74
A/CNK*	1.05	1.08	1.25	1.13	0.1
U	0	0	0	0	0
Th	31	8	28	22	102
Ce	36	39	27	34	5
La	13	18	14	15	2
Pb	9	2	12	8	4
Ba	512	31	227	257	197
Zr	92	132	87	104	20
Y	15	22	19	19	3
Sr	128	63	49	80	34
Rb	141	11	267	140	104
Ga	11	15	10	12	2
Zn	4	1	5	3	2
Cu	0	0	0	0	0
Ni	4	1	1	2	1
Co	0	6	8	5	3
Cr	60	18	91	56	30
S	26	26	25	26	0
Nb	11	20	10	14	4
K/Rb	231	327	180	246	61
Rb/Sr	1.1	0.2	5.4	2.2	2.3

* : molar-ratio of Al2O3 to CaO+Na2O+K2O

σn : Standard deviation

Mean: Arithmetical mean

Mineralogical compositions and coordinates of the quartz-alkali syenites

634	or+ab+qtz+ep	83665-93098
637	ab+or+qtz+ep	83323-93230
658	or+qtz+ab	82285-93190

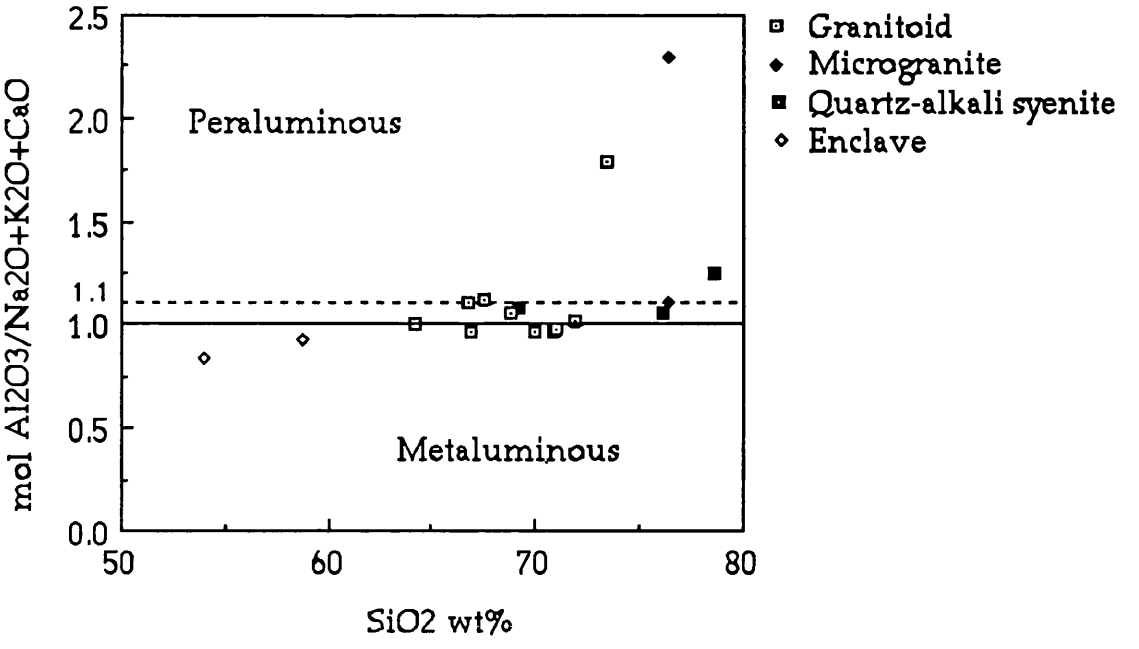

Figure 66: Molar Al2O3/(Na2O+K2O+CaO) versus SiO2 wt%.

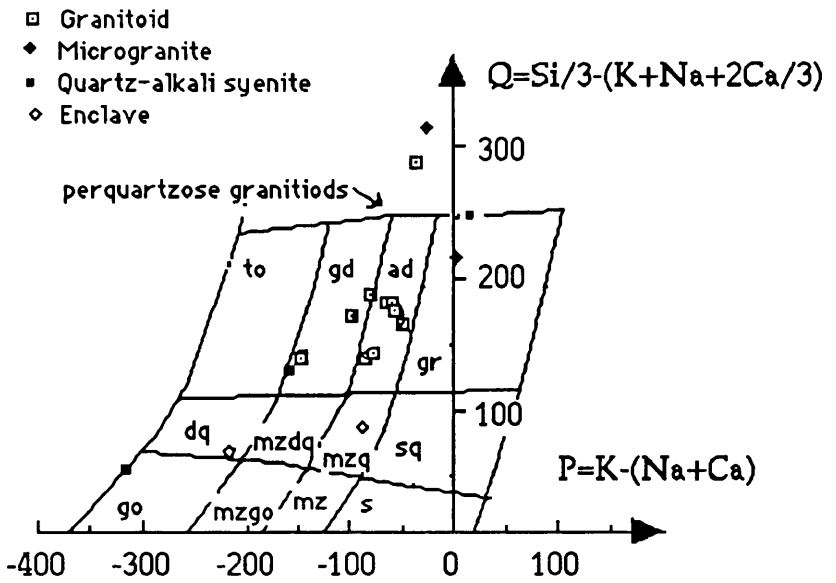

Figure 67: Nomenclature diagram of the granitoids, microgranites, quartz-alkali syenites and enclaves (Debon&LeFort, 1982). The two parameters are in millications(10^3 gram-atoms) for 100 g of rock or mineral(see Table 47 for calculation). Q parameter is proportional of the weight content of quartz. gr: granite, ad: adamellite, gd: granodiorite, to: tonalite, sq: quartz-syenite mzq: quartz monzonite, mzdq: quartz monzodiorite, dq: quartz diorite (quartz gabbro-quartz anorthosite), s: syenite, mz: monzonite, mzgo: monzogabbro, monzodiorite, go: gabbro (diorite-anorthosite)

Table 47: Example calculation of the different parameters for the diagram of Debon &Le Fort(1982). Column 1: Chemical analysis, in weight percent of metallic oxides. Fe2O3t, total iron as ferric oxide; L.I., loss on ignition. Column 2: molecular weight of the different oxides. Column 3; factor obtained by dividing the molecular weight by the number of metallic atoms (cations) in the oxide formula. Column 4: number of millications(10^3 gram-atoms) per 100 grams, obtained by dividing values from column 1 by the corresponding factor of column 3, and then multiplying by 10^3. Column 5: Parameters are calculated from the millicationic values. In the B and Mg/(Mg+Fe) parameters, Fe represents Fe^{2+} + Fe^{3+}. Quartz, dark minerals and feldspars + muscovite (weight percentages) are obtained by dividing Q, B and F by 5.55.

	1 Oxide %	2 Molecular weight	3 Factor	4 Millications	5 Parameters	
SiO2	74.16	60.06	60.06	Si=1235	Q=Si/3(K+Na+2Ca/3)	=178
Al2O3	14.89	101.94	50.97	Al=292	P=K-(Na+Ca)	=-78
Fe2O3t	0.59	159.70	79.85	Fe3+=7	A=Al-(K+Na+2Ca)	=41
FeO	-	71.85	71.85	Fe2+= -	B=Fe+Mg+Ti	=12
MnO	0.10	70.93	70.93	Mn= 1	F=555-(Q+B)	=365
MgO	0.16	40.32	40.32	Mg= 4	Na+K	=225
CaO	0.75	56.08	56.08	Ca= 13	K/(Na+K)	=0.36
Na2O	4.49	62.00	31.00	Na=145	Mg/(Fe+Mg)	=0.36
K2O	3.75	94.19	47.10	K =80		
TiO2	0.06	79.90	79.90	Ti = 1	Quartz	% 32.1
L.I.	0.59			weight	Dark minerals	% 2.2
Total	99.54			%	Feldspars+muscovite	% 65.7

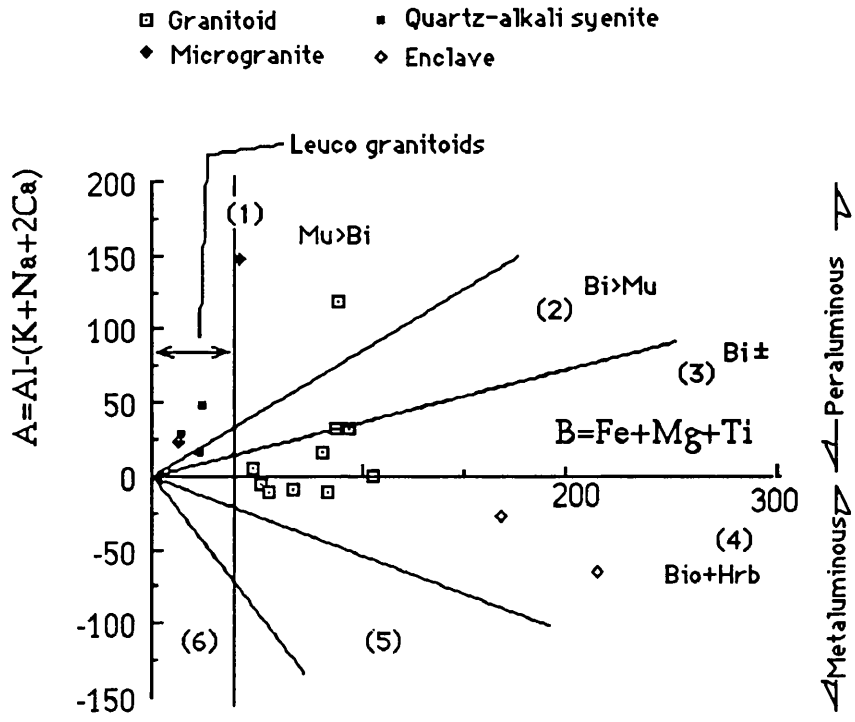

Figure 68: a)Characteristic mineral and classification diagrams of Debon&Le Fort, 1982 (Bi: Biotite, Mu: Muscovite, Hrb: Hornblende).

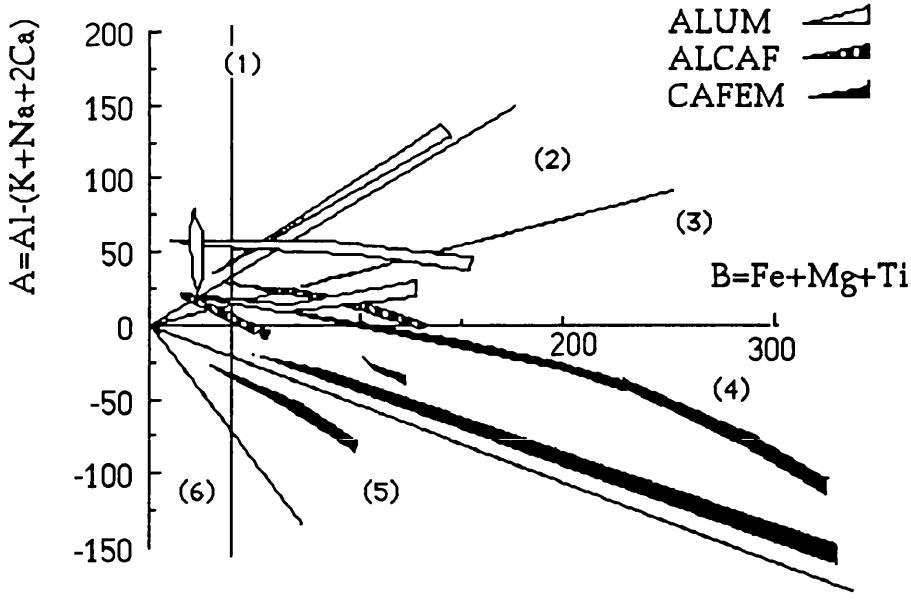

b) For comparison, typical trends corresponding to aluminous (Alum), alumino-cafemic(Alcaf) and cafemic(Cafem) are shown. Other explanations are as in Fig.67.

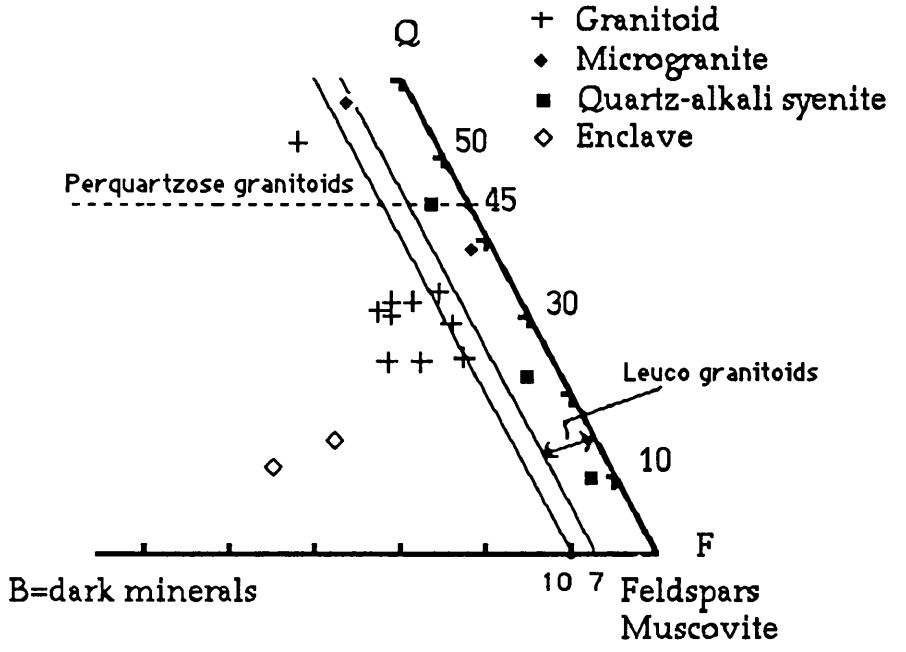

Figure 69: a)The classification diagram of cafemic and alumino-cafemic associations(Debon&Le Fort, 1982). The parameters , in weight percentages, are calculated from chemical analyses; see Table 47.

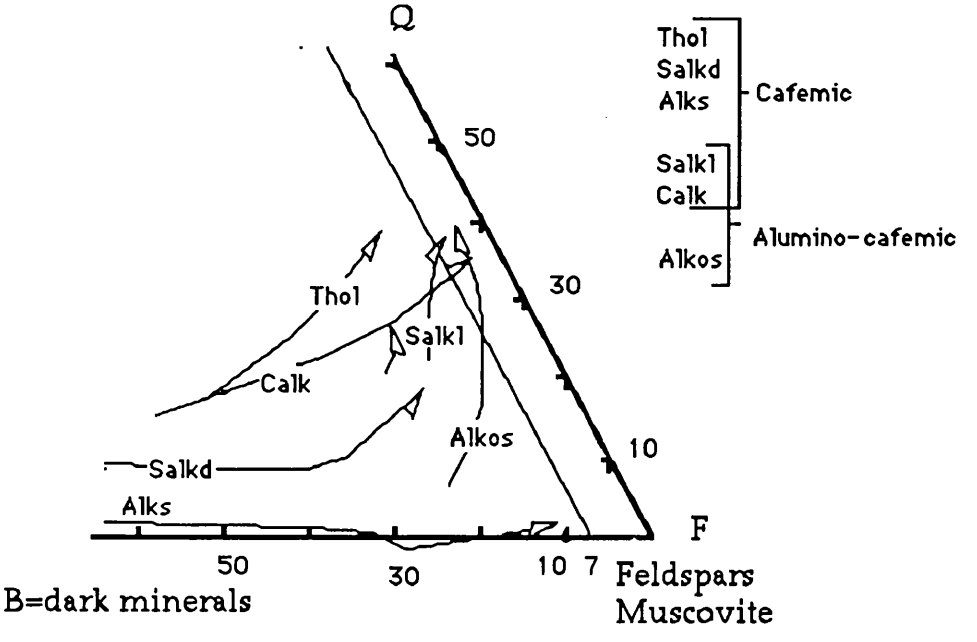

Fig.69-b: Reference system of typical trends is shown for comparison (after Debon & Le Fort, 1982). Other explanations as in Figure 67. THOL:tholeiitic; CALK: calkalkaline; SALKD, SALKL: dark- and light- coloured subalkaline; ALKS: dark-coloured alkaline saturated; ALKOS: light-coloured alkaline oversaturated.

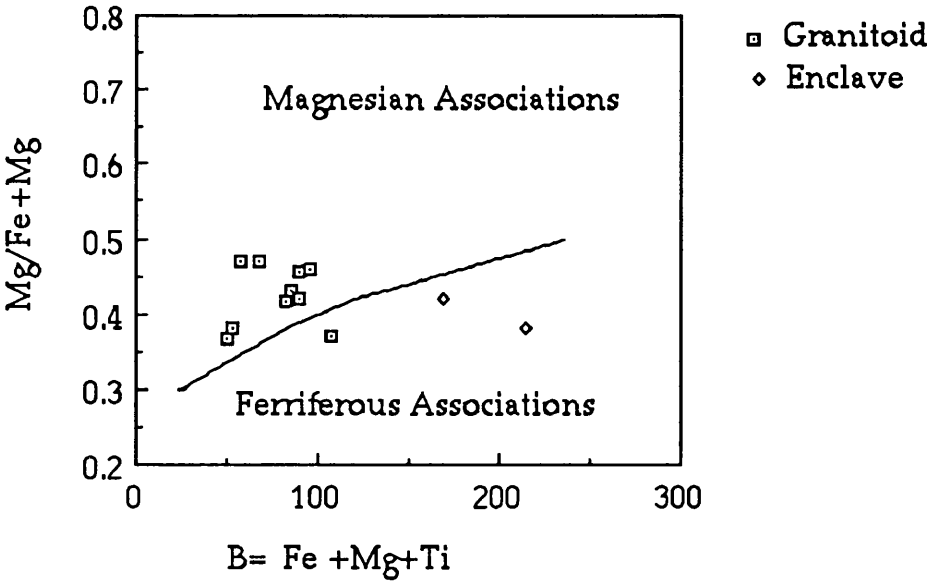

Figure 70: Mg/(Fe+Mg) against Fe+Mg+Ti diagram(after Debon&Le Fort, 1988). The two parameters are in millications (10^3 gram-atoms) (see Table 47 for calculations). Fe: total iron. Other explanations as in Fig. 67.

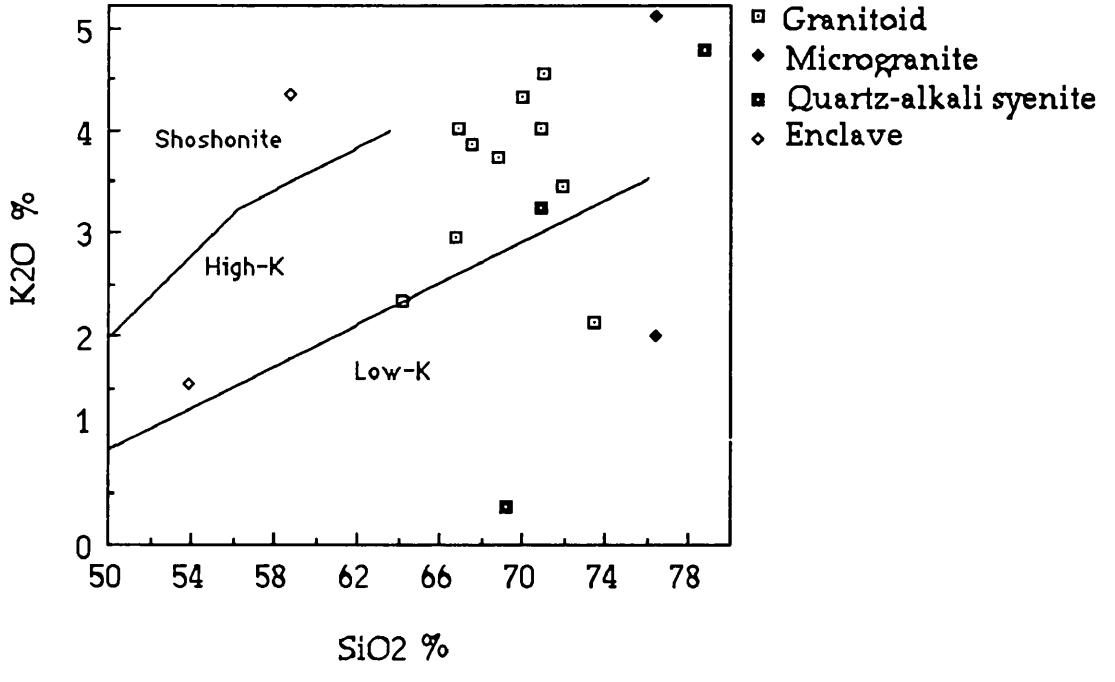

Figure 71: K2O versus SiO2 (boundaries from Peccerillo & Taylor,1976).

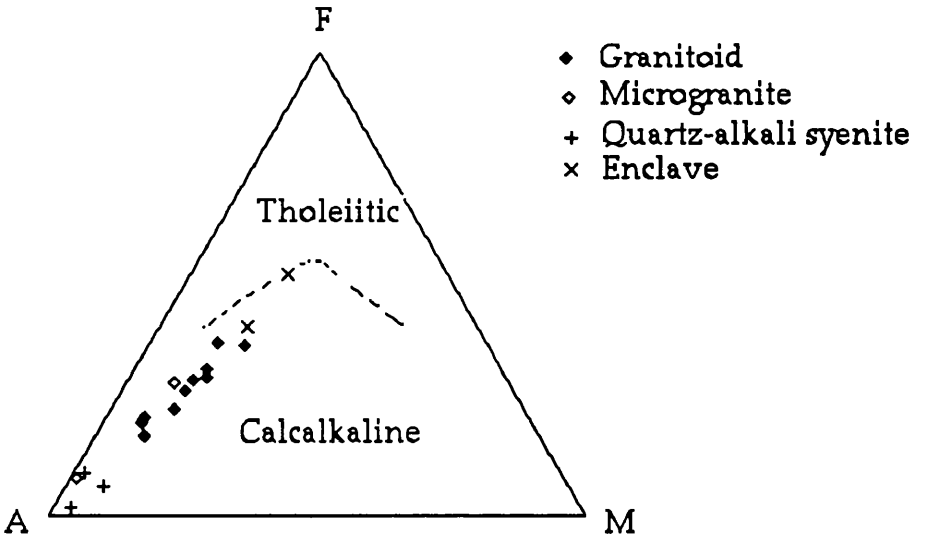

Figure 72: AFM triangular diagram (fields after Irvine & Baragar, 1971).

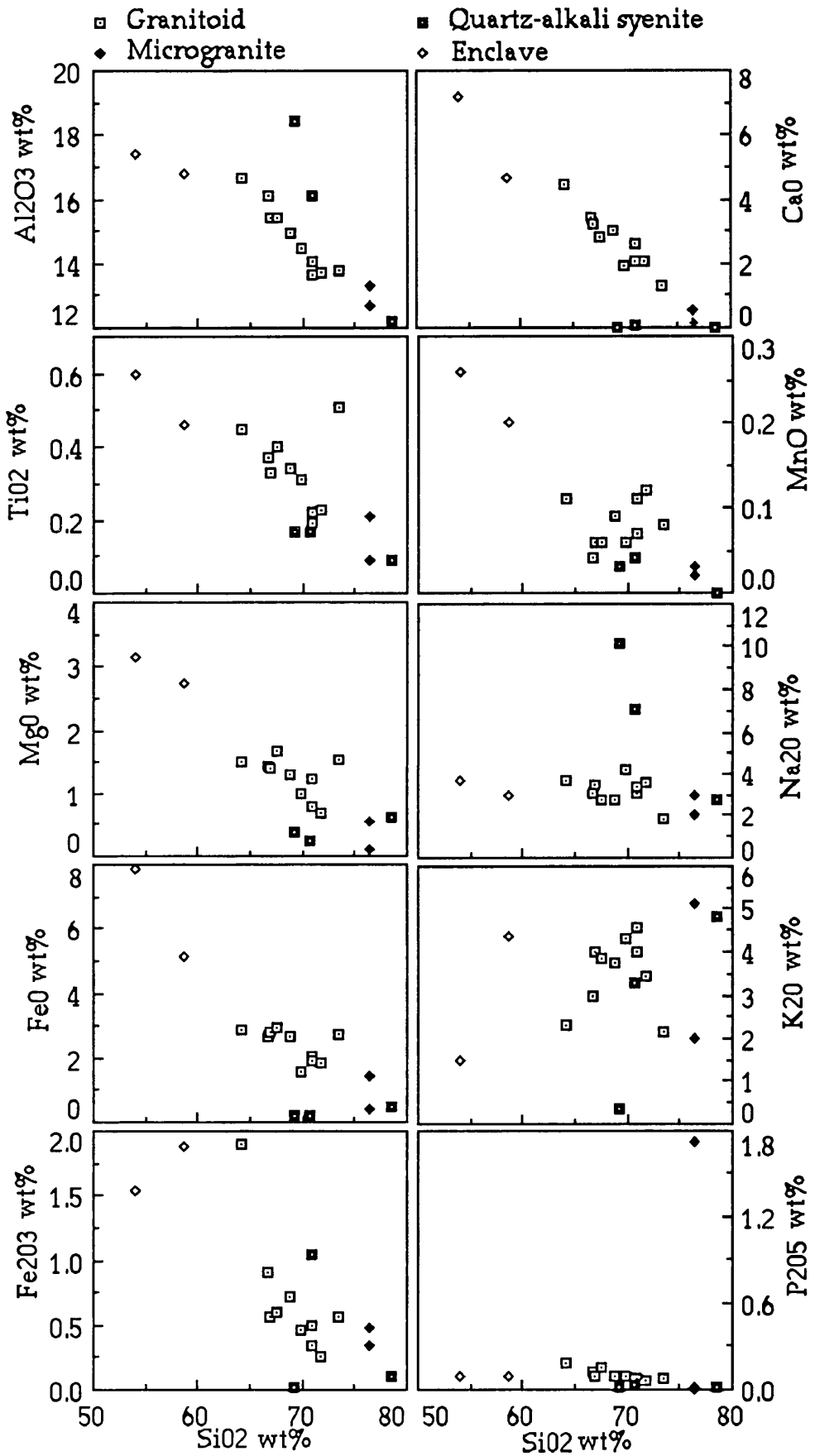

Figure 73: Harker diagram for the granitoids, microgranites, quartz-alkali syenites and enclaves.

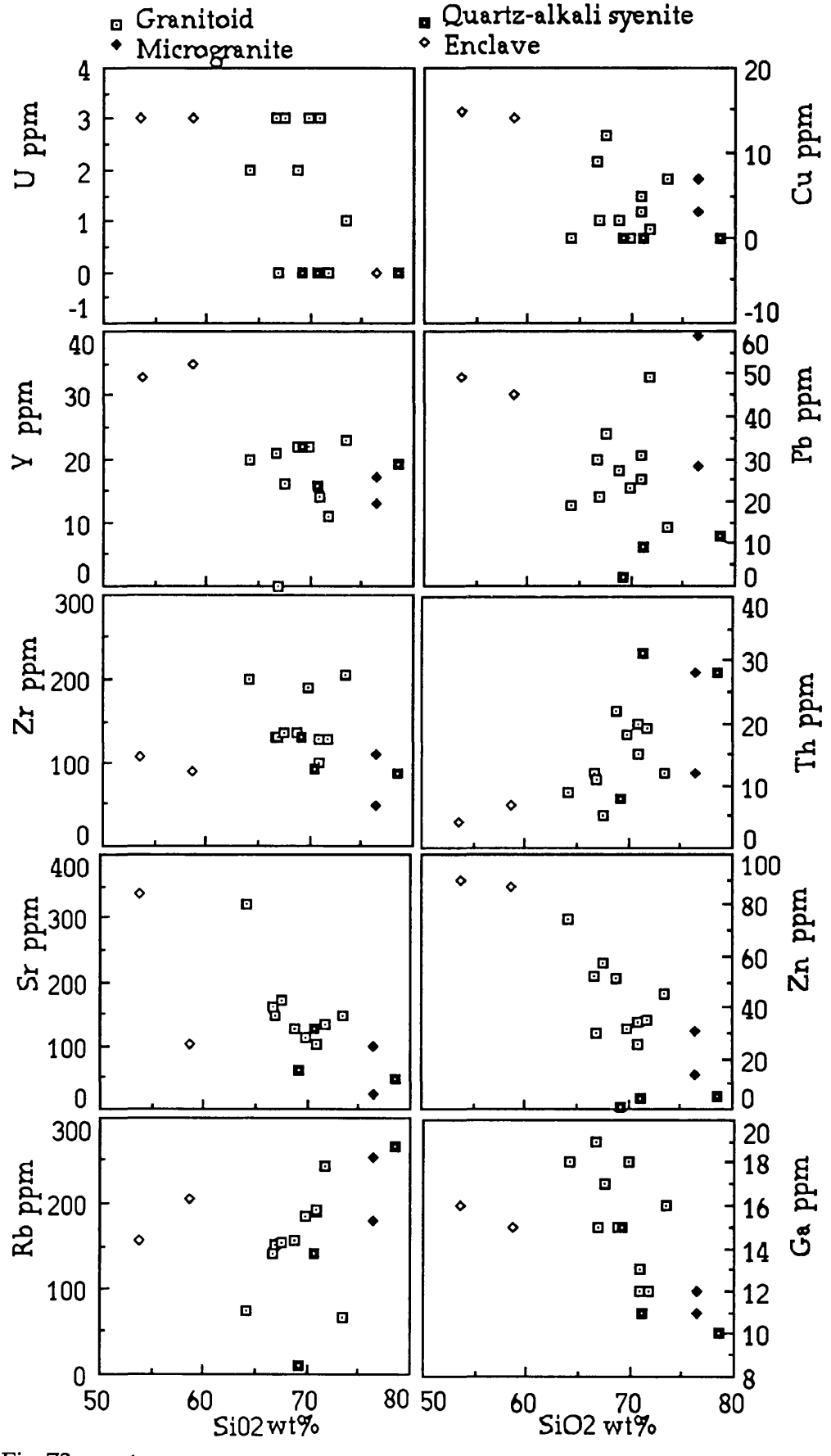
Granitoid
Microgranite
Quartz-alkali syenite
Enclave
U ppm
Cu ppm
Y ppm
Pb ppm
Zr ppm
Th ppm
Sr ppm
Zn ppm
Rb ppm
Ga ppm
SiO2 wt%
SiO2 wt%

Fig.73. cont.

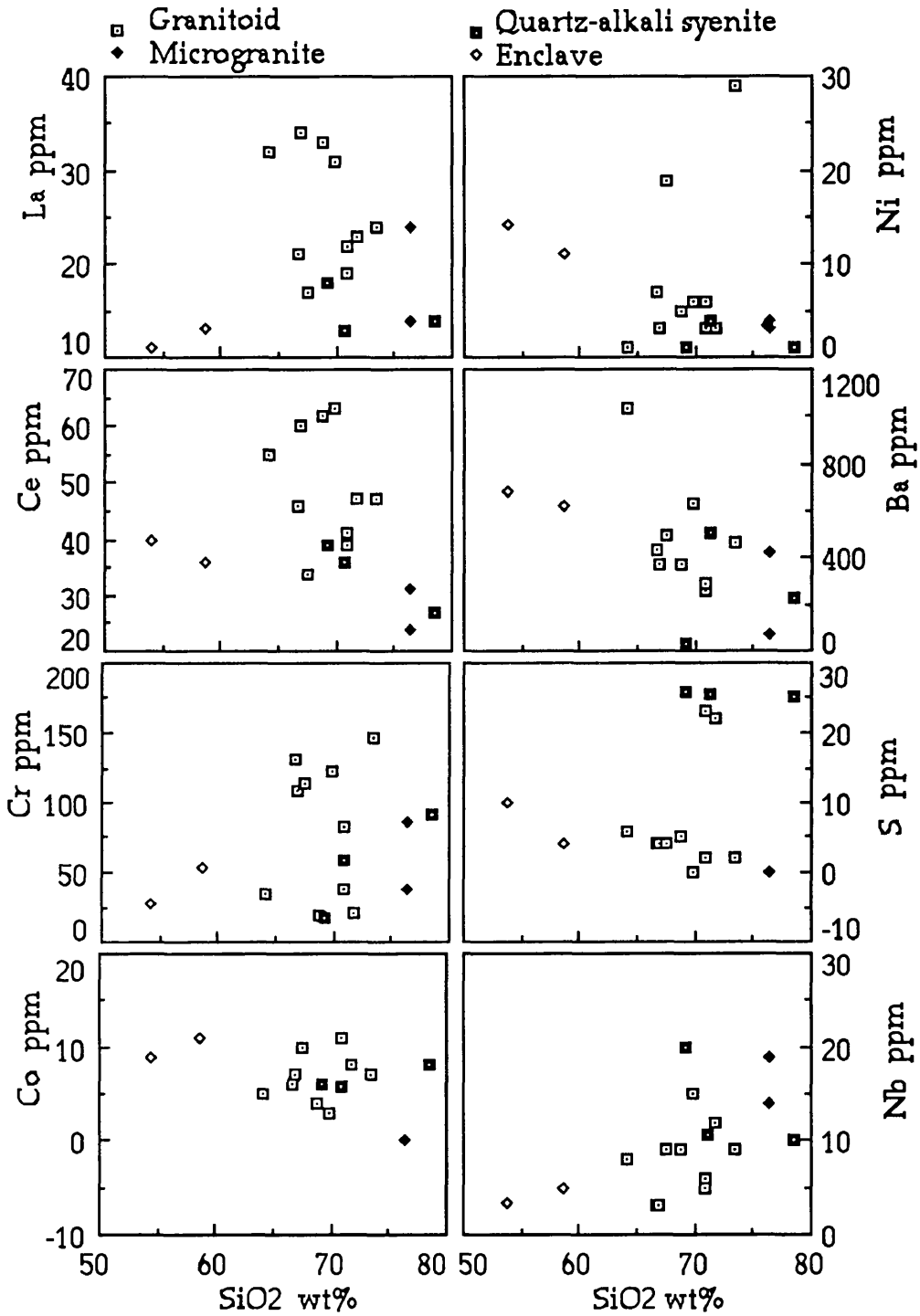
Granitoid
Microgranite
Quartz-alkali syenite
Enclave
La ppm
Ni ppm
Ce ppm
Ba ppm
Cr ppm
S ppm
Co ppm
Nb ppm
SiO2 wt%
SiO2 wt%

Fig.73. cont.

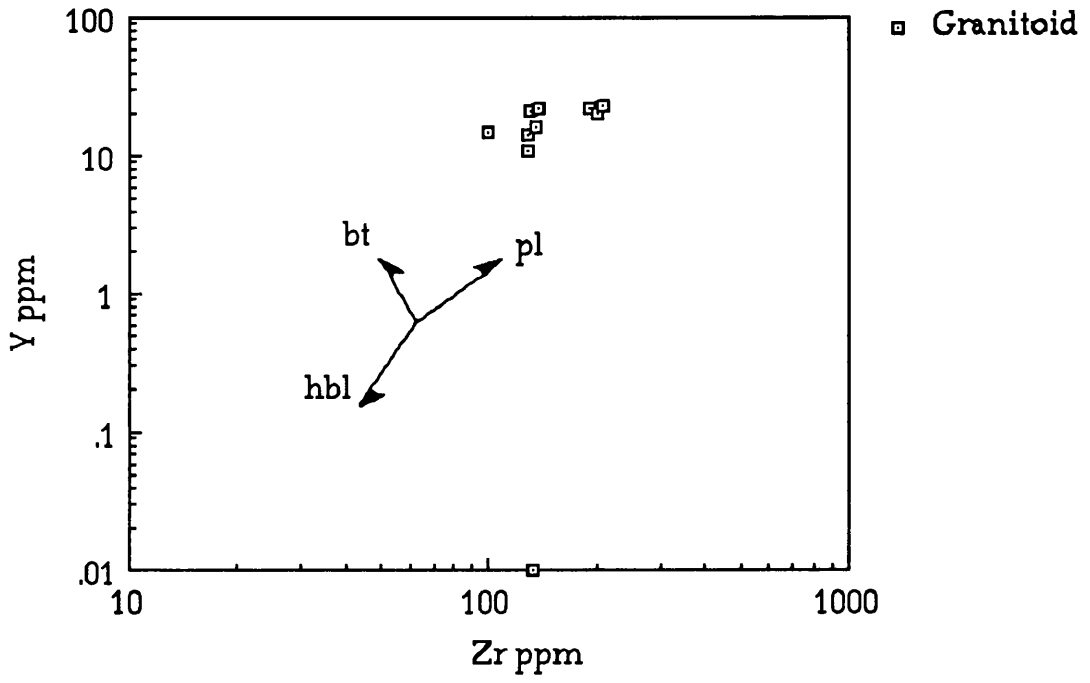

Figure 74: Y versus Zr. The vectors showing fractional crystallization of the minerals are taken from Beckinsale, 1979.

hbl: hornblende, bt: biotite, pl: plagioclase

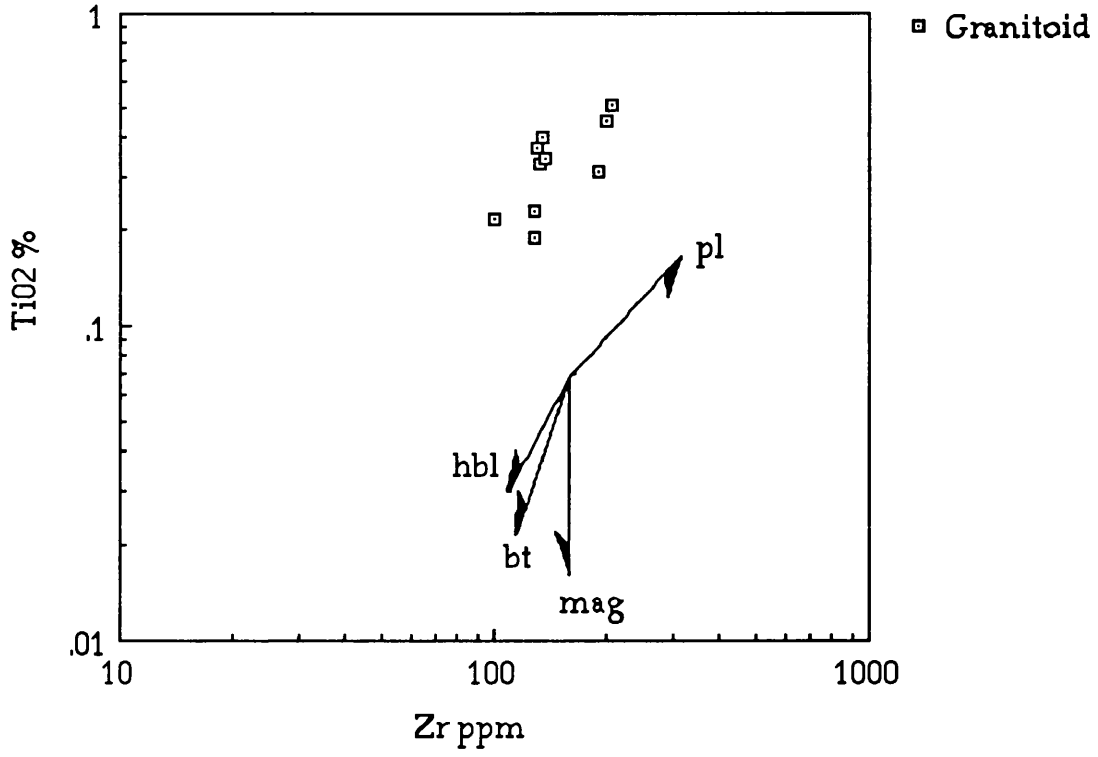

Figure 75: TiO2 versus Zr. Calculated vectors from Atherton & Sanderson,1985.

pl: plagioclase, hbl: hornblende, bt: biotite, mag: magnetite.

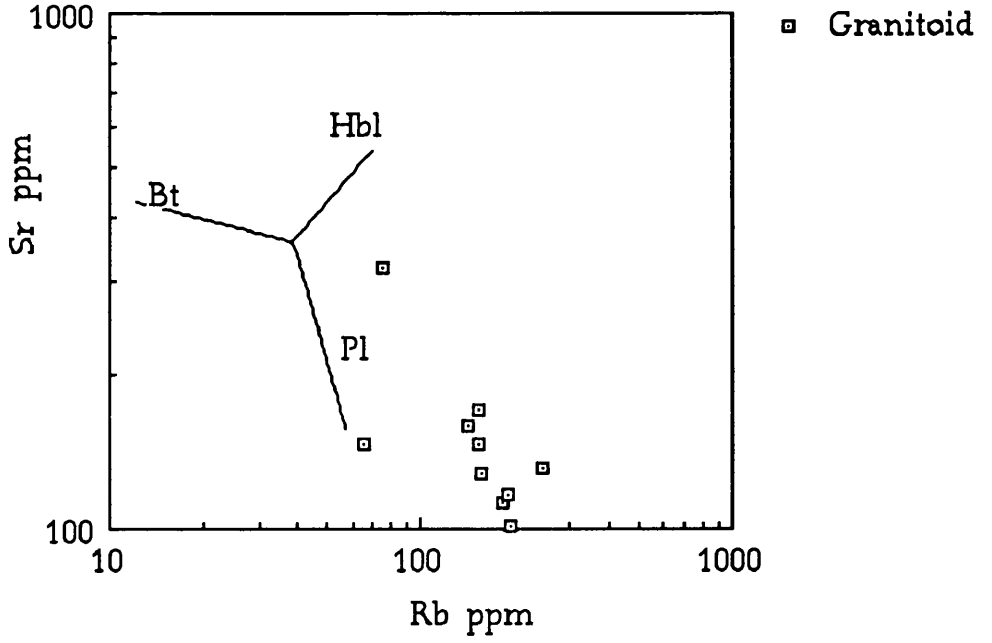

Figure 76: Sr versus Rb. Vector from Bussel, 1988.

Bt: Biotite, Hbl: Hornblende, Pl: Plagioclase

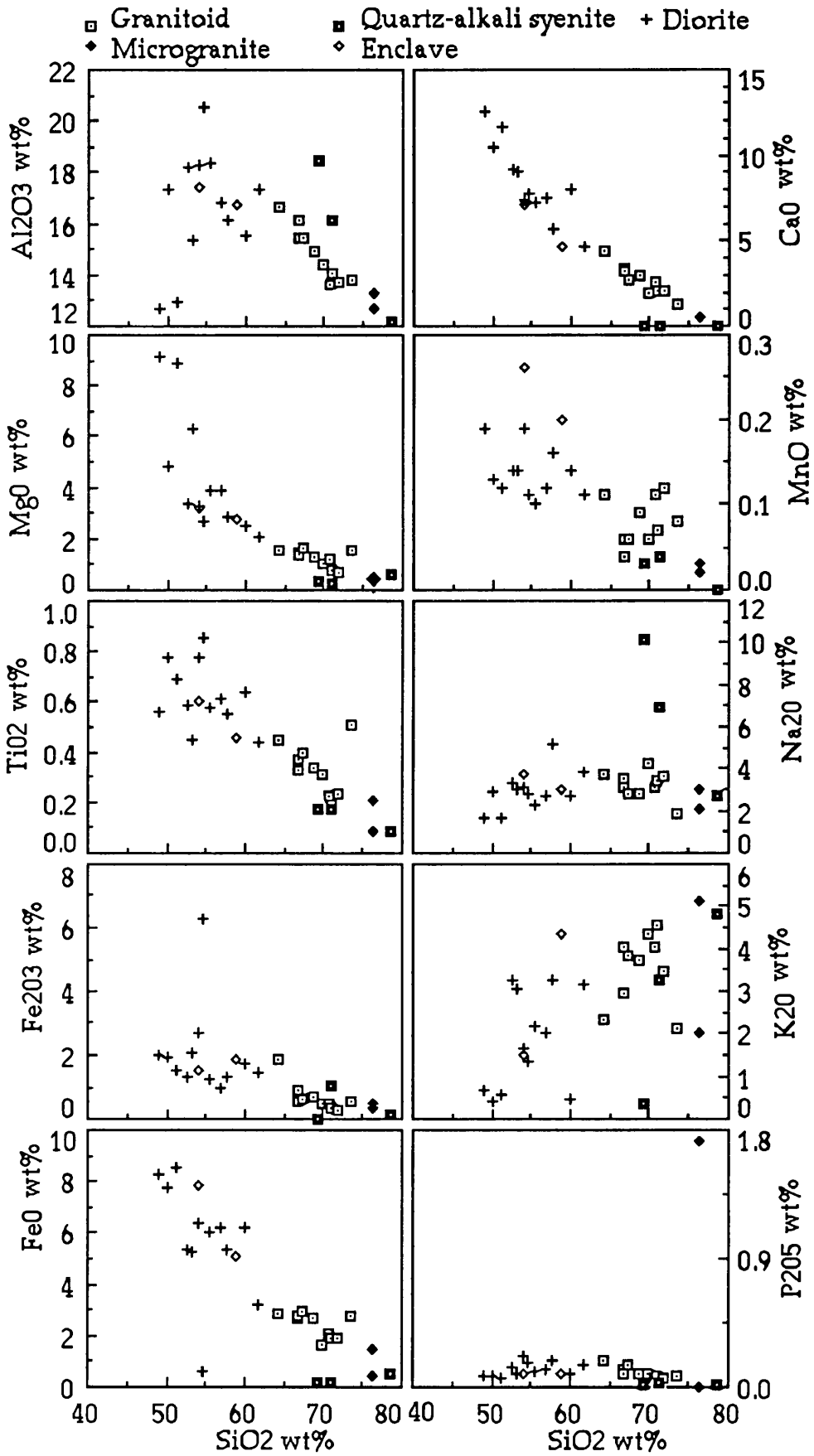

Figure 77: SiO2 versus major oxides.

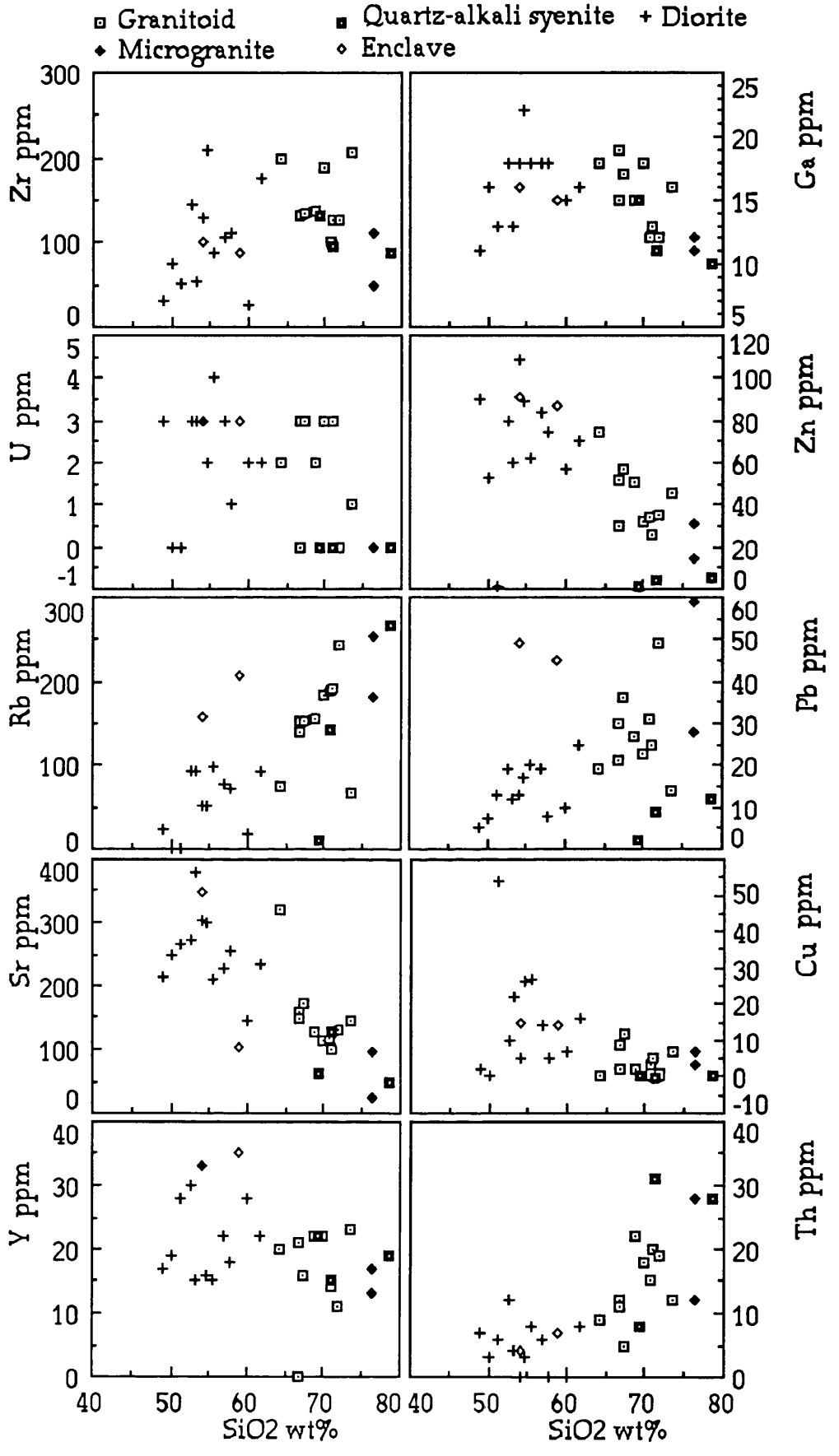

Figure 78: SiO2 versus trace elements.

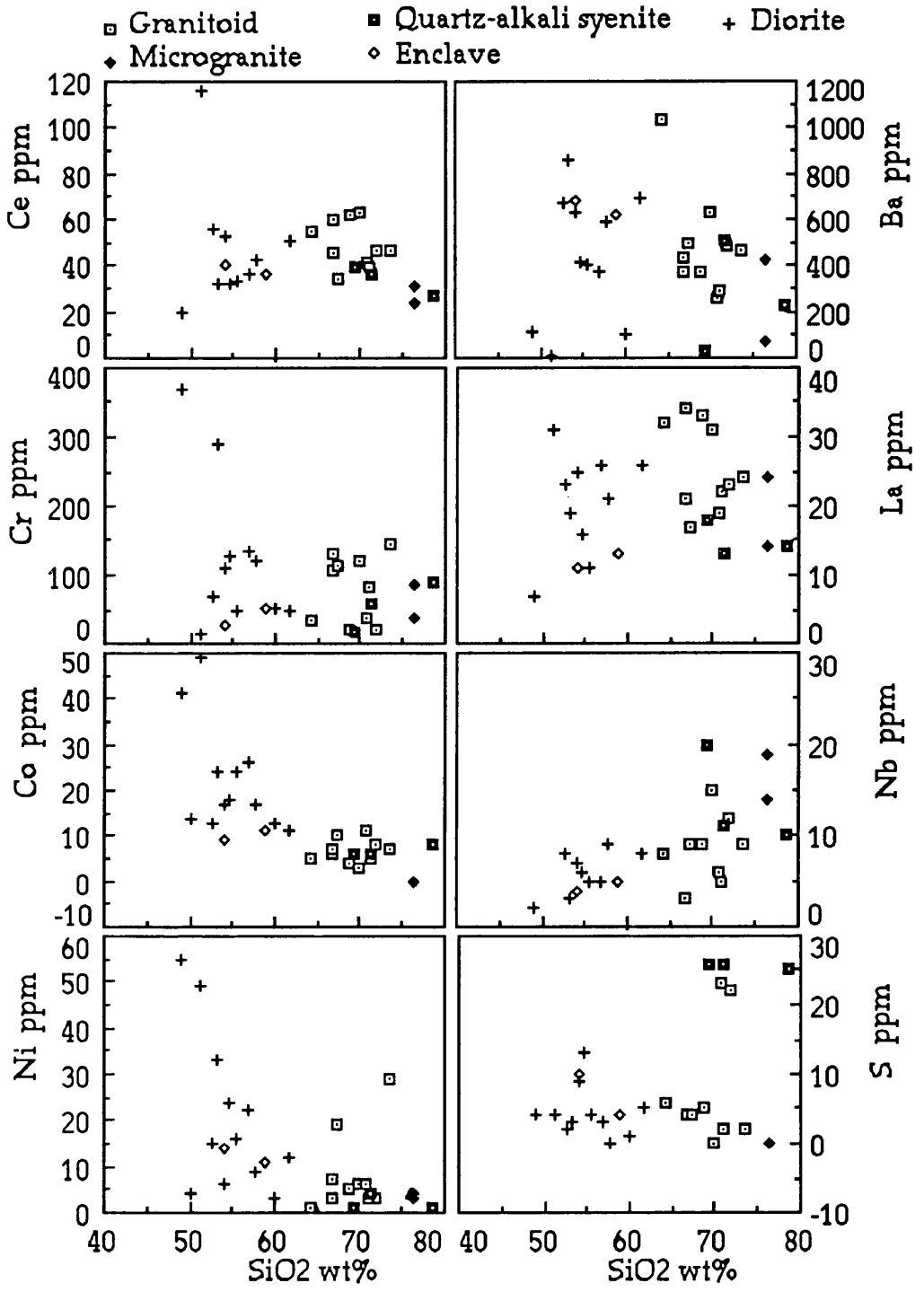
Granitoid
Quartz-alkali syenite
Diorite
Microgranite
Enclave
Ce ppm
Ba ppm
Cr ppm
La ppm
Co ppm
Nb ppm
Ni ppm
S ppm
SiO2 wt%
SiO2 wt%

Fig. 78: Cont.

Table 48: Test of the granitoid(437) fractionation from the diorite(388).

recalculated analyses (wt.pcent. basis)

comp	init(388)	final	hbl	plg
SiO2	50.81	73.30	52.58	45.39
TiO2	0.68	0.51	0.16	0.00
Al2O3	12.82	13.78	3.74	34.31
Fe*2O3	10.93	3.59	14.64	0.34
MnO	0.12	0.08	0.32	0.01
MgO	8.82	1.54	14.74	0.17
CaO	11.51	1.30	12.56	18.09
Na2O	1.59	1.84	0.88	1.54
K2O	0.58	2.14	0.38	0.15
P2O5	0.06	0.08	0.00	0.00
H2O	1.98	1.67	0.00	0.00
CO2	0.10	0.19	0.00	0.00
S%	0.00	0.00	0.00	0.00
Cr2O3	0.00	0.00	0.00	0.00
NiO	0.00	0.00	0.00	0.00

	bulk comp. of added or subtr.matl.	obs.diff., between magmas	calc.diff. between magmas	obs.-calc. (residuals)
SiO2	50.46	22.491	21.222	1.269
TiO2	0.11	-0.174	0.370	-0.545
Al2O3	12.75	0.957	0.954	0.003
Fe*2O3	10.43	-7.333	-6.352	-0.980
MnO	0.23	-0.039	-0.141	0.102
MgO	10.45	-7.279	-8.278	0.999
CaO	14.19	-10.213	-11.981	1.768
Na2O	1.07	0.242	0.711	-0.469
K2O	0.31	1.552	1.697	-0.145
P2O5	0.00	0.020	0.074	-0.054
H2O	0.00	-0.314	1.549	-1.863
CO2	0.00	0.091	0.176	-0.086
S%	0.00	0.000	0.000	0.000
Cr2O3	0.00	0.000	0.000	0.000
NiO	0.00	0.000	0.000	0.000
total				0.000

sum of the squares of the residuals = 10.7253

phase name	amount as wt.pct.of init.magma	amount as wt.pct.of all phases	amount as wt.pct.of added phs	amount as wt.pct. of subtrd.phs
Hornblende	-65.54	70.53	0.00	70.53
Plagioclase	-27.38	29.47	0.00	29.47
Totals rel. to initial magma =			0.00	92.92

*: Fetot as Fe2O3, hbl: hornblende, pl: plagioclase
obs.diff: observed difference, eqns: equations

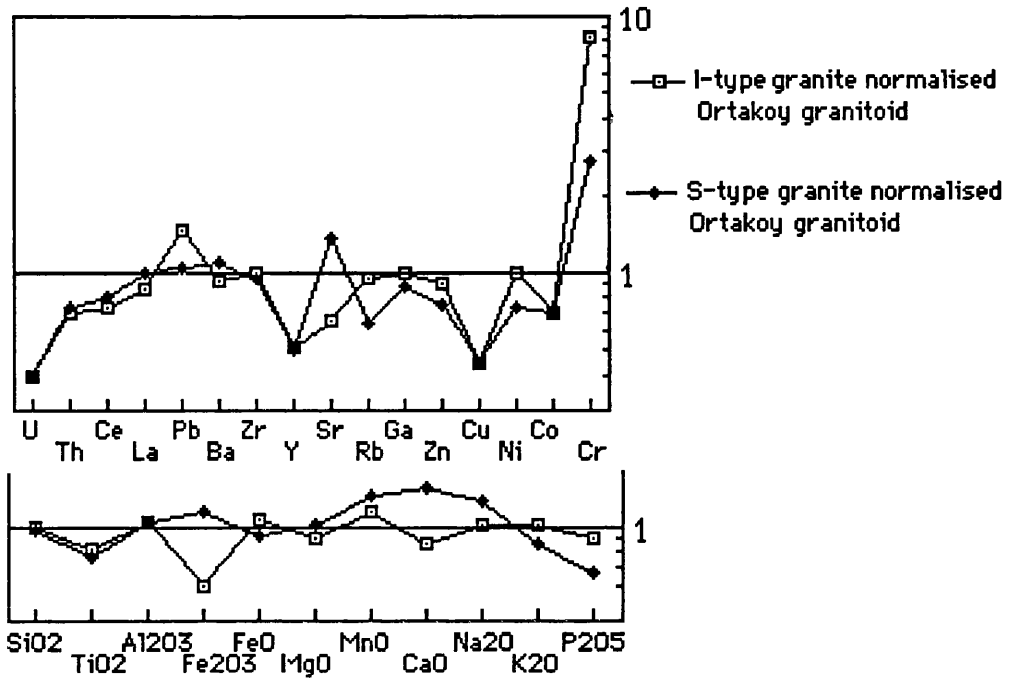

Figure 79: I- and S-type granite normalised Ortakoy granitoid pattern. Normalised values are from Lochland, Australia(Chappell&White, 1992). Note y axis is logarithmic

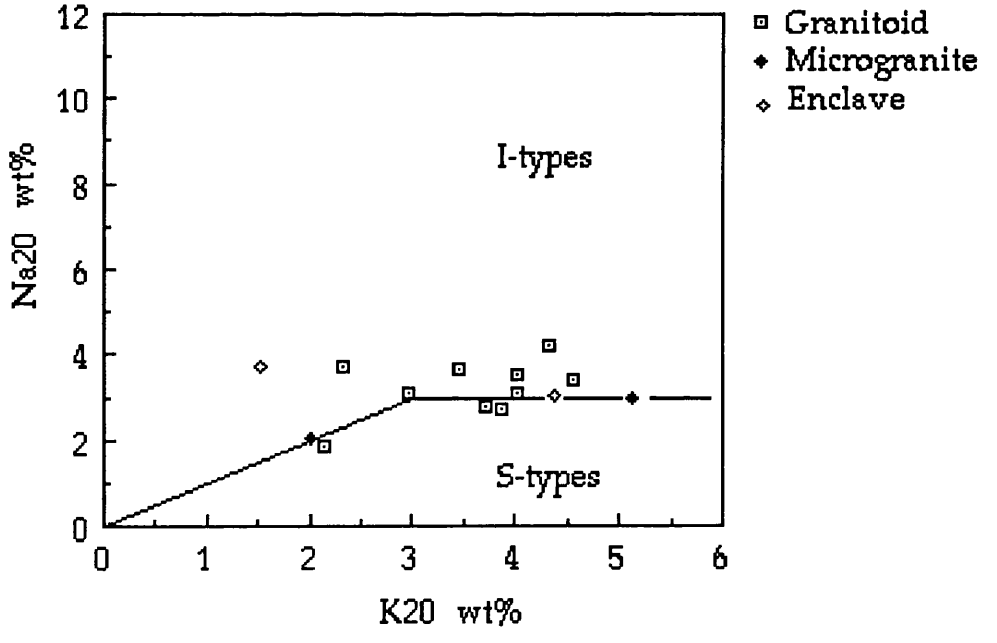

Figure 80: Variation of Na2O and K2O. I- and S-type boundaries of Lachlan Fold Belt from Chappell & White, 1984.

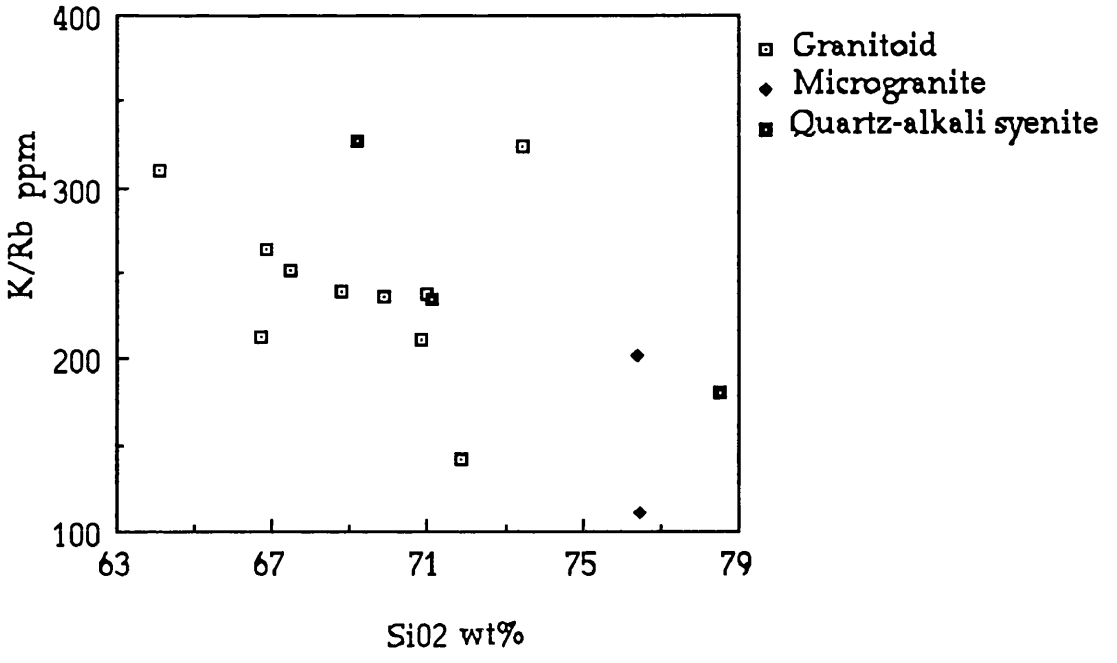

Figure 81: Diagram showing melt-rich granite with decreasing K/Rb and increasing SiO2(Wyborn et al.,1992).

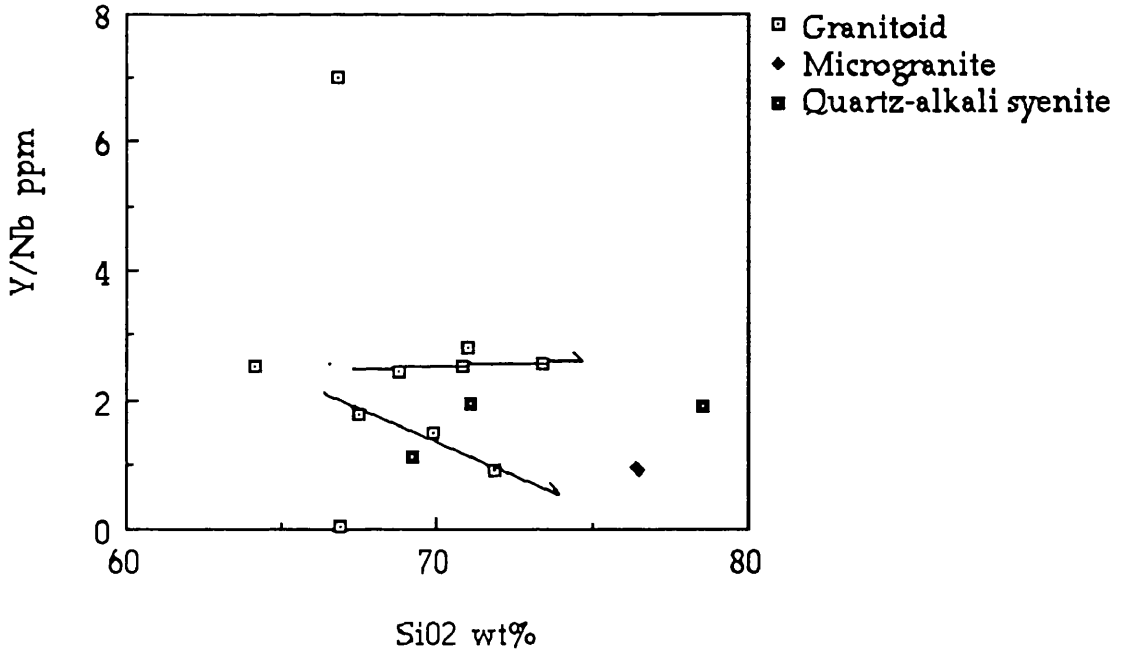

Figure 82: SiO2 versus Y/Nb.

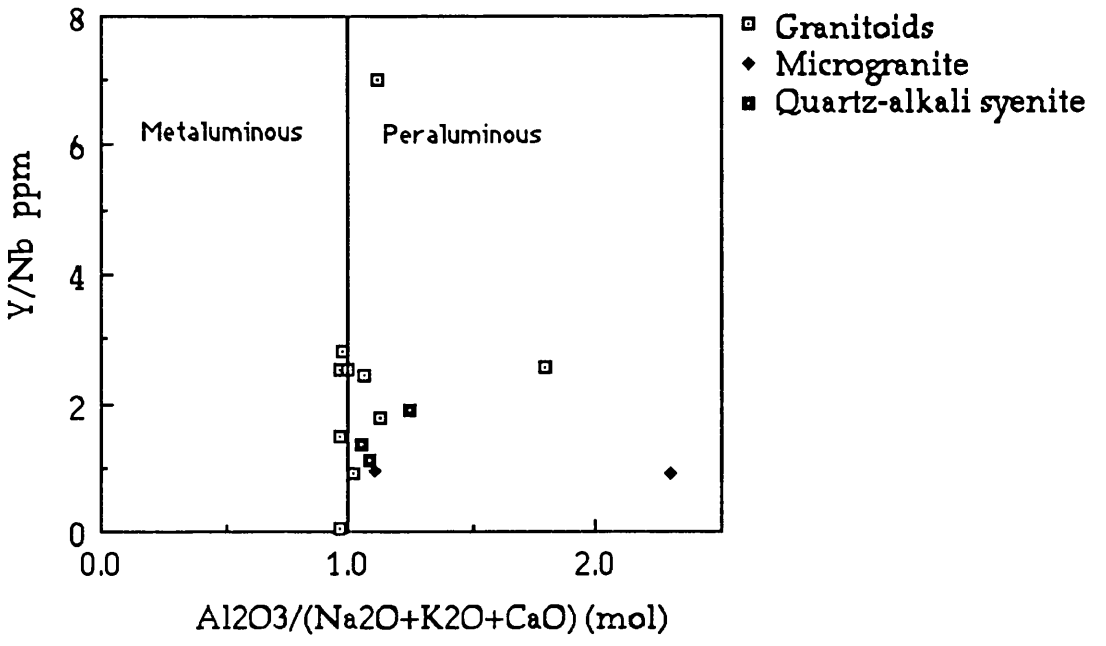

Figure 83: Plot of Y/Nb versus mol Al2O3/(Na2O+K2O+CaO).

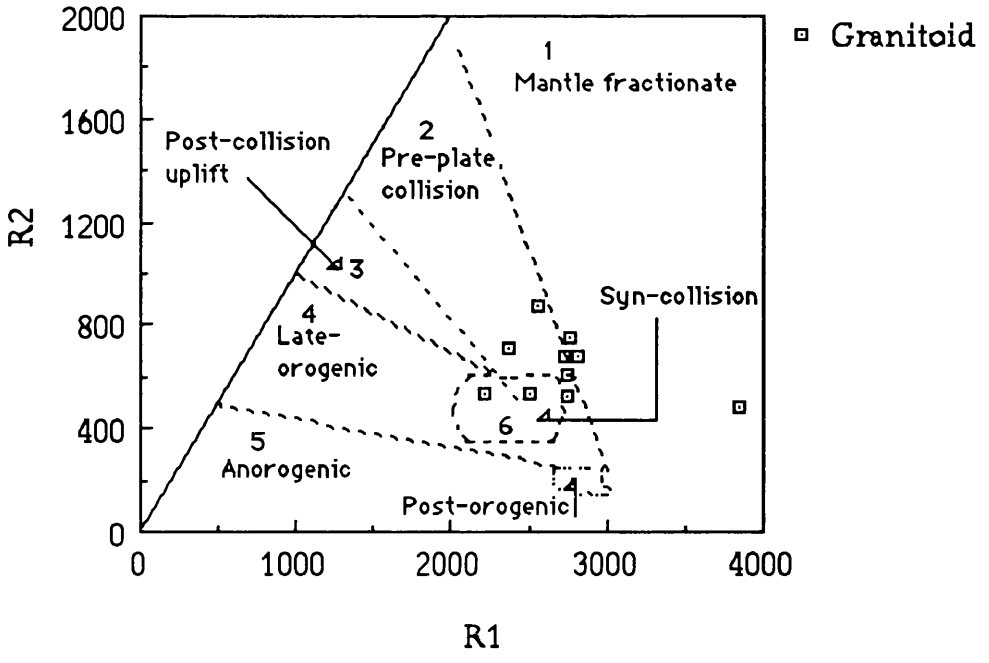

Figure 84: R1-R2 multicationic diagram (after de la Roche et al, 1980; and Batchelor & Bowden,1985). Petrological equivalents (after Lameyre & Bowden, 1982): group 1- tholeiitic; group 2- calc-alkaline and trondjhemitic; group 3- high-potassic calc-alkaline; group 4- sub-alkaline monzonitic; group 5- alkaline and peralkaline; group 6- anatectic two-mica leucogranites.

R1= 4Si-11(Na+K)-2(Fe+Ti), R2= 6Ca+2Mg+Al (as cation) .

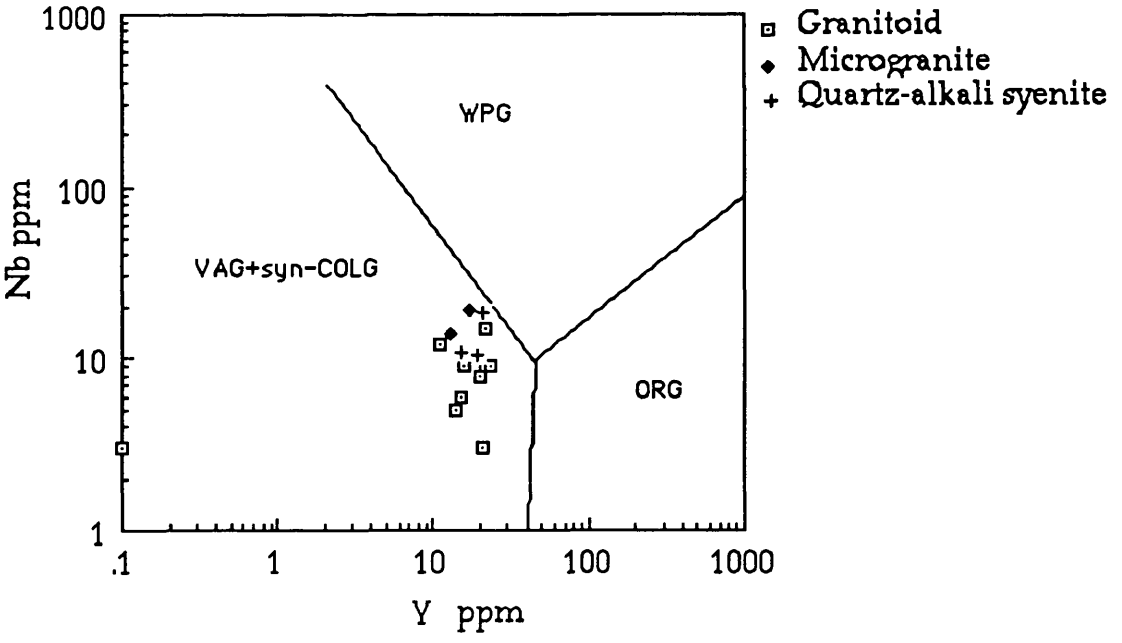

Figure 85: Nb-Y diagram of Pearce et al. (1984).

VAG: Volcanic arc granitoids, syn-COLG: syncollision granitoids

WPG: within plate granitoids, ORG: Ocean ridge granites

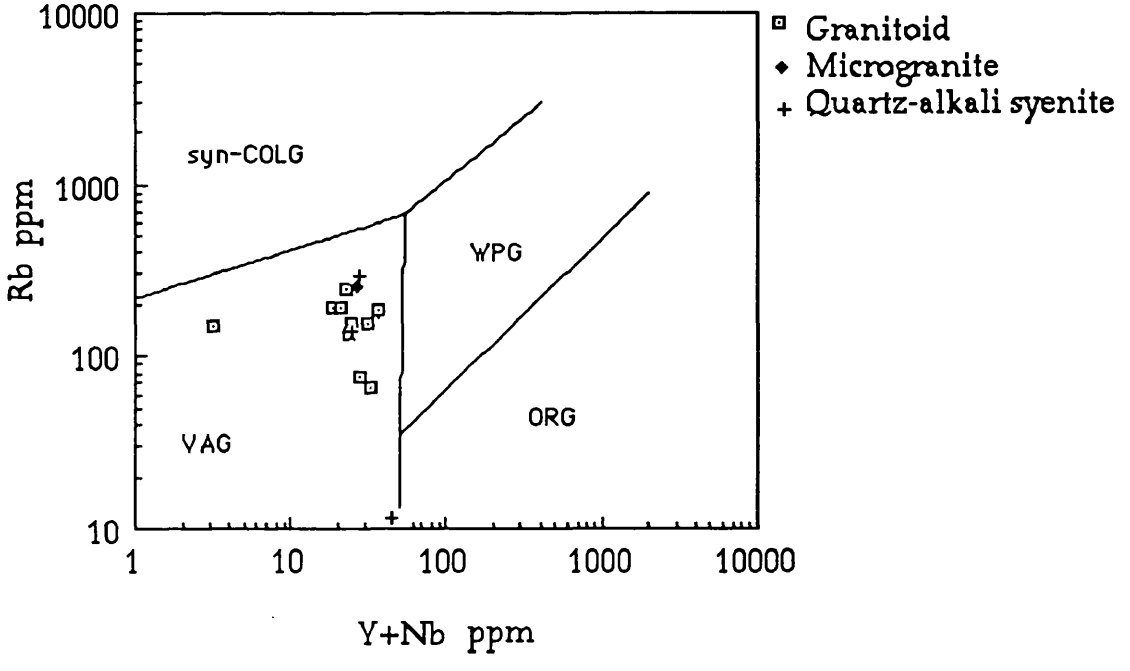

Figure 86: Rb versus Y+Nb (lines after Pearce et al., 1984).

VAG: Volcanic arc granitoids, syn-COLG: syncollision granitoids

WPG: within plate granitoids, ORG: Ocean ridge granitoids

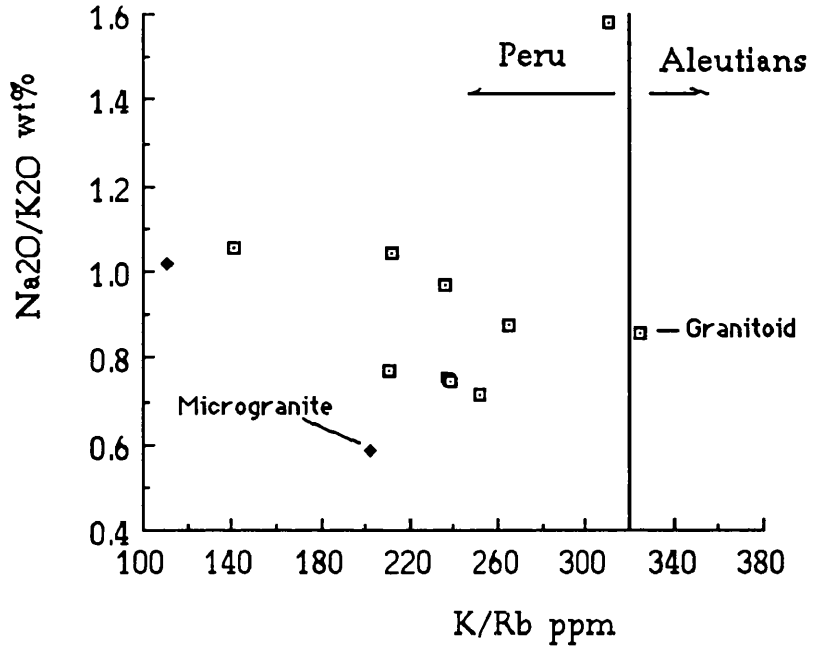

Figure 87: Diagram showing correlation of the Ortakoy granitoids with continental (Peru) and Island arc(Aleutians). Fields from Mpodozis & Kay (1992).

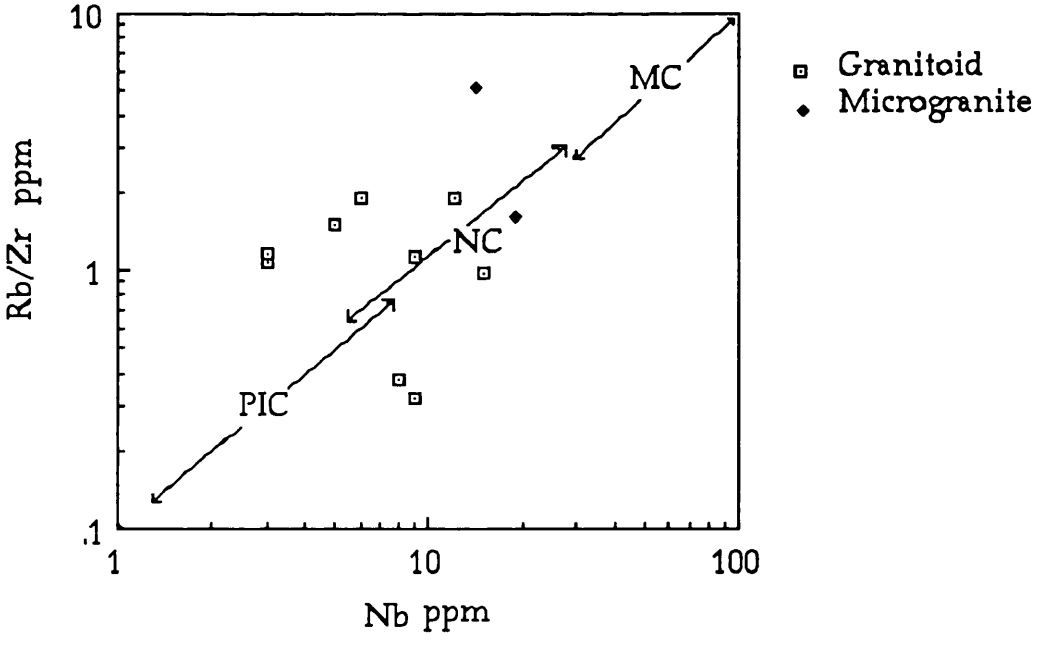

Figure 88: Rb/Zr versus Nb (after Brown et al., 1984). MC: Mature continental arcs NC: Normal continental arcs PIC: Primitive island arcs and continental arcs.

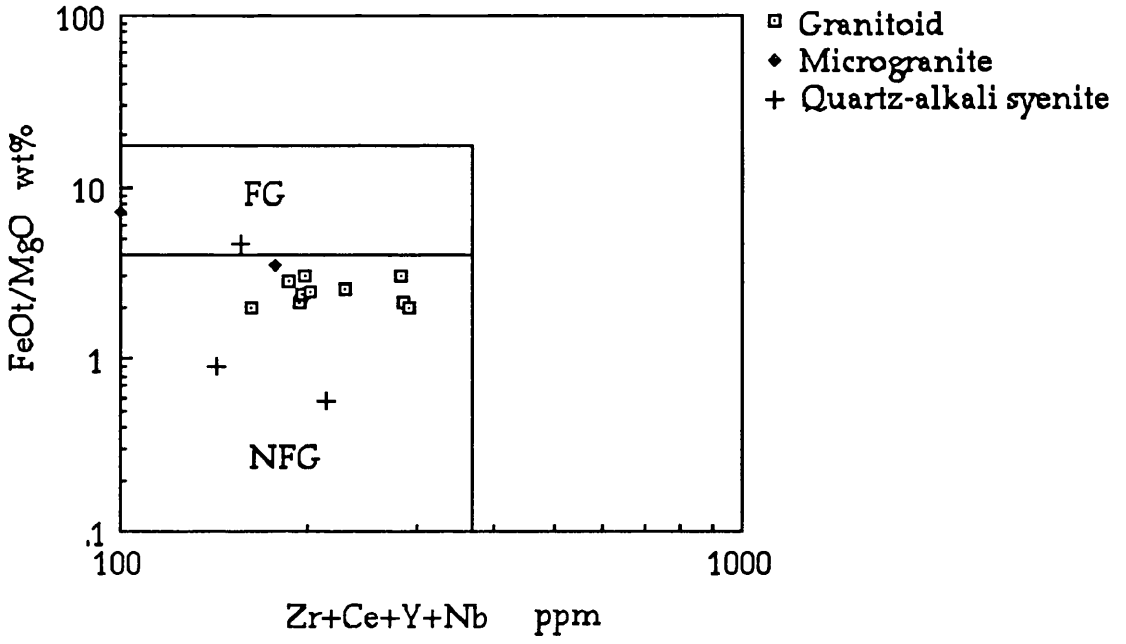

Figure 89: FeOt/MgO against Zr+Ce+Y+Nb (after Whalen, 1987). FG: Fractionated granite, NFG: Unfractionated M-, I- and S-type granite.

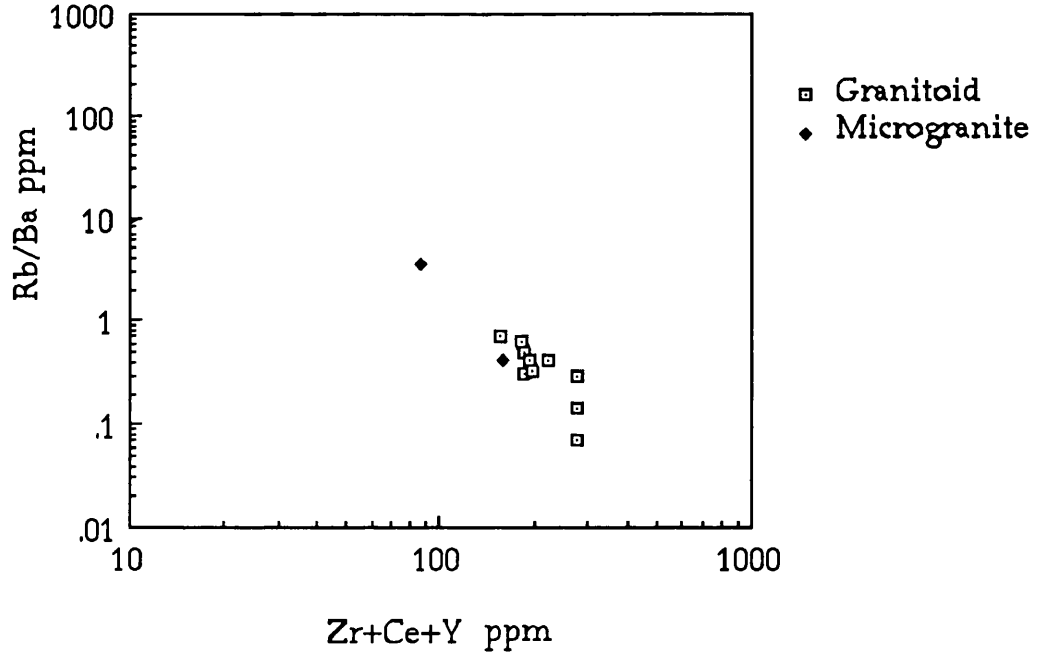

Figure 90: Rb/Ba versus Zr+Ce+Y+Nb

Table 49: Test of fractionation of the microgranite (744) from the granitoid (573)

recalculated analyses (wt.pcent. basis)

comp	init(573)	final(744)	plg	hbl	bt
SiO2	64.16	76.48	59.36	44.11	35.69
Tio2	0.45	0.21	0.04	1.15	3.54
Al2O3	16.68	13.29	25.30	7.69	19.91
Fe*2O3	5.08	2.09	0.30	22.39	23.53
MnO	0.11	0.03	0.02	1.43	0.22
MgO	1.51	0.54	0.00	9.78	7.11
CaO	4.44	0.15	7.00	10.96	0.00
Na2O	3.69	2.04	7.41	1.63	0.58
K2O	2.33	2.00	0.57	0.87	9.43
P2O5	0.18	1.73	0.00	0.00	0.00
H2O	1.30	1.15	0.00	0.00	0.00
CO2	0.07	0.29	0.00	0.00	0.00
S%	0.00	0.00	0.00	0.00	0.00
Cr2O3	0.00	0.00	0.00	0.00	0.00
NiO	0.00	0.00	0.00	0.00	0.00

	bulk comp. of added or subtr.matl.	obs.diff., between magmas	calc.diff. between magmas	obs.-calc. (residuals)
SiO2	53.40	12.325	12.254	0.070
TiO2	0.62	-0.240	-0.216	-0.024
Al2O3	20.18	-3.391	-3.659	0.268
Fe*2O3	8.04	-2.991	-3.160	0.169
MnO	0.41	-0.080	-0.202	0.122
MgO	3.17	-0.970	-1.398	0.428
CaO	7.49	-4.292	-3.900	-0.392
Na2O	5.32	-1.651	-1.741	0.091
K2O	1.36	-0.330	0.339	-0.669
P2O5	0.00	1.551	0.919	0.632
H2O	0.00	-0.150	0.611	-0.761
CO2	0.00	0.220	0.154	0.066
S%	0.00	0.000	0.000	0.000
Cr2O3	0.00	0.000	0.000	0.000
NiO	0.00	0.000	0.000	0.000
total				0.000

sum of the squares of the residuals = 1.8962

phase name	amount as wt.pct. of init.magma	amount as wt.pct. of all phases	amount as wt.pct. of added phs.	amount as wt.pct. of subtrd.phs
plg	-34.70	65.36	0.00	65.36
hbl	-14.13	26.61	0.00	26.61
bt	-4.26	8.03	0.00	8.03
totals rel. to initial magma =			0.00	53.09

* : Fetot as Fe2O3

hbl: hornblende, bt: biotite ort: orthoclase plg: plagioclase

obs diff: observed difference, eqns: equations , wt. pct: weight percentage

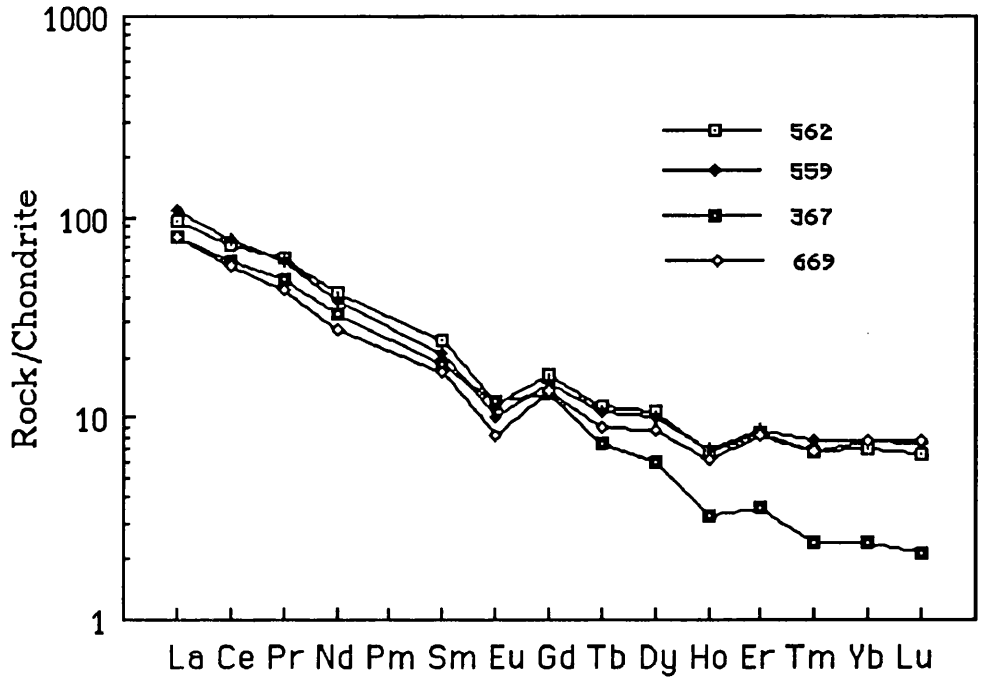

Figure 91: Normalised REE (Boynton, 1984) patterns of the granitoid

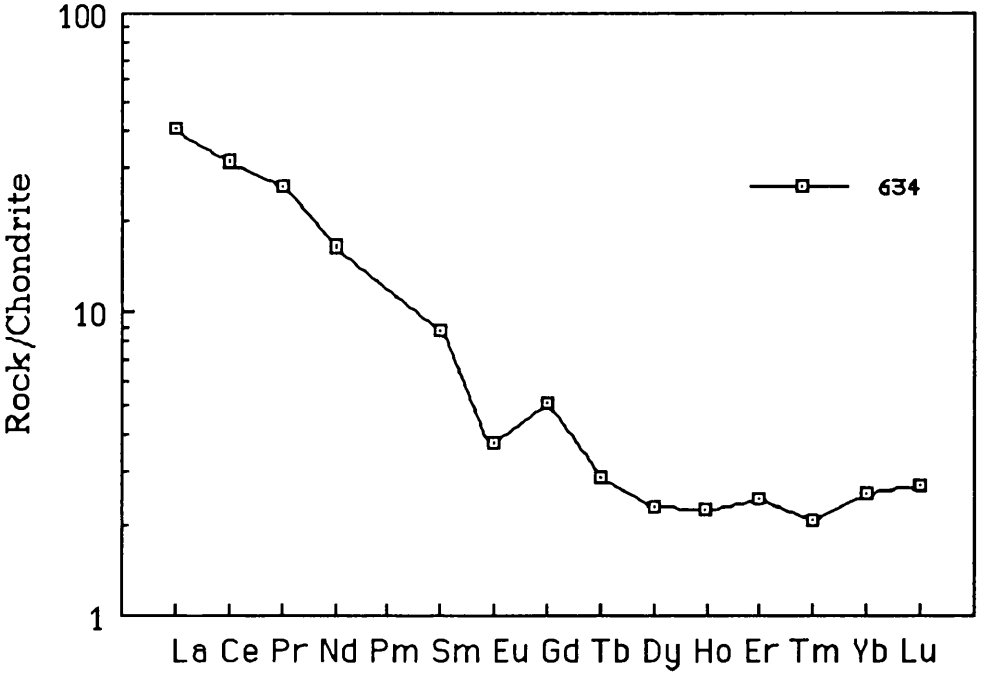

Figure 92: Normalised REE (Boynton, 1984) pattern of the quartz-alkali syenite.

IV.6 PECENEK FORMATION

IV.6.1 Tuff

IV.6.1.1. Major and trace elements

The chemical composition of the Ortakoy tuffs is almost uniform being subalkaline (Fig. 93 a) and rhyolitic. As compared with the composition of average rhyolite (Le Maitre, 1976), the tuffs show slight enrichment in SiO2, Al2O3, MgO and CaO and slight depletion in Fe2O3, FeO and Na2O (Table 50).

Cainozoic volcanism in Central Anatolia started with andesitic lavas and ignimbirites of Lower Pliocene age and continued with rhyolite domes, basalt, perlite and obsidian (Ercan et al., 1987). The Ortakoy tuff of Pliocene age may represent a rhyolitic member of the volcanic succession in the region. The existence of basalt gravels with An_{91} in the tuff confirms the existence of Cainozoic basaltic volcanism prior to the rhyolitic volcanism in Cental Anatolia.

IV.6.1.2. Conclusions

The Ortakoy tuffs are subalkaline and rhyolitic in composition and preceded by basaltic volcanism. They show slight enrichment in SiO2, Al2O3, MgO and CaO and slight depletion in Fe2O3, FeO and Na2O relative to the composition of average rhyolite (Le Maitre, 1976).

Table 50: Chemical analyses of the tuffs and average composition of rhyolite(from Le Maitre, 1976)

Sample No	673	675	674	563	Mean	σn	Rhyolite
SiO2	74.52	74.16	72.68	72.96	73.58	0.78	72.82
TiO2	0.23	0.22	0.24	0.22	0.23	0.01	0.28
Al2O3	13.73	13.53	13.71	13.60	13.64	0.28	13.27
Fe2O3	1.27	1.35	0.88	1.32	1.15	0.28	1.48
FeO	0.33	0.33	0.80	0.35	0.45	0.20	1.11
MgO	0.69	0.68	0.67	0.98	0.75	0.13	0.39
MnO	0.06	0.10	0.07	0.05	0.07	0.02	0.06
CaO	1.29	1.32	1.37	1.30	1.32	0.03	1.14
Na2O	2.96	2.88	2.64	2.91	2.85	0.12	3.55
K2O	3.96	3.91	3.95	4.26	4.02	0.14	4.30
P2O5	0.05	0.05	0.04	0.06	0.05	0.01	0.07
H2O	1.15	1.60	1.95	1.85	1.64	0.31	
CO2	0.25	0.30	0.35	0.30	0.30	0.03	
Total	100.49	100.43	99.35	100.16			
U	0	0	0	5	1	2	
Th	31	30	30	27	29	2	
Ce	51	57	57	53	54	3	
La	32	32	31	29	31	1	
Pb	24	23	23	21	23	1	
Ba	614	644	651	609	629	18	
Zr	138	125	128	132	131	5	
Y	7	8	7	12	8	3	
Sr	152	155	145	144	149	5	
Rb	177	175	165	152	167	10	
Ga	13	12	10	12	12	1	
Zn	23	24	22	28	24	2	
Cu	1	3	0	3	2	1	
Ni	7	5	1	4	4	2	
Co	9	8	9	1	7	3	
Cr	6	28	6	10	12	9	

Mineralogical composition and coordinates of the tuffs.
673: plg+bt (9642-8632)
675: plg+bt (9637-8552)
674: plg+bt (9613-8532)
563: plg+bt (9625-8530)

σn : Standard deviation
Mean : Arithmetical mean

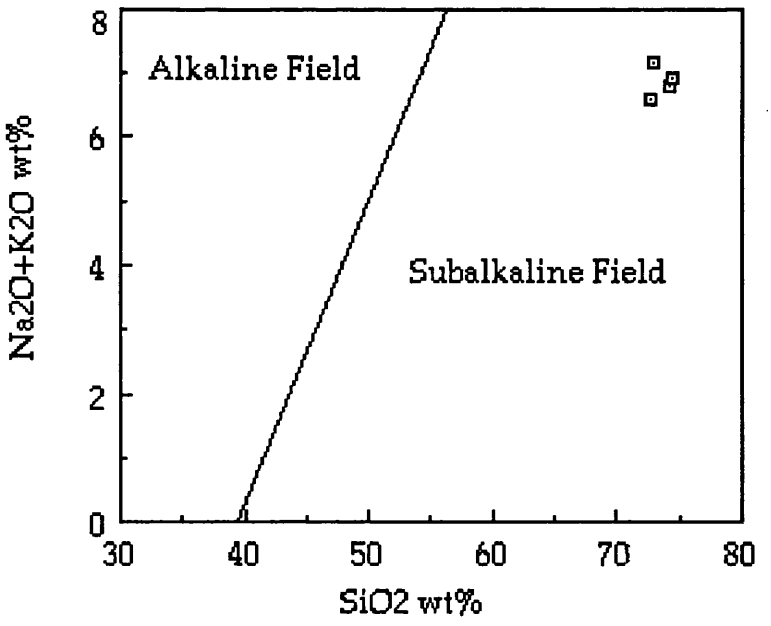

Figure 93 a: Na2O+K2O versus SiO2 (fields after Irvine & Baragar, 1971).

IV.6.2 Limestone

The composition of the limestone is essentially that of calcite influenced by clasts of igneous and metamorphic rocks and grains of quartz, orthoclase, plagioclase, muscovite and pyroxene. Dolomite is absent and this is confirmed by the low MgO, 0.48 (Table 51).

Table 51: Major element analyses of the limestones

Sample	50	59	58	Mean	σn
SiO2	5.98	6.05	6.42	6.15	0.19
TiO2	0.06	0.05	0.05	0.05	0.00
Al2O3	1.32	1.39	1.38	1.36	0.03
Fe2O3	0.42	0.39	0.33	0.38	0.04
FeO	0.13	0.13	0.07	0.11	0.03
MgO	0.47	0.54	0.43	0.48	0.04
MnO	0.03	0.03	0.02	0.03	0.00
CaO	49.26	49.74	50.28	49.76	0.42
Na2O	0.00	0.00	0.00	0.00	0.00
K2O	0.29	0.16	0.33	0.26	0.07
P2O5	0.03	0.02	0.03	0.03	0.00
H2O	2.25	1.95	1.85	2.02	0.17
CO2	39.50	40.10	38.50	39.4	0.70
Total	99.74	100.55	99.69		

Coordinates of the analysed samples
50: 94010-88820
59: 93850-88710
58: 93770-88665

Mean : Arithmetical mean
σn : Standard deviation

V PETROGENESIS OF THE METAMORPHIC AND MAGMATIC ROCKS

The geological history of the metasediments in the Kirsehir area was explained by Seymen(1984). This is applicable to the present area. The sedimentary sequence starts with muds and lesser shore-barrier sands, which were deposited in a shore environment. Gradually, carbonate precipitation became dominant as terrestrial detritus declined. Finally, an open-shelf environment was formed in which carbonate precipitated alone. On the whole, the metasediments in the massif developed transgressively in an Atlantic type continental edge.

The marbles of the Seksenusagi Formation with their low diversity microfossil assemblage, the existence of coral and the lack of any spores indicate a shelf environment of restricted circulation away from areas of sediment derived from a vegetated terrestrial environment. Towards the top of the Gobektepe Formation marble became the sole lithology which suggests an open shelf environment.

Magmatism in the Ortakoy part of the region starts with a continental basaltic magmatism, represented by amphibolites in the metasediments. During Upper Cretaceous and Paleocene time, the most intensive part of the magmatism occured, which resulted in the intrusion of the tholeiitic Ekecekdagi gabbros(?), tholeiitic to calc-alkaline diorites and calc-alkaline granitoids. These are correlated with a subduction zone. Isotopic studies of granitoids formed at active continental margins such as the Peninsular Ranges Batholith of California reveal that compositional variations in these acidic rocks were largely inherited from the source region from which the acidic magma was derived by partial melting (Silver&Chappell, 1988). High level processes such as fractional crystallisation, and local assimilation have a relatively minor influence on the composition of the acidic rocks. Similarly, Pankhurst et al.(1988) also showed by isotopic studies of granitoids

in Andean region of South America and Antarctic Peninsula that contamination of granitic magmas largely occur in the source region, and high level contamination has minor effect on the composition of granitic magmas.

The emplacement of mantle derived basic magma into the lower crust can supply enough heat to initiate melting (Burnham, 1979; Huppert&Sparks, 1988). This magma can assimilate lower crustal rocks prior to any significant differentiation, and can be modelled as an assimilation-fractional crystallisation process in which mafic magma supplies the heat for assimilation. The volume of assimilated crustal rocks could be much less than that of the primary magma. Finally, granites could represent anatectic melts of deep crustal rocks . This model may also involve crustal melting and hybridization of the end member liquids. Huppert&Sparks (1988) investigated experimentally that a 10-1500 m thick basaltic sill which intruded into the continental crust would require only 2-200 years to solidify , during which time large volumes of convective silicic magmas could be formed. Relatively low density melts at the floor rise and mix into overlying magma and thus form hybrid andesitic magmas.

Applying the model to the studied area, the Ekecekdagi gabbro would be representative of the basic magma which triggered the melting to produce the diorites and the granitoids. Because the exposed volume of the Ortakoy pluton is much more than that of the Ekecekdagi gabbro, it is necessary to assume substantial unexposed gabbro in the crust below the acidic rocks. Present diorites and granitoids may represent a mixture of mantle and lower crustal derived magmas, coupled by fractional crystallisation with possible minor high level contamination. The granitoids would therefore be much more contaminated with melted crust than the diorites. The acidic rocks became melt dominated rather than restite dominated by this contamination, which was evidenced by decreasing K/Rb with increasing

SiO2(Wyborn et al.,1992). Y/Nb variation, in general unchanged by crustal contamination(Eby, 1990), also implies the heterogeneity at the source of the granitoids.

Ortakoy magmatic rocks show a coherent trend on an AFM diagram (Fig.93 b) therefore fractional crystallisation may be an important process in their petrogenesis.

The Ekecekdagi gabbro was considered as an intrusive rock in the above explanation. However, the gabbro may belong to an uncompleted ophiolitic sequence as the contact of the Ekecekdagi gabbro with the metamorphic rocks has not been seen in the field and the existence of a negative Ce anomaly in the gabbro (but not in the granitoids and diorites), may be due to gabbro and sea-water interaction. In that case, after the gabbro was emplaced into the metamorphic rocks as an allochthonous unit the Ortakoy pluton intruded into the metamorphic rocks and the Ekecekdagi gabbro.

The magmatism in the Ortakoy area ends with the production of basaltic and rhyolitic rocks in the Pliocene.

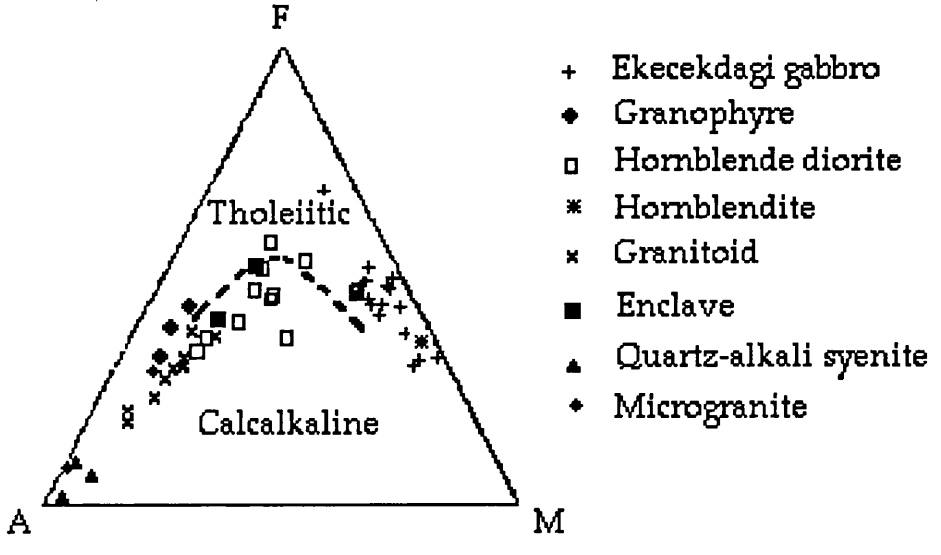

Figure 93 b: AFM diagram of Ortakoy intrusives (Fields after Irvine & Baragar, 1971)

VI METAMORPHISM

VI.1 REGIONAL METAMORPHISM

VI.1.1 Semipelites and psammites

The psammites, with their quartz-rich nature, are less indicative of metamorphic conditions than the semipelites. Widespread retrograde and contact metamorphism, destroyed the characteristic regional metamorphic mineral assemblages making it difficult to determine the P-T conditions of regional metamorphism. In spite of these difficulties, the mineral assemblage which is thought to be representative of early regional metamorphism in the semipelite is:

Quartz + sillimanite (fibrolite) + biotite + plagioclase (%An23-25) + garnet ± ilmenite /hematite.

The garnet is commonly replaced by biotite and quartz while the sillimanite is grown within, and fringes, the biotite. The biotite is quite rich in TiO2, up to 3.7wt % with $Mg/(Mg+Fe_t^*)$ values varying between 0.22 and 0.39.

The garnet occurs sporadically probably because of biotite replacement and low-pressure in the massif. The bulk composition of the metasediments is probably also another factor in controlling garnet growth: high Mg^/(Mg+Fe) ratios in the semipelite(0.64) and psammite (0.59) are not in favour of the garnet formation. Symmes and Ferry (1992) suggested that the small MnO contents of normal pelitic schists (X_{Mn}, Mn^/(Fe+Mg+Mn) = 0.01-0.04) are both sufficient and necessary for stability of garnet. The average value of X_{Mn} in the Ortakoy semipelite (0.008) is smaller than the lower limit of Symmes and Ferry(1992) for garnet

*: Fet as FeO
^: Mol proportion

formation, 0.01 while X_{Mn} in the Ortakoy psammite, 0.01 is just on the lower limit. On the whole combined factors such as low pressure, unsuitable bulk rock composition and biotite destruction by biotite lead to low garnet contents.

The sillimanites occur as fibrolite in both semipelitic and migmatitic gneiss. In metamorphic rocks of upper amphibolite and granulite facies, partial melting has been suggested to produce sillimanite (fibrolite) if the quartzofeldspathic components segregate and form leucosomes between melanosomes that are enriched in aluminium, via leaching of base cations by solutions (Vernon, 1979, 1987). In contrast, Yardley (1977 b) ascribed sillimanite formation to the breakdown of garnet to muscovite and staurolite. In the migmatitic gneiss, metasomatism (base cation-leaching) may be responsible for the development of the sillimanite but for the gneiss, the garnet breakdown is also involved as some garnet pseudomorphism by sillimanite can be observed under the microscope.

Sericite, chlorite and muscovite are later minerals which formed by retrograde metamorphism.

VI.1.2 Migmatites

In the migmatitic gneiss, leucosomes containing quartz, orthoclase and plagioclase develop between melanosomes which are made of biotite, fibrolite and ilmenite. The composition of the plagioclase is roughly same in the neosome(%An 23-29) and paleosome (%An 23). If the leucosomes were melts, they should have contained feldspars more sodic than those of the paleosomes (Yoder et al., 1957). Therefore, the migmatites lacking the plagioclase differentiation effect can not be anatectic (Yardley, 1977 b). But some migmatites that are known as anatectic on the basis of leucosome

compositions, textures and field relations lack the plagioclase differentiation effect (Ashworth, 1976). According to Menhert and Busch(1982) who found almost the same plagioclase composition in leucosomes and melanosomes in the initial stage of migmatitization, anorthite content of plagioclase can change only if the melt is clearly separated from its starting material. The feldspars could also have re-equilibrated by diffusion between the zones after crystallisation of the melt Olsen(1983).

Partial melting could occur above the second sillimanite isograd in a low pressure metamorphism (Yardley, 1989). Incongruent melting for muscovite in the presence of a fluid phase is represented by the equilibrium:

muscovite+quartz+plagioclase+vapour = sillimanite+melt.

Vapour-present melting reactions may occur where local vapour is retained or where infiltration of vapour takes place (Grant, 1985). In the absence of free water, the melting depends upon muscovite. Such amounts of water are usually not sufficient to saturate a melt formed by the breakdown of the hydrates and the water released during this process is dissolved in the melt without formation of a vapour phase(Burnham, 1967). Therefore, it is likely that migmatites would be formed by a vapour absent reaction, called dehydration melting in the terminology of Thompson (1982). This is common in the crust (Clemens&Vielzeuf, 1987).

VI.1.3 Carbonates

In calc silicate metasediments, the assemblage of calcite + diopside + quartz + plagioclase ± tremolite ± orthoclase ± scapolite(meionite) ± sphene±zircon±opaque appears.

VI.1.4 Amphibolites

The assemblage of hornblende (magnesio-hornblende and magnesio-hastingsite)+anorthite+diopside+quartz±sphene is characteristic in the amphibolites which equilibrated finally at 761± 75 °C(at 4kb pressure), determined by the hornblende-plagioclase thermometer of Blundy and Holland(1990). The plagioclase with % An 87 in the sample (685) was used, since plagioclase with An ≥ 92 is not eligible for the calculation of the geothermometer. The estimated equilibrium temperature of the amphibolite is high compared with the one determined from the semipelitic gneiss but is compatible if the errors are taken into the consideration. The temperature was also determined for andesine and hornblende in Table 12 (sample 689) using the hornblende-plagioclase thermometer. The result of the calculation, 935± 75 °C at 4kb pressure shows that the andesine and hornblende in the amphibolite (sample 689) are probably not in equilibrium. Since there is no development of orthopyroxene in the amphibolite, it is unlikely that the temperature significantly exceeded 700 °C

The occurrence of chlorite within the biotite, formed from hornblende is attributed to retrograde metamorphism.

VI.1.5 Timing of Metamorphism

The regional metamorphic rocks in the Ortakoy part of the Middle Anatolia Massif record the effect of a single episode of regional metamorphism producing garnet, biotite sillimanite (the semipelitic and psammitic gneiss) hornblende, diopside and anorthite (amphibolites). As

no fabric was developed by the D2 deformation, the regional metamorphism might have formed during or after D1 deformation.

As shown in petrography chapter by SEM studies, plagioclase with andesine composition in amphibolite may have formed by later fluids.

VI.1.6 Conclusions

During or after D1 deformation, the regional metamorphism induced the crystallisation of the garnet, biotite, sillimanite(semipelite and psammite), hornblende, anorthite and diopside (amphibolite).

The presence of sillimanite instead of kyanite in the semipelitic rocks and hornblende, anorthite and diopside in the metabasic rocks indicate that the Ortakoy metasediments were metamorphosed under upper amphibolite facies conditions (second sillimanite grade). This is confirmed by geothermometer studies (Fig. 94) from the different metamorphic assemblages which yield between 608-761 °C at 4 kb. pressure.

The scarcity of garnet in the semipelites is probably due to a combination of low pressure and unsuitable composition combined with destruction of garnet to biotite Fibrolite largely grow by replacement of biotite

The metasediments partially melted via the reaction of the muscovite breakdown (incongruent melting) under fluid absent conditions.

The high grade metamorphic rocks have undergone limited retrogression to greenschist facies assemblages resulting in the replacement

of sillimanite and K-feldspar by muscovite, and breakdown of garnet to biotite.

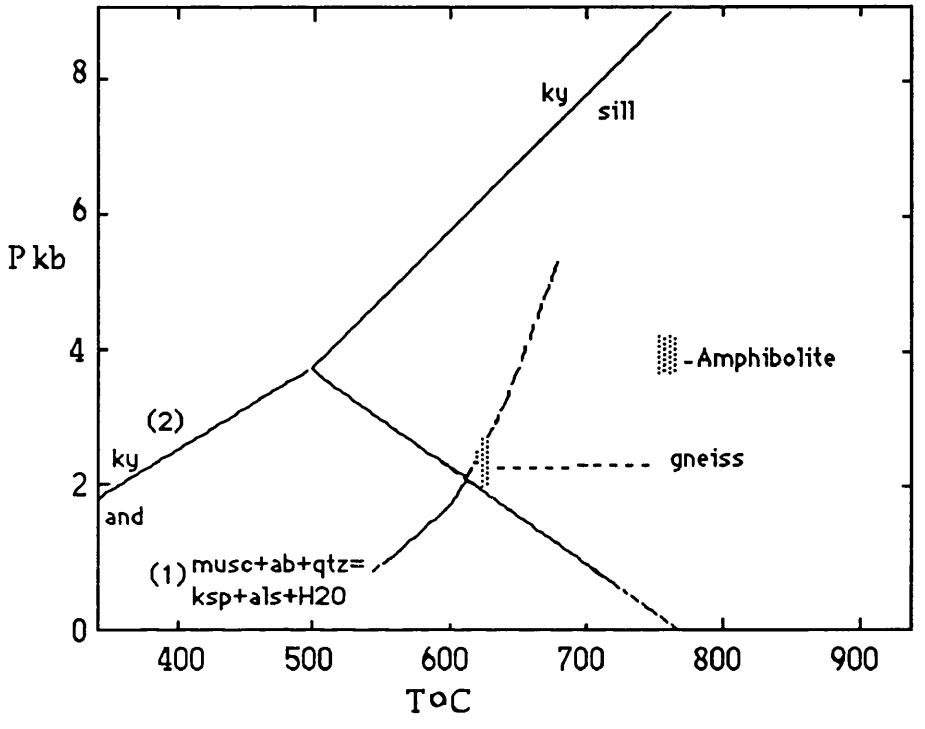

Figure 94: P-T diagram of the Ortakoy metamorphics. Al2SiO5 phase boundary(1) and muscovite breakdown reaction (2) are taken from Holdaway (1971) and Thompson (1974).

VI.2 LOCAL METAMORPHISM

VI.2.1 Contact metamorphism

In general, the igneous rocks in the area, the Ekecekdagi gabbro and the Ortakoy pluton are undeformed. The contact metamorphic aureole of the Ortakoy pluton, (the contact of the Ekecekdagi gabbro with the Ortakoy metamorphics has not been observed) overprints the regional metamorphic assemblages, indicating that they were emplaced after the regional metamorphism and the development of the regional foliation in the massif.

Some pelitic rocks next to the granitoid suffered from contact metamorphism and a mineral assemblage of biotite, cordierite, orthoclase and plagioclase crystallised. The cordierite is full of inclusions of quartz, biotite, muscovite and opaques which prevented microprobe analysis. The two feldspar geothermometer of Haselton et al.(1983) gives 619°C equilibrium temperature at 4 kb pressure for this hornfels.

The occurrence of small andalusite rombs within sillimanite in the semipelitic gneiss is attributed to the contact metamorphism.

Semipelitic rocks that are surrounded by Ortakoy pluton show contact metamorphic: tourmaline (schorl) in both contaminated granite and xenolithic gneiss while garnet with a rim enriched in Mn appears only in the contaminated granite. Therefore, it is likely that the Ortakoy pluton contributed to the tourmalinisation which is common in the semipelite and psammite. Sericitisation and chloritisation, which often accompanies the tourmalinisation might have been formed, or have been induced by the contact metamorphism. The fact that the Ortakoy metasediments are

found as roof pendants within the igneous rocks may support this.

The paragneissic granite consisting of quartz, cordierite, biotite, plagioclase(26-35 %An), orthoclase and garnet is suggested to have formed from semipelite by contact metamorphism of the Ekecekdagi gabbro and, or the Ortakoy pluton. At 4 kb pressure, the granite was finally equilibrated at 533±50 ^{o}C (from the garnet-biotite geothermometer of Frank and Spear, 1978) and, or at 526 ^{o}C, obtained from two feldspar geothermometer of Haselton et al.(1983).

Inclusions in the paragneissic granite contain idioblastic garnet which shows breakdown to the assemblage of biotite, cordierite, orthoclase and plagioclase(%An 28-40). The mineral assemblages are projected on an AFM diagram(Fig. 95). The reason why the AFM diagram of Barker (1961) chosen, rather than that of Thompson(1957) is the lack of muscovite in the samples. The garnet-biotite geothermometer of Ferry and Spear(1978) gives 681±50^{o}C equilibrium temperature for these inclusions (at 4 kb P). Using Holland and Powell(1990)'s updated thermodynamic dataset, 4.17±0.29 kb. average pressure is obtained(see petr. chapter).

Within the carbonate xenoliths, some Ca-silicate mineral assemblages vis. garnet, diopside, hedenbergite, tremolite, sphene, epidote and plagioclase(bytownite and anorthite) developed under the hornblende-hornfels facies conditions.

VI.2.1.1 Conclusions

The regional metamorphic mineral assemblages in the massif are overprinted by a contact one induced by Ortakoy magmatism. As a result of this, there formed pelitic hornfels consisting of biotite, cordierite, orthoclase and plagioclase; paragneissic granites and their pelitic inclusions, both of which are made of cordierite, biotite, plagioclase(26-40%), orthoclase and garnet; skarn zone in carbonate xenoliths, and andalusite in the semipelitic gneiss. The temperature ranges from 681(±50) to 533 (± 50) °C at 4.17(±0.29) kb. in contact metamorphism.

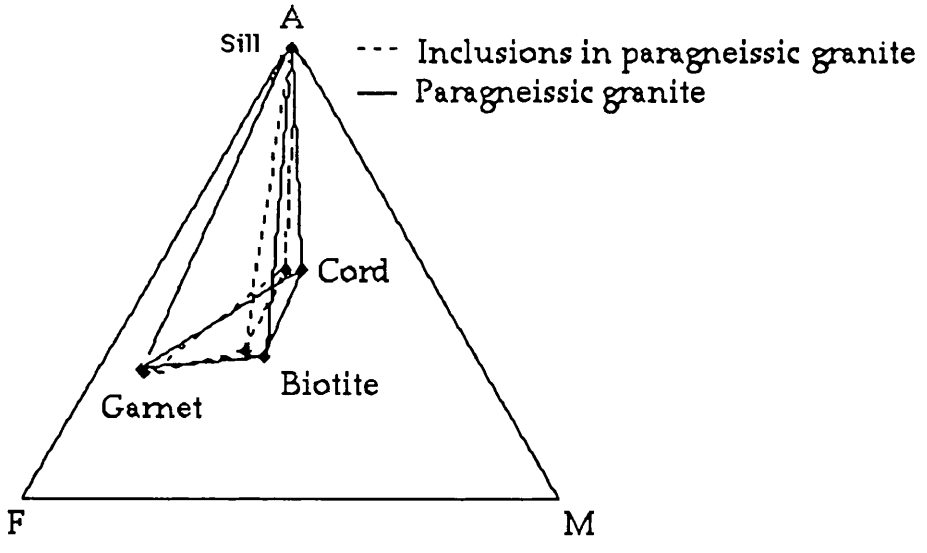

Figure 95: AFM (molar Al2O3, FeO and MgO) projection of the paragneissic granite and its inclusions.

VI.2.2 Dislocation metamorphism

Varying degrees of late shearing, mylonitisation and cataclastic effects record late stage dislocation metamorphism approximately E-W direction.

VII STRUCTURE

VII.1 FOLDS

In general, except for bedding in the marbles, bedding has been replaced by a D1 foliation in the metasediments due to syntectonic movements during or before upper amphibolite facies metamorphism when migmatites developed.

Around Sirayalardagi (Seksenusagi Form.) and Akcaagil tepe (Gobektepe Form.), the folds of quartzite in marble have their axial planes roughly parallel to the bedding in the marble. Observations and measurements around these outcrops lead to the conclusion that these small folds formed in relation with a refolded D2 anticline that is plunging eastwards. The D3 fold developed around Seksenusagi within the gneisses of the Seksenusagi formation is a refolded isoclinal syncline which may be related to the formation of the refolded anticline and this interpretation is made for the Seksenusagi formation on the cross sections of the geological map of the Ortakoy area (Appendix-1b). The structure of a refolded anticline is also well defined by marbles in gneiss around Osmanagatepe. No fabric development has been observed in D2 folds, that is, the common foliation in the gneiss must have been developed during D1 folding which has not produced any folds that have been recognised. Accordingly, Tolluoglu (1989) stated the foliation formed prior to the D2 deformation. Some crenulation cleavage oriented E-W developed by D3 folds.

Following D3 were generally open D4 folds with steep axial plane. Spaced cleavages ESE-WNW oriented formed by D4 folding.

The area where the regional metamorphic rocks crop out has been divided into six subareas (Appendix-3), and measurements of bedding and foliation in five of these have been plotted on an equal area diagram using a computer program called Sods (Farrow, 1992). D3 folds appear in 1, 5a and 5b subareas with 60'28*, 88'8 and 85'30 fold axes (Figs. 96 -a, -b, -c). No clear fold pattern is seen in the equal area diagrams of the other sub-areas due to superimposed folds(Figs. 96-d,-e,-f). The axes of minor folds have also been plotted on an equal area diagram (Figs. 97-a,-b,-c). In 4a and 6 subareas, the axes of D3 folds plunge to the E while D3 folds in subarea 4b plunge towards the W. The D4 folds plunge towards SSW and E-SE in 4a and 4b subareas .

After three deformation phases, the Middle Anatolia Massif fractured as a result of late stage deformation due to regional uplift of the massif. The joint system in the Ekecekdagi gabbro, hornblende diorite and granitoid developed in WSW-ENE direction (Fig.s 98, 99 and 100)

The alignment of feldspar phenocrysts in the granitoids especially the granitoid mapped on the 1/5000 scale next to Sirayalardagi is plotted on a rose diagram(Fig. 101). Though it is not well defined in the diagram, some mineral alignment in an ESE direction(>30% of crystals) appears. It is also compatible with the D3 fold axis in the 5b subarea, closest metamorphic rocks to the granitoid in which the feldspar alignment was measured.

60,28 *: 28 is plunge, 60 is the direction of the plunge

VII.2 FAULTS

These faults develop both at the contact of the magmatic intrusions and the metamorphics, and also between the different igneous units. The faults also develop within individual igneous rock bodies, especially in the granitoids. The main faults are WNW-ESE, longest fault occurs in the granitoid next to the Ekecekdagi gabbro. But other fault direction strike E-W.

VII.3 CONCLUSIONS

It has been deduced that Ortakoy part of the Middle Anatolia Massif underwent four phases of deformation: D1 during the formation of the metamorphic rock fabric, D2 which produced folds varying from isoclinal to tight while D3 folds have open limbs. D4 folds are usually open with steep axial plane. The massif was then uplifted inducing the development of the WSW-ENE dominated joint sets in the Ekecekdagi gabbro, hornblende diorite and granitoid and the formation of WNW-ESE faults.

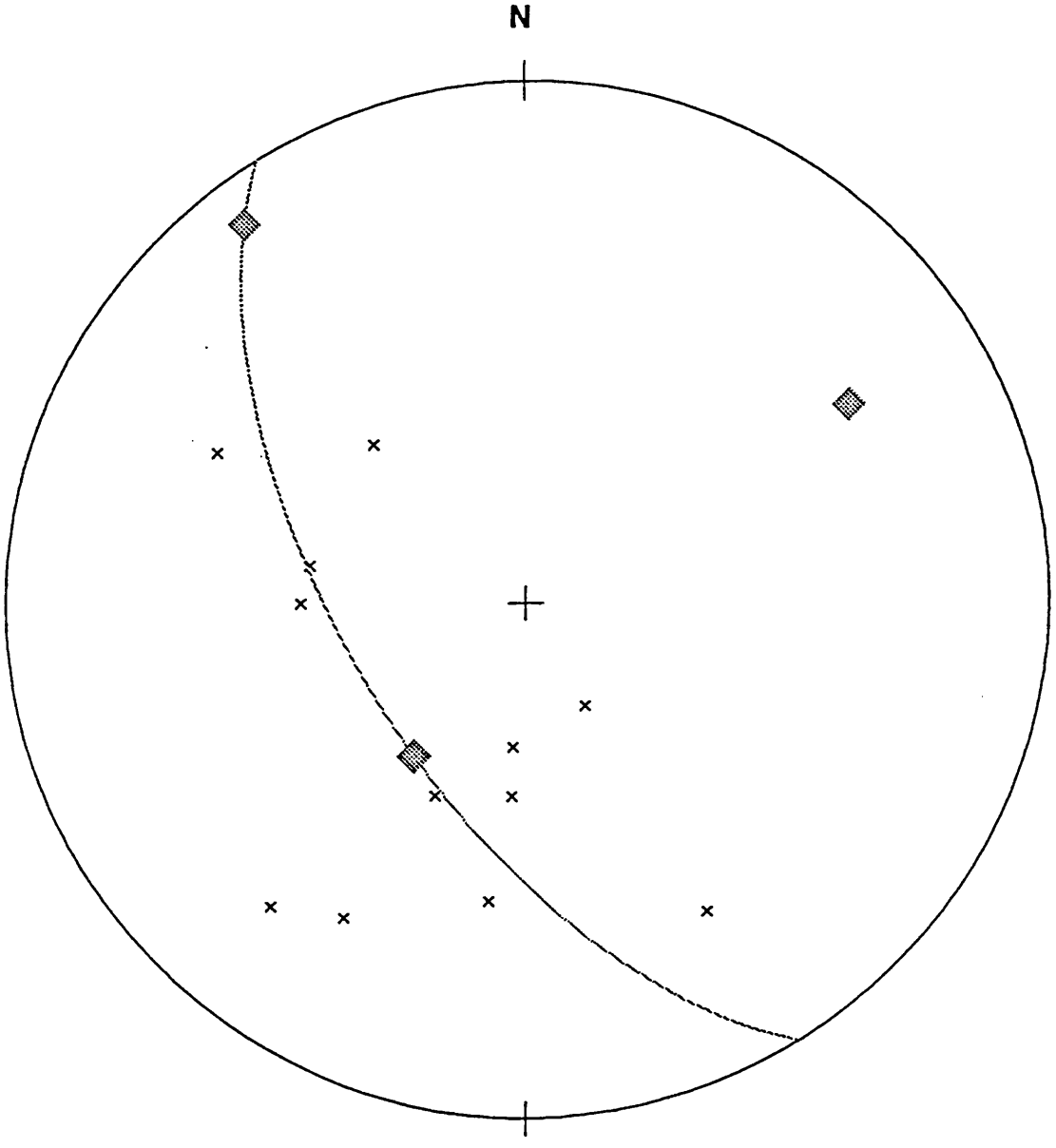

Figure 96 a: Equal area diagram of the bedding in 1 subarea

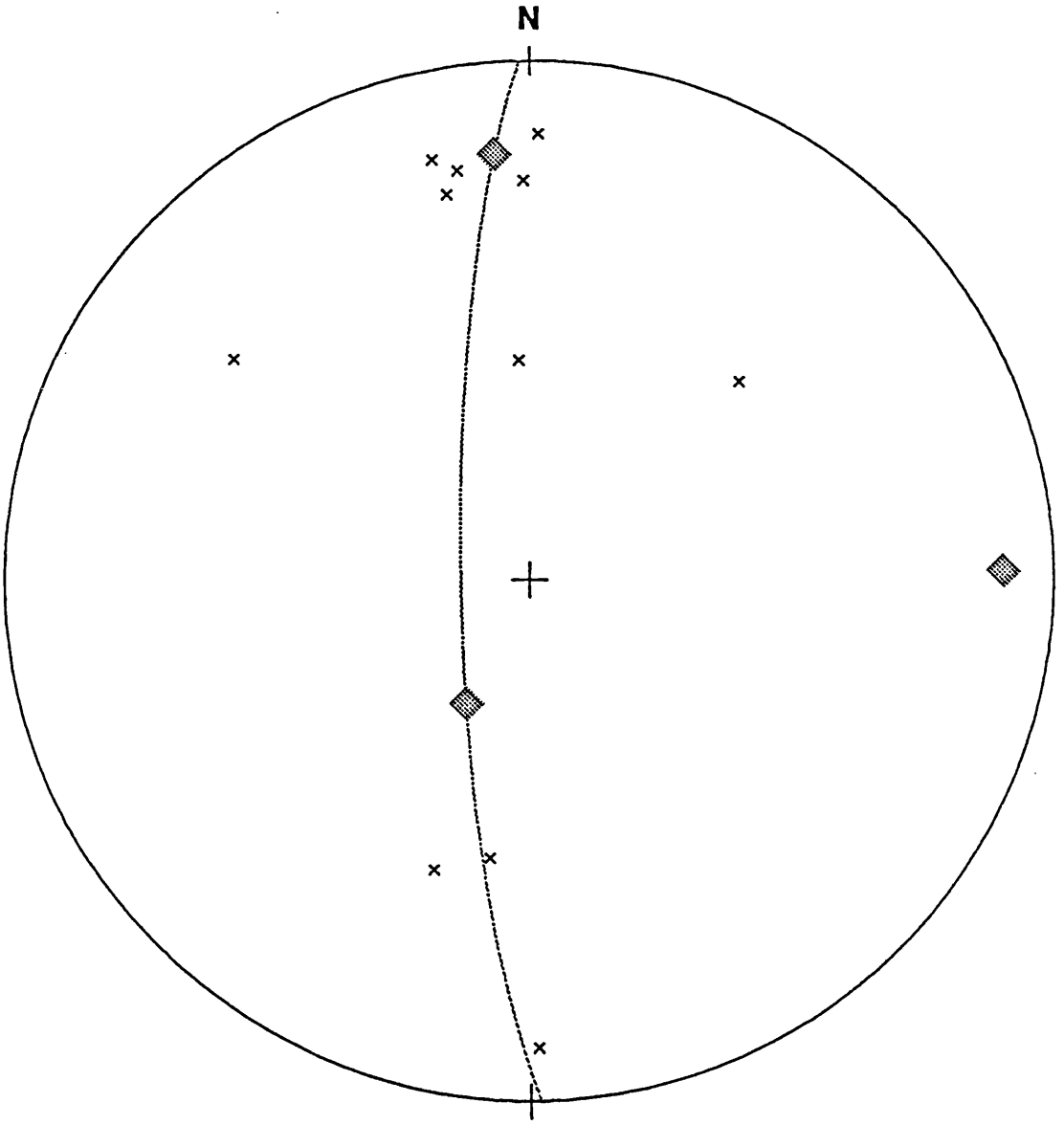

Figure 96 b: Equal area diagram of the bedding and foliation in 5a subarea.

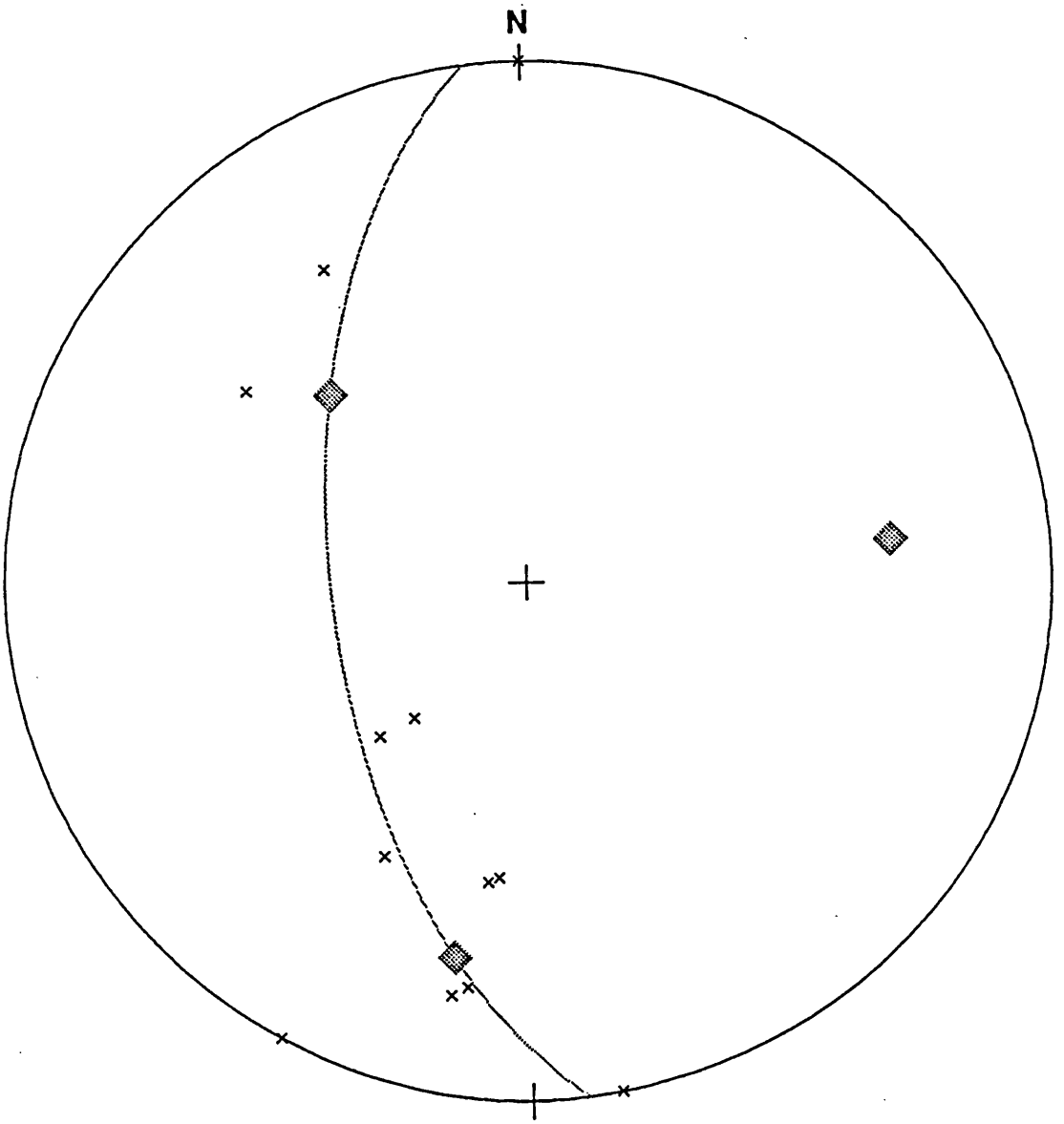

Figure 96 c: Equal area diagram of the bedding in 5b subarea.

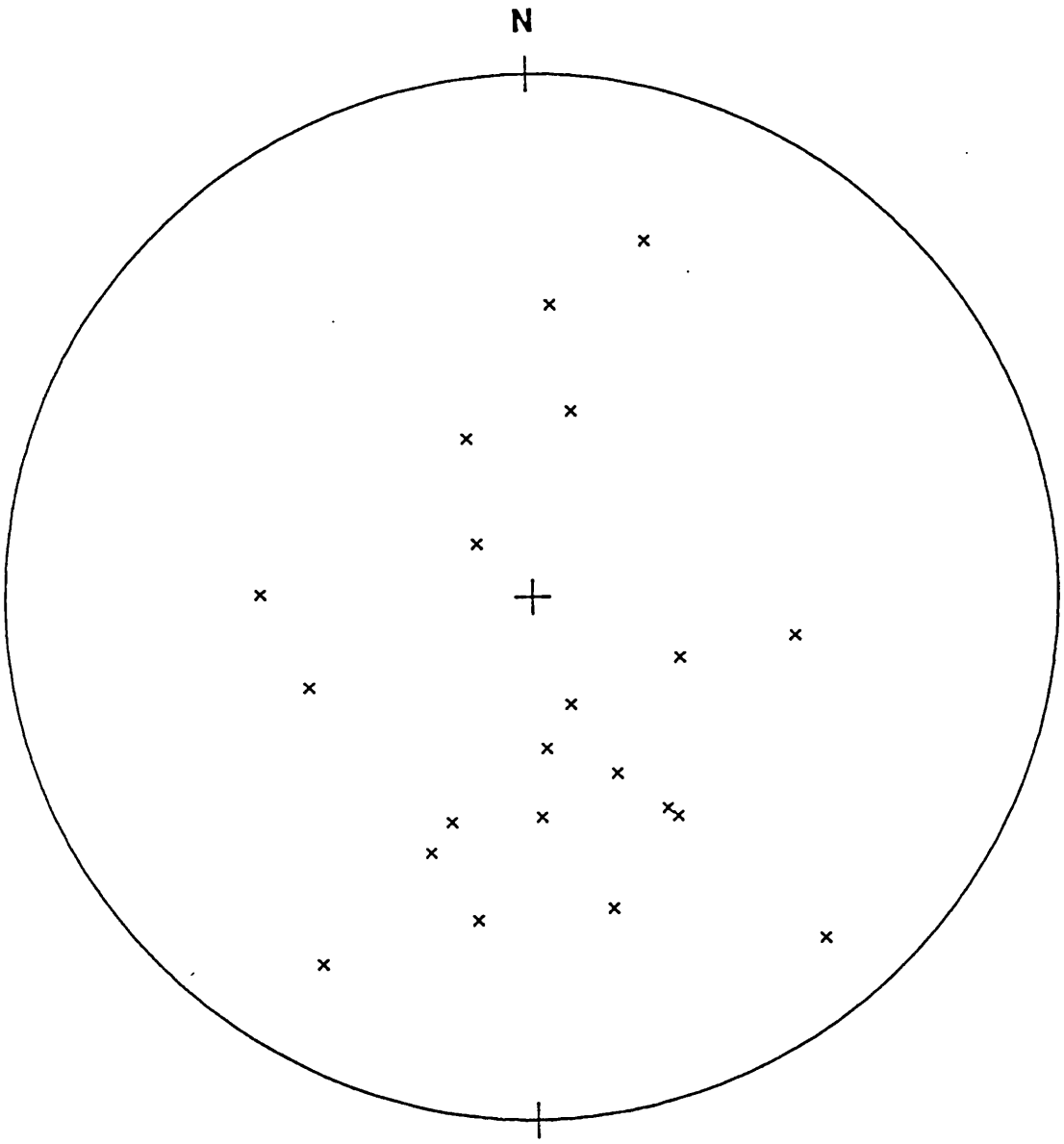

Figure 96 d: Equal area diagram of the bedding in 2 subarea.

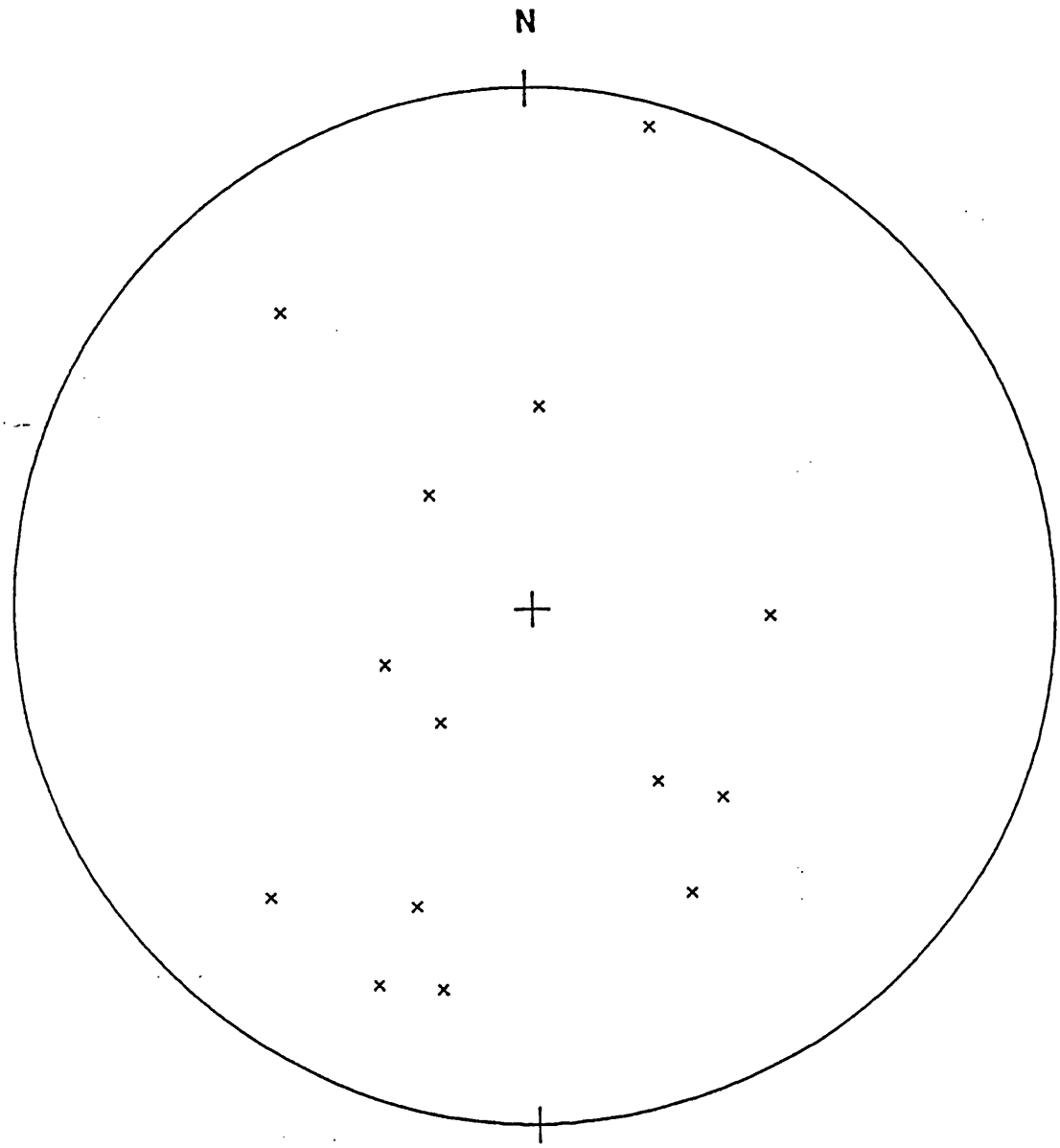

Figure 96-e: Equal area diagram of the bedding and foliation in 3 subarea.

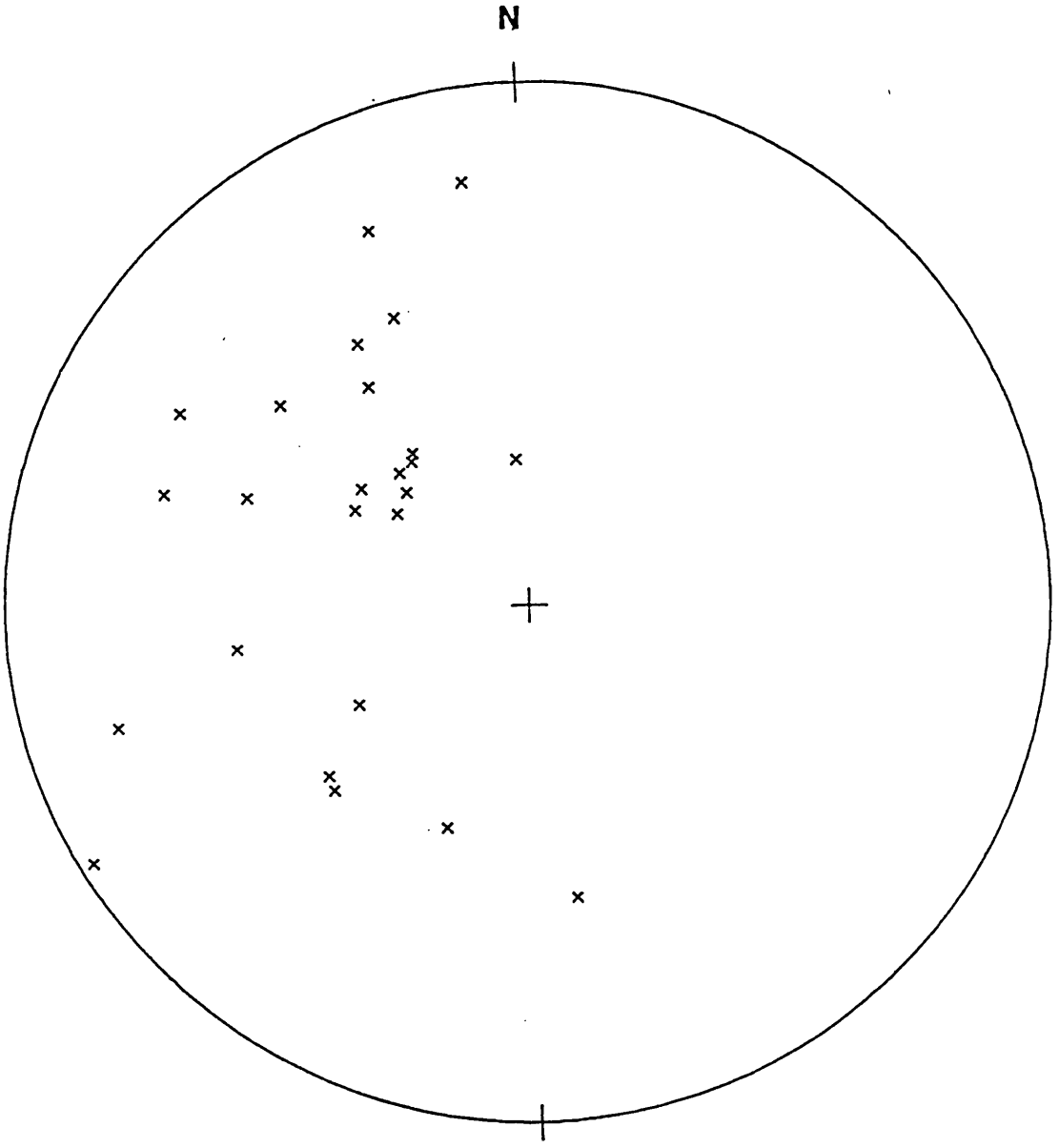

Figure 96-f: Equal area diagram of the bedding and foliation in 4a and 4b subarea.

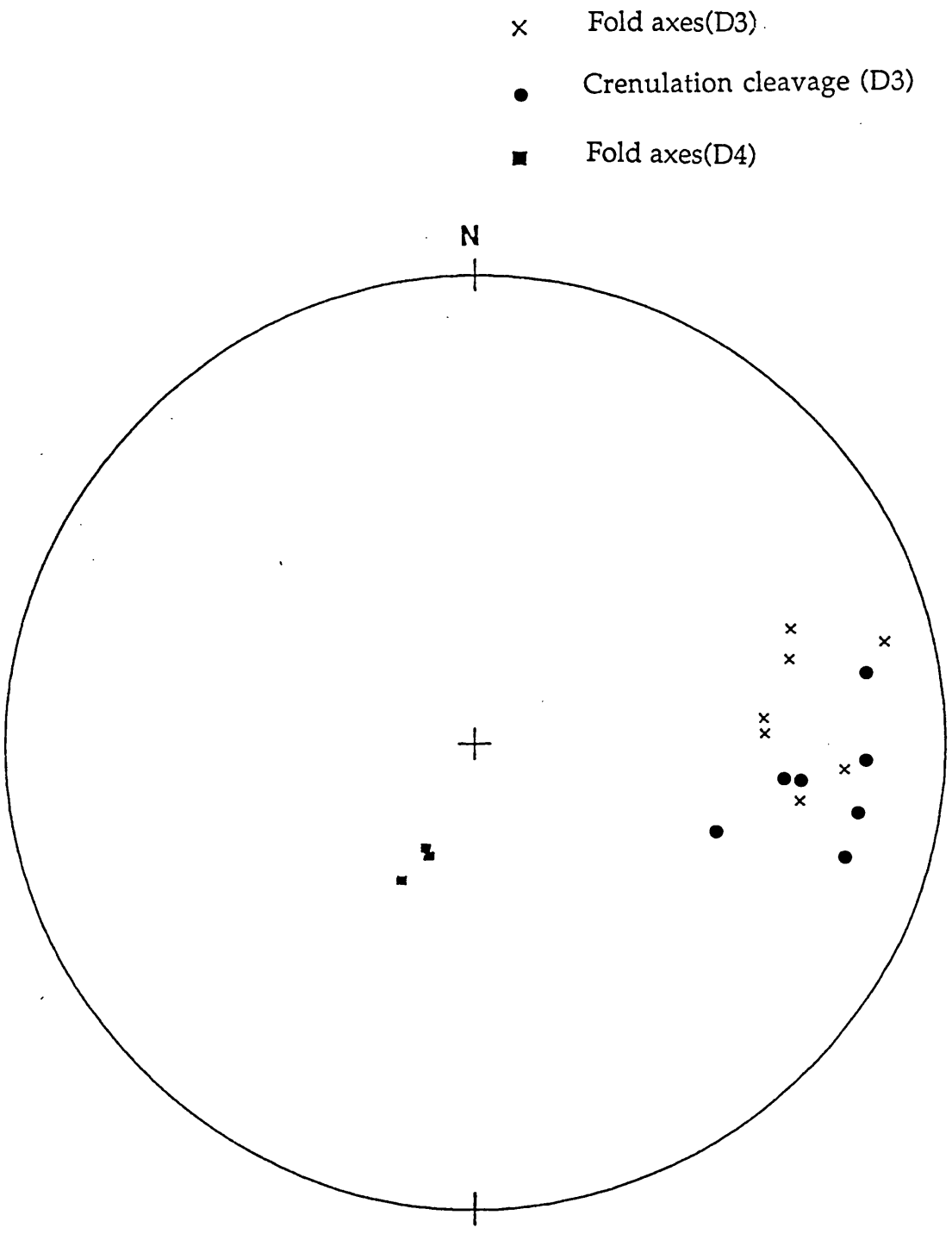

Figure 97a: Equal area diagram of the fold axes and crenulation cleavage in 4a subarea.

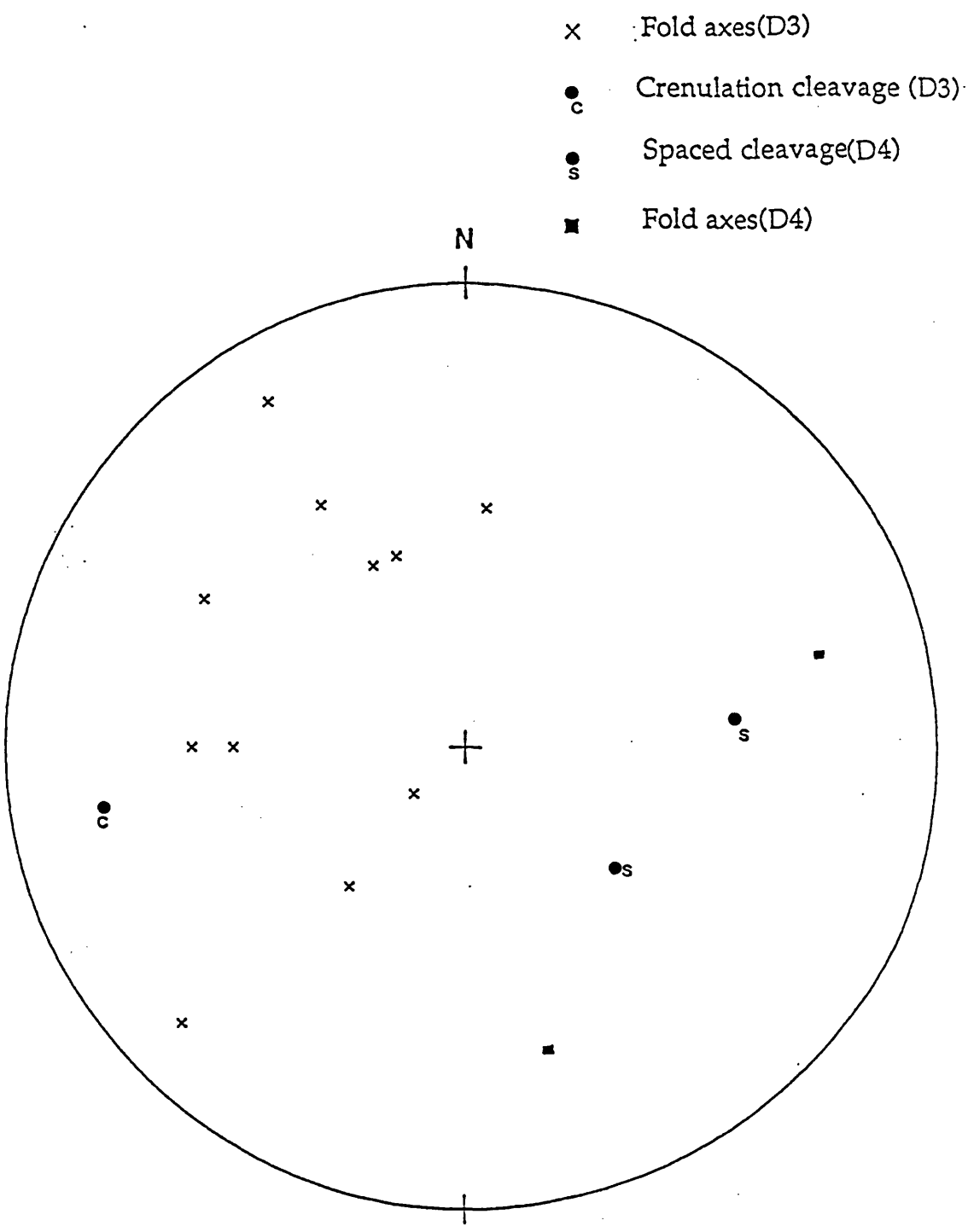

Figure 97 b: Equal area diagram of the fold axes, crenulation and spaced cleavages in 4b subarea.

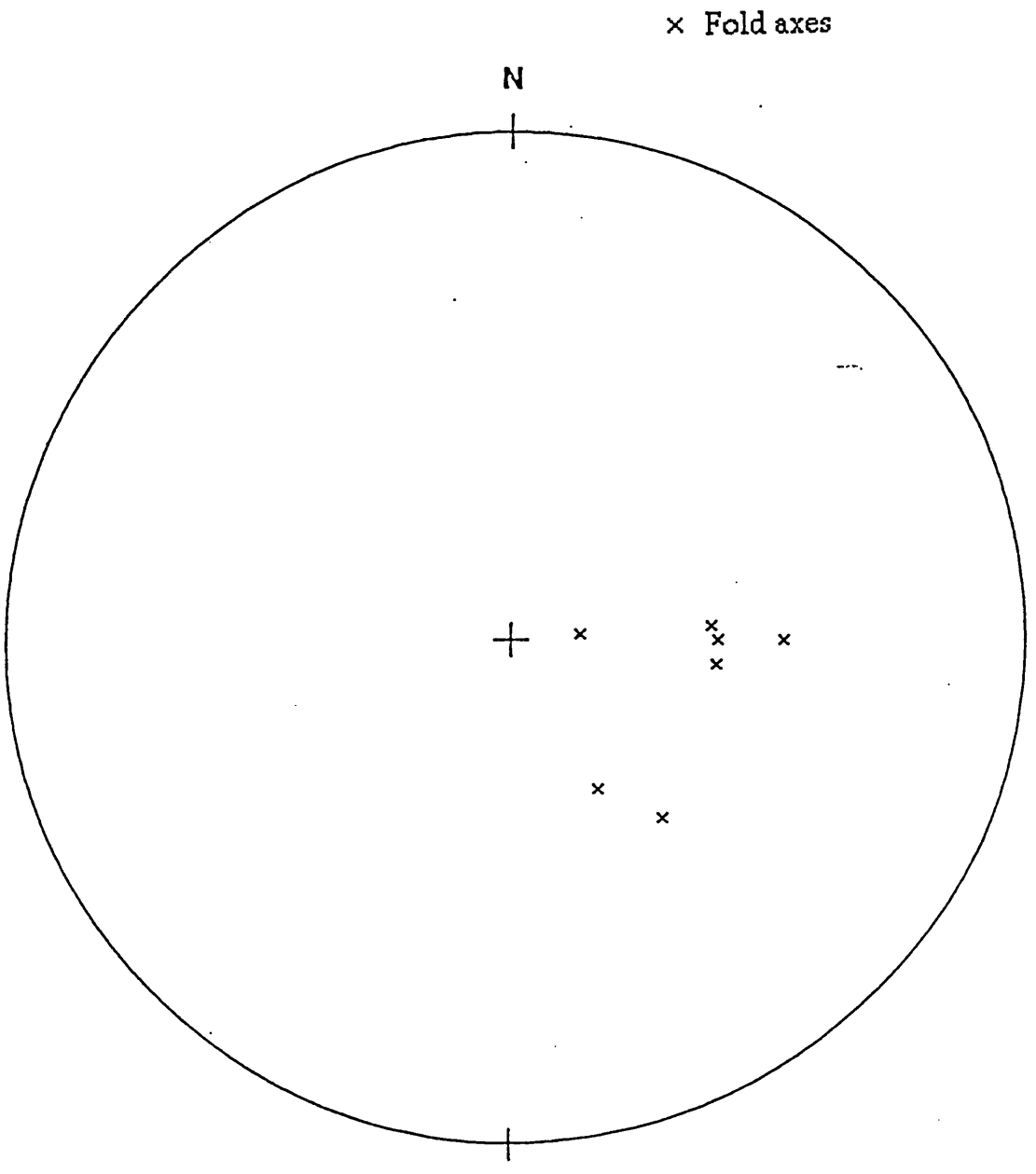

Figure 97 c: Equal area diagram of the fold axes in 6 subarea.

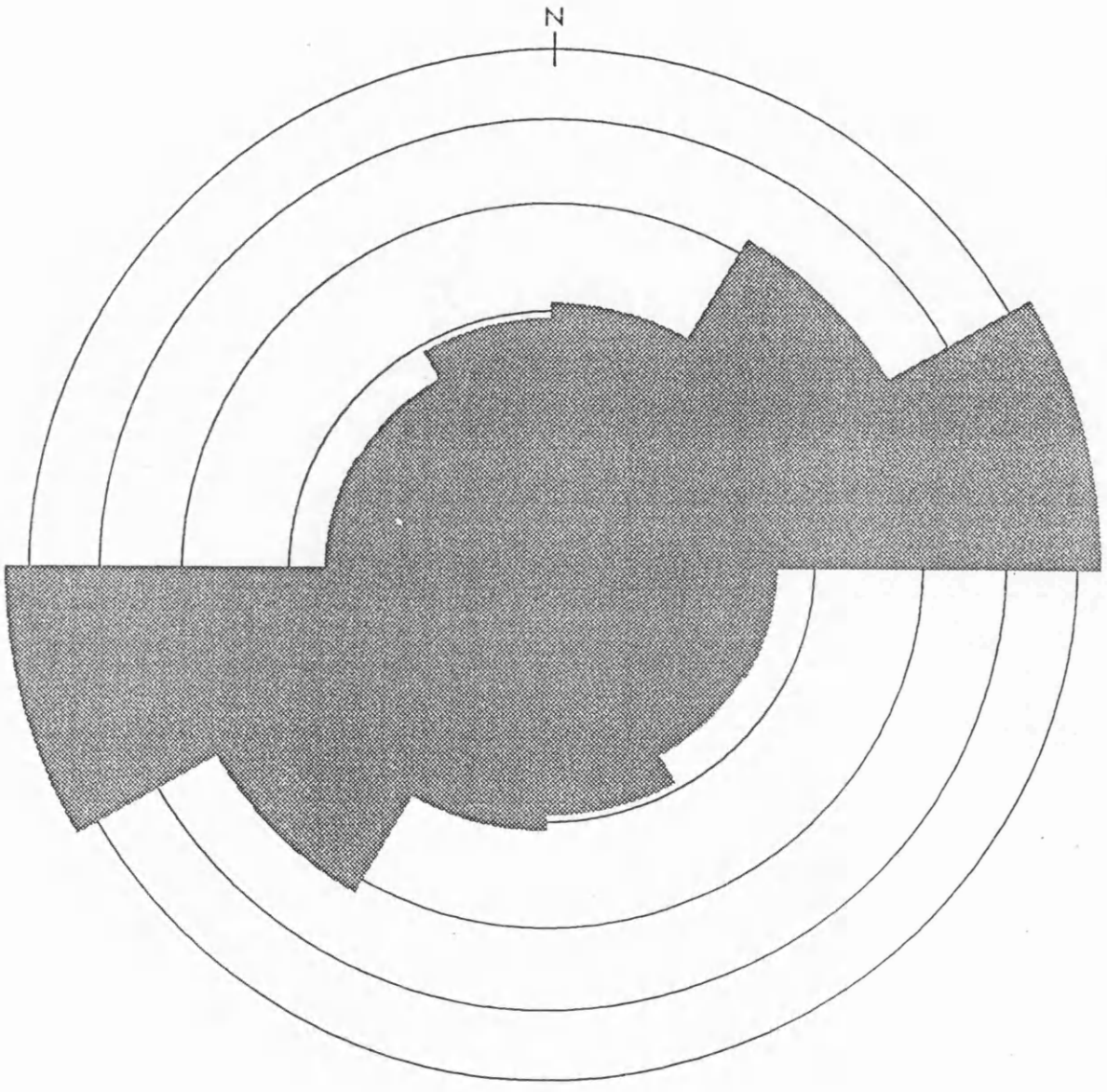

Figure 98: Rose diagram of the joints in the Ekecekdagi gabbro (291 joints).

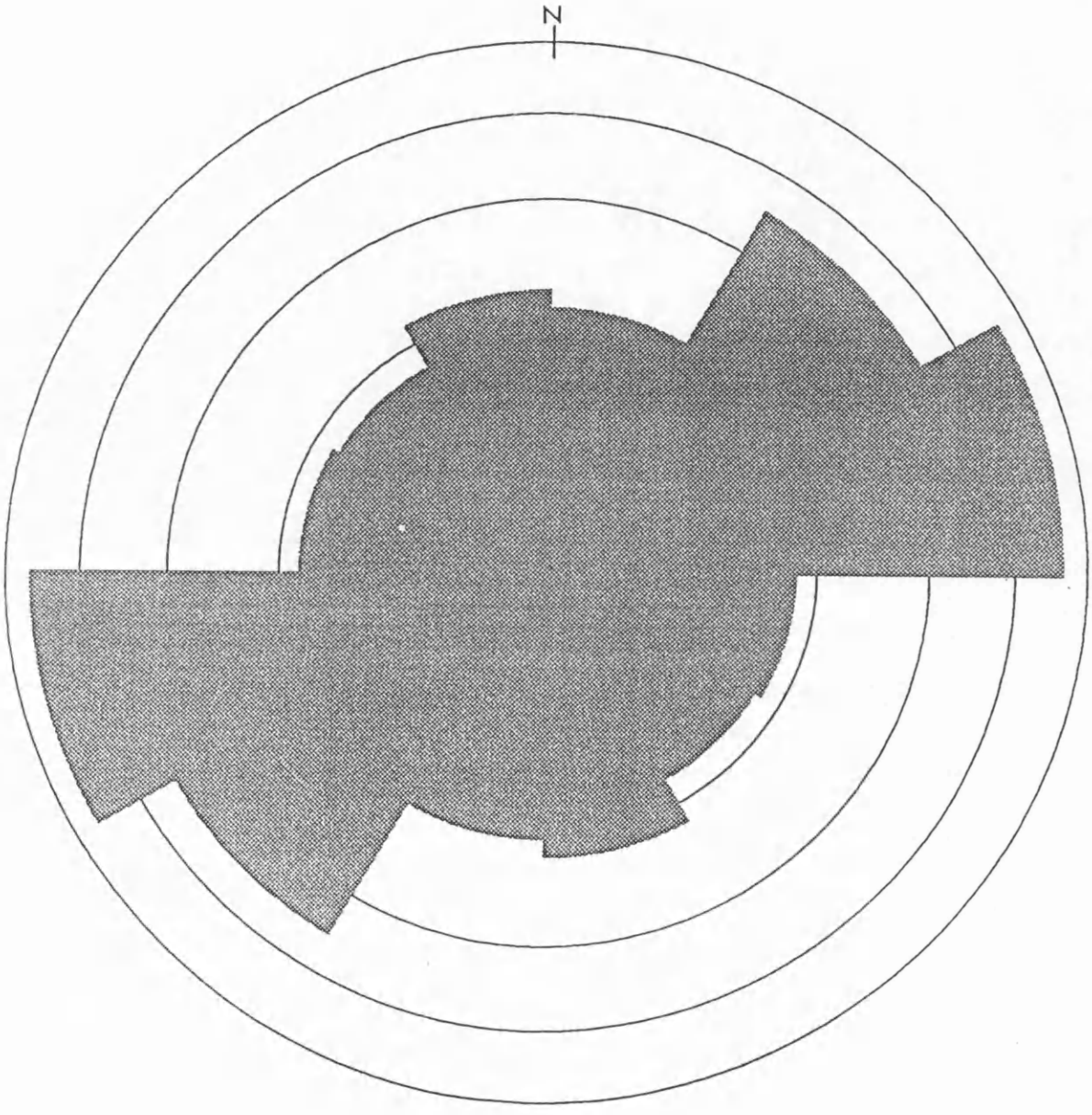

Figure 99: Rose diagram of the joints in the hornblende diorites(221 joints).

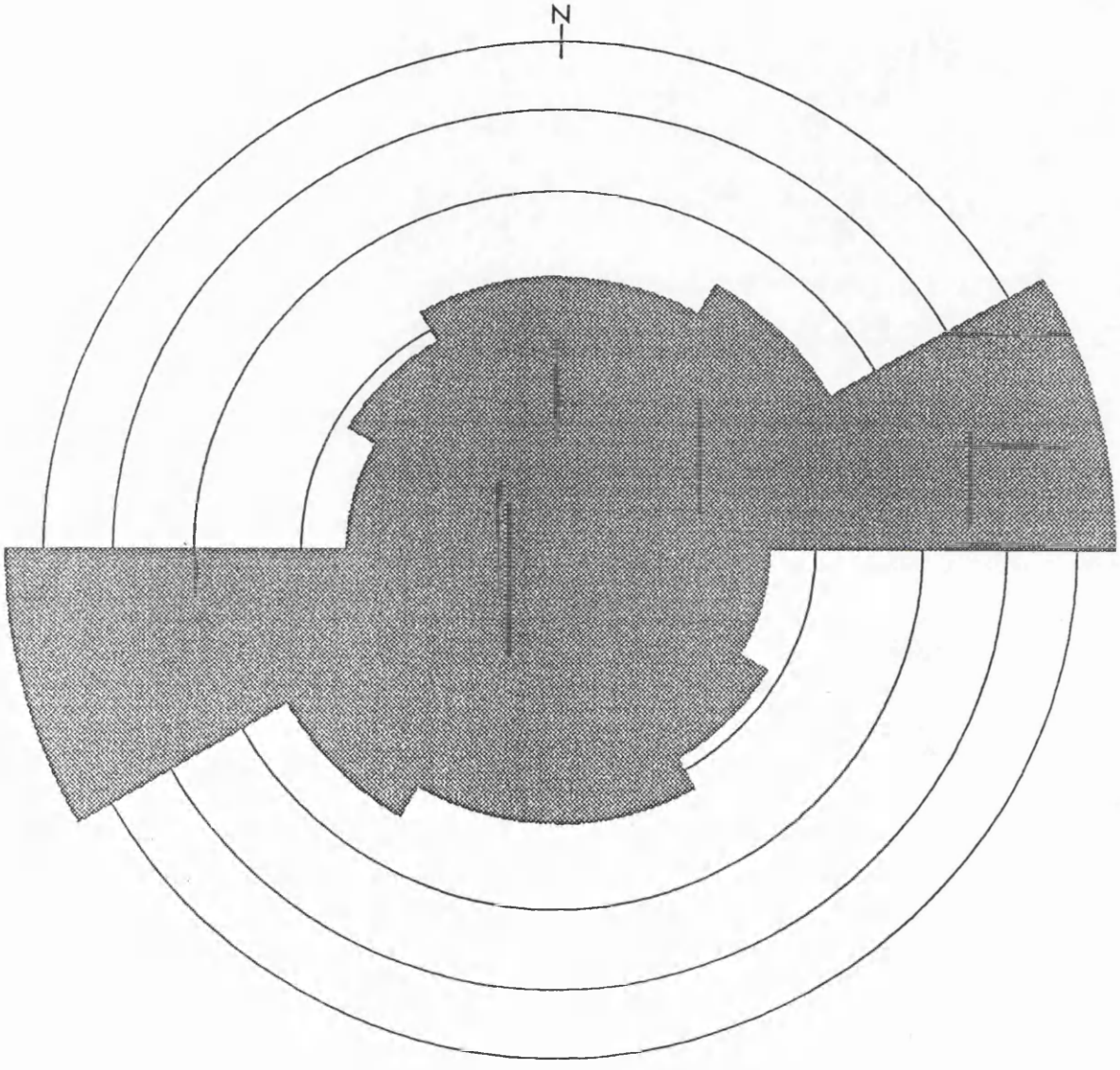

Figure 100: Rose diagram of the joints in the granitoids (641 joints)

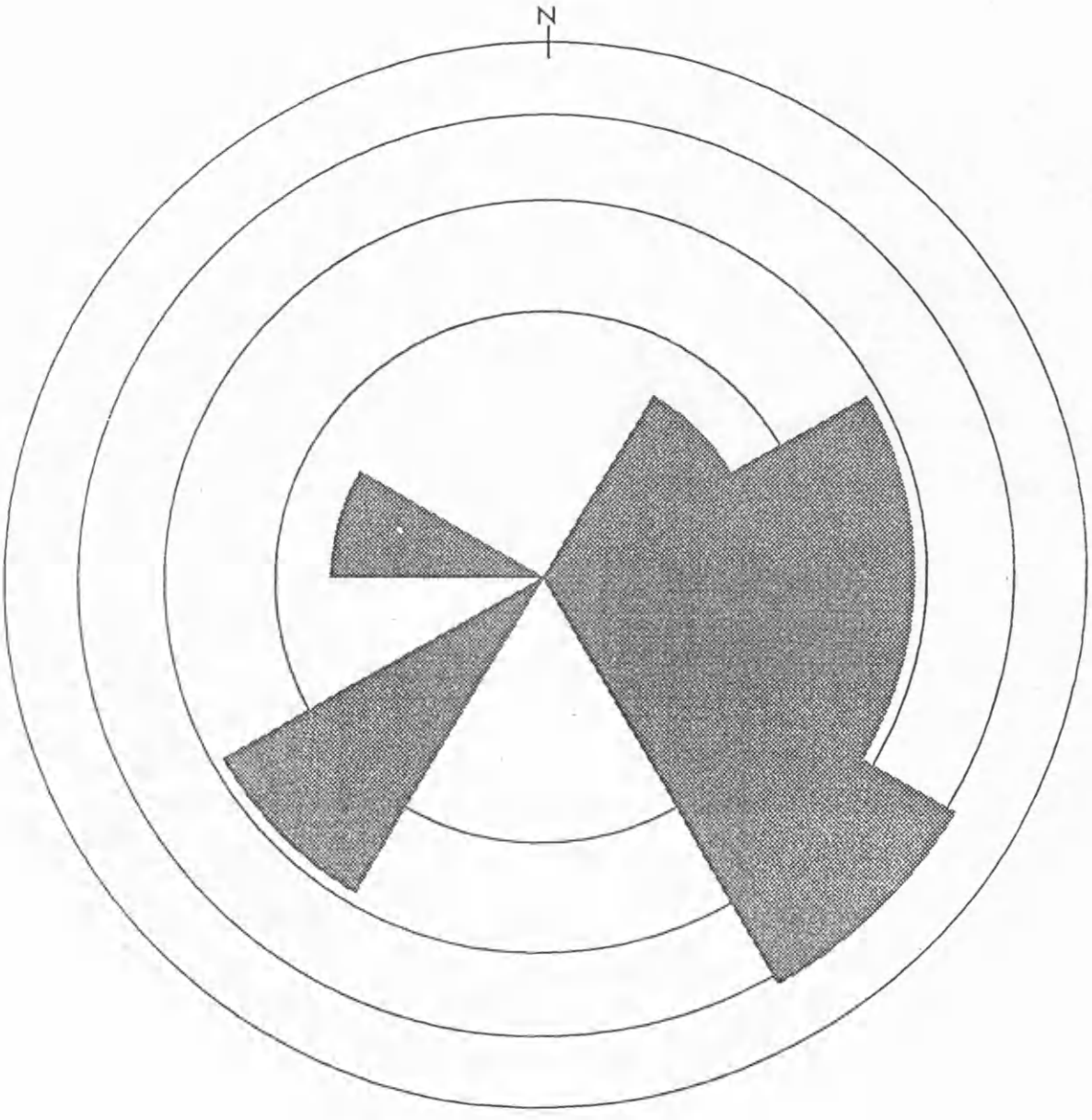

Figure 101: Rose diagram of the feldspar alignment in the granitoids (16 measurements).

VIII GEOLOGICAL HISTORY OF THE ORTAKOY DISTRICT

The geological history of the Ortakoy district starts with weathering and transportation of the Ortakoy semipelites and psammites from a craton (Gondwanaland?) in pre-Devonian time (Lower Paleozoic). The source of the sediments possibly suffered from moderate chemical weathering and was made of acidic igneous and volcanic rocks (probably fractionated) with possible minor basic-ultrabasic contributions. During Silurian-Devonian time, the semipelites and psammites with minor carbonates (Seksenusagi Formation) were deposited in a shelf environment of restricted circulation away from areas of sediment derived from a vegetated terrestrial environment, at an Andean type continental margin and possibly a continental island arc. Later, the carbonate was deposited alone as terrestrial detritial matter declined in an open shelf environment in Upper Paleozoic time, most probably in the Devonian-Carboniferous.

The amphibolites, continental basic rocks were later emplaced within the sediments between the Devonian to Permian. They were metamorphosed together under upper amphibolite facies conditions with the formation of some migmatites during or after D1 deformation which induced formation of the main foliation during the Permian-Carboniferous. D2, D3 and D4 deformations took place in the massif between Permian and Upper Cretaceous. Metasediments were intruded by voluminous hornblende diorite, hornblendite, biotite-hornblende granitoid (I-type), microgranite (fractionated I-type) and quartz-alkali syenite in a volcanic arc environment, during the Upper Cretaceous and Paleoecene. The tholeiitic Ekecekdagi gabbro may have been intruded before the intrusions of the Ortakoy pluton or been emplaced onto

metamorphic rocks as an allochthonous unit in the Upper Cretaceous.

Metasediments may be uplifted and eroded during or after Upper Cretaceous. Magmatic activity continued in the Pliocene with basaltic and rhyolitic flows. Meanwhile block faulting in the massif created a shallow lagoon where tuffaceous material, detritial material from the basement and limestone were deposited.. During and after the lake dried out, some palesols formed. Collovium and alluvium were developed by faulting in the Ekecekdagi gabbro and by alteration of the various lithologies in streams in the Quaternary.

IX SUMMARY OF THE CONCLUSIONS

1. The geological maps of the Ortakoy area at 1: 25 000 scale covering ~380 km^2, that of Sirayalardagi at 1: 5 000 covering 2 km^2 , and structural map of Ortakoy metamorphics have been completed (Appendix-Ia,b, -II, and -III)

2. The lithostratigraphic units of the Ortakoy area show the Seksenusagi Formation of Silurian-Devonian age is the oldest formation and includes migmatitic gneiss, migmatitic granite; biotite-, sillimanite-, garnet-, muscovite-, sericite-bearing semipelitic and psammitic gneiss with interlayers of marble, quartzite, calc-silicatic gneiss, rare tremolite-bearing gneiss and amphibolite. This is overlain by the Gobektepe Formation of Upper Palaeozoic age (Devonian-Carboniferous), which is mainly made of marble with lesser quartzite, biotite-, sillimanite- and garnet-bearing semipelitic and psammitic gneiss, rare amphibolite and tremolite bearing gneiss.

The Ekecekdagi gabbro including hornblende-gabbro and very rare banded gabbro may have been emplaced in the metamorphic rocks as an allochthonous unit or intruded into the metasediments before the intrusion of the Ortakoy pluton. The metasediments were then intruded and hornfelsed by the Ortakoy pluton containing hornblende diorite, biotite hornblende granitoid, microgranite and quartz-alkali syenite. Igneous and metamorphic rocks are overlain by the Pecenek Formation including rhyolitic tuff and limestone of Pliocene age. Collovium and alluvium are the last occurrence in the studied area.

3. The first fossil to be discovered in the massif has been found. Heliolitinae (Heliolitidae fam.) Paeckelmannophora sp can be recognised within the marbles of the Seksenusagi Formation, which gives an early Silurian to late Devonian age while the acritarchs, Leiosphaeridia and Lophosphaeriduim sp, give a broad Cambrian to Devonian range. The age of the metamorphism can be constrained as Carboniferous-Permian. It predates the rifting in Anatolia, which starts in the Permo-Trias and continues to the Lower Cretaceous (Sengor &Yilmaz, 1981).

4. Petrography reveals some minerals which had not previously been known in the area: garnet, andalusite, accessory picotite and cassiterite in semipelitic and psammitic gneisses; anorthite in the amphibolite; scapolite in the impure marble; corundum and hercynite in contact metamorphic samples; hercynite in the gabbro, tschermakite in the granophyre; hercynite in the hornblendite; and minerals of the late fractionate of the migmatitic granite (garnet, andalusite and gahnite) and that of the paragneissic granite and pelitic inclusions (garnet, biotite, sillimanite, cordierite and plagioclase and accessory magnetite, zircon, apatite and cassiterite).

5. Geochemical characteristic of the metasediments, tholeiitic gabbro and Ortakoy pluton were determined:

Sheet silicates were a dominant factor in controlling the composition of the Ortakoy metasediments. Various elements, namely K, Fe+3, Ti, Rb, Zr and possibly Ba, Ni and Zn were probably added in sheet silicates to the original sediments. A similar clay mineral end member, illite with substantial Si and Fe, was added to all Ortakoy sediments in various proportions

The metasediments were largely derived from non mafic sources, particularly acidic igneous and volcanic rocks (probably fractionated) with possible minor basic-ultrabasic contributions and deposited in an Andean type continental margin or continental island arc.

The Ortakoy granitoids are metaluminous to slightly peraluminous, high-K (Peccerillo and Taylor,1976), magnesian and possibly cafemic(Debon le Fort, 1988), and calcalkaline (Irvine and Baragar, 1971) in character.

The chemical and mineralogical composition of the hornblendite, diorites, granitoids and microgranites of the Ortakoy pluton represent different batches of the magma which possibly originated by mixing of mantle and lower crustal derived magmas, coupled with fractional crystallisation with possible minor high level contamination. The acidic rocks became melt dominated rather than restite dominated by this contamination, which is shown by decreasing K/Rb with increasing SiO2(Wyborn et al.,1992). Y/Nb variation in the granitoids also implies heterogeneity at the source of the granitoids. The chemical composition of the granitoids were altered by hybridisation processes such as mass-to-mass mixing and mechanical transfer

6. During or after D1 deformation, the metasediments suffered a single episode of regional prograde-metamorphism corresponding to the upper amphibolite facies conditions (second sillimanite grade) resulting in the formation of migmatite with muscovite breakdown (incongruent melting) under fluid absent conditions, and the crystallisation of hornblende, anorthite, diopside and sillimanite in the metabasic and semipelitic rocks. This is confirmed by geothermometer studies from the different metamorphic assemblages which yield between 608-761 ^{o}C at 4 kb.

pressure. The high grade metamorphic rocks have undergone limited retrogression to greenschist facies assemblages resulting in the replacement of sillimanite and K-feldspar by muscovite, and breakdown of garnet to biotite

The scarcity of garnet in the semipelites is probably due to a combination of low pressure and unsuitable composition combined with destruction of garnet to biotite

Hornfelsing resulted from the intrusions of Ortakoy pluton and Ekecekdagi gabbro(?).

7. The Ortakoy part of the Middle Anatolia Massif underwent four phases of deformation: D1 during the formation of the metamorphic rock fabric, D2 which produced folds varying from isoclinal to tight while D3 folds have open limbs and developed approximately in E-W directions. D4 folds are usually open with steep axial plane and plunging roughly towards SE. The massif was then uplifted inducing the development of the WSW-ENE dominated joint sets in the Ekecekdagi gabbro, diorite and granitoid and the formation of WNW-ESE faults.

8. Any model of the plate tectonic history must take account of the following:

a: The Ortakoy semipelite and psammites of Silurian-Devonian age, including quartzite were derived from a craton adjoining an active continental margin or continental island arc

b: The Ortakoy metasediments are a transgressive sequence which is characterised, from bottom to the top by decreasing of semipelite and psammite and increasing of carbonate .

c: After the metasediments were deposited, the amphibolites having a within plate geotectonic setting were emplaced

d: The Ortakoy granitoids of Upper Cretaceous-Paleocene age are high K calc-alkaline in character, indicative of an active continental margin(Pearce et al., 1984). The post tectonic granitoids can not be distinguished from the syntectonic granitoids as both plot in the volcanic arc field (Pearce et al.,1984) However, field data e.g. sharp contact between the granitoids and country rocks suggests that the granitoids belong to a shallow-seated pluton and are post tectonic.

These explanations may be synthesised as follow. The Ortakoy semipelitic and psammitic gneisses may have been derived in pre-Silurian time via weathering of Gondwanaland which was made of acidic igneous and volcanic rocks with possible minor basic-ultrabasic contributions and were deposited at an active continental margin and possibly in part in a continental island arc during Silurian-Devonian time. The environment became a passive continental margin which is characterised by transgressive deposition of open shelf carbonates during the Devonian and Carboniferous, and particularly emplacement of the continental amphibolites of within plate character. The sediments were latter intruded by voluminous post-tectonic granitoids of active continental margin type in Upper Cretaceous-Paleocene. As a tensional tectonic regime was dominant in the Anatolia block between Permian and Upper Cretaceous times (Sengor &Yilmaz,1981), the metamorphism in Ortakoy would be Permian-

Carboniferous. However, the time gap between the metamorphism and the intrusion of the post-tectonic granitoids is rather large. The non-existence of the pre-Upper Cretaceous formations in the MAM indicates that the massif acted as a rigid block after the metamorphism, between the Permian and Upper Cretaceous. The Ekecekdagi gabbro is of uncertain origin, and it is not clear whether it is allochthonous or not.

X REFERENCES

Aranovich, L.Ya., Lavrent'eva, I.V. and Kosyakova, N.A., 1988, Calibration of the biotite-garnet and biotite-orthopyroxene geothermometers corrected for the variable Al level in biotite, *Geochemistry, 50-59.*

Arikan, Y., 1975, Tuz golu havzasinin jeolojisi ve petrol imkanlari, *M.T.A. Der., 85, Ankara, 17-37.*

Arni, P., 1938, Kirsehir-Keskin ve Yerkoy zelzelesi hakkinda, *MTA Enstitusu Yayinlari, seri B, no1, Ankara.*

Ashworth, J.R., 1976, Petrogenesis of migmatites in the Huntly-Portsoy area, north-east Scotland, *Min.Mag., 40, 661-682.*

Atabey, E., Papak, I., Tarhan, N., Akarsu, B. and Taskiran, M.A., 1987, Ortakoy (Nigde)-Tuzkoy(Nevsehir)-Kesikkopru(Kirsehir) yoresinin jeolojisi, M.T.A. Gen. Mud.Jeo.Dai.Bsk., *derleme, 64.*

Ataman, G., 1972, Ankara'nin guneydogusundaki granitik-granadiyoritik kutlelerden Cefalik dagin radyometrik yasi hakkinda on calisma. *Hacettepe Fen ve Muh. Bil. Derg.,2/1,44-49.*

Atherton, M.P.,1968, The variation in garnet, biotite and chlorite composition in medium grade pelitic rocks from the Dalradian, Scotland, with particular reference to the zonation in garnet, *Con. Min. Pet., 18, 347-371.*

Atherton, M.P. and Sanderson, L.M., 1985, The chemical variation and evolution of the super-units of the segmented Coastal Batholith, In Pitcher, W.S., Atherton, M.P., Cobbing, E.J. and Beckinsale, R.D.(eds) Magmatism at a plate edge, *208-227.*

Ayan, M., 1963, Contribution a l'etude petrographique et geologique de la region situee au Nord-Est de Kaman (Turquie), *MTA Enst. yayinlari, no: 115, 332.*

Bacon, R.C., 1986, Magmatic inclusions in silicic and intermediate volcanic rocks, *J.Geoph.Res., 91(36), 6091-6112.*

Barbarin, B., 1990, Granitoids: main petrogenetic classifications in relation to origin and tectonic setting, *Geo.J.,25, 227-238.*

Barbarin, B. and Didier, J., 1992, Genesis and evolution of mafic microgranular enclaves through various types of interaction between coexisting felsic and mafic magmas, *T.R.S.E.: Earth Scie., 83, 145-153.*

Barker, F., 1961, Phase relations in cordierite-garnet-bearing Kinsman quartz monzonite and the enclosing schist, Lovewell Mountain quadrangle, New Hampshire, *Am. Min., 46, 1166-1176.*

Batchelor, R.A. and Bowden, P., 1985, Petrogenetic interpretation of granitoid rock series using multicationic parameters, *Chem.Geo., 48, 43-55.*

Bavinton, O.A. and Taylor, S.R., 1980, Rare earth element geochemistry of Archean metasedimentary rocks from Kambalda, Western Australia, *Geo.Cosmo.Acta., 44, 639-648.*

Bayhan, H. and Tolluoglu, U., 1987, The mineralogical-petrographical and geochemical characteristics of Cayagazi syenitoid (Northwest of Kirsehir province), *Yerbilimleri, 14, 109-120.*

Baykal, F., 1941, Krikkale-Kalecik ve Keskin-Bala mintikalarinda jeolojik etudler, *MTA Enst., derleme, Rap.no 1448 (yayinlanmamis).*

Beckinsale, R.D., 1979, Granite magmatism in the tin belt of southeast Asia, In Atherton, M.P. and Tarney (eds) Origin of granite batholiths: geochemical evidence, *Shiva, Orpington, U.K., 34-44.*

Beekman, P.H., 1966, Hasandagi-Melendiz dagi bolgesindeki Pliosen ve Kuvaterner volkanizma faaliyetleri, *M.T.A.Der., 66, Ankara, 88-104.*

Bhatia, M.R., 1983, Plate tectonics and geochemical compositions of sandstones, *J. Geo.,91, 611-627.*

Bhatia, M.R. and Crook, K.A.W., 1986, Trace element characteristics of greywackes and tectonic setting discrimination of sedimentary basins, *Con. Min. Pet.,92, 181-193.*

Bhatia, M.R. and Taylor, S.R.,1981, Trace element geochemistry and sedimentary provinces: a study from the tasman geosynclines, Australia. *Chem. Geo., 33, 115-125.*

Bingol, E., 1974, 1/2 500 000 olcekli Turkiye Metamorfizma Haritasi ve bazi metamorfik kusaklarin jeotektonik evrimi uzerine tartismalar. *MTA Enst.Der., 83, 178-184.*

Blumenthal, M.M., 1946, Die neue geologische Karte der Turkei und einige ihrer stratigraphischen-tektonischen Grundzuge. *Eclogae Geol.Helv., 39/2, 277-289.*

Blundy, J.D. and Holland, T.J.B.,1990, Calcic amphibole equilibria and a new amphibole-plagioclase geothermometer, *Con.Min.Pet.,104, 208-224.*

Boynton, W.V., 1984, Cosmochemistry of the rare earth elements: Meteorite studies, In Henderson, P.(ed) Rare earth elements, *Elsevier, 63-114.*

Brinkman, R., 1971, The geology of western Anatolia, In Geology and history of Turkey, *Petroleum Expl. Soc. of Libya, Tripolis, 171-190.*

Brookins, D.G., 1989, Aqueous geochemistry of rare earth elements, In Lipin, B.R. and McKay, G.A.(eds) Geochemistry and mineralogy of rare earth elements, Reviews in Mineralogy, *Min.Soc.Am., 201-225.*

Brown, G.C., Thorpe, R.S. and Webb, P.C., 1984, The geochemical characteristics of granitoids in contrasting arcs and comments on magma sources, *J.Geo.Soc.Lon., 141, 413-426.*

Buchardt, W.S., 1954, Orta Anadolu'da yapilan 1/100 000 olcekli jeolojik harita calismalari hakkinda rapor, *MTA Enst., Der. Rap. No:2675 (yayinlanmamis)*

Burnham, C.W., 1967, Hydrothermal fluids at the magmatic stage . In Barnes H.L.(ed) , Geochemistry of hydrothermal ore deposits, *Holt, Reinhart and Winston, New York, 38-76.*

Burnham, C.W., 1979, The importance of volatile costituents, In Yoder, H.S. (ed) the evaluation of the Igneous Rocks , *Princeton Univ.Press., Princeton, New Jersey, 439-482.*

Bussel, M.A., 1988, Structure and petrogenesis of a mixed-magma ring dyke in the Peruvian Coastal Batholith: eruptions from a zoned magma chamber, In the origin of granites, *T.R.S.E: Earth Sci., 87-104.*

Castro, A., Moreno-ventas, I. and de la Rosa, J.D. 1990, Microgranular enclaves as indicator of hybridisation processes in granitoid rocks Hercynian Belt, Spain, *Geo. J., 25, 391-404.*

Cawthorn, R.G. and O'Hara, M.J.,1976, Amphibole fractionation in calcalkaline magma genesis, *Am.J.Sci., 276, 309-329.*

Chappell, B.W.& White, A.J.R., 1974, Two contrasting granite types, *Pac.Geo., 8, 173-174.*

Chappell, B.W. and White, A.J.R., 1984, I- and S-type granites in the Lachlan Fold belt, southeastern Australia, In Keqin, X. and Guangchi, T.(eds) Geology of granites and their metallogenic relations, *Beijing, Science Press, 87-101.*

Chappel, B.W. and White, A.J.R., 1992, I- and S-type granites in the Lachlan Fold Belt, *T.R.S.E. : Earth Scie., 1-26.*

Clarke, D.B., 1992, Granitoid rocks, *Chapmen&Hall, 280.*

Clemens, J.D. and Vielzeuf, D., 1987, Constrains on melting and magma production in the crust, *E.P.S.Letters., 287-306.*

Conrad, W.K., Nicholls, I.A., and Wall,V.J., 1988, Water-saturated and -undersaturated melting of metaluminous and peraluminous crustal compositions at 10 kb: evidence for the origin of silicic magmas in Taupo Volcanic Zone, New Zealand, and other occurrence, *J.Pet., 29, 765-803.*

Cox, K.G., Bell, J.D. and Pankhurst, R.J., 1979, The interpretation of igneous rocks, *George Allen&Unwin Ltd., 450.*

Cullers, R.L. and Graf, J.L., 1984, Rare earth elements in igneous rocks of the continental crust: predominantly basic and ultrabasic rocks, In Henderson, P.(ed) Rare earth element geochemistry, *Elsevier, 237-274.*

de La Roche, H., Leterrier, J., Grand Claude, P. and Marchal, M., 1980, A classification of volcanic and plutonic rocks using R1-R2 diagrams and major element analyses-its relationships with current nomenclature, *Chem. Geo., 29, 183-210.*

Debon, F and Le Fort, P., 1982, A chemical-mineralogical classification of common plutonic rocks and associations, *T.R.S.E., Earth Scie., 73, 135-149.*

Debon, F and Le Fort, P., 1988, A cationic classification of common plutonic rocks and their magmatic associations: principles, method, applications, *Bull.Min., 111, 493-510.*

Didier, J.,1973, Granites and their enclaves. *Elseviers ,393.*

Drop, G.T.R.,1987, A general equation for estimating Fe3+ concentrations in ferromagnesian silicates and oxides from microprobe analyses, using stoichiometric criteria, *Min. Mag, 51, 431-450.*

Eberz, G.W and Nicholls, I.A., 1988, Microgranitoid enclaves from the Swifts Creek Pluton SE-Australia: textural and physical constraints on the nature of magma mingling process in the plutonic environment, *Geol.Runds., 77/3, 713-736.*

Eby, G.N., 1990, The A-type granitoids: A review of their occurrence and chemical characteristics and speculations on their petrogenesis, In Woolley, A.R. and Ross, M.(eds) Alkaline igneous and carbonatites. *Lithos, 26, 115-134.*

Ellis, D.J. and Thompson, A.B.,1986, Subsolidus and partial melting reactions in the quartz-excess CaO+MgO+Al2O3+SiO2+H2O system under water-excess and water deficient conditions to 10 kb: some implication for the origin of peraluminous melt from mafic rocks, *J.Pet., 27, 91-121.*

Ercan, T., Yildirim, A. and Akbasli, A., 1987, Characteristic features of the volcanism between Gelveri (Nigde) and Kizilcin (Nevsehir), *Jeomorfoloji dergisi, 15, 27-36.*

Erguvanli, K., 1954, Kirsehir dogusunun jeolojisi hakkinda rapor, *MTA Enst., Der.Rap. No: 2373 (yayinlanmamis).*

Erkan, Y., 1976 a, Kirsehir cevresindeki rejiyonal metamorfik bolgede saptanan izogradlar ve bunlarin petrolojik yorumlanmalari, *Yerbilimleri,2, 23-54.*

Erkan, Y., 1976 b, Orta Anadolu Masifi'ndeki karbonatli kayaclarda plajiyoklaz bilesimi ile metamorfizma arasindaki iliskilerin incelenmesi, *Yerbilimleri, 2,107-111.*

Erkan, Y., 1977, Orta Anadolu Masifi'nin guneybatisinda (Kirsehir bolgesinde) etkili rejiyonal metamorfizma ile amfibol minerallerinin bilesimi arasindaki iliskiler, *TJK Bul., 21, 43-50.*

Erkan, Y., 1978, Kirsehir Masifin'de granat minerallerinin kimyasal bilesimi ile rejiyonal metamorfizma arasindaki iliskiler. *TJK Bul., 21, 43-50.*

Erkan, Y., 1980 a, Amfibolit sorunu ve Orta Anadolu amfibolitlerinin olusum ve kokenlerinin incelenmesi, *Yerbilimleri, 5-6, 61-76.*

Erkan, Y., 1980 b, Orta Anadolu Masifi'nin kuzeydogusunda (Akdagmadeni, Yozgat) etkili olan bolgesel metamorfizmanin incelenmesi, *TJK Bult., 23, 213-218.*

Erkan, Y. and Ataman, G., 1981, Orta Anadolu Masifi'nin (Kirsehir yoresi) metamorfizma yasi uzerine K/Ar yontemi ile bir inceleme. *T.J.K. 35. Bilimsel ve Teknik Kurultayi bildiri ozetleri, 33.*

Farrow, C., 1992, Structural orientation data system(SODS), unpublished, *Glasgow, 15.*

Ferry,J.M. and Spear, F.S.,1978, Experimental calibration of the partioning of Fe and Mg between biotite and garnet, *Con.Min. Pet., 66, 113-117.*

Floyd, P.A., Winchester, J.A. and Park, R.G., 1989; Geochemistry and tectonic setting of Lewisian clastic metasediments from the early Proterozoic Loch Maree Group of Gairloch, NW Scotland, *Pre. Res., 45, 203-214.*

Frey, F.A., Chappel, B.W. and Roy, S.D., 1978, Fractionation of rare-earth elements in the Tuolumne Intrusive series, Sierra Nevada Batholith, California, *Geology, 6, 239-242.*

Goncuoglu, N.C., 1977, Geologie des weslichen Nigde-Massivs, PhD thesis, *Rheinischen Friedrich-Wilhelms-Univ., Bon, 180.*

Gorur, N., Oktay, F.Y., Seymen, I. and Sengor, A.M.C., 1984, Paleo-tectonic evolution of the Tuz golu basin complex, Central Turkey: sedimentary record of a Neo-Tethyan closure, In Dixon, J.E. and Robertson, A.H.F.(eds) The geological evolution of the Eastern Mediterranean, *Special Publication of the Geological Society, 17, 467-482.*

Grant, J.A., 1985, Phase equilibria in partial melting of pelitic rocks In Ashworth, J.R.(ed) Migmatites, *Glasgow, Blackie and Son, 86-144.*

Groome, D.R. and Hall, A., 1974, The geochemistry of the Devonian lavas of the northern Lorne Plateau, Scotland, *Min.Mag., 39,621-640.*

Gulson, B.L.,Lovering, J.F., Taylor, S.R., White, A.J.R., 1972, High-K diorites, their place in the calc-alkaline associations and relationship to andesites, *Lithos, 5, 269-279.*

Hanson, G.N., 1980, Rare earth elements in petrogenetic studies of igneous systems, *Ann. Rev. Earth Planet. Sci., 8, 371-406.*

Hanson, G.N.,1989, An approach to trace element modeling using a simple igneous system as an example, In Lipin, B.R. and McKay, G.A.(eds) Rare earth elements, *Min.Soc.Am, 21, 79-97.*

Harvey, P.K., Taylor, D.M., Hendry, R.D. and Bancroft, F.,1973, An accurate fusion method for the analysis of rocks and chemically related minerals by x-ray fluorescence spectrometry, *X-ray spectrometry, 21, 33-44.*

Haselton, H.T., Hovis, G.L., Hemingway, B.S. and Robie, R.A., 1983, Calorimetric investigation of the excess entropy of mixing in analbite-sanidine solid solutions: lack of evidence for Na, K short range order and implications for two-feldspar thermometry, *Am.Min., 68, 398-413.*

Helz, R.T., 1973, Phase relations of basalts in their melting ranges at P_{H2O}=5 kb as a function of oxygen fugacity. Part 1 Mafic phases, *J. Pet., 14, 249-302.*

Helz, R.T., 1976, Phase relations of basalts in their melting ranges at P_{H2O} = 5 kb. Part II. Melt compositions, *J.Pet., 17, 139-193.*

Henderson, P., 1982, Inorganic goechemistry, *Pergamon, Oxford, 353.*

Hibbard, M.J., 1981, The mixing origin of mantled feldspars, *Con.Min.Pet., 76, 158-170.*

Hill, R.I., Silver, L.T. and Taylor, H.P.Jr., 1986, Coupled Sr-O isotope variations as an indicator of source heterogeneity for the Northern Peninsular Ranges Batholith, *Con.Min.Pet., 92, 351-361.*

Holdaway, M.J., 1971, Stability of andesite and the aluminium silicate phase diagrams, *Am.J.Sci., 271, 97-131.*

Holden, P., Halliday, A.N. and Stephens, W.E., 1987, Neodymium and strontium isotope content of microdiorite enclaves points to mantle input to granitoid production. *Nature , 330, 53-56.*

Holden, P., Halliday, A.N.,Stephens, W.E. and Henney, P.J., 1991, Chemical and isotopic evidence for major mass transfer between mafic enclaves and felsic magma, *Chem.Geol.,92,135-152.*

Holland, H.D., 1978, The chemistry of the atmosphere and oceans, *Wiley, New York, 351.*

Holland,T.J. and Powell,R., 1990, An enlarged and updated internal consistent thermodynamic dataset with uncertainties and correlations: the system K2O-Na2O-CaO-MgO-MnO-FeO-Fe2O3-Al2O3-TiO2-SiO2-C-H2O2, *J. Met. Geo.,8,89- 124.*

Hollister,L.S.,1966, Garnet zoning: An interpretation based on the Rayleigh fractionation model, *Science, 154,1647-1651.*

Humphris, S.E., 1984, The mobility of the rare earth elements in the crust, In: P., Henderson, Ed. Rare Earth Element Geochemistry, *Elsevier, Amsterdam,317-342.*

Huppert, H.E.and Sparks, R.S.J., 1988, The fluid dynamics of crustal melting by injection basaltic sills, *T.R.S.E.: Earth Sci., 79, 237-243.*

Irvine, T.N. and Baragar, W.R.A., 1971, A guide to the chemical classification of the common volcanic rocks, *Can.J.Earth Sci., 8, 523-548.*

Jenner, G.A., Fryer, B.J. and McLennan, S.M., 1981, Geochemistry of the Yellowknife Super Group, *Geo.Cosmo.Acta, 45, 1111-1129.*

Jolliff, B.L., Papike, J.J. and Laul, J.C., 1987, Mineral recorders of pegmatite internal evolution: REE contents of tourmaline from the Bobingersoll pegmatite, South Dakota, *Geo.Cosm.Acta, 51, 2225-2232.*

Ketin, I., 1955, Yozgat bolgesinin jeolojisi ve Orta Anadolu Masifi'nin tektonik durumu. *TJK Bult., 6, 1-40.*

Ketin, I., 1959, Uber alter und Art der kristellinen gesteine und Erzlagestatten in Zentral-Anatolien: *Berg und Hutenmannische Monatshefte, 104/8, 163-169.*

Ketin, I., 1963, 1/500 000 olcekli Turkiye Jeoloji Haritasi "Kayseri" paftasi, *M.T.A.yay., Ankara, 83.*

Ketin, I., 1966, Tectonic units of Anatolia (Asia Minor). *MTA Bull., 66, p 23-35*

King, R.W., Kerrich, R.W. and Daddar, R., 1988, REE distributions in tourmaline: an INAA technique involving pretreatment by B volatilization, *Am. Min., 73, 424-431.*

Kober, L., 1931, Das Alpine Europ., Berlin.

Kretz, R.,1983, Symbols for rock forming minerals, *Am. Min. , 68, 277-279.*

Kretz, R.,1990, Biotite and garnet compositional variation and mineral equilibria in Grenville gneisses of the Otter Lake area, Quebec, *J.Met.Geo., 8, 493-506.*

Lahn, E., 1949, Orta Anadolu Masifinin jeolojisi hakkinda, *TJK Bul., 2,No:1*

Lamayre, J. and Bowden, P., 1982, Plutonic rock type series: discrimination of various granitoid series and related rocks, *J.Vol.Geo.Res., 14, 169-186.*

Le Bas, M.J., LeMaitre, R.W., Sreickeisen, A. and Zanettin, B., 1986, A chemical classification of volcanic rocks based on total alkali-silica diagram, *J. Pet., 27-3, 745-750.*

Le Maitre, R.W.,1976, The chemical variability of some common igneous rocks, *J.Pet., 17/4, 589-637.*

Leake, B.E., 1964, The chemical distinction between ortho- and para-amphibolites, *J. Pet. 5-2, 238-254.*

Leake, B.E., 1978, Nomenclature of amphiboles, *Min.Mag., 42, 533-563.*

Leake, B.E., Hendry, G.L., Kemp, A., Plant, A.G., Harvey, P.K., Wilson, J.R., Coates, J,S., Aucott, J.W., Lunel, T. and Howarth, R.J., 1969, The chemical analyses of rock powders by automatic x-ray fluorescence, *Chem.Geo., 5, 7-86.*

Leuchs, K., 1943, Der Bauplen Von Anatolian. *N. 3b . Miner. Geol. Paul. Mh., B, 33-72*

Lorenc, M. and Saavedra, J., 1989, Comparison of granite enclaves from the Iberian Peninsula with the autholiths of some Hercynian granitoids of southern Poland, *Krystalinikum, 20, 85-101.*

Lorenc, M.W., 1990, Magmatic mafic enclaves in granitoids of northern Sierra de Paiman, Argentina, *Geo.J., 25, 405-412.*

Maas, R. and McCulloch, M.T., 1991, The Provenance of Archean clastic metasediments in the Narryer Gneiss Complex, W Qestern Australia: Trace element geochemistry, Nd isotopes and U-Pb ages for detritial zircons, *Geo. Cosmo. Acta., 55, 1915-32.*

Macdonald, G.A. and Katsura, T., 1964, Chemical composition of Hawaiian lavas, *J. Pet., 5, 82-133.*

Maniar, P.D. and Piccoli, P.M., 1989, Tectonic discrimination of granitoids, *G.S.A.B., 101, 635-643.*

McLennan, S.M.,1989, Rare earth elements in sedimentary rocks: influence of provenance and sedimentary processes In: Lipin, B.R. and McKay, G.A.(eds) geochemistry and mineralogy of rare earth elements, Reviews in mineralogy, *Min.Soc.Am., 21, 169-200.*

McLennan, S.M., Taylor, S.R. and Kroner, A., 1983, Geochemical evolution of Archean shales from the Pilbara Supergroup, Western Australia, *Geo.Cosmo.Acta, 47, 1211-1222.*

McLennan, S.M., Taylor, S.R. and McGregor, V.R., 1984, Geochemistry of Archean metasedimentary rocks from West Greenland, *Geo.Cosm.Acta., 48, 1-13.*

McLennan, S.M., Taylor, S.R., McCulloch, M.T. and Maynard, J.B.,1990, Geochemical and Nd-Sr isotopic composition of deep sea turbidites: Crustal evolution and plate tectonic associations, *Geo. Cosmo.Acta, 54, 2015-2050.*

Menhert,K.R.,1968, Migmatites and the origin of granitic rocks, *Elsevier ,Amsterdam, 393.*

Menhert, K.R. and Busch, W, 1982, The initial stage of migmatite formation, *Neues Jb.Min. Ab.,145, 211-238.*

Miyashiro, A., 1974, Volcanic rock series in island arcs and active continental margins, *Am. J. Sci., 274, 321-355.*

Miyashiro,A.and Shido,F.,1973, Progressive compositional change of garnet in metapelite, *Lithos.,6,13-20.*

Mpodozis, C. and Kay , S.M., 1992, Late Paleozoic to Triassic evolution of the Gondwana margin: Evidence from Chilean Frontal Cordilleran Batholiths (28°S to 31°S), *G.S.A.B., 104, 999-1014.*

Nance, W.B. and Taylor, S.R., 1977, Rare earth element patterns and crustal evolution- II. Archean sedimentary rocks from Kalgoorlie, Australia, *Geo.Cosmo.Acta., 41, 225-231.*

Naslund, H.R.,1983, The effect of oxygen fugacity on liquid immiscibility in iron bearing silicate melts, *Am.J.Sci.,283, 1034-1059.*

Nesbitt, H.W. and Young, G.M.,1982, Early Proterozoic climate and plate motions inferred from major element chemistry of lutites, *Nature,299, 715-717.*

Okay, A.C., 1954, Kayseri, Nigde ve Tuzgolu arasindaki bolgenin jeolojisi, *MTA Rap. No:2701(yayinlanmamis)*

Olsen, S.N., 1983, A quantitative approach to local mass balance in migmatites, In Atherton, M.P and Gribble, C.D.(ed.s) Migmatites, melting and metamorphism, *Shiva, Nantwich, 201-233.*

Pankhurst, R.J., Hole, M.J. and Brook, M., 1988, Isotope evidence for the origin of Andean granites, *T.R.S.E.: Earth Sci., 79, 123-133.*

Peacock, M.A., 1931, Classification of igneous rock series, *J. Geo., 39, 54-67.*

Pearce, J.A. and Cann, J.R., 1973, Tectonic setting of basic volcanic rocks determined using trace element analyses, *E. P.S. Letters, 19, 290-300.*

Pearce, J.A., Harris, N.B.W. and Tindle, A.G., 1984, Trace element discrimination diagrams for the tectonic interpretation of granitic rocks, *J.Pet., 25, 956-983.*

Pecerillo, A. and Taylor, S.R., 1976, Geochemistry of Eocene calc-alkaline volcanic rocks from the Kastamonu area, northern Turkey, *Con.Min.Pet., 58, 63-81.*

Perchuk, L.L. and Lavrent'eva, I.V., 1983, Experimental investigation of exchange equilibria in the system cordierite-garnet-biotite. In: Advances in Physical Chemistry, 3, 199-299, *Springer-Verlag, New York.*

Pichler, H. and Zeil, W., 1972, The Cenozoic rhyolite-andesite association of the Chilean Andes, *Bull.Volc.,35,424-452.*

Pisoni, C., 1961, Ortakoy(Aksaray), Nevsehir, Avanos ve Incesu bolgelerinin jeolojisi ve petrol imkanlari*(tercume Malkoc, A.), 19.*

Pitcher, W.S., 1983, Granite type and tectonic environment, In Hsu,K.(ed) Mountain building processes, *Academic press,London, 19-40.*

Pitcher, W.S., 1987, Granites and yet more granites forty years on, *Geol.Runds., 76, 51-79.*

Powell,R. and Holland,T.J.B.,1988, An internally consistent thermodynamic dataset with uncertainties and correlations 3.Application to geobarometry, worked examples and a computer program, *J. Met. Geo. ,6, 173-204.*

Riley, J.P., 1958, Simultaneous determination of water and carbon dioxide in rocks and minerals, *Analyst, 83/ 982 , 42-49.*

Roenner, F., 1958, Ekzojen-endojen metamorfizma munasebetleri hakkinda bir etud. Kirsehir Masifi' nde (Merkezi Anadolu) bir granit mermer kontagindaki musahedeler, *M.T.A.Der., 50, 59-79.*

Roser, B.P. and Korsch, R.J.,1988, Provenance signatures of sandstone mudstone suites determined using discriminant function analysis of major element data, *Chem. Geo., 67, 119-139.*

Sengor, A.M.C. and Yilmaz, Y., 1981, Tethyan evolution of Turkey: a plate tectonic approach, *Tectonophysics, 75, 181-241.*

Senior, A. and Leake, B.E.,1978, Regional metasomatism and the geochemistry of the Dalradian metasediments of Connemara, Western Ireland, *J. Pet., 19, 585-625.*

Sewell, R.J., Darbyshire, D.P.F., Langford, R.L. and Strange, P.J., 1992, Geochemistry and Rb-Sr geochronology of Mesozoic granites from Hong-Kong, *T.R.S.E.: Earth Sci., 83, 269-280.*

Seymen, I., 1981, Kaman(Kirsehir) dolayinda Kirsehir Masifi'nin stratigrafisi ve metamorfizmasi. *TJK Bult., 24/2, 7-14.*

Seymen , I., 1982, Kaman dolayinda Kirsehir masifinin jeolojisi. Docentlik tezi, *I.T.U.Mad.Fak., Istanbul.*

Seymen, I., 1984, Kirsehir Masifi Metamorfitlerinin jeolojik evrimi, *T.J.K . Ketin Simpozyumu, 133-148.*

Shand, S.J., 1947, Eruptive rocks. Their genesis, composition, classification, and their relation to ore-deposits, *3rd edition, J.Wiley&Sons, Newyork, 488.*

Shaw, D.M.,1968, A review of K-Rb fractionation trends by covariance analysis, *Geo. Cosmo. Acta.,32, 573-602.*

Silver, L.T.and Chappel, B.W., 1988, The Peninsular Ranges Batholith: an insight into the evolution of the Cordilleran batholiths of southwestern North America, *T.R.S.E.Earth Sci., 79, 105-121.*

Stormer, J.C. and Nicholls, J., 1978, XLFRAC: A program for the interactive testing of magmatic differentiation models, *Comp.Geosci., 4, 143-159.*

Symmes, G.H. and Ferry, J.M., 1992, The effect of whole-rock MnO content on the stability of garnet in pelitic schists during metamorphism, *J.Met.Geo.,10, 221-237.*

Taylor, S.R. and McLennan, S.M., 1985, The Continental crust : its composition and Evolution, *Blackwell Scient. Pub., 296.*

Thompson, A.B., 1974, Calculation of muscovite-paragonite-alkali feldspar phase relations , *Con.Min.Pet., 44, 173-194.*

Thompson, A.B., 1982, Dehydration melting of pelitic rocks and the generation of H2O-undersaturated granitic liquids, *Am.J.Sci.,282, 1567-1595.*

Thompson, J.B., 1957, The graphical analyses of mineral assemblages in pelitic schists, *Am.Min., 42, 842-858..*

Tolluoglu, A.U., 1989, Mesoscopical tectonic features of the Kirsehir metamorphites, *Yerbilimleri, 15, 89-103.*

Tracy,R.J.,1982, Compositional zoning and inclusions in metamorphic minerals in Ferry, J.M.,ed., Characterization of metamorphism through mineral equilibria, Reviews in Mineralogy, *Min.Soc. Ame. , 10,355-397.*

Tracy,R.J., Robinson,P. and Thompson, A.B., 1976, Garnet composition and zoning in the determination of temperature and pressure of metamorphism, central Massachusetts, *Am. Min., 61,762-775.*

Tromp, S., 1942, Nigde-Incesu, Kizilirma ve Tuzgolu arasinda bulunan mintikalarin jeolojik etudu, *MTA Der Rap.No: 1456 (yayinlanmamis).*

Tulumen, E., 1980, Akdagmadeni(Yozgat) yoresinde petrografik ve metalojenik incelemeler, *K.T.U., Yerb.Fak., Dok.Tezi.*

Tuttle, O.F. and Bowen, N.L., 1958, Origin of granite in the light of experimental systems in the system NaAlSi3O3-KAlSi3O8-SiO2-H2O, *G.S.A.Mem., 74, 153*

Vache, R., 1963, Akdagmadeni kontakt yataklari ve bunlarin Orta Anadolu kristalinine karsi olan jeolojik cercevesi, *MTA Der., 60, 22-36.*

Van der Moolen, I. and Paterson, M.S., 1979, Experimental deformation of partially melted granite, *Cont.Min.Pet., 70, 299-318.*

Van der plas,L. and Tobi,A.C.,1965, A chart for judging the reliability of point counting results, *Am. J. Sci.,263, 87-90.*

Veizer, J., Hoefs, J., Lowe, D.R. and Thurston, P.C., 1989, Geochemistry of Precambrian carbonates: II. Archean greenstone belts and Archean sea water, *Geo. Cosmo. Acta, 53, 859-871.*

Vernon, R.H., 1979, Formation of late sillimanite by hydrogen metasomatism (base-leaching) in some high grade gneiss. *Lithos, 12, 175-185.*

Vernon, R.H., 1984, Microgranitoid enclaves in granites: globules of hybrid magma quenched in a plutonic environment, *Nature, 309, 438-439.*

Vernon, R.H., 1987, Growth and concentration of fibrous sillimanite related to heterogeneous deformation in K-feldspar-sillimanite metapelites, *J.Met.Geo., 5, 51-68.*

Vielzeuf, D. and Halloway, J.R., 1988, Experimental determination of the fluid-absent melting relations in the pelitic system; consequences for crustal differentiation, *Con.Min.Pet., 98, 257-276.*

Watson, E.B.,1976, Two liquid partition coefficients: Experimental data on geochemical implications, *Con. Min.Pet.,56, 119-134.*

Wedepohl, K.H., 1969, The handbook of Geochemistry,*V. Springer-Verlag.*

Weissermel, W., 1939, Abhandlungen der Preussischen Geologischen Landesanstait, N.F., 190, 131.

Whalen, J.B., Currie, K.L. and Chappel, B.W., 1987, A-type granites: Chemical characteristics, discrimination and petrogenesis, *Con.Min.Pet.,95, 407-419.*

Wildeman, T.R. and Condie, K.C., 1973, Rare earths in Archean greywackes from Wyoming and from the Fig Tree group, South Africa, *Geo.Cosmo.Acta., 37, 439-453.*

Wilkinson, J.F.G., 1986, Classification and average chemical compositions of common basalts and andesites, *J. Pet., 27, 31-62..*

Wilson, J.R. and Leake, B.E., 1972, The petrochemistry of the epidiorites of the Tayvallich Peninsula, North Knapdale, Argyllshire, *Scot. J. Geo., 8, 215-252.*

Winchester, J.A. and Floyd, P.A., 1977, Geochemical distributions of different magma series and their differentiation products using immobile elements, *Chem.Geo., 20, 325-343.*

Woodsworth,G.J.,1977, Homogenization of zoned garnets from pelitic schists, *Can. Min.,15, 230-242.*

Wright, A.E. and Bowes, D.R., 1979, Geochemistry of the appinite suite. In The Caledonides of the British Isles, *Geo.Soc.Lon.,699-704.*

Wyborn, L.A.I., Wyborn, D., Warren, R.G. and Drummand, B.J.,1992, Proterozoic granite types in Australia implications for lower crust composition, structure and evolution, *TRSE: Earth Sci., 83, 201-209.*

Wyllie, P.J., 1983, Experimental studies on biotite- and muscovite-granites and some crustal magmatic sources, In Atherton, M.P. and Gribble, C.D.(eds), Migmatites, melting and metamorphism, *Shiva, Cheshire, 12-26*

Wyllie, P.I.,1984, Constrains imposed by experimental petrology on possible and impossible magma sources and products, *Phil.Trans.Roy.Soc.Lon., A310, 439-456.*

Yaman, S., 1985, Akcakent(Cicekdagi-Kirsehir) yoresi florit yataklarinin jeolojisi ve sivi kapanim calismalari, T.J.K., Bult., 28, 743-78.

Yardley,B.W.D.,1977 a, An empirical study of diffusion in garnet, *Am. Min., 62,793-800.*

Yardley, B.W.D., 1977 b , The nature and significance of the mechanism of sillimanite growth in the Connemara Schists, Ireland, *Con.Min.Pet., 65, 53-58.*

Yardley, B.W.D., 1989, An introduction to metamorphic petrology, *Longman Scientific&Technical, 248.*

Yasar, M., Erkan, C., Bas,H., Celik,E., Aygun, M., Bilgic, T.,Kayakiran, S., Ayak, F. ve uygun, M.A., 1982, Tuz golu havzasi projesi raporu, *MTA Rap., 2/178*

Yoder, H.S., Steward, D.B. and Smith, J.R., 1957, Ternary feldspars, *Yb.Carneige Inst. Wash., 56, 206-214.*

Yoder, H.S., 1976, Generation of basaltic magma, *National Academy of Sciences, 265.*

Zorpi, M.J., Coulon, C., Orsini, J.B. and Cocirta, C., 1989, Magma mingling, zoning and emplacement in calcalkaline granitoid plutons, *Tectonophysics, 157, 315-329.*

Zorpi, M.J., Coulon, C and Orsini, J.B., 1991, Hybridisation between felsic and mafic magmas in calcalkaline granitoids- a case study in northern Sardinia, Italy, *Chem. Geol., 92, 45-86.*

APPENDIX-3 (EK-3)

A STRUCTURAL MAP OF ORTAKOY (AKSARAY) METAMORPHICS (ORTAKOY METAMORFIKLERININ YAPISAL HARITASI)

Kerim KOCAK, 1992

SYMBOLS (ISARETLER)

- : Formation boundary (Formasyon siniri)
- : Possible formation boundary(Muhtemel formasyon siniri)
- : Bedding (Tabakalanma)
- : Foliation (Foliyasyon)
- : Strike slip fault (Dogrultu atimli fay)
- : Dip slip fault (Egim atimli fay)
- : Possible fault (Muhtemel fay)
- : Plunge of anticline(F2)(Antiklinalin dalimi,,F2)
- : Plunge of overturned anticline(F2) (Ters donmus antiklinalin dalimi,F2)
- : Plunge of anticline (F3) (Antiklinalin dalimi,F3)
- : Major overturned anticline (Ana ters donmus antiklinal), F2
- : Major anticline(Ana antiklinal),F2
- : Subarea (Asalan)

Minor Fold (Kucuk kivrim)

N

Scale: 1/25 000

0 500 1000 m

APPENDIX-2 (EK-2)

A GEOLOGICAL MAP OF SIRAYALARDAGI

(SIRAYALARDAGININ JEOLOJIK HARITASI)

Kerim KOCAK , 1992

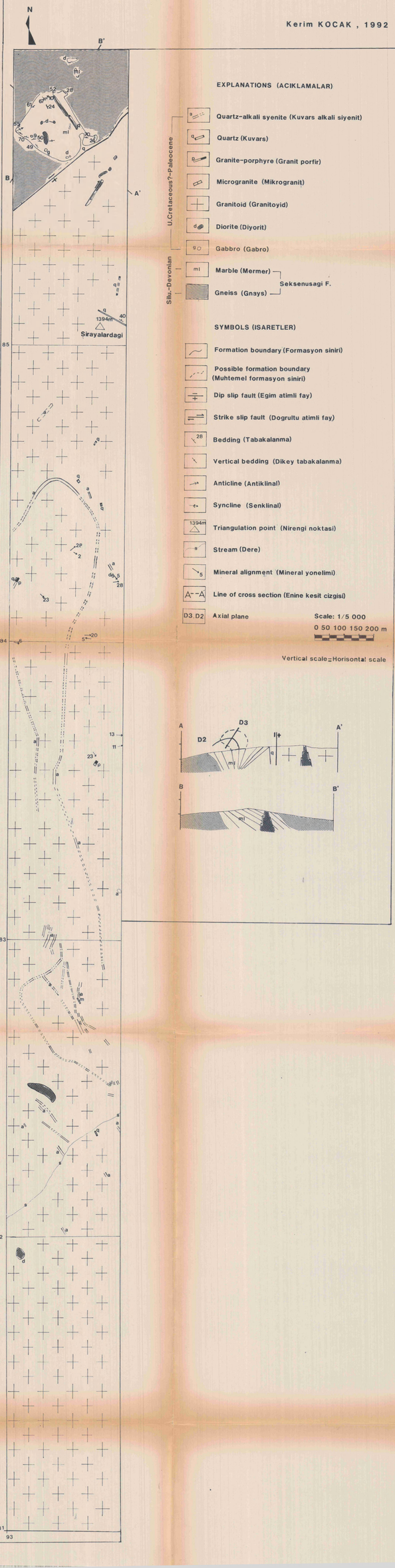

(APPENDIX-1b (EK-1b) ORTAKOY(AKSARAY)JEOLOJIK HARITASININ ENINE KESITLERI

CROSS SECTIONS FOR THE GEOLOGICAL MAP OF ORTAKOY, TURKEY

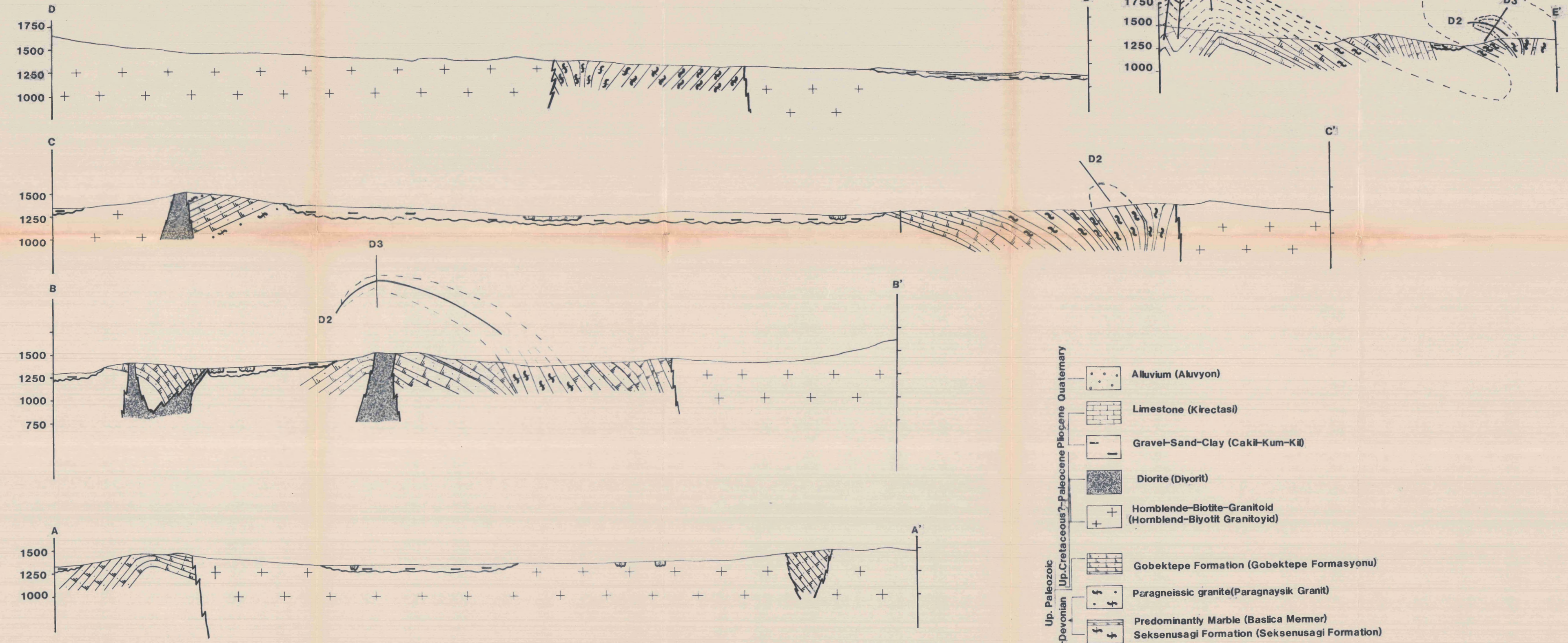

APPENDIX-1A [EK 1A]

[ORTAKOY, AKSARAY YORESININ JEOLOJIK HARITASI]

A GEOLOGICAL MAP OF ORTAKOY AREA, TURKEY KERİM KOÇAK, 1991

N

HARUNDAGI
Dede T.
1505 m.
Gokler
Bogelek T.
1311 m.
Abdiusagi
Saytepe
Cafertepe
Namlikisla
Akpinar
Catalcesme
Yenice
Hocabeyli
ÇALDAGI
1475 m.
ÇALDAĞI
1495 m.
Hacimahmutusagi
Kabakulak
Haciibrahimusagi
Gobek T.
ORTAKOY
Kochasan Hu.
Balci
Kepir
Armutlu T
Osmanaga T.
Seksenusagi
Sirayatardagi
Demirli D.
Kocaoz D.
PINAR DAGI
Bagozu D.
Elma D.
Sultancayi D.
Fakicik
Sinandi
Gökkaya
Yerli T.
1538 m.
EKECEK DAĞI
2137 m.
Edek
Ozdere

A A' B B' C C' D D' E E'

SYMBOLS (ISARETLER)

- Formation Boundary (Formasyon Siniri)
- Possible Formation Boundary (Muhtemel Formasyon Siniri)
- Transitional Formation Boundary (Gecisli Formasyon Siniri)
- Dip Slip Fault (Egim Atimli Fay)
- Strike Slip Fault (Dogrultu Atimli Fay)
- Possible Fault (Muhtemel Fay)
- Strike and Dip of Foliation (Foliasyon dogrultu ve egimi)
- Strike and Dip of Bedding (Tabaka dogrultu ve egimi)
- Horizontal Bedding (Yatay Tabakalanma)
- S — Skarn
- Aplite (Aplit)
- Pegmatite (Pegmatit)
- Quartz (Kuvars)
- Microdiorite (Mikrodiyorit)
- 1495 m. — Triangulation Point (Nirengi Noktasi)
- Stream (Dere)
- Dam (Baraj)
- Road (Yol)
- Mineral Alignment (Mineral Yonelimi)
- A — A' Line of cross section (Enine kesit cizgisi)

EXPLANATIONS (ACIKLAMALAR)

Quaternary
- Alluvium (Aluvyon)
- Collúvium (Yamac Molozu)

Pliocene — Pecenek Formation
- Limestone (Kirectasi)
- Gravel-Sand-Clay (Cakıl-Kum-Kil)
- Tuff (Tuf)

Up. Cretaceous - Paleocene
- al — Quartz-alkali syenite (Kuvars-alkali siyenit)
- Microgranite (Mikrogranit)
- g : Biotite-hornblende granitoid (Biyotit-hornblend granitoyid)
- H — Hornblendite (Hornblendit)
- Hornblende diorite (Hornblend diyorit)
- Ekecekdagi gabro (Ekecekdagi gabro)

Up. Paleozoic - Silu.-Devonian
- a : Amphibolite (Amfibolit) Gobektepe Formation (Gobektepe Formasyonu)
- Paragneissic granite (Paragnaysik granit)
- m : Predominantly Marble (Baslica Mermer) Seksenusagi Formation (Seksenusagi Formasyonu)

Scale : 1/25.000

0 500 1000 1500 m.